FINAL REPORT

Advanced Nanocrystalline Cobalt Alloys and Composites as Alternatives for Chromium and Nickel Plating in Repair Operations

SERDP Project WP-2609

AUGUST 2019

Dr. Jonathan McCrea
Integran Technologies Inc.

SERDP
DOD ▪ EPA ▪ DOE

REPORT DOCUMENTATION PAGE

Form Approved
OMB No. 0704-0188

1. REPORT DATE *(DD-MM-YYYY)*	**2. REPORT TYPE**	**3. DATES COVERED** *(From - To)*
19/08/2019	SERDP Final Report	9/21/2016 - 9/21/2018

4. TITLE AND SUBTITLE

Advanced Nanocrystalline Cobalt Alloys and Composites as Alternatives for Chromium and Nickel Plating in Repair Operations

5a. CONTRACT NUMBER
16-C-0042

5b. GRANT NUMBER

5c. PROGRAM ELEMENT NUMBER

6. AUTHOR(S)
Jonathan McCrea

5d. PROJECT NUMBER
WP-2609

5e. TASK NUMBER

5f. WORK UNIT NUMBER

7. PERFORMING ORGANIZATION NAME(S) AND ADDRESS(ES)
Integran Technologies, Inc
6300 Northam Drive
Mississauga, Ontario Canada L4V1H7

8. PERFORMING ORGANIZATION REPORT NUMBER
WP-2609

9. SPONSORING/MONITORING AGENCY NAME(S) AND ADDRESS(ES)
Strategic Environmental Research and Development Program (SERDP)
4800 Mark Center Drive, Suite 16F16
Alexandria, VA 22350-3605

10. SPONSOR/MONITOR'S ACRONYM(S)
SERDP

11. SPONSOR/MONITOR'S REPORT NUMBER(S)
WP-2609

12. DISTRIBUTION/AVAILABILITY STATEMENT
DISTRIBUTION STATEMENT A. Approved for public release: distribution unlimited.

13. SUPPLEMENTARY NOTES

14. ABSTRACT
Integran Technologies Inc., in collaboration with Cirrus Materials Science and Corrdesa, successfully completed SERDP Project WP-2609, in which a cost-effective nanostructured cobaltphosphorus (nCoP) composite alloy was successfully developed for the repair and refurbishment of damaged components for use within the US Department of Defense (DoD). Validation testing performed in the project demonstrated that the novel nanostructured composite coatings meet and/or exceed the properties and performance of electroplated nickel coatings and Electrolytic Hard Chrome (EHC) and can be successfully applied to steel and aluminum components.

15. SUBJECT TERMS
Electrodeposited Nickel replacement, Electrolytic Hard Chromium replacement, Integran, Nanocrystalline Cobalt Phosphorus, DC-rectifier compatible, Low Temperature Electroplating, 2nd Phase particle reinforcement, Improved Taber Wear Performance, Cirrus Materials, Dopant technology, Aluminum reinforcement via cladding, Corrdesa, Computational Optimization Methods, Tarnish Resistant Coatings, PVD

16. SECURITY CLASSIFICATION OF:			**17. LIMITATION OF ABSTRACT**	**18. NUMBER OF PAGES**	**19a. NAME OF RESPONSIBLE PERSON**
a. REPORT	**b. ABSTRACT**	**c. THIS PAGE**			Jonathan McCrea
UNCLASS	UNCLASS	UNCLASS	UNCLASS	190	**19b. TELEPHONE NUMBER** *(Include area code)* 416-675-6266

Prepared By: **Ijya Srivastava**
Project Engineer

Reviewed By: **Jonathan McCrea**
VP Technology

Approved By: **Gino Palumbo**
President/CEO

Revision History Log

Revision Level	Date	Comments
00	December 21, 2018	Initial Release
01	February 15, 2019	Revised based on comments from SERDP Project Office
02	August 19, 2019	Removed "Proprietary/Confidential" markings

DISCLAIMER

Integran Technologies Inc. takes reasonable steps to ensure that all work performed shall meet the industry standards and that all reports shall be reasonably free of errors, inaccuracies or omissions. **INTEGRAN TECHNOLOGIES INC. DOES NOT MAKE ANY WARRANTY OR REPRESENTATION WHATSOEVER, EXPRESS OR IMPLIED, WITH RESPECT TO THE MERCHANTABILITY OR FITNESS FOR ANY PARTICULAR PURPOSE OF ANY INFORMATION CONTAINED IN THIS REPORT OR THE RESPECTIVE WORKS OR SERVICES SUPPLIED OR PERFORMED BY INTEGRAN TECHNOLOGIES INC.** Integran Technologies Inc. does not accept any liability for any damages, either directly, consequentially or otherwise resulting from the use of this report.

EXECUTIVE SUMMARY

Integran Technologies Inc., in collaboration with Cirrus Materials Science and Corrdesa, successfully completed SERDP Project WP-2609, in which a cost-effective nanostructured cobalt-phosphorus (nCoP) composite alloy was successfully developed for the repair and refurbishment of damaged components for use within the US Department of Defense (DoD). Validation testing performed in the project demonstrated that the novel nanostructured composite coatings meet and/or exceed the properties and performance of electroplated nickel coatings and Electrolytic Hard Chrome (EHC) and can be successfully applied to steel and aluminum components.

The development efforts in the project built upon the core Nanostructured Cobalt-Phosphorus technology that was successfully demonstrated and validated at FRC-SE in ESTCP Project WP-0411. The main accomplishments in the project include:

nCoP Process Optimization – Integran successfully optimized the nCoP deposition process such that nanostructured CoP coatings could be produced using DC-rectifiers at lower bath operating temperatures (as low as 70°C). Demonstration and validation testing confirmed that properties (hardness, wear, hydrogen embrittlement) were comparable to the standard nCoP coating previously demonstrated in WP-0411.

Nanometal Matrix Composite Development – nCoP-composite coatings were successfully developed based on two different fabrication methods: i) co-deposition of second phase particulate (from particle suspension baths) showed significant improvement in abrasive wear performance over the baseline nCoP coating, achieving Taber wear as low as ~ 4mg/1000cycles (down from 18mg/1000cycles), and ii) development of nCoP-composite coatings based on the Cirrus Materials Science dopant technology in which co-deposited nanoparticles are formed in-situ achieved a Taber wear as low as ~ 11mg/1000cycles. Ductility testing performed on nCoP-composite samples fabricated from both methods showed that reasonable ductility was retained with the inclusion of the particles.

Substrate Compatibility for Repair Applications – The nCoP process was successfully demonstrated to be suitable for repair of steel and aluminum substrates; providing good galvanic corrosion compatibility and excellent adhesion. The high hardness and excellent wear resistance of the nCoP coating was found to provide significantly enhanced surface durability to both steel and aluminum substrates. The excellent structural properties of the nanometal coating was also found to significantly enhance mechanical properties of aluminum substrates with a relatively thin layer of nanometal coating. Three-point bend tests performed on aluminum substrates coated with 100µm thick nCoP coatings showed a two-fold increase in flexural strength.

Demonstration of Novel Localized Repair Method for Thick Repairs – A novel localized repair method was demonstrated on a modified nCoP-composite plating chemistry. Integran's Encased Contact Free (ECF) plating setup involves a fully contained plating head that can be attached to surfaces requiring repair. Plating solution is then pumped through the plating head resulting localized plating without the mess typically associated with brush plating. Testing performed in the project demonstrated that the method was compatible with the nCoP-Composite coatings developed in the project.

Key words: Electrodeposited Nickel replacement, Electrolytic Hard Chromium replacement, Integran, Nanocrystalline Cobalt Phosphorus, DC-rectifier compatible, Low Temperature Electroplating, 2nd Phase particle reinforcement, Improved Taber Wear Performance, Cirrus Materials, Dopant technology, Aluminum reinforcement via cladding, Corrdesa, Computational Optimization Methods, Tarnish Resistant Coatings, PVD

TABLE OF CONTENTS

TABLE OF FIGURES

LIST OF TABLES

LIST OF ACRONYMS

Al	Aluminum
Al_2O_3	Aluminum Oxide
AMS	Aerospace Material Specifications
ASTM	American Society for Testing and Materials
B4C	Boron Carbide
Co	Cobalt metal
CoP	Cobalt-Phosphorus alloy
Cr	Chromium metal
Cr_3C_2	Chrome Carbide
DC	Direct Current
DOD	Department of Defense
DOE	Design of Experiments
ECF	Encased Contact Free Plating Apparatus
EHC	Electrolytic Hard Chrome
EN	Electroless Nickel
ESOH	Environmental Safety and Occupational Health
ESTCP	Environmental Security Technology Certification Program
HV	Vickers Hardness (also see VHN)
ICP-MS	Induction Coupled Plasma – Mass Spectroscopy
LOS	Line of Sight
ML	Multilayer
MSDS	Materials Safety Datasheet
NAVAIR JAX	Naval Air Station Jacksonville
Ni	Nickel Metal
NiB	Nickel boron
NiP	Nickel phosphorus
Ni-W	Nickel-tungsten
NLOS	Non-line-of-sight
nm	Nanometer
NSS	Neutral Salt Spray
nCoP	Nanostructured Cobalt-Phosphorus alloy
OCP	Open Circuit Potential
P	Phosphorus element
PoD	Pin-on-Disk
PP	Pulse Plating
PVD	Physical Vapour Deposition
REACH	Regulation on Registration, Evaluation, Authorisation and Restriction of Chemicals
SBIR	Small Business Innovative Research
SEM/EDX	Scanning electron microscopy/ Energy-dispersive X-ray spectroscopy
SERDP	Strategic Environmental Research and Development Program
Si	Silicon
SiC	Silicon Carbide
Sm	Samarium metal

SWR	Sliding wear rate
T	Temperature
TEM	Transmission Electron Microscope
TDS	Technical Datasheet
Ti	Titanium
TiO_2	Titanium Dioxide
TWI	Taber wear index
µ	Coefficient of friction
µm	micrometer
UoA	University of Auckland
US	United States
USAF	United States Air Force
VHN	Vickers Hardness Number (also see HV)
XRD	X-ray Diffraction
ZnNi	Zinc-Nickel Alloy
Zr	Zirconium
ZrO_2	Zirconium Dioxide

Acknowledgements

The investigators would like to acknowledge Strategic Environmental Research and Development (SERDP) Program for facilitating the opportunity to research Nanostructured coatings as an environmentally benign alternates to electrodeposited Ni and EHC and the novel technology of in-situ particle formation systems in electroplating.

1. INTRODUCTION

1.1 Nickel and Chromium Plating

Electrodeposited nickel and hard chromium coatings are extensively used throughout the DoD for the repair and overhaul of damaged components. Hard chromium coatings (0.25 to 10 mil thick) impart wear and erosion resistance to components in both industrial and military applications. The most common (and most practical) means of depositing such hard chromium deposits has been through the use of chromic acid baths containing hexavalent chromium (Cr^{+6}). Health risks associated with the use of Cr^{+6} baths have been recognized since the early 1930's, wherein skin irritation and inflammation, particularly in the nasal passages, were identified. More recently, such Cr^{+6} baths have been shown to enhance the risk of cancer of the lung and nose. As a result of its toxicity, exposure levels of hexavalent chrome ions have been limited.

Due to the increase in operational costs associated with compliance to new rules including implementation of systematic procedures for cleanliness (i.e., ensuring walls and all horizontal surfaces are free of contaminants), and due to overall loss in productivity resulting from re-allocation of resources, there is tremendous pressure to find an environmentally-benign alternative to hard chrome. Similarly, use of nickel compounds is being limited in order to reduce operational risks resulting from possible inhalation, ingestion, and dermal contact. Although significant progress has been made in the development of less harmful 'trivalent Cr' (Cr^{+3}) plating processes, a reliable industrial process has yet to emerge for use as a suitable repair technology.

From the above summary, it is apparent that any alternative technology to hard chromium or nickel electroplating, in addition to necessarily yielding significantly-reduced environmental and health risks, must as a minimum achieve the hardness and low coefficient of friction provided by hard chromium, and must be amenable to industrial application. The industrial application refers to the ability to address ease of use and ability to coat inner diameters and complex shapes – a holistic solution. Moreover, as a result of some of the technical drawbacks identified with hard chromium technology, opportunities exist for significant improvements, particularly with regard to: 1) increasing deposition rates, 2) reducing the risk of substrate embrittlement, 3) enhancing ductility, and 4) improving spalling and corrosion resistance. As outlined in the following sections, nanocrystalline cobalt alloys and composite coatings are fully compatible with current hard chromium plating infrastructure, and have displayed properties which render them a superior alternative to hard chromium and nickel coating technologies for repair.

1.2 Proposed Alternative Solution

In the current project presented herein, Integran Technologies Inc., in collaboration with Cirrus Materials Science and Corrdesa, executed an advanced technology development program for environmentally-benign nanoscale cobalt alloy composite coatings as a replacement for current nickel and chromium electroplating for repair and overhaul of DoD weapon platforms. Nickel electroplating is by far the most extensively applied metal finishing technology [i], and this project sought to allow the complete elimination of nickel at rework, maintenance, and manufacturing facilities within the DoD. The nanoscale composite coating approach, which is based upon electroplating, would allow for the retention of numerous benefits associated with nickel and chromium electroplating technologies (i.e., line-of-sight (LOS) and non-line-of-sight (NLOS)

application, excellent coating adhesion, dimensional consistency and superior surface finish). The nanoscale composite coating approach would also allow for the use of existing plating infrastructure within the defense sector. This will significantly reduce the time and cost to practical implementation. Moreover, the proposed nanoscale technology is expected to provide significant performance and life-cycle cost benefits over current nickel and chromium plating technology. The proposed program leverages the success of previous SERDP and ESTCP projects related to the development of nanostructured cobalt alloys as an alternative to hard chrome coatings, and it would take advantage of the current nanostructured cobalt-phosphorus (Nanovate™ CoP) plating infrastructure at FRC-SE for a streamlined technology transfer to DoD operations.

This project involves the continued development of Integran's existing nanocrystalline cobalt-phosphorus (nCoP) electrodeposition process (Nanovate™ R3010[1], SAE AMS 2428[2], MIL-DTL-32502[3]).

There are a number of features of nCoP coatings that make them ideally suited for repair and overhaul of damaged/worn components. For example, the nCoP deposit has an average grain size in the range of 5-15nm as observed by direct observation in bright-field imaging using transmission electron microscopy (TEM), which results in an optimal combination of strength and ductility. The nCoP coatings are also fully-dense and free of pits, pores, or cracks, whereas EHC is inherently micro-cracked. From a corrosion stand-point, the fully-dense nCoP provides a continuous barrier to resist corrosion, an advantage over cracked hard chrome which is shown by the improved performance in neutral salt spray corrosion testing (ASTM B117). Due to EHC's inherent microcracks, it cannot be used as a structural repair, and a nickel underlayer is typically required for repair of damaged steel components. Furthermore, from a galvanic corrosion perspective, nCoP provides a better galvanic couple with steel (and aluminum) than nickel coatings due to the closer open circuit potential (OCP) in salt water. For a full comparison between EHC and nCoP, please refer to Appendix A.

The current process to deposit nCoP coating however, requires the use of pulse plating rectifiers in order to obtain the optimized nCoP microstructure. The use of pulse (PP) rectifiers can be cost-prohibitive due to high capital expenditures required for procurement and provide a significant barrier to the widespread adoption of the technology within the DoD. Therefore, the development of a nCoP process that is compatible with direct current (DC) rectifiers and lower operating temperatures while still producing coatings with excellent abrasive wear performance was highly desirable to reduce this barrier to implementation.

This project focused on two main development activities: i) the continued optimization of the nCoP process to allow use of DC-rectifiers and to reduce operating temperature, and ii) the investigation of a nanocomposite coating system based on a nanocrystalline cobalt-phosphorus matrix embedded with second-phase hard particles to improve abrasive wear performance. Two parallel approaches to creating these composite structures were investigated: the first approach involved novel technology from Cirrus Materials Science whereby nanoparticles are formed in-situ and subsequently co-deposited in the plating bath; in the second approach conventional co-deposition

[1] http://www.integran.com/services/corrosion---wear-resistant-coatings
[2] http://standards.sae.org/ams2428/
[3] https://global.ihs.com/doc_detail.cfm?document_name=MIL-DTL-32502&item_s_key=00627875

of suspended hard ceramic particles was investigated. In order to minimalize cost associated with technology implementation, Integran and Cirrus collaborated with Corrdesa LLC to employ complementary state-of-the-art computational fluid dynamics, electroplating, and corrosion design software to aid in materials selection and optimize deposition rates.

The nanoscale composite coating technology will be suitable for line-of-sight (LOS) and non-line-of-sight (NLOS) applications, accompanied with excellent coating adhesion, dimensional consistency and superior surface finish. The technology will also allow for the use of existing plating infrastructure within the defense sector thereby providing further reduction in time and implementation costs.

This report discusses the technical approach taken to address project objectives and highlights the relevant findings.

1.3 Health & Safety and Environmental Impact of Integran's Nanostructured Cobalt Processes

Today, cobalt metal is widely used in the manufacture of pigments, HVOF thermal spray coatings, Li-ion batteries, catalysts, superalloys and magnets. With regards to ESOH concerns, best practices regarding standard health and safety precautious currently being followed for nickel and chrome plating and grinding processes should also be followed for all light and heavy metal-based fabrication processes, including Integran's nanostructured Cobalt coatings. During the electrodeposition process, workers handling liquid mixtures will require personal protective equipment already in-use within electroplating operations (i.e., eyewear, safety shoes, etc.). As will almost all processes, there is a Permissible Emission Limit (PEL) for cobalt. The PEL for Co metal is 0.1 mg(Co)/m^3. From work conducted in the SERDP PP-1152 and ESTCP WP-0411 programs, however, the Cobalt present in mist when the tank is in operation is well below the PEL. Cobalt is not covered under the Clean Air Act regulations.

With regards to the specific environmental concerns with respect to cobalt coatings and cobalt salts used and applied in the proposed development efforts, the current status of the toxicity of cobalt is that there is "inadequate evidence for the carcinogenicity of cobalt and cobalt compounds in humans", International Agency for Research on Cancer (IARC). Cobalt, or any of the cobalt containing chemicals used and applied in the proposed development efforts are ***not*** listed as a known carcinogen in any organization (EPA, IARC, U.S. Department of Health and Human Services 13th Report on Carcinogens (13th ROC)). Only Cobalt sulfate is listed in 13th ROC and IARC as a substance that is possibly carcinogenic to humans based on animal studies; however, cobalt sulfate is not used or produced in the nano CoP process. This is in contrast to Hexavalent chromium and nickel compounds; where: Hexavalent Chromium is listed as a "Known Carcinogen" (EPA, IARC, 13th ROC), Nickel compounds are listed as "Known Carcinogens" (EPA, IARC, 13th ROC), and Nickel metal is listed as "A substance reasonably anticipated to be a human carcinogen" (13th ROC). The EPA has also determined that nickel refinery dust and nickel sub-sulfide are human carcinogens (http://www.atsdr.cdc.gov). Presently, the EPA does not classify cobalt for carcinogenicity.

Five Cobalt salts have been proposed for prioritization for addition into Annex XIV of REACH.

This means that certain uses of these cobalt compounds could become subject to Authorization under REACH. Pre-authorization of cobalt salts by suppliers would enable use of the chemicals for manufacture within the EU jurisdiction. The addition of cobalt salts does not preclude importation of nCoP coated articles manufactured outside the EU. Major chemical suppliers have indicated that they intend to register for authorization for surface finishing users. The current position of the cobalt REACH consortium is that a prioritization process at this stage is premature and cannot be concluded as a number of technical data is still being collected and reviewed to ensure a complete understanding of these cobalt salts' numerous uses. More specifically, the Cobalt REACH consortium believes[4]: i) the prioritization of these five salts is based on the wrong assumption of their inter-changeability: industrial processes designed for one of the salts cannot be changed to use another salt for practical and chemical reasons, ii) most uses/applications are already covered by existing and robust EU legislation and thus should be exempted; and iii) an Annex XIV listing will not contribute to a higher level of human health or environmental protection given that there is negligible consumer exposure and worker exposure is strictly regulated under existing legislation. To obtain more information refer to the Cobalt Development Institute.

Integran recently completed cytotoxicity and biocompatibility evaluation of nanostructured cobalt plated components with a leading medical surgical instrument manufacturer. The components passed their requirement for temporary use in the human body.

[4] www.cobaltreachconsortium.org/authorization

2. OBJECTIVES

The project presented herein sought to develop an alternative repair technology for worn components that is free of chromium and nickel. Based upon previous proprietary developments by the applicants in the area of nanostructured metal and metal-matrix composites, applied by electroplating and selective (brush) plating, a materials technology development and optimization program was conducted to specifically target the cost-effective repair of damaged components and structures.

The overall technical objective of the project was to develop and validate an alternative repair technology based on electrodeposited nanostructured cobalt that meets and/or exceeds the properties and performance of i) electroplated nickel coatings in both Class 1 (corrosion protection) and Class 2 (engineering plating) applications, as specified in military and aerospace standards for bulk component plating such as MIL-STD-868A and AMS-QQ-N-290; ii) electrolytic hard chrome coatings per AMS-QQ-C-320; and iii) for selective plating, repair, and rebuilds as outlined in MIL-STD-865C.

In order to develop a nanocrystalline cobalt-phosphorus alloy to meet the above requirements the primary technical objectives of the project were as follows:

1. Optimize a nanocrystalline cobalt-phosphorus electrodeposition process for repair operations that is based on conventional DC rectifiers in order to reduce infrastructure costs associated with pulse plating;
2. Develop novel nanocomposite coating systems consisting of a nanocrystalline cobalt-phosphorus matrix embedded with second-phase hard particles in order to improve Taber wear performance of nanocrystalline cobalt-phosphorus systems; composite coatings will be created by
    a. Co-deposition of suspended particles, and
    b. Novel in-situ particle formation and deposition of nanoparticles (Cirrus Materials Science technology);
3. Evaluate suitable equipment to enable brush plating for specialized repair using the optimized material; and
4. Reduce repair implementation cost by utilizing state-of-the-art computational fluid dynamic, electroplating, and galvanic corrosion design software in order to optimize deposition rates and aid in material selection.

3. TECHNICAL APPROACH / METHODS & MATERIALS

To address the project objectives, the workplan for this project was divided into the following five tasks:

- *TASK 1 Development and optimization of nCoP matrix material:* development of plating process for matrix material deposition on steel and aluminum substrates.
- *TASK 2 Development of process to co-deposit hard ceramic, second phase particles:* entails development of the process to co-deposit hard ceramic second-phase particles using particle- suspension plating baths as well as Cirrus dopant technology based baths.
- *TASK 3 Development of specialized repair methods via brush plating:* development of brush plating method, plating deposits developed in Tasks 1 and 2, suitable for repair applications
- *TASK 4 Optimized (final) process stand-up:* Scale-up of the process developed in the preceding tasks and optimization of the coating process.
- *TASK 5 Coating characterization, testing and evaluation:* Characterization of deposits produced in Task 4, used for feedback for effective process and material optimization and validation

The overall project breakdown is as follows: Task 1 was aimed at optimizing the nCoP matrix, Task 2 involved the investigation of co-deposition of second phase particles in the nCoP matrix to enhance mechanical properties, and Task 3 involved the design and development of nCoP and nCoP-particle brush plating system suitable for repair operations and consequent scale up in Task 4 and validation testing in task 5. The findings of every task were used in the development of the succeeding tasks.

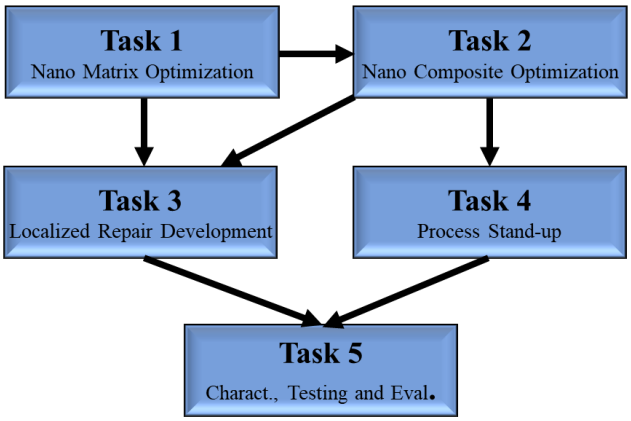

Figure 1 Project Flow Chart

3.1 TASK 1 Development and Optimization of nanostructured CoP matrix material

The main objective of this task was to further optimize the nCoP plating process to address some of the usability-issues identified at the conclusion of ESTCP project no. WP-0411. Factors include process compatibility with DC-rectifiers, and operation at lower bath temperatures (i.e. < 85°C). Additionally, as the intent of the coating is for repair and overhaul of steel and aluminum components, the process needs to be compatible with steel and aluminum with acceptable levels of adhesion.

An additional goal of this task was to better understand the corrosion behaviour of the nCoP material. Nano CoP forms a coherent cobalt oxide surface layer in corrosive environments, which has a yellowish-brown appearance. Even though the oxide is not detrimental to its performance, (i.e. no decrease in corrosion or wear performance) an improvement in aesthetics is desirable. The effect of various additives to the nCoP process on the corrosion behaviour of the alloy was also investigated in this Task.

3.1.1 Task 1A Beaker-scale development of nanostructured CoP matrix

i. nCoP Benchmark Chemistry DOE

Integran's existing nCoP chemistry (used to produce deposits as defined in MIL-DTL-32502) was used as the benchmark solution to conduct the initial optimization DOE. The preliminary DOE investigated the following conditions:

- Pulse conditions: Direct Current (DC), Pulse Plating (PP)
- Plating temperature: 65, 75, 85°C

ii. Effect of Organic Additives

The second DOE investigated the effect of various additives to the existing CoP chemistry; specifically the following two additives were investigated:

a. Nanovate™ B18: an organic, anionic surfactant
b. Nanovate™ A24: an organic, grain refining additive

For each additive, effect of the parameters listed in Table 1 on quality of the nCoP was studied.

Table 1 Operating conditions investigated in the second optimization DOE (additive investigation)

Parameter	Range/Operating conditions
Nanovate™ A24	Low, High
Nanovate™ B18	With, Without
Temperature (°C)	65, 75, 85
Pulsing conditions	DC, PP1, PP2

iii. Effect of Samarium (III) Sulphate Octahydrate

It has been reported in the academic literature that the addition of rare earth salts to nickel electroplating systems can significantly improve corrosion resistance [1]. Presence of rare earth elements have been found to result in a compact nanostructure due to their incorporation into the deposit during plating [1, 2]. Possibly, the compounds that form in solution may encourage the formation of a passive film that increases the material's corrosion resistance [1-3]. Lopez *et al* [1] specifically studied the effect of addition of Samarium (III) Sulphate Octahydrate into a nickel electroplating system and found its addition to be beneficial to the corrosion resistance. Therefore, Samarium salt additions to the nCoP plating solution was investigated was to improve corrosion properties of the deposit plated under various plating conditions.

iv. Effect of Phosphorus

The effect of phosphorus content on deposit quality and properties was also investigated. The main goals for investigating the effect of Nanovate^{TM} A59 on the deposit were:

a. to evaluate dependence of mechanical properties on wt% P over a relatively narrow range
b. to provide samples with varying wt% P content for corrosion evaluation

3.1.2 Task 1B Optimization and Development of nCoP matrix on Carbon-Steel substrates

Based on the results of Task 1A, an optimized nCoP plating chemistry was selected for scale-up to a 60L plating tank for further evaluation of the stability of plating chemistry and consistency in deposit quality.

In this task the optimized nCoP matrix was evaluated for specific application onto high and low carbon steels, following the basic procedures described in military specifications pertaining to nickel plating (MIL-STD-868A and AMS-QQ-N-290)

To evaluate the compatibility of the optimized nCoP chemistry with regards to plating on carbon steel substrate, a DOE was conducted that evaluated the effect of the operating parameters listed in Table 2 on deposit quality and properties.

Table 2 Parameters investigated in nCoP matrix optimization on carbon steel

Parameter	Range/Operating conditions
Temperature (°C)	65, 75, 85
Current density (mA/cm^2)	50, 80, 135
Pulsing conditions	DC, PP

3.1.3 Task 1C Optimization and Development of nCoP matrix on Aluminum substrates

The Nano CoP process was also optimized and evaluated for specific application to aluminum alloy 6061-T6. To evaluate the effect solution pH has on the nCoP deposit quality, an alternate nCoP plating chemistry was evaluated based on Integran's pure Nano Cobalt chemistry with phosphorous additions (referred to herein as R3311). The effectiveness of double zincate surface pre-treatment procedure i.e. was also evaluated. The compositional and mechanical properties of deposits were determined.

3.1.4 Task 1D Corrosion Testing: Potentiodynamic Polarization

Potentiodynamic polarization testing was performed by Corrdesa LLC to assist in the characterization of the corrosion performance of the nCoP deposits produced with varying phosphorus content (0 – 1.5 wt%P) from the two different plating solutions. Polarization tests were performed in order to capture the electrochemical behavior of electrodeposited Co-P compositions. Prior to performing the polarization test, the samples were immersed in the electrolyte for either 1hr or 3-4 days, during which time, the OCP was monitored. Electrochemical cell used for polarization testing is shown in Figure 2.

A potentiodynamic sweep at 0.5 mV/s was carried out on an area of $1cm^2$. The test conditions were as follows:

1. 3.5 wt% NaCl
2. naturally aerated bulk conditions
3. near neutral pH 6.5-7.5
4. temperature 25-27°C

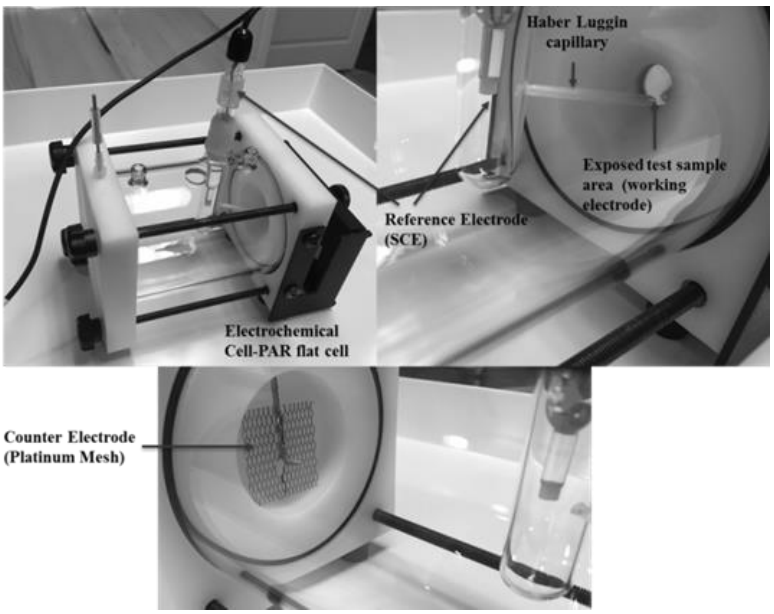

Figure 2 Electrochemical cell used for polarization testing.

The results were used to determine the effect that phosphorus concentration and particle deposit concentration has on corrosion behavior of the nCoP alloy, to help identify the optimal deposition composition. The results were also be used to carry out Computational Galvanic Corrosion Modeling (using corrosion Djinn software) to determine the optimal deposition composition for galvanic compatibility with different materials used in weapons platforms throughout the DoD.

Corrdesa also performed analysis via electroplating simulations of the electrolyte to the possible effects of solution flow on evaluate plating efficiency, throwing power, and plating uniformity.

Successful completion of the polarization tests will help establish a suitable processing 'window' for deposition. Emphasis will also be placed on modelling a suitable plating set-up to maximize the plating rate for the process to minimize the time required for heavy build repairs.

3.2 TASK 2 Development of Nanostructured Cobalt Composite Coatings

The optimized nCoP chemistry developed in Task 1A was utilized throughout all the nanocomposite coating trials performed Task 2. The objective of this Task was to successfully co-deposit second phase particles within the optimized nCoP matrix thereby producing a composite nCoP coating with enhanced mechanical performance.

3.2.1 Task 2A Co-deposition of second phase particles from suspension baths

In this task, detailed DOEs were carried out to determine suitable levels of solution particle concentration, particle size (nanoparticles, microparticles), particle type, particle combinations, additives that may optimize particle co-deposition. The particle type, concentrations and size investigated in the various DOEs are listed in Table 3 Particle types, concentrations and sizes investigated in Task 2A. Both standard and the newly optimized nCoP process conditions were used for depositing the nanocomposite coatings.

Table 3 Particle types, concentrations and sizes investigated in Task 2A

Particle type	Particle Size (nm)
Chrome carbide, Cr_3C_2	800 - 1300
Silicon carbide, SiC	40, 500, 1000
Alumina, Al_2O_3	800
Diamond	700

Furthermore, the effect of various additives on particle co-deposition was also investigated:

1. *Nanovate^{TM} A59*

The effect of P in-solution concentration on particle co-deposition was studied. Previous experimentations have led to the understanding that P solution doping levels can influence the co-deposition of other bath constituents (see Task 1A, subsection *iv*). Three P levels were investigated:

- Low P (~0 - 0.5 wt% P in deposit)
- Medium P (~0.5 -1 wt% P in deposit)
- High P (~1 - 1.5 wt% P in deposit)

2. *Nanovate^{TM} B19 (cationic surfactant)*

Literature notes that the use of a cationic surfactant enhances the co-deposition of ceramic particles [4, 5].

Three surfactant concentrations were investigated on particle systems found to be successful in previous efforts. Table 4 shows the concentration and the standard operating conditions. For select chemistries, deposits were plated using the successful alternative plating conditions identified in Task 1A (i.e. 75°C and 80mA/cm^2).

Table 4 Operating parameters used for depositing nCoP composite coatings with the cationic surfactant additions

Parameter	Range/Operating conditions
Surfactant concentration	low, med, high
Temperature (°C)	75, 85
Current density (mA/cm^2)	80, 135
Pulsing conditions	DC

Throughout the development of nCoP-particle system, successful deposits underwent in-depth characterization and analysis.

3.2.2 Task 2B Cirrus Dopant Evaluation in nCoP Solution

The efforts made in this task included the identification and development of a "dopant" additive to achieve the necessary conditions for formation of nano-particles in a stable suspension in the target electrolyte. The desired outcome was the formation of nano-particles that are of a characteristic (size, charge, structure) that allows them to be co-deposited uniformly throughout the coating matrix, thus reinforcing and strengthening the coating[6,7,8]. In this task, Cirrus applied their technology to:

i. appraise the target electrolyte,
ii. tailor a dopant for that electrolyte, and
iii. confirm the desired reinforcement and strengthening has been achieved.

This includes the following subtasks:

a. nCoP Process Stand-up at Cirrus:
b. Evaluate Dopant Compatibility with nCoP Chemistry
c. Determine Preferred Doping Levels
d. Confirm Coating Performance
e. Determine Bath Management Parameters
f. Support Import of Dopant in Experimental Quantities

In support of Cirrus's efforts, Integran provided 40L of baseline nCoP plating solution developed in Task 1A and accompanying Technical Data Sheet. Monthly update meetings were held to ensure synergistic development of the nCoP-particle systems.

Appendix B contains a detailed report on progress made at Cirrus Materials Science regarding the Dopant-nCoP development work.

3.3 TASK 3 Brush Plating for repair systems

Brush-plating is a technique which makes it possible to deposit metal over a localized area

without the need for part immersion, giving it a decided advantage for selective repair.

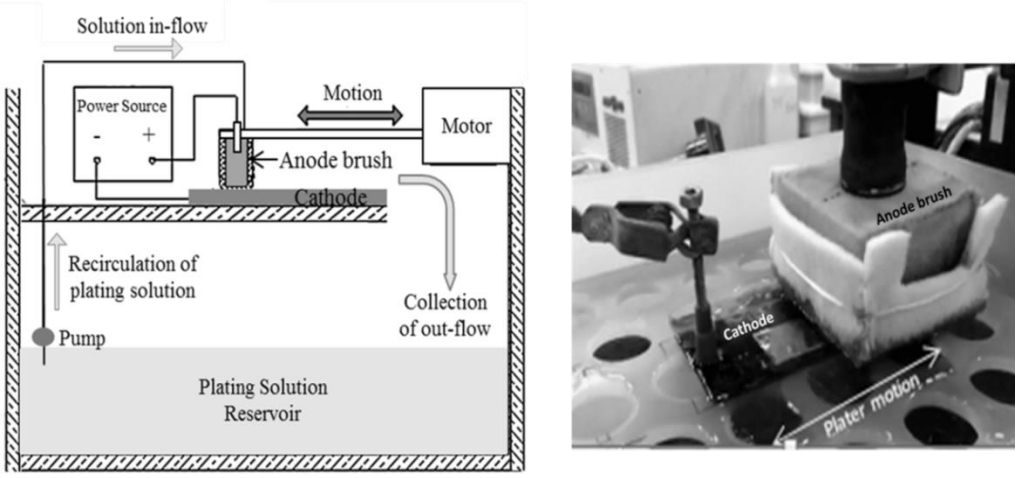

Figure 3 Schematic and picture demonstrating brush plating mechanism.

For this task, the optimized coating systems from Tasks 1 and 2 were used to develop a specialized repair method using brush plating. Figure 3 shows the standard brush plating set-up/mechanism. Work performed in this task involved the investigation of suitable brush plating equipment through the execution of detailed DOEs to study process variables including:

i. Particulate concentration,
ii. Solution replenishment i.e. flow rate.
iii. Brush motion (speed, distance)
iv. Absorbent material type.
v. Operating parameters (temperature / current density)

Brush plated nCoP coatings were applied to carbon steel coupons and underwent in-depth characterization and property analysis, including:

1. Deposit Quality Visual – Visual assessment of lustre and uniformity of the deposit
2. Composition - X-ray Fluorescence Spectroscopy (XRF/ Energy Dispersive X-Ray Spectroscopy (EDS)
3. Crystal Structure & Grain size – X-Ray Diffraction (on select samples)
4. Microhardness - Vicker's Microhardness tested following ASTM B578
5. Abrasive wear including Taber Wear (mg/1000 cycles using C-17 wheels), Pin on Disk (coefficient of friction, and sliding wear),
6. Grain structure (XRD),
7. Composition (SEM/EDS),

3.4 TASK 4 Final Process Stand-up

The final optimized plating systems that were down-selected from the previous tasks were scaled-up at Integran to a 60L plating tank for final demonstration/validation testing. The processes that were selected for evaluation include:

1. Baseline CoP: used to plate at standard and alternative conditions
2. CoP-Particle System: (CoP-Diamond and CoP-SiC-Diamond)
3. CoP-Cirrus Dopant Systems: CoP- Titania and CoP-Alumina

A short DOE was conducted to determine/confirm the optimal windows of operation for the scaled-up process for each system, as compared to the earlier beaker trials. For example, following the transfer of dopant technology, the first task at Integran was to replicate the nCoP-dopant process developed by Cirrus. This was necessary to:

i) Determine the reproducibility of the deposit properties achieved at the beaker scale.
ii) Determine process stability and bath-life on a pilot-scale

Following sufficient optimization and confirmation of process repeatability, test coupons were fabricated for property and performance testing in Task 5.

3.5 TASK 5 Coating characterization, testing and evaluation

The core demonstration/validation tests that were performed as part of this task for the development and optimization of the coating included:

- Deposit characterization: composition, microstructure, surface finish
- Mechanical testing: microhardness, coating ductility
- Wear testing: pin-on-disk, Taber wear
- Corrosion testing: salt spray cabinet, galvanic compatibility
- Hydrogen embrittlement testing: sustained load testing on notched bars

Tests were conducted in a manner that prevented duplication and maximize use of each test specimen. For example, where possible, more than one test was performed on each specimen. The number and type of tests that could be run on any one specimen was determined by the destructiveness of the test. Table 5 shows the list of tests, ASTM standard followed for qualification.

Table 5 List of Engineering requirements and testing standards

	Engineering Requirement	Qualification Test	Reference ASTM standard	Evaluation Description
1	Appearance	Visual	N/A	Standard visual (x1) inspection will be carried out for surface uniformity on all samples produced for the various coating systems.
2	Thickness	Cross-section	ASTM E3, ASTM B487 ASTM E1621	Thickness was assessed via two methods: on mass add-basis and on cross-sectioned deposits as per ASTM E3 and ASTM B487 for thickness of electroplated layers. The key motivation to assess thickness is to determine plating efficiency.
3	Composition	Cross-section		Composition of the deposits was assessed on 2 samples per coating type, following method defined in ASTM E1621 and via SEM/EDS analysis.
4	Micro-hardness	Vickers Hardness	ASTM E92	Microhardness was evaluated on two samples per coating type (minimum thickness of 100µm).
5	Grain structure	XRD	ASTM B930	Determine grain structure – size and texture and whether addition of dopants or particle influences it.
6	Corrosion	Salt Spray	ASTM B117	Time to red rust, carried out on 50um and 100um thick coatings to determine effect of thickness on corrosion protection. Substrates inspected at cycles of 24, 48, 72, 100, 200, 400, 600, 800, and 1000 h.
		LPR (+ OCP)		To determine recommended phosphorus content for optimum corrosion resistance and impact of particles and dopant. Polarization data acquisition was done according to NAVAIR protocol for galvanic corrosion.
		Galvanic Compatibility		Determine galvanic compatibility of CoP material with typical aerospace materials including 4130 steel and Al 7075.
7	Hydrogen Embrittlement	ASTM F519	ASTM F519	Determine hydrogen embrittlement of CoP materials.
8	Wear	Taber Wear	ASTM D4060	Taber wear test, comparing results with the ones achieved on a beaker scale and EHC.
		PoD	ASTM G99	To determine coefficient of friction and sliding wear rate.

4. RESULTS AND DISCUSSION

4.1 TASK 1 Nanostructured CoP Development

The continued optimization of the nCoP matrix began in October 2016. The efforts in this task were aimed at addressing the following project objective:

- Optimize a nanocrystalline cobalt-phosphorus electrodeposition process for repair operations that is based on conventional DC rectifiers in order to reduce infrastructure costs associated with pulse plating.

4.1.1 Task 1A Beaker-scale development of nanostructured CoP matrix

Task 1A was further divided into sub-tasks in order to systematically carry out beaker scale development of nCoP matrix plating chemistry and operating conditions: (i) nCoP benchmark, (ii) investigation of Nanovate™ B18 (anionic surfactant), (iii) Nanovate™ A24 (organic additive), (iv) rare earth element (samarium (III) – based salt), and (v) Nanovate™ A59 (source of phosphorous). An example beaker setup is shown in Figure 4.

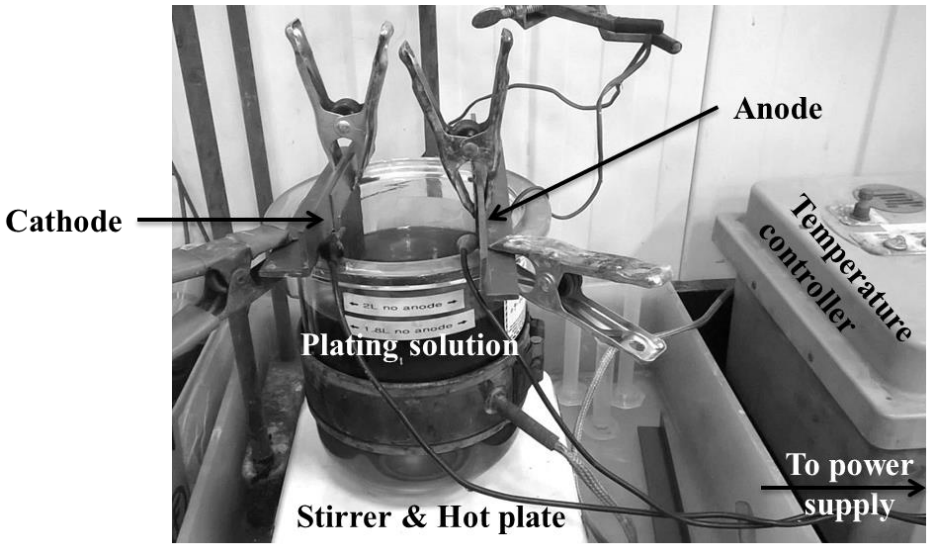

Figure 4 Beaker setup used in nCoP-matrix development work.

i. nCoP Benchmark Chemistry DOE

The first DOE established a benchmark based on Integran's nCoP (R3010) plating chemistry and operating conditions. This allowed for a standardized assessment of deposits achieved via future DOEs. Figure 5 shows the hardness of nCoP coatings deposited at various pulse conditions and temperatures.

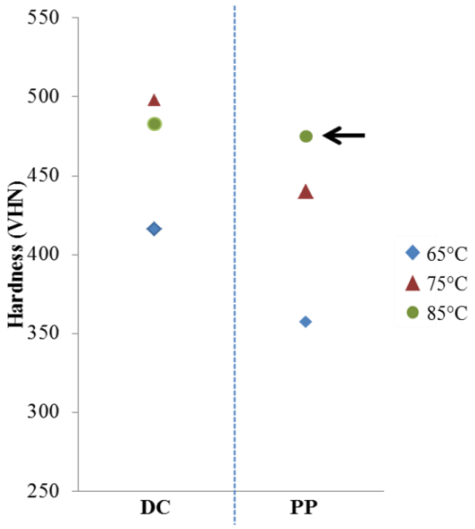

Figure 5 Effect of electrical parameters and plating temperature on hardness

As reflected in the figure above, the hardness of the deposit, when plated under normal conditions was lower than expected. The standard tank plated Nanovate R3010, plated at 85°C and 135mA/cm^2, has a hardness of 500 - 600 VHN, while in this benchmark hardness is only 473VHN. This is believed to be the result of a lower Phosphorus (P) content in the deposit due to the limitations of plating on a small scale (2L beaker) as listed below:

- insufficient plating solution flow: adequate agitation is essential to maintaining a consistent concentration of plating ingredients in order to replenish ions at the cathodic surface,
- temperature gradients within the beaker,
- pronounced current density effects.

In general, it is well known that solution flow can influence the co-deposition of elements in alloy plating systems, as is believed to be the case with with co-deposited Phosphorus with cobalt. It has been observed that limited flow in beaker plating results in lower P levels (between 0.4 - 0.6 wt% P) in the deposit and therefore lower hardness. An X-Ray Diffraction Pattern indicating a nanocrystalline grain structure as seen in Figure 6 which confirms a similar microstructure between beaker and tank plated material. While the beaker scale experiments do not fully replicate the tank scale results, the general trends are believed to be consistent and thus the beaker scale studies are useful for developing quick understanding of the critical variables prior to scaling to larger tanks.

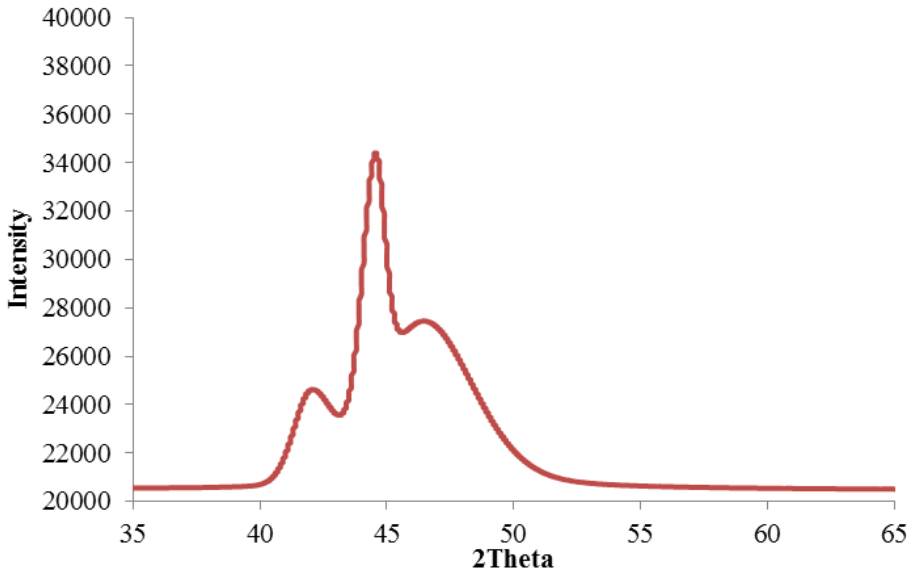

Figure 6 XRD patterns of benchmark nCoP

In effort to study the effect of multiple variables on deposit properties, studies at a beaker level were continued to develop trends pertaining influence of additives and plating conditions on the deposit properties. For the initial set of DOEs carried out in Task 1A, subtasks ii-iv on a beaker scale, the lower hardness was accepted as the benchmark; however a detailed assessment of the influence of P concentration in the deposit on the hardness was investigated, and is reported later in section *iv*. Recognizing the scaling effects, an additional DOE/ trials were carried at the beginning of the Tank scale-up trials to confirm the trends and results determined at the beaker scale were still relevant.

ii. Effect of organic additives

Organic additives can be used to influence deposit properties in conventional electroplating processes. In this DOE, two proprietary additives were investigated: anionic surfactant Nanovate™ B18 and Nanovate™ A24. Both have been used with Integran's other Nanovate™ alloys.

a. Effect organic additives: Nanovate™ B18

The effect of an addition of anionic surfactant (Nanovate™ B18) on deposit quality and properties was investigated over a range of pulse conditions and temperatures. The resulting hardness and deposit quality are shown in Figure 7.

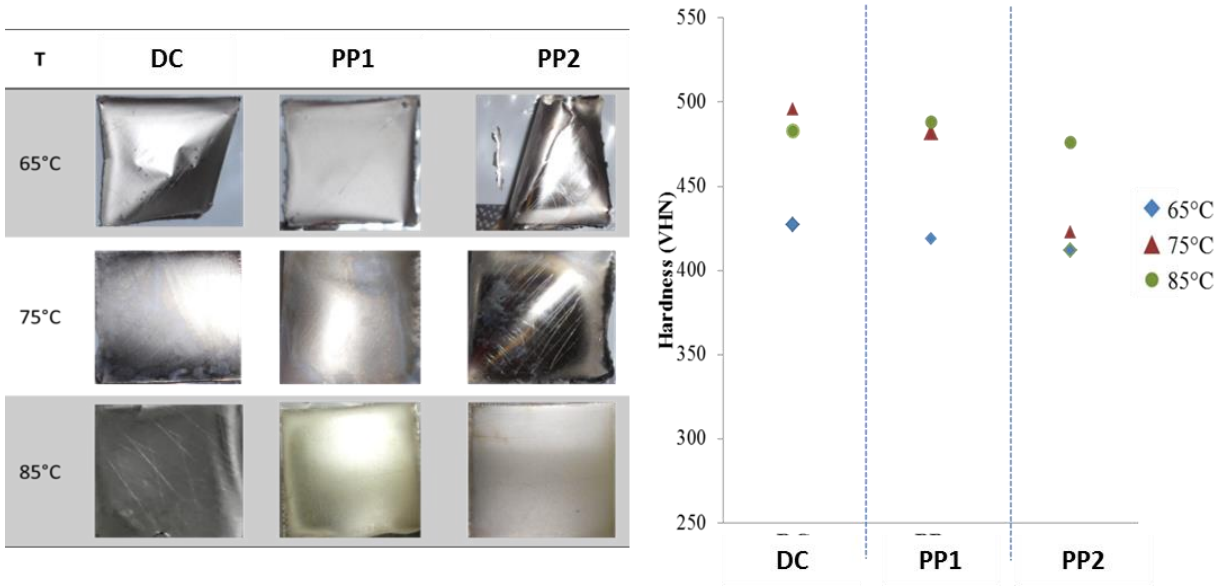

Figure 7 Effect of electrical parameters and plating temperature on hardness (L) and quality/uniformity of the corresponding deposits (R)

As noted in the benchmarking trials, the deposits contained low amounts of phosphorus (≤0.5wt% P). However, under the assumption that the low hardness is due to low wt% P for all plating conditions tested, the deposit quality in terms of aesthetics and hardness was relatively comparable for 75°C and 85°C under DC and PP plating conditions. This finding was in-line with the first project objective of developing a nanocrystalline cobalt-phosphorus electrodeposition process for repair operations that is based on conventional DC rectifiers.

In order to validate these positive results, it was essential to scale-up the nCoP – Nanovate™ B18 chemistry and repeat this DOE. In support of this effort, a 60L tank was set up. The repetition of this DOE at a larger scale would eliminate uncertainty related to solution flow – P's deposition. The outcome of this DOE is discussed in detail in Task 1B.

b. Effect organic additives: Nanovate™ A24

The effect of an addition of an organic additive (Nanovate™ A24) on ability to achieve a nanostructure by plating under DC conditions was also investigated. Deposits were produced under various plating temperatures and pulse conditions. Figure 8 shows the resulting hardness and x-ray diffraction patterns of the samples produced in the DOE. No positive change in mechanical properties was noted with Nanovate™ A24 additions, in fact the hardness was found to decrease for most conditions. A significant change in the crystallographic texture was observed, as shown by the XRD patterns. Since there was no benefit observed with the addition of Nanovate™ A24 under any plating condition, no further investigation with this additive were conducted.

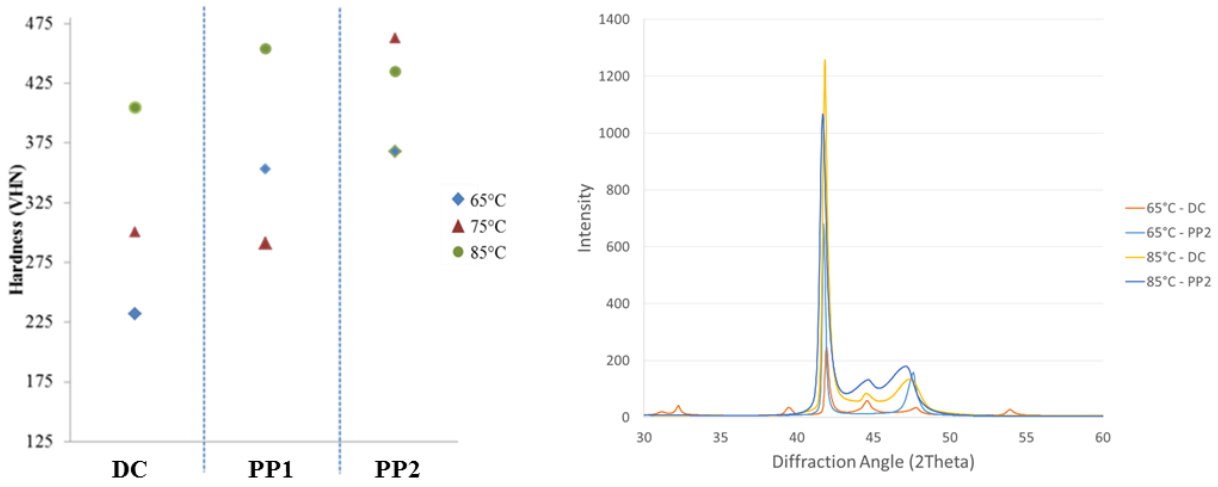

Figure 8 Effect of electrical parameters and plating temperature on hardness and the corresponding XRD pattern.

iii. Effect of Samarium (III) Sulphate Octahydrate, $Sm_2(SO_4)_3 \cdot 8H_2O$

As noted in the technical approach section (Section III), the addition of Samarium Sulphate Octahydrate into a nickel electroplating system was found to be beneficial to the corrosion resistance. Our findings indicate that, deposition of Sm was noted to be highly dependent on flow and temperature, where higher flow, lower T resulted in higher co-deposition.

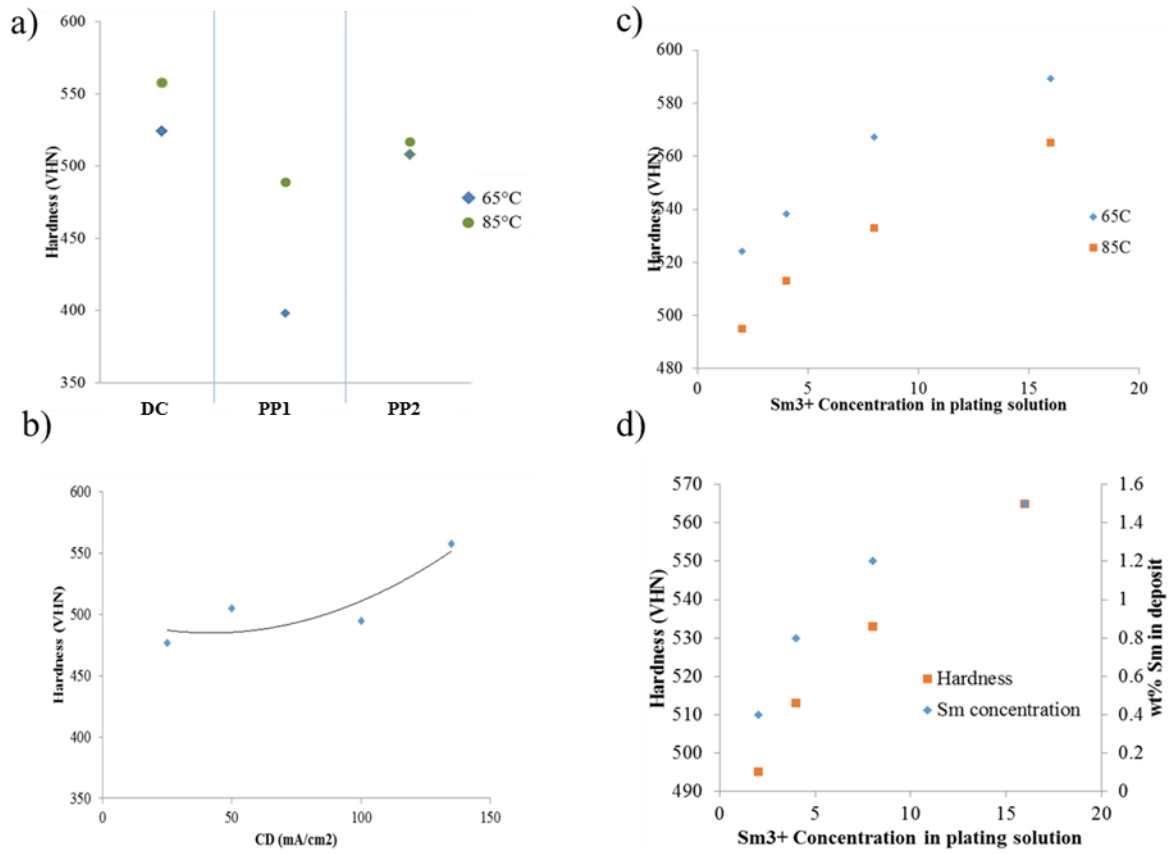

Figure 9 Effect on hardness given: a)various electrical parameters; b) plating current densities (mA/cm^2) @ 85°C plating T; c) Sm^{3+} concentration in solution (g/L) & plating T (°C); and d) Sm concentration in solution (g/L) and deposit (wt%) @ 85°C plating T, 100mA/cm^2.

As seen in Figure 9, with a minor addition of 2 g/L Samarium salt to the nCoP solution, an improvement in hardness was achieved at 65°C and DC conditions. Hardness was also found to increase with increasing current density and Sm salt concentrations, likely due to higher co-deposition of Sm at those conditions. This was considered as a positive result as it indicated promised towards addressing the first project objective.

It was also observed that the microhardness varied significantly (±60 VHN) within a given deposit. This could be due to poor distribution of Sm throughout the deposit which could have arisen from either poor distribution of Sm in the plating solution and/or inadequate agitation during plating.

As there is limited control over agitation at a beaker level, a surfactant (Nanovate^{TM} B18) and

phosphorous (in the form of Nanovate™ A59) were added to the plating solution in effort to promote distribution. At a fixed operating conditions and Sm^{3+} concentration the addition of the surfactant resulted in ~12% increase in hardness (from 495 VHN to 554 VHN) and the addition of A59 resulted in ~15% increase in hardness (from 495 VHN to 570 VHN).

This increase in hardness can be attributed to the following:

- higher co-deposited amounts of samarium (SEM/EDX results indicated an increase from 0.4 wt%Sm to 1.0 wt%Sm),
- higher co-deposited amounts of phosphorus (SEM/EDX results indicated an increase from 0.5 wt%P to 0.8 wt% P),
- improved distribution of samarium in nCoP matrix (low variability in hardness and wt%Sm from SEM/EDX results indicated uniform distribution of Sm in the deposit).

In order to assess corrosion behavior, salt spray corrosion testing was conducted for a total of 1000hrs. The test followed ASTM B117-16: Standard Practice for Operating Salt Spray (Fog) Apparatus, and was conducted on benchmark 100µm nCoP and 100µm nCoP-Samarium coating systems. The progression of corrosion was observed at 24h, 48h, 72h, 96h, 200h, 500h and 1000h intervals and revealed that all deposits performed exceptionally well in the test with no signs of red rust up to 1000hrs. The test also revealed that the addition of Samarium (III) Sulphate did not significantly affect the formation of the cobalt oxide tarnish compared to the standard nCoP deposit. Interestingly, these deposits did show some level of hydrophobicity where nCoP-Samarium deposits measured a contact angle of 108° (Wenzel and Cassie-Baxter state) as compared to the standard nCoP deposits which measured contact angle of 84° (Wenzel and Cassie-Baxter state). However, the added hydrophobicity did not appear to have a significant benefit with regards to the tarnish resistance of nCoP.

iv. Effect of Nanovate™ A59 (Source of Phosphorus)

The goal of this subtask was to determine the relationship between the content of Phosphorus in the deposit with the mechanical properties of the deposit over a relatively narrow concentration range. This would allow deposits to be produced with the same properties and performance as the tank plated nCoP (Nanovate™ R3010), thereby compensating for flow related-P deposition limitations at a beaker scale. The hardness and X-ray diffraction results at the various phosphorus levels are shown in Figure 10.

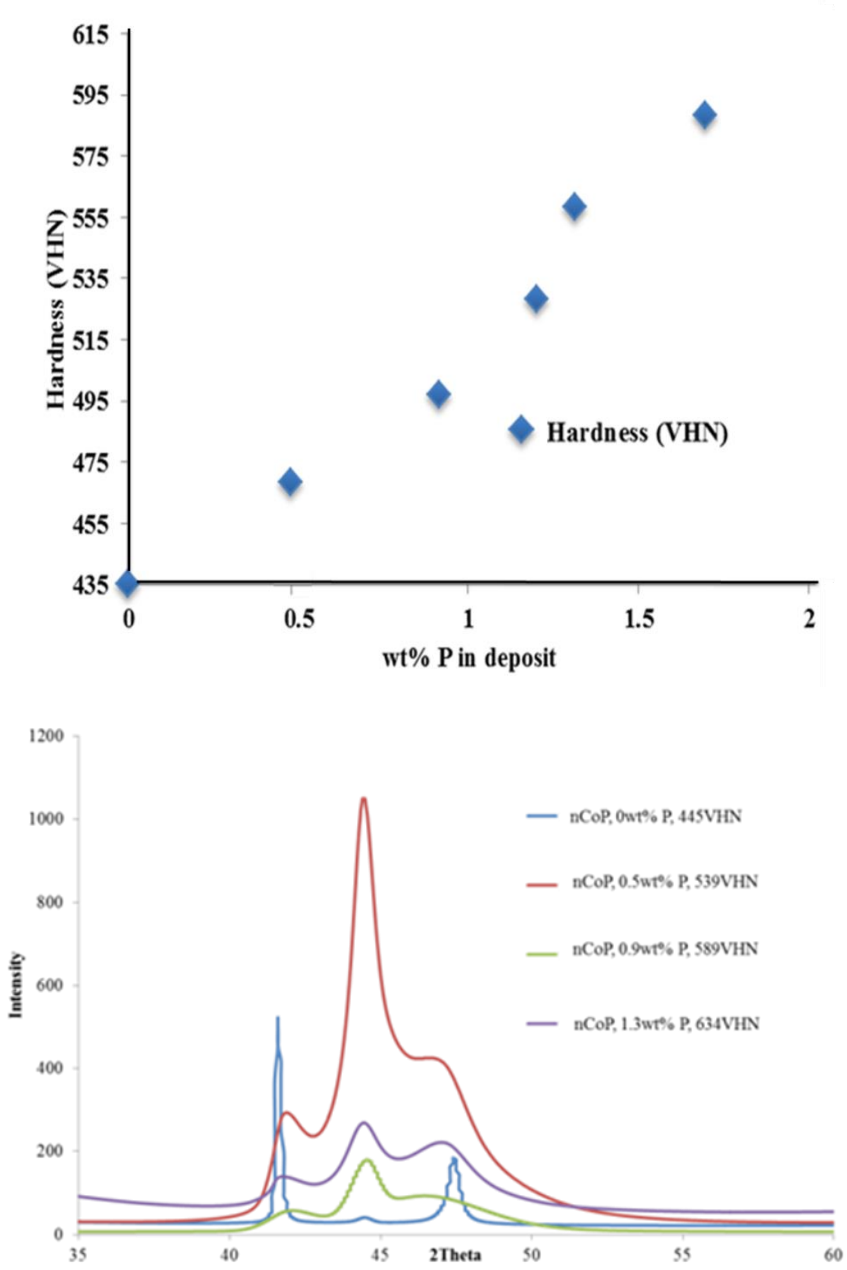

Figure 10 Effect of scaling P in electrolyte on hardness, co-deposited P in deposit and grain structure

The phosphorus content in deposit was measured using SEM/EDX. As seen in Figure 10, the hardness in the deposit is strongly dependant on the wt% P in the deposit. Based on these results, the beaker plating chemistry required to obtain a deposit content between 1 to 2wt%P was established. The subtask goal of obtaining a beaker-suitable plating solution was achieved and the level of phosphorous in the solution for beaker plating was established for all future beaker-scale experimentations. These findings were also shared with Cirrus Materials Science, as they were in the process of optimizing dopant-nCoP systems (See Task 2B) at a beaker scale.

4.1.2 Task 1B Optimization and Development of nCoP matrix on Carbon Steel

This task was carried out in the 60L tank shown in Figure 11 using the plating chemistry down-selected in Task 1A-ii.

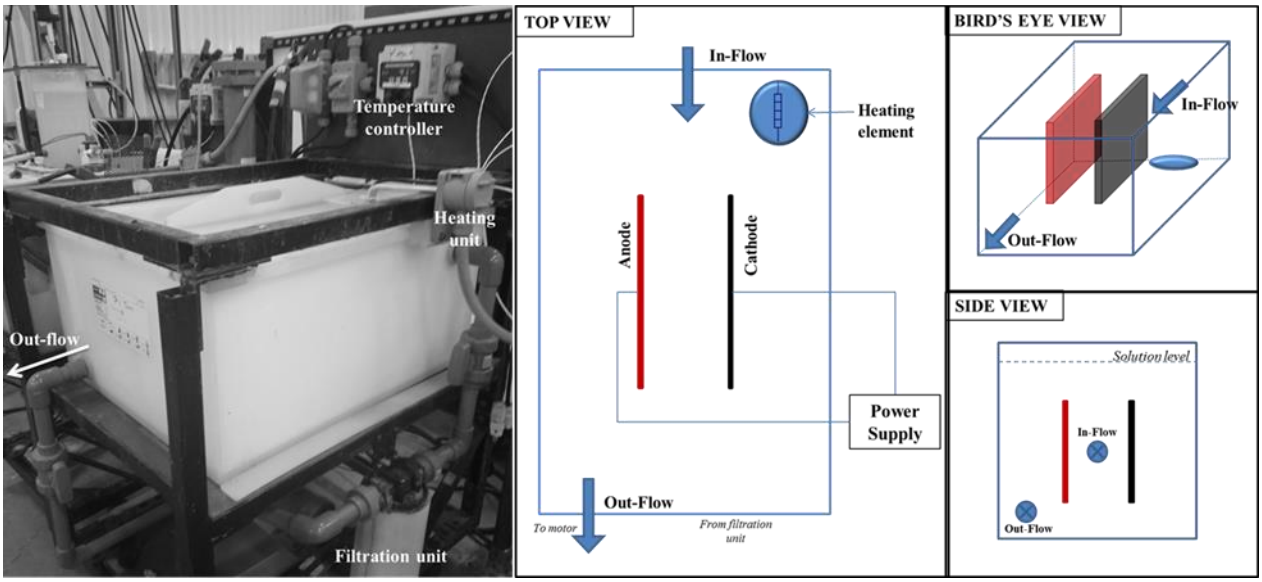

Figure 11 Photograph and schematic showing one of the two tanks setup at Integran

The DOE investigated in Task 1A, subtask *ii* was repeated on carbon-steel substrates for validation of the new optimized plating chemistry and comparison of properties and performance with Integran's original nCoP process (R3010). The use of pump-agitated 60L tank for the production of samples in this sub-task addressed the scaling-related concerns observed earlier in the project. Optimization and plating on carbon-steel substrate also permitted coating of Taber wear panels for abrasive wear testing as well as hydrogen embrittlement bars for hydrogen embrittlement testing. The results of the optimization DOE are shown in Figure 12.

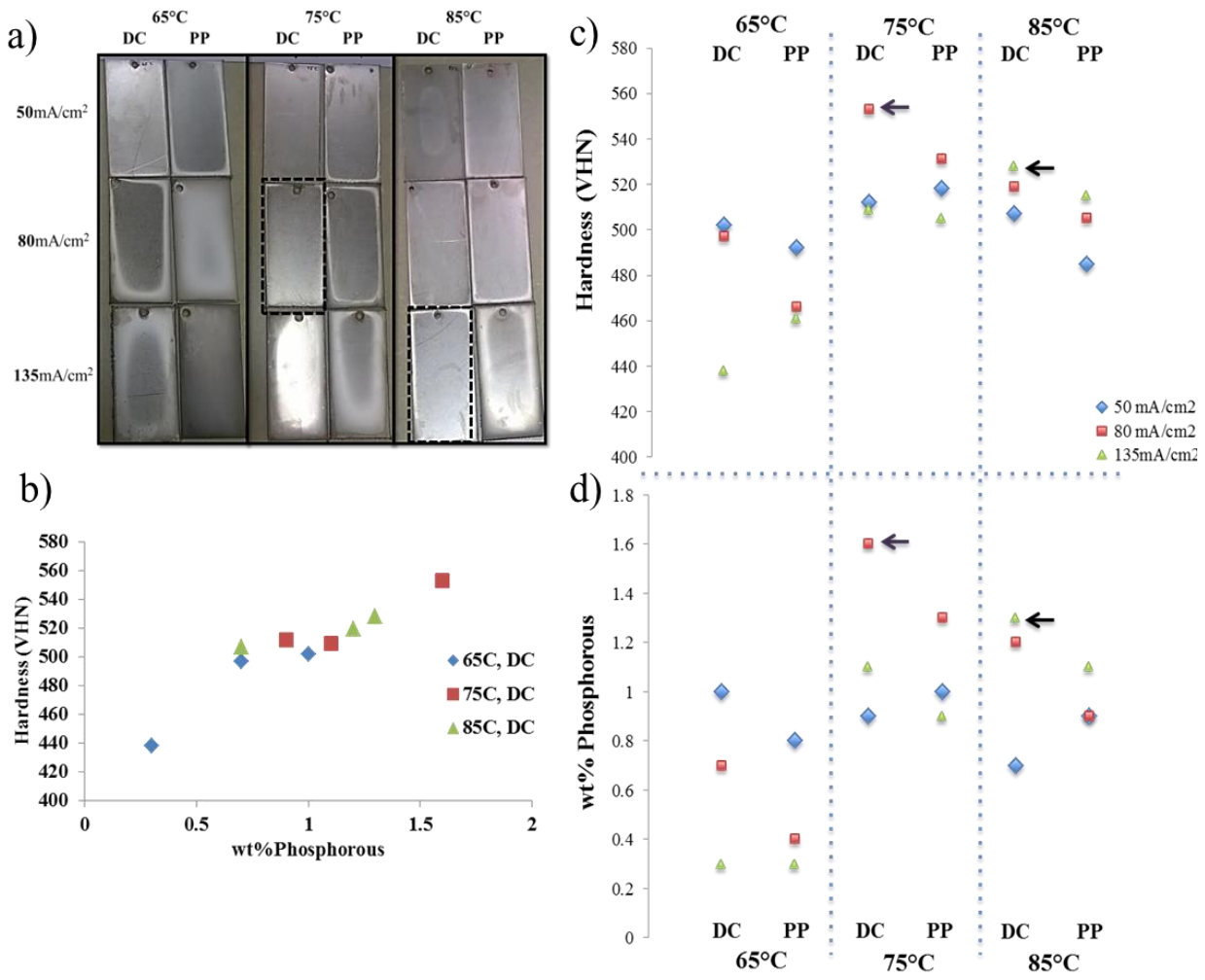

Figure 12 Optimization DOE results: a) deposits obtained, b) graph indicating hardness *wrt* wt% P in deposit, and c) hardness and d) wt% phosphorus as a function of electrical conditions (current density, pulsing parameters) and plating temperature

For satisfactory adhesion between nCoP coatings and mild steel substrates, an alkaline cleansing pre-treatment step followed by 30% HCl activation of substrate process yielded satisfactory results.

The results demonstrated that the optimized plating chemistry was able to produce equivalent electrodeposits under DC conditions compared to the standard pulse plating process, thereby achieving the first project objective i.e. nanostructured cobalt phosphorus coating that can be plated using DC rectifiers.

In addition, this plating chemistry is also suitable for plating at lower CD (80 mA/cm^2) and lower operating temperatures (75°C), thereby achieving the project's secondary goal. These findings are deemed advantageous as the lower CD and lower operating temperature make this chemistry more production-viable (operator-friendly) and compatible with masking-wax used during part processing. Furthermore, it is also suitable for plating on geometrically complex parts as well as polymers.

For qualification purposes, further characterization of deposits plated under these alternative operating conditions was carried also out. Table 6 provides a summary of various measured properties for nCoP deposited using the two sets of conditions.

Table 6 Mechanical properties of standard and alternative plating conditions

Plating conditions	wt% P in deposit	Hardness (VHN)	Taber Wear Index (TWI)	Pin on Disk (Al_2O_3 pin)	
				Average Coefficient of friction (μ)	Sliding wear rate* (10E-6 mm^3/Nm)
75°C, 80 mA/cm^2, DC	**1.3**	553	18.47	0.63	13.68
85°C, 135 mA/cm^2, DC	**1.1**	528	18.32	0.58	12.41

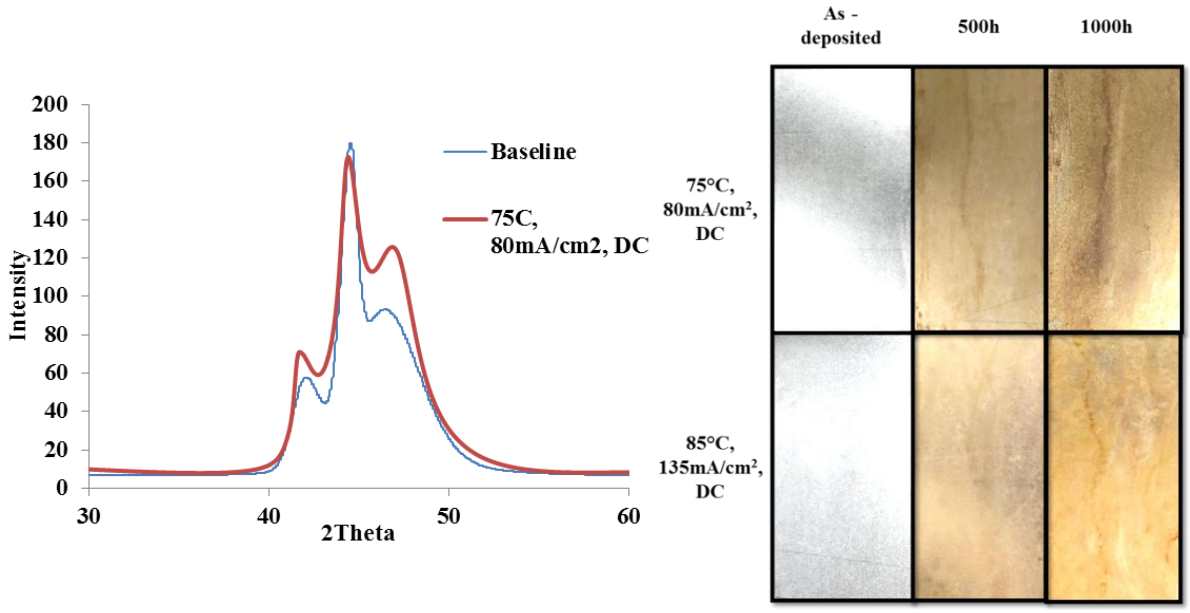

Figure 13 XRD pattern (L) and Salt Spray corrosion panels (R) of nCoP plated under standard conditions (85°C, 135 mA/cm^2, DC) and alternative conditions (75°C, 80 mA/cm^2, DC)

Hydrogen Embrittlement bars following ASTM B519 were plated using the standard and alternative conditions. Figure 13 compares the XRD pattern and salt spray corrosion behaviour of the deposits produced at the standard conditions and alternative conditions.

For validation purposes and in order to assess electrolyte stability, chemical analysis and monitoring of Co and P element, pH, surface tension was carried out. Chemical analysis was performed using Inductively Coupled plasma (ICP) spectrometry. Additionally, stability of deposit quality was assessed via the production of coatings (monitoring runs), produced under the same conditions on a monthly-basis. Coating quality was assessed via visual analysis and microhardness measurements. The process was found to be stable and the operation ranges were established.

4.1.3 Task 1C Optimization and Development of nCoP matrix on Steel and Aluminum

4.1.3.1 Steel

A 1/8" thick 4140 steel plate was coated with 100µm CoP and subjected to a bend test as per ASTM B571. No delamination was noted in between the CoP coating and 4140 substrate (see Figure 14). Due to high strength of the coating and substrate the bend test was carried out manually, Instron tester could not be used due to force/load limitations.

4.1.3.2 Aluminum

Aluminum is an attractive structural material due to its low density; however the weight advantages come at the cost of strength. This gap can possibly be addressed by the use of a thin, high strength structural nanometal coating without a significant increase in weight. Therefore, there is significant interest to investigate the ability to coat onto Nano CoP coatings onto aluminum substrates and assess the added value proposition in terms of mechanical properties.

The adhesion between aluminum and nCoP coating is also important. Given the nature of the surface of aluminum (i.e. proclivity to form a protective oxide), the aluminum underwent a double zincate activation process followed by a copper strike. Full copper encapsulation was required, since any exposed aluminum could potentially lead to corrosion of the aluminum by the acidic nCoP plating solution. Due to the susceptibility of aluminum to corrode in the low pH nCoP solution, an alternate nCoP plating solution with a higher pH was investigated (i.e. to prevent attack of the underlying aluminum and compromise adhesion between aluminum substrate and nanometal coating). The higher pH nCoP process was based on a modification Integran's pure Cobalt process (R3310). Plating trials were firstly performed at the beaker scale and later scaled-up to a 45L tank

This alternative chemistry was successful in achieving nanocrystalline cobalt phosphorus deposits (referred to as R3311), and it operates at a lower temperature of 65°C and displayed excellent compatibility with aluminum. The structural benefit of coating aluminum with Integran's nanometal in terms of enhanced strength was assessed in three-point bend testing of 15.24cm x 2.54cm x 3mm Aluminum test bars coated with 50µm of nCoP (Figure 14, 15).

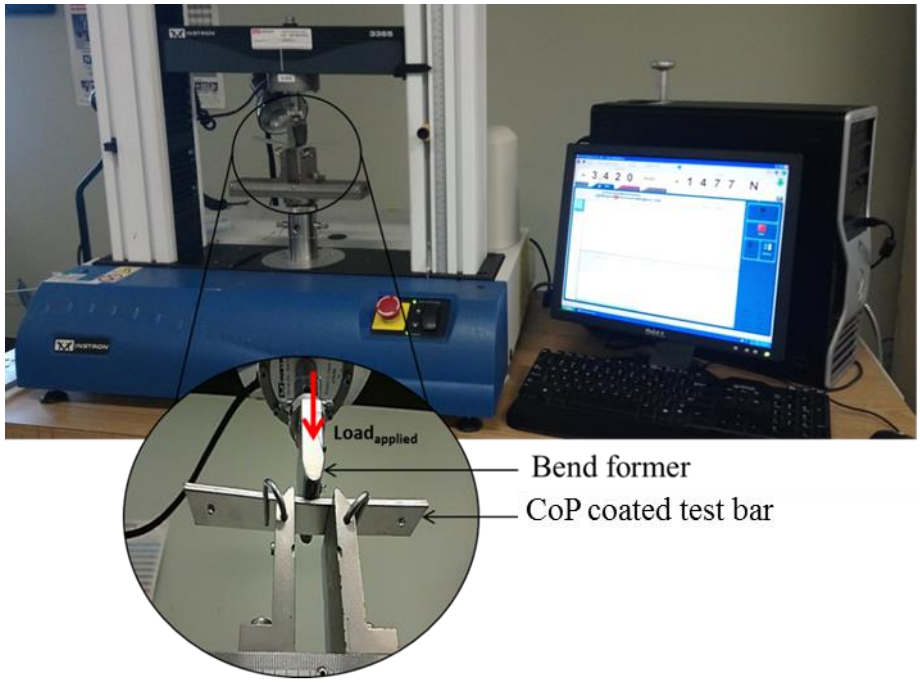

Figure 14 Bend-adhesion test setup for aluminum (Instron 3365)

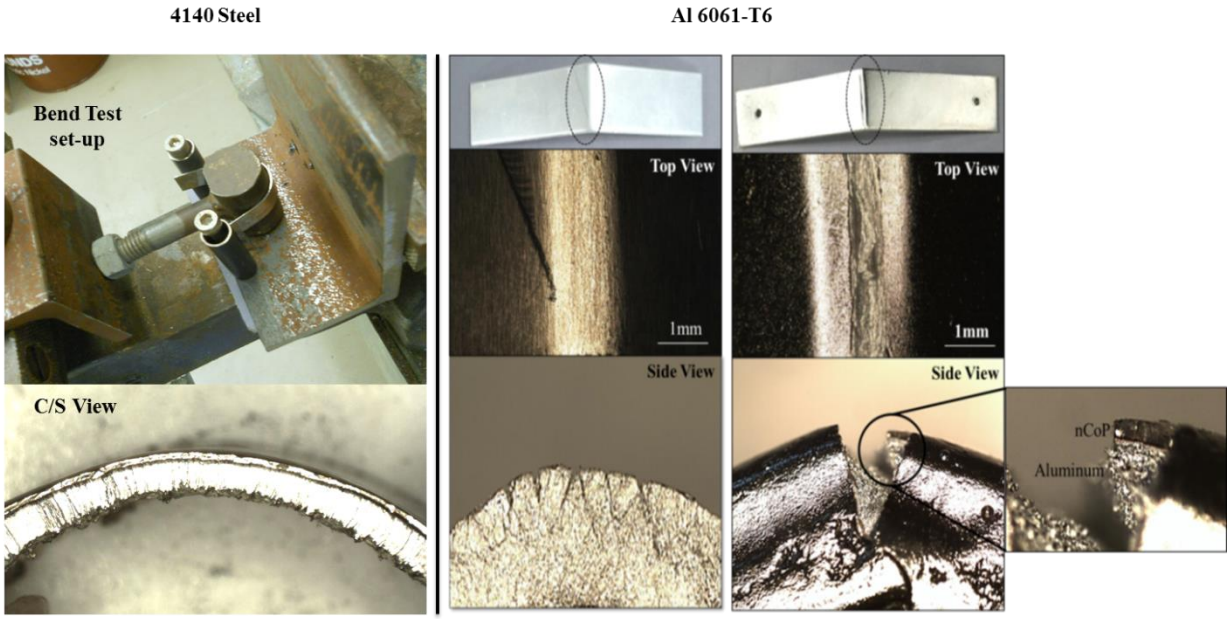

Figure 15 L – Figure showing bend test used on CoP coated 4140 steel and the cross-section showing no delamination between coating and substrate. Note how the coating deforms with the steel. R - Figure showing the cracked fracture surface post bend-adhesion test of bare Al 6061-T6 and nanometal on Al 6061-T6. NOTE: maintained adhesion between nanometal and Al substrate

Figure 16 shows the flexural stress-strain curve and the corresponding hardness graph of a bare aluminum bar compared to the same bar coated with 50µm Nanovate™ coating. A significant increase in flexural strength and stiffness as well as hardness was observed.

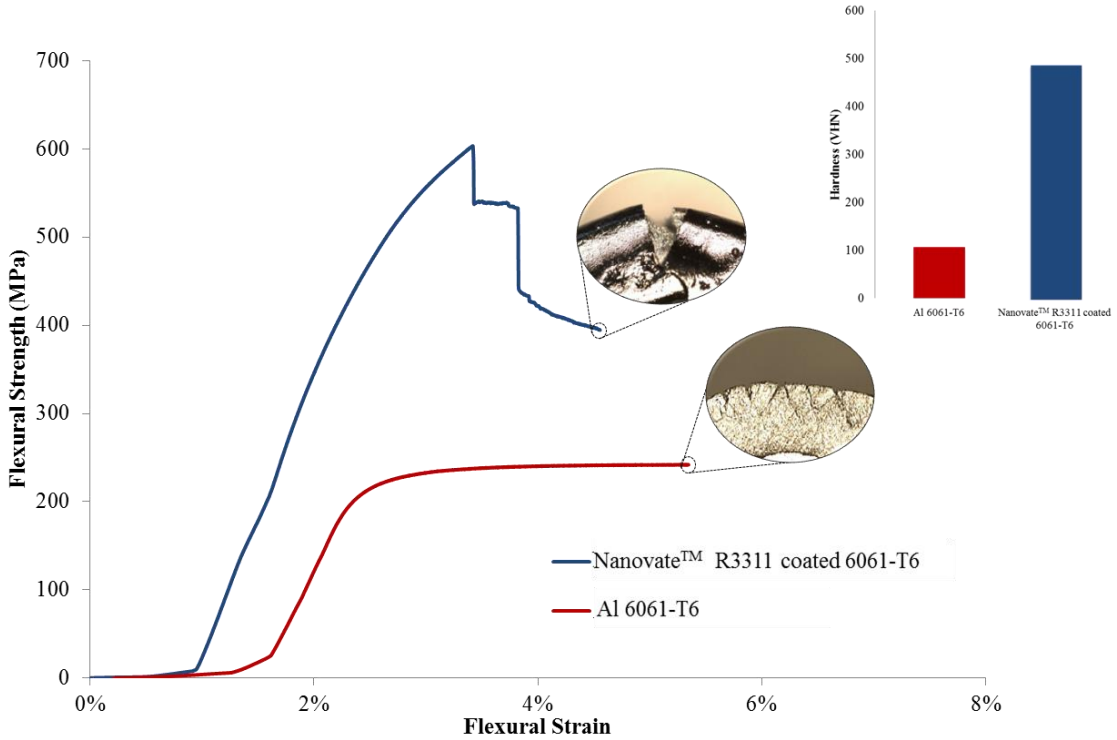

Figure 16 Flexural stress-strain curve and corresponding hardness graph demonstrating the added advantage of 50µm Nanovate™ R3311 coating. Test sample: 15.24cm x 2.54cm x 3mm Aluminum test bars coated with 50µm of nCoP

To further the understanding of the R3311 process and to compare it with the newly established DC-compatible nCoP process, the hardness with respect to phosphorus content was also determined (Figure 17).

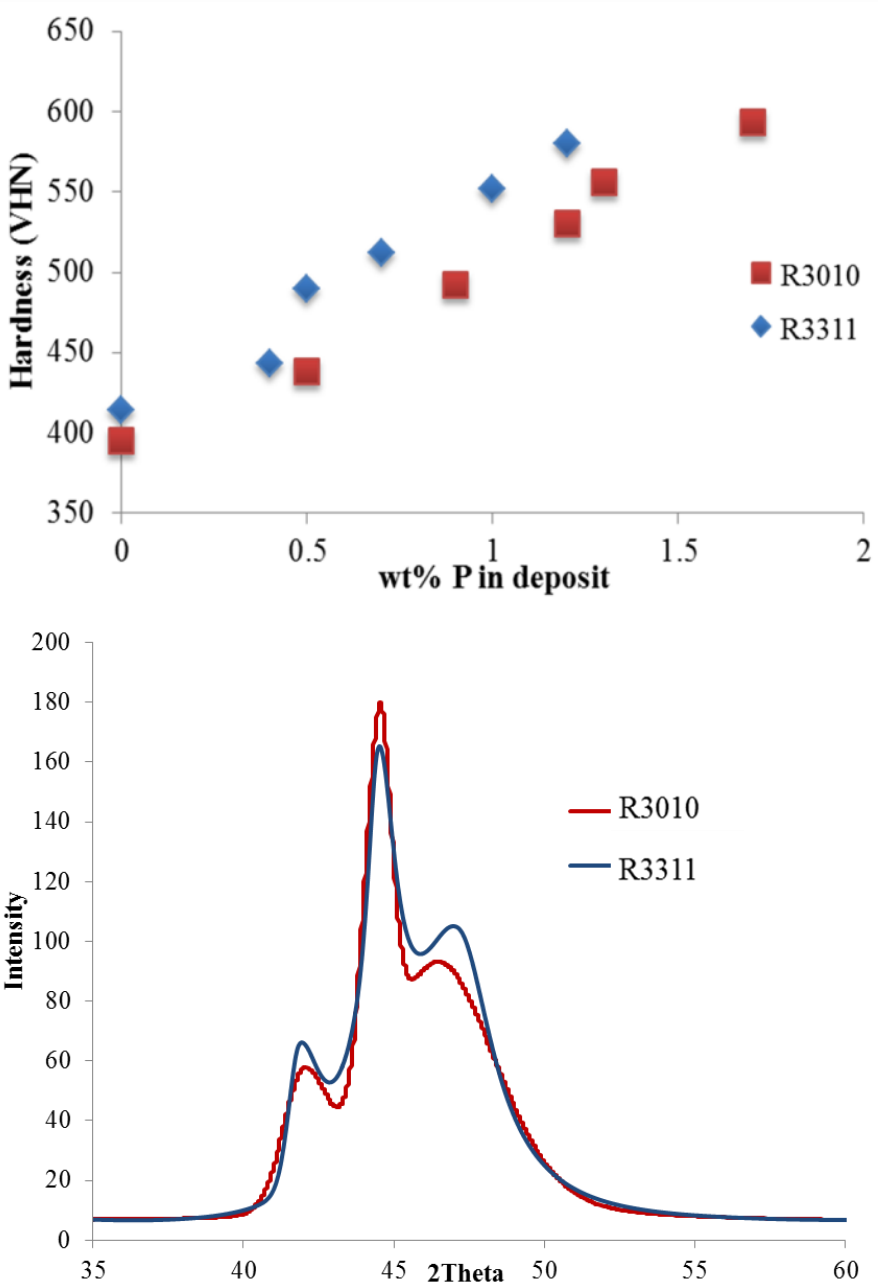

Figure 17 Effect of wt% P on hardness and XRD pattern of standard nCoP (R3010) and the new nCoP (R3311)

A relatively thin (100µm) coating of nCoP (R3311) applied to the aluminum was found to impart significant structural reinforcement in terms of flexural strength (greater than 2x the flexural strength) and stiffness with only a minor weight penalty, thereby maintaining aluminum's weight saving advantage. Additionally, given the significantly enhanced surface hardness (increased from 100VHN to ~600VHN), the application of nanometal on aluminum should result in significantly improved surface durability, wear/scratch resistance and impact resistance.

4.1.4 Task 1D Polarization behaviour of nCoP R3010 and nCoP R3311 by Corrdesa

In parallel to Tasks 1A, 1B and 1C, the corrosion polarization behaviour of nCoP R3010 and nCoP R3311 coatings with varying phosphorus content was tested by Corrdesa. The aim was to determine the optimal phosphorus content for corrosion resistance in deposits with 0 wt% P to 2 wt% P. In support of these efforts, Integran provided free-standing foils as well as coatings on steel substrates. The use of free-standing nCoP foils for testing was intended to eliminate possible substrate interference and to ease identification of signs of post-corrosion pitting. Long term open circuit potential (OCP) and resulting polarization behavior were measured. Polarization data for 10 minutes, 1 hour, and 3 to 4 days of immersion period was obtained. The phosphorus content for the two chemistries tested included: no P (0.0 wt% P), Low P (<0.5 wt% P), Med P ($0.5 \leq$ wt% P ≤ 0.9) and High P ($1.0 \leq$ wt% P ≤ 1.3).

Polarization tests performed after 10 min of immersion indicated that deposits containing no P have the most noble corrosion potentials. As seen in Figure 18, the samples with no P content appeared to have slightly lower corrosion current densities than the higher P samples.

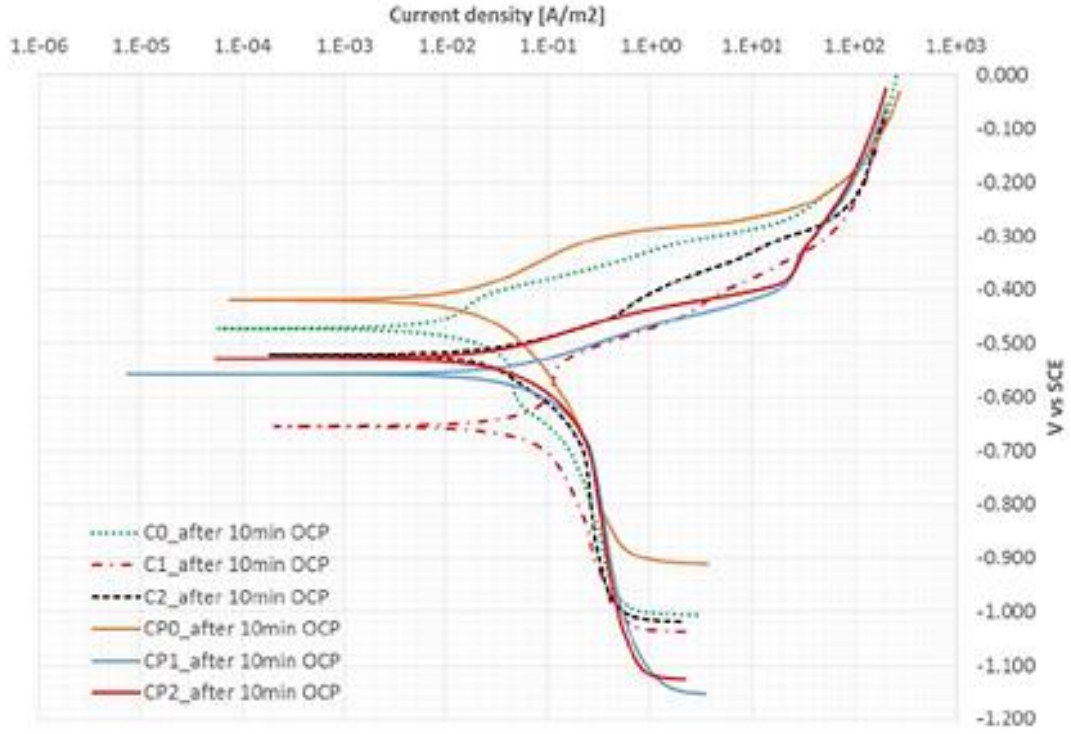

Figure 18 Polarization behaviour after 10 minutes of immersion, where C-series corresponds to R3311 and CP-series corresponds to R3010, and three phosphorus contents (0 = no P, 1 = Low P and 2 = Med P)

Prior studies have indicated stabilization of the OCP after 50 to 100 hours of immersion. Therefore it is plausible that given the short exposure time (10 minutes), the differences observed in the measured polarization curves may be within the associated statistical error of the measurements. Integran's preliminary findings from salt spray indicated that after long term exposure, the higher P deposits showed better corrosion resistance i.e. reduced kinetics after longer immersion, as

compared to lower P deposits. Further testing was carried out by Corrdesa to validate this phenomenon and understand polarization behaviour with respect to exposure time and the role of P determining corrosion performance.

The impact of bath chemistry and longer immersion times on corrosion behavior was investigated. After longer immersion times (2.5/3.5 days), both R3010-Med P (CP2 in Figure 19) and R3311-Med P (C2 in Figure 19) appeared to exhibit more defined passivation behaviour than after shorter immersion times (1-1.5hr). This would suggest a film may be forming on the surface. When inspecting the samples post-polarization (as shown in Figure 19), optical images of the corroded surfaced show more discoloration after the longer immersion times, again suggesting that a film is indeed forming. Future work would involve comparing the effect of immersion time on the low to no P containing samples to see if a similar phenomenon (i.e. passivation behaviour) occurs.

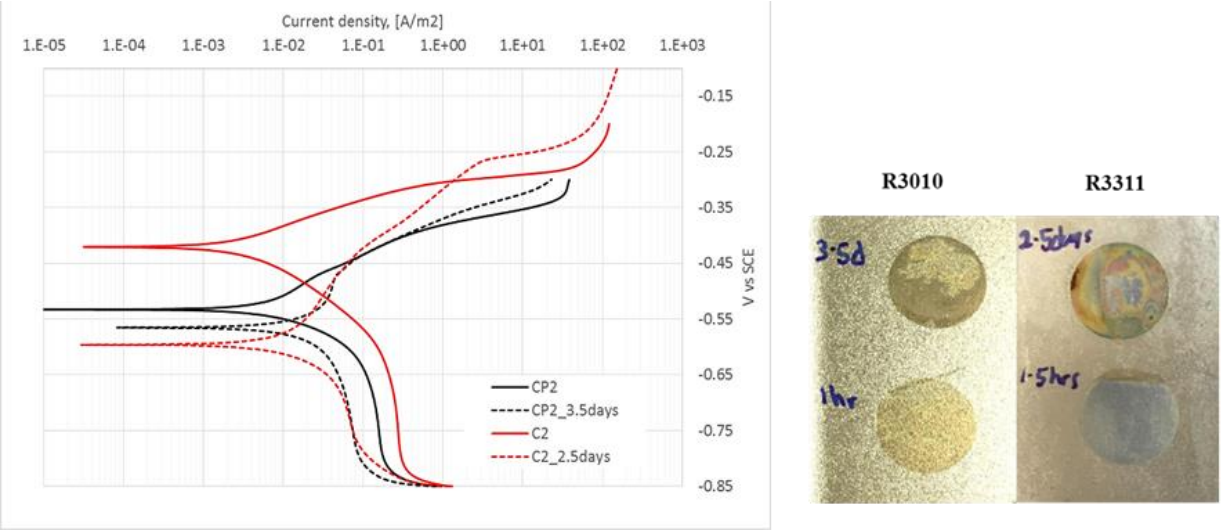

Figure 19 Polarization behavior of R3010 and R3311 after 1h and 2.5-3.5 days immersion time and the corresponding samples post-testing

4.2 TASK 2 Development of Nanostructured Cobalt Composite Coatings

The work performed in this task was performed with the objective of developing novel nanocomposite coating systems that consist of a nanocrystalline cobalt-phosphorus matrix embedded with second-phase hard particles in order to improve Taber wear performance of nanocrystalline cobalt-phosphorus systems. Two different methods were evaluated for producing the composite coatings:

a. Co-deposition of second-phase ceramic particles,
b. Novel in-situ particle formation and deposition of nanoparticles (Cirrus Materials Science Dopant technology).

4.2.1 Task 2A Co-deposition of second phase particles from particle suspension baths

In this task, Integran investigated the effect of particle type, size, combinations, and additives in particle suspension baths on deposit property and performance.

4.2.1.1 Particle size variance

The first stage of development of a nCoP-particle nanocomposite system investigated the co-deposition of SiC of three particle sizes (40nm, 500nm and 1µm) into a nCoP matrix. The relationship between particle loading concentration in the plating solution and influence on Vickers microhardness and Taber wear resistance is shown in Figure 20.

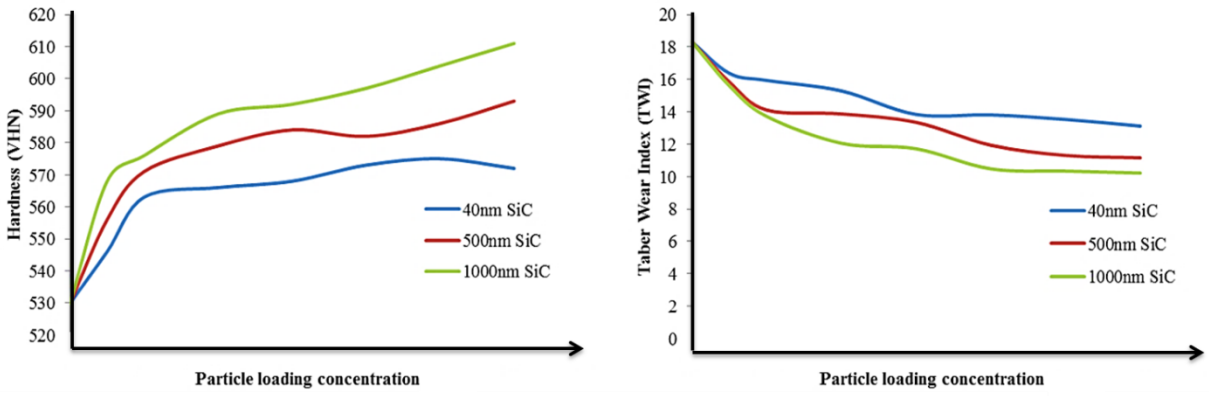

Figure 20 Effect of particle size on hardness and Taber wear

Higher particle loading/doping concentrations were found to result in improved hardness and wear resistance for all particle sizes. In general, the bigger the particle size the higher the hardness and the lower the Taber wear. This may be due to decreased co-deposition of 2nd phase particle in smaller particles size-systems. It should be noted that while SiC could not be seen in the cross-sections with optical and SEM imaging, XRF and SEM/EDS measurements indicated presence of Si in the deposit, thus suggesting effective co-deposition. There was also an increase in surface roughness of the deposits, which taken together with the improvement in mechanical properties (hardness and taber wear performance) seem to be a indicator for successful SiC co-deposition. The coefficient of friction and sliding wear rate both increase with particle additions. Appendix D

contains the detailed deposit coefficient of friction and sliding wear rates for samples produced with SiC particulate of various sizes as a function of bath loading. The use of additives to enhance particle co-deposition was investigated next.

4.2.1.2 Effect of additive Nanovate™ A59 (Phosphorous concentration)

Following the observation made in Task 1A-iv with Sm co-deposition, the effect of phosphorous concentration in solution on the co-deposition of SiC was investigated. The particle size for this study was fixed to 500nm while the P content was varied from 0.5 to 1.3 wt%P. As previously observed in Task1A, subsection *iv*, P appears to play a role in co-deposition of other alloying constituents.

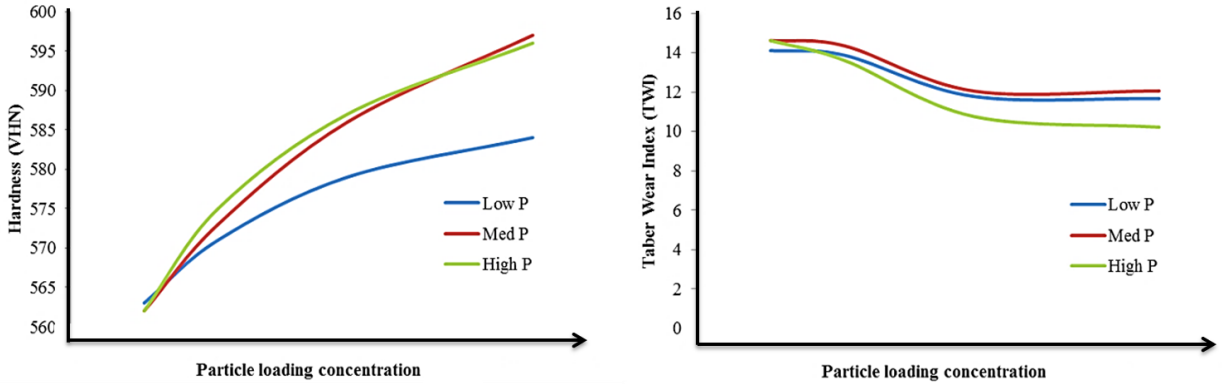

Figure 21 Effect of additive Nanovate A59 in particle systems on hardness and taber wear.

As demonstrated in the graphs (Figure 21), an improvement in Taber wear and hardness is observed with increasing phosphorous and particle loading concentrations. While there is only marginal improvement in Taber wear resistance, a significant improvement in hardness is observed. This implies that increasing P in plating solution results in higher P in the deposit (higher hardness) but it does not significantly influence the co-deposition of 2nd phase particles (similar TWI).

4.2.1.3 Effect of Particle type

Four different types of particles were investigated: 1000nm Silicon Carbide (SiC), 800nm Chrome Carbide (Cr_3C_2), 800nm Alumina (Al_2O_3) and 700nm Diamond particles. Figure 22 shows the hardness and Taber resistance of nCoP deposits produced from baths with the different particle types as a function of the particle load in the bath.

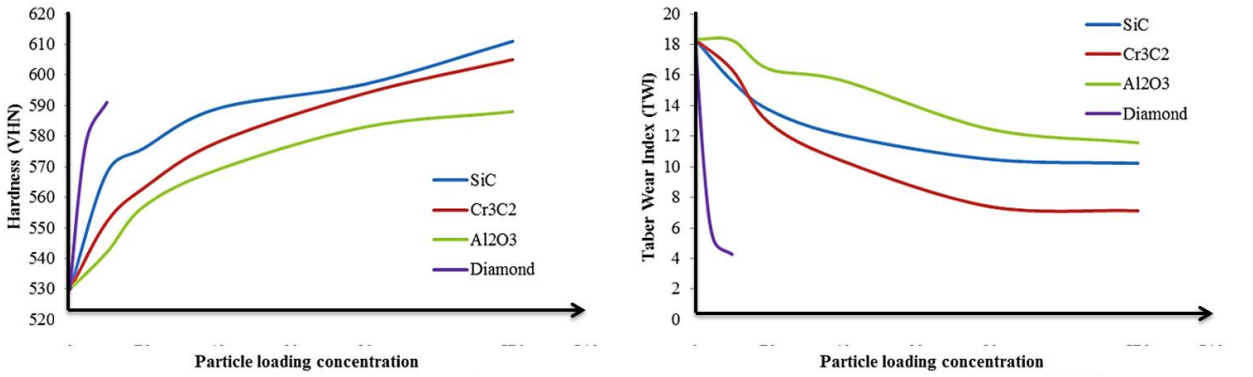

Figure 22 Effect of particle type on hardness and Taber wear.

As seen in the Figure 22, diamond particles result in the highest hardness and lowest Taber wear index per unit particle addition. The nCoP-SiC system showed the second best performance in terms of hardness, however nCoP-Cr_3C_2 composite system showed the second best Taber performance. It is believed that both systems should be well suited for high temperature applications. The effect of high temperature aging on these composite coating was also evaluated (please refer to the following section). In addition to mechanical performance, these deposits were provided to Corrdesa for polarization testing.

In-house 1000h salt spray corrosion testing, following ASTM B117-16: Standard Practice for Operating Salt Spray (Fog) Apparatus was performed on nCoP-composite coatings with different particle types. The following coatings, all produced using the standard plating conditions, 150µm thick, were tested:

1. Baseline nCoP
2. nCoP – SiC
3. nCoP – Cr_3C_2
4. nCoP – Al_2O_3
5. nCoP – Diamond

As seen in Figure 23, all the nanocomposite coatings were found to tarnish in a similar fashion as Baseline nCoP, however there was no evidence of red rust or other signs of substantial corrosion (pitting) even after 1000hrs of exposure. Between 24h and 200h of exposure there is no significant change in appearance. Similar to baseline nCoP, the corrosion product formed is a solid layer i.e. non-powdery. The Cr_3C_2 deposit formed a brown –black tarnish that later turned yellow-brown like the corrosion product formed on the other deposits.

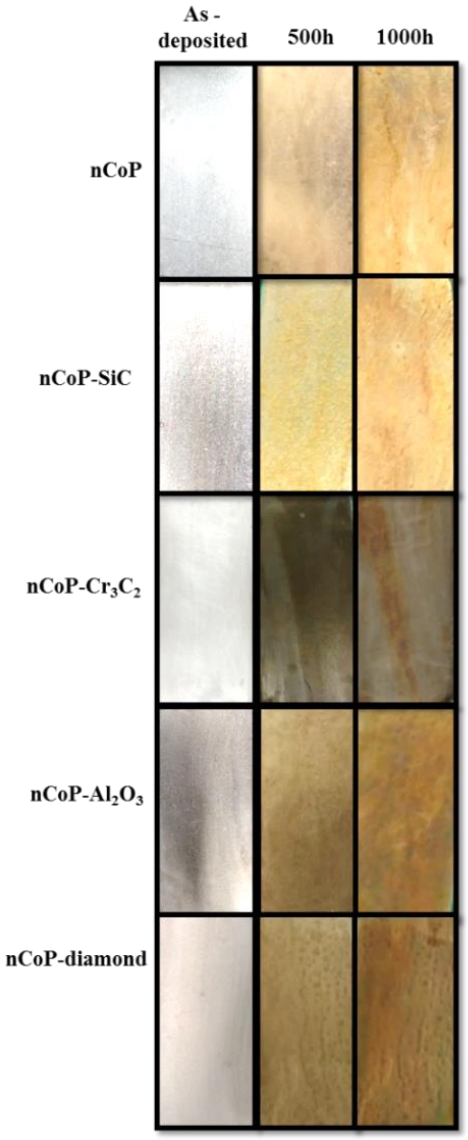

Figure 23 Salt Spray corrosion samples for the various particle systems.

4.2.1.4 Effect of heat treatment on various particle-systems

The effect of heat treatment at 425°C for various durations (1hour, 24hours, and 100 hours) on hardness was investigated. This aging study was carried out on nCoP, nCoP-SiC, nCoP-Cr_3C_2 systems. Figure 24 shows the Hardness and Taber wear Index for the different nanocomposite coatings at different aging times.

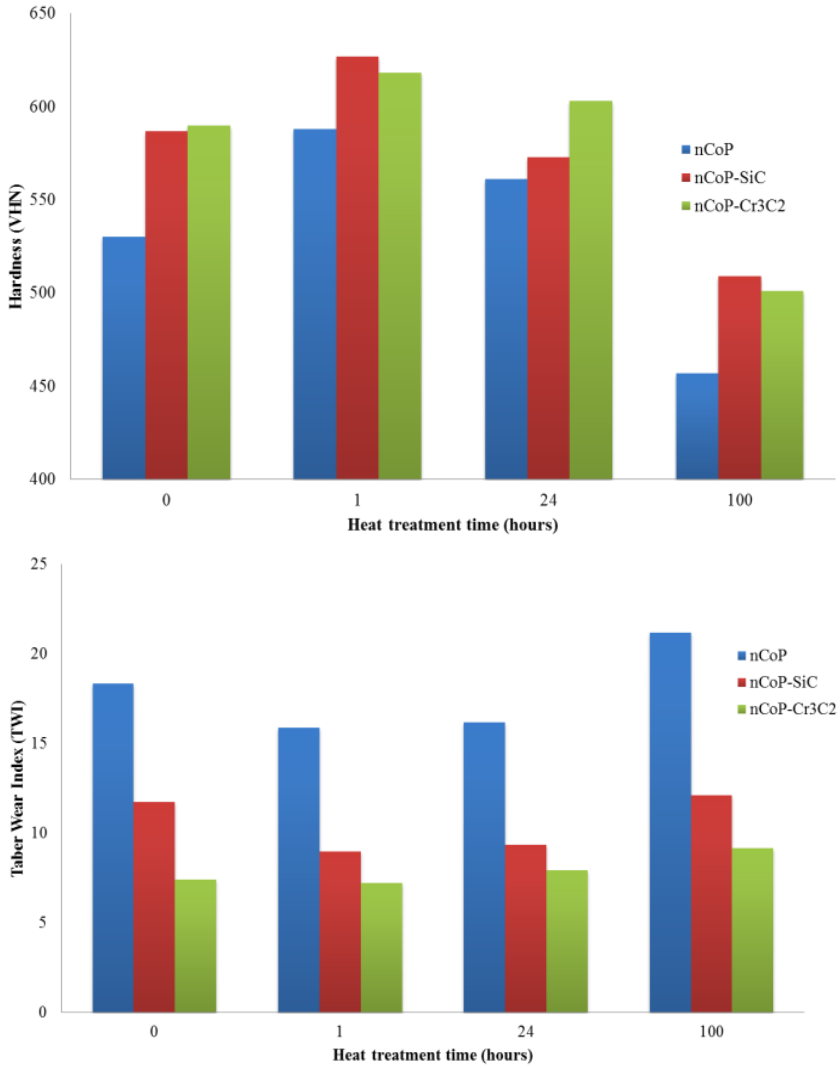

Figure 24 Effect of heat treatment on hardness and Taber wear rate.

Results indicated an increase in hardness after 1 hour of heat treatment, and a steady drop in hardness sometime thereafter. This can be attributed to two competing mechanisms: precipitation hardening (dominating between $0 \leq$ hours ≤ 1) [9] and grain growth (dominating $\geq$1hour). A general trend between hardness and Taber wear was noticed – the higher the hardness the lower the Taber wear, in accordance with Archard's law [10]. Both hardness and Taber wear were found to diminish at the longer heat treatment times, however the nCoP-particle systems were found to retain these properties better than the nCoP system.

4.2.1.5 Particle combinations and hybrid systems

Various combinations of particle systems were investigated. Following the findings of the previous sub-studies, some particle types and sizes were found to co-deposit more than others. It was therefore theorized that mixing these particles may have a synergistic influence on co-deposition. For example, in the SiC system, particle size is a limiting factor, where more success was achieved in co-deposition of bigger particle sizes. Also, certain particles such as diamond, given their hardness and Taber wear performance, are probably more likely to co-deposit than SiC. Therefore it is possible that combining multiple particle types or sizes may promote the co-deposition of the other. Figure 25 shows the hardness and Taber wear resistance of various coatings with different combinations of co-deposited SiC and diamond particles.

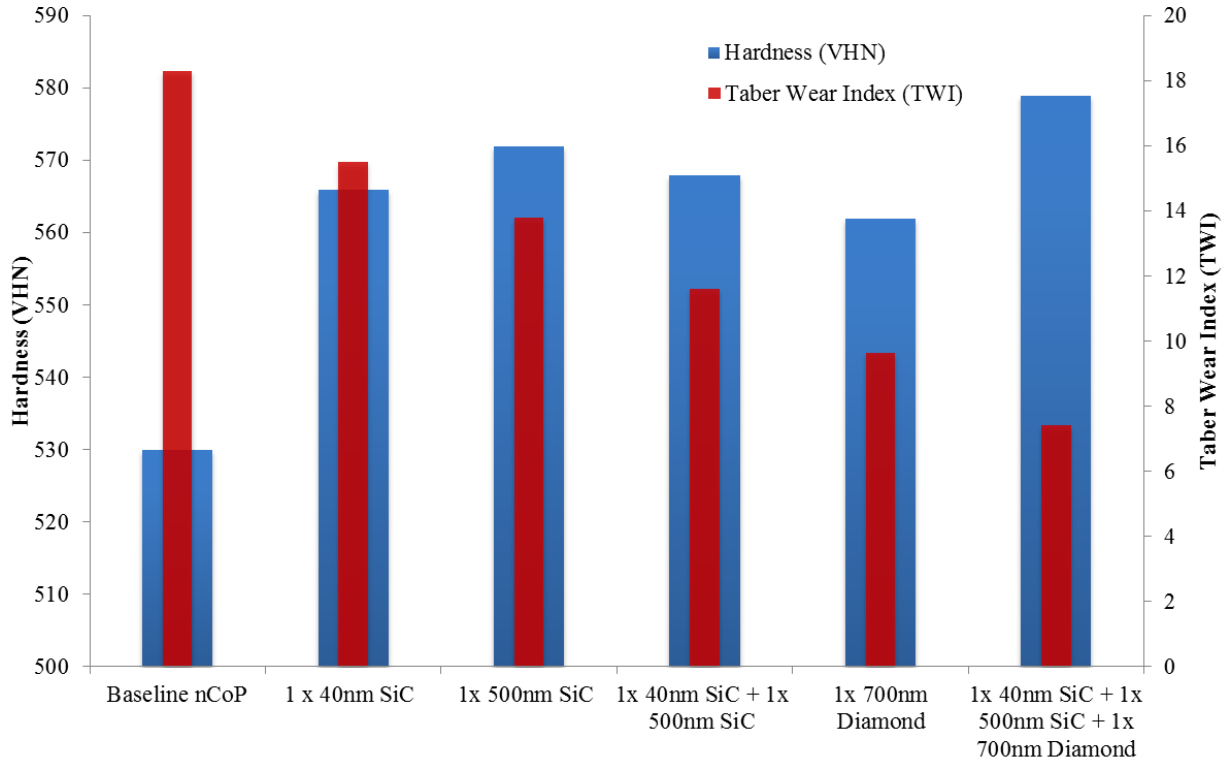

Figure 25 Effect of combining particle types and sizes on mechanical performance.

As seen in Figure 25, combining 40nm and 500nm SiC particles, while maintaining the overall particle concentration resulted in an improvement in Taber wear resistance and averaging of hardness (following rules of mixture). Whereas, a further minor addition of Diamond resulted in further improvement in Taber wear resistance and hardness.

Further increases in the particle loading concentration of the SiC and Diamond combinations, leads to a further increase in hardness and Taber wear resistance, as shown in Figure 26. This result further validates the theory of synergistic co-deposition.

Various combinations of SiC and Cr_3C_2 also showed a similar trend, as shown in Figure 27. With the hybrid SiC/Cr_3C_2 nCoP-particle composite systems, superior hardness and Taber wear resistance were achieved compared to the nanocomposite coatings with a single particle type.

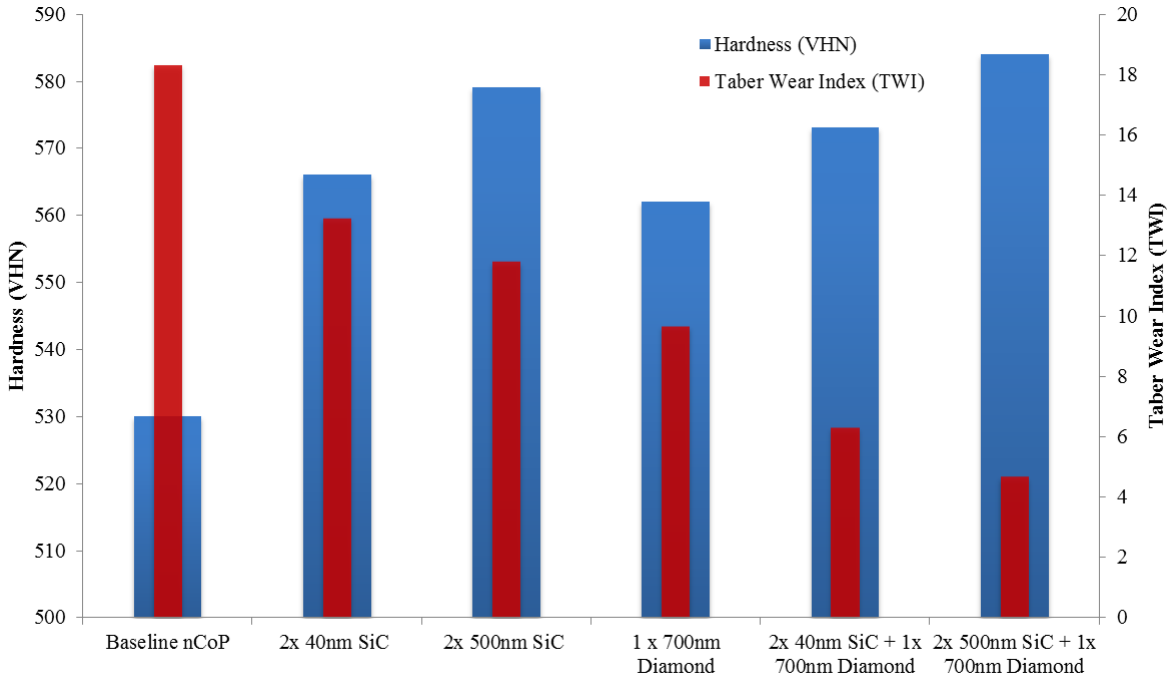

Figure 26 Effect of combining particle types, sizes and particle loading concentration on mechanical performance.

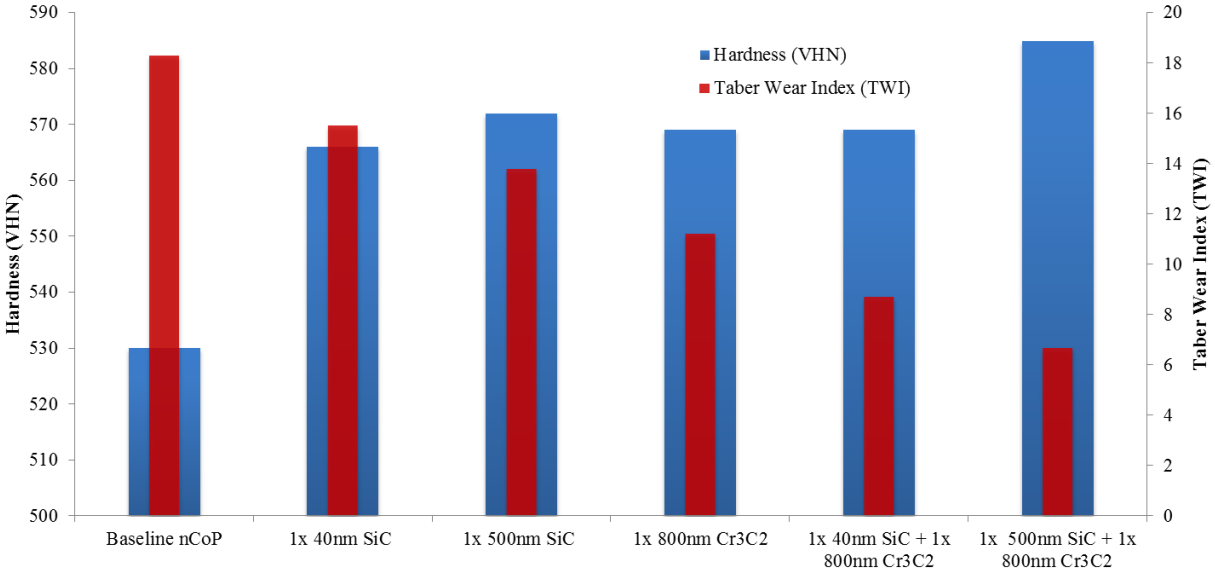

Figure 27 Effect of particle type combination on mechanical performance.

4.2.1.6 Effect of Nanovate™ B19- cationic surfactant

The cationic surfactant B19 was added to the chemistry with the purpose of influencing particle co-deposition. Theoretically, modifying the plating solution surface tension should enhance particle dispersion in-solution which in turn could influence particle co-deposition [4, 5]. Figure 28 shows the effect of B19 additions on the hardness and Taber wear resistance of SiC/Diamond hybrid nanocomposite coatings. In general, the addition of the cationic surfactant resulted in an increase in hardness and decrease in Taber wear Index. The use of B19, however, resulted in a decrease in material ductility. With the addition of 1x B19, the ductility dropped from ~4-5% elongation to 0.71%. Further drops in ductility were observed with increasing B19 concentration, decreasing to 0.60% elongation with 2x B19, and 0.54% elongation with 4x B19. Ductility measurements were determined using ASTM B489: Standard Practice for Bend Test for Ductility of Electrodeposited and Autocatalytically Deposited Metal Coatings on Metals. As seen in Figure 28, a slight improvement in hardness and Taber wear was achieved with a 1X addition of B19, and increasing the B19 concentration to 2X and 4X did not result a significant improvement in hardness or wear resistance over the 1x addition.

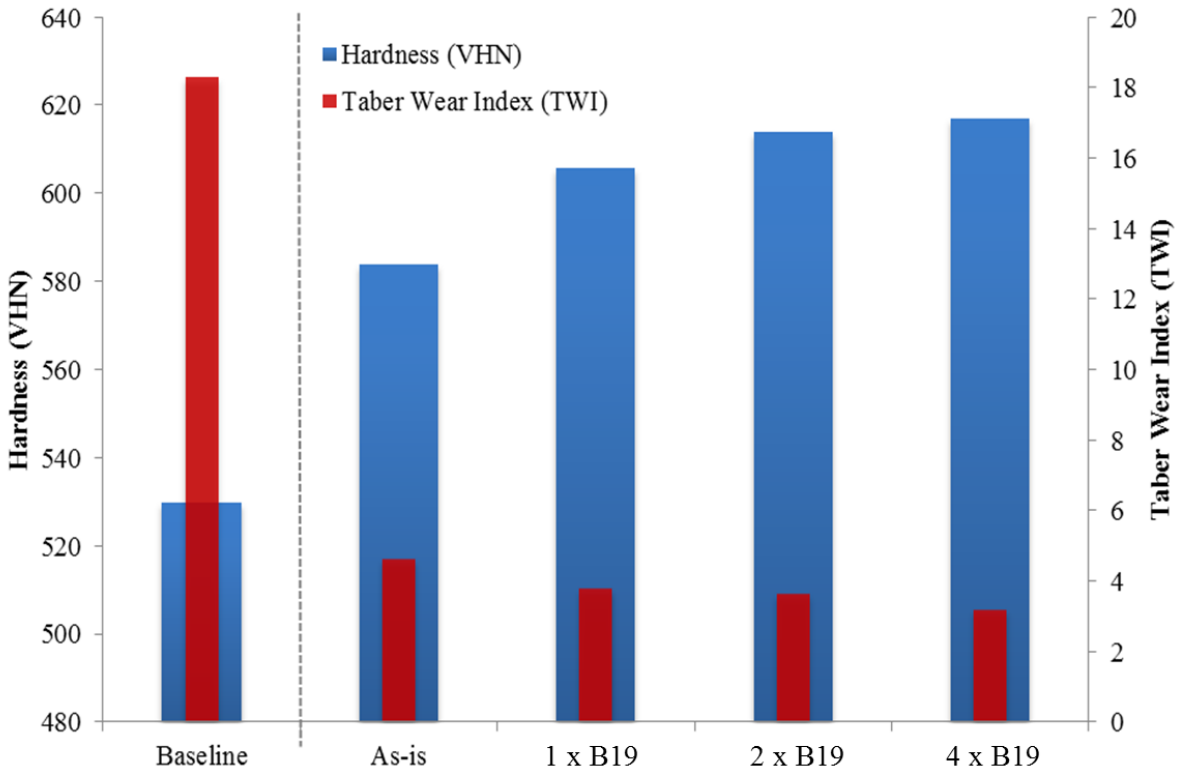

Figure 28 Effect of B19 concentration on mechanical performance of 2x 500nm SiC + 1x 700nm Diamond chemistry.

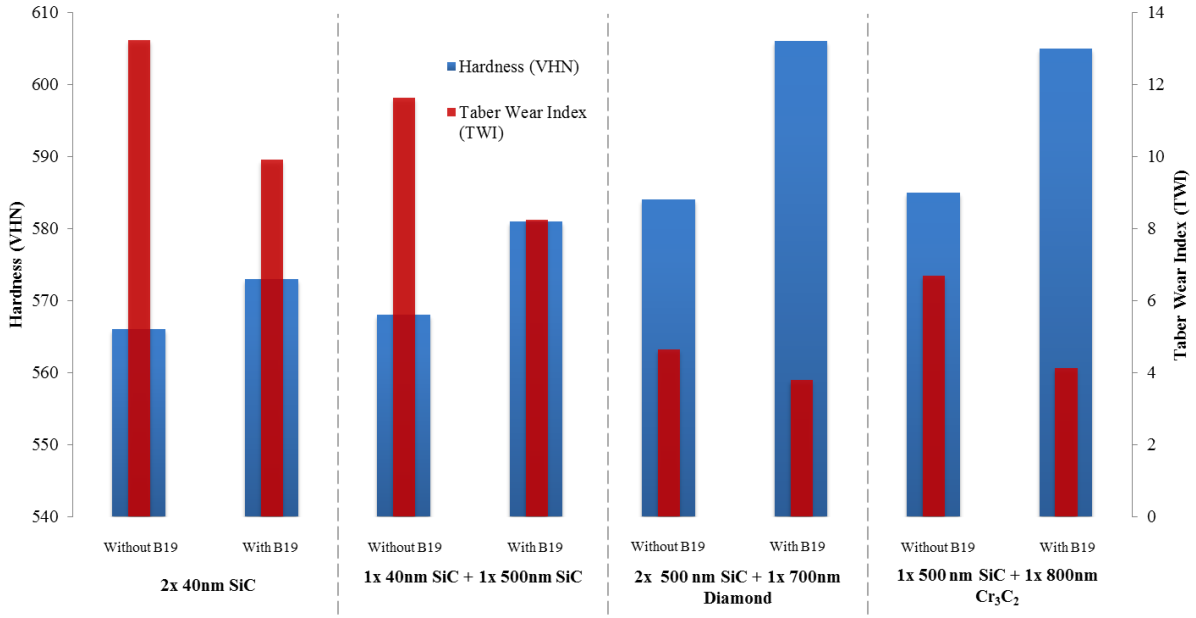

Figure 29 Effect of B19 on various particle and particle hybrid systems.

Figure 29 shows the effect of B19 additions on various particle and particle hybrid systems. As seen in the figure, the addition of B19 results in improvement in hardness and decrease in Taber wear rate for the various particle types and combinations. This improvement is accredited to either enhanced uniform distribution or higher content of particles in CoP matrix or both.

Hybrid nCoP-particle composite systems with B19 displayed excellent hardness and Taber wear results, where TWI achieved is very close to that of EHC, thereby addressing the second project objective.

4.2.1.7 Effect of plating conditions

As identified in Task 1, process optimization led to the ability to reduce the operating temperature and current density of the nCoP process. In this task, the effect of these varied operating conditions on nCoP-particle deposit property and performance was evaluated and compared to the standard operating conditions.

Table 7 Mechanical properties of various hybrid systems as compared to the baseline nCoP

	85°C, 135 mA/cm^2, DC				75°C, 80 mA/cm2, DC			
			Pin on Disk (Al_2O_3 pin)				Pin on Disk (Al_2O_3 pin)	
	Hardness (VHN)	TWI	Coefficient of friction (μ)	Sliding wear rate* (10E-6 mm^3/Nm)	Hardness (VHN)	TWI	Coefficient of friction (μ)	Sliding wear rate* (10E-6 mm^3/Nm)
Nanovate™ nCoP	528	18.32	0.58	12.41	553	18.47	0.63	13.68
2x 800nm Cr_3C_2	594	7.39	0.59	26.33	589	8.44	0.55	19.3
1x 500nm SiC + 1x 800nm Cr_3C_2	585	6.68	0.64	27.62	592	6.29	0.54	24.52
1x 500nm SiC + 1x 800nm Cr_3C_2 + 1x B19	605	4.12	0.61	28.23	614	5.89	0.63	26.74

As seen in Table 7, there is no significant difference in properties of deposits plated under standard conditions (85°C, 135 mA/cm^2, DC) as compared to alternative conditions (75°C, 80 mA/cm^2, DC). Therefore plating under the alternative conditions is a viable option and can be used in the future Tasks. Table 8 highlights the systems that displayed ≥50% improvement in Taber wear performance over baseline nCoP (R3010). Properties of EHC are also included for comparison purposes.

Table 8 Particle systems that showed ≥50% improvement in taber wear performance over baseline nCoP

Particle system description (type, concentration)	Hardness, VHN	Taber wear, TWI (mg/1000 cycles, C-17 wheels)
EHC (as previously documented)	800-1200	3.2
nCoP	528	18.32
2x 500nm SiC + 1x 700nm Diamond + 1x B19	606	3.78
1x 500nm SiC + 1x 800nm Cr_3C_2 + 1x B19	605	4.12
2x 500nm SiC + 1x 700nm Diamond	584	4.63
2x 40nm SiC + 1x 700nm Diamond	573	6.28
1x 500nm SiC + 1x 800nm Cr_3C_2	585	6.68

4.2.2 Task 2B Cirrus Dopant Evaluation in nCoP Solution

The initial evaluation of the Cirrus Dopant with the nCoP process was performed at Cirrus Material Science, at their facilities in Auckland, New Zealand. After a standard nCoP benchmark was established, the experiments were performed to test the compatibility of Zr, Ti and Al - based dopants with Integran's nCoP process. It was found that the aqueous based dopants were more compatible with nCoP plating chemistry than the solvent based. At the conclusion of the Year 1 of the project, Cirrus reported that:

"The organic dopants produce the better improvements in mechanical properties; however the formulations were not stable in the low pH of the nCoP. The titania generating dopants agglomerate and precipitate after a few hours while the zirconia generating dopants precipitate after a few days. The aqueous alumina dopant produces moderate hardness and wear resistance improvements; however, it shows consistent stability in the nCoP bath. The reason for this difference may be the size of particles created by the dopant with Alumina typically creating particles of approximately 40-nm, while organic dopants create particles below 12nm. Cirrus that the smaller particles more easily integrate with the nCoP grain structure and thus result in improved coating properties." The full interim report on the investigations made by Cirrus Materials, is included in Appendix B.

A second generation of aqueous-based alumina and titania dopant system was developed and scaled-up to 1.5L and 5L plating setup in order to produce samples to send to Integran for abrasive (Taber) wear testing.

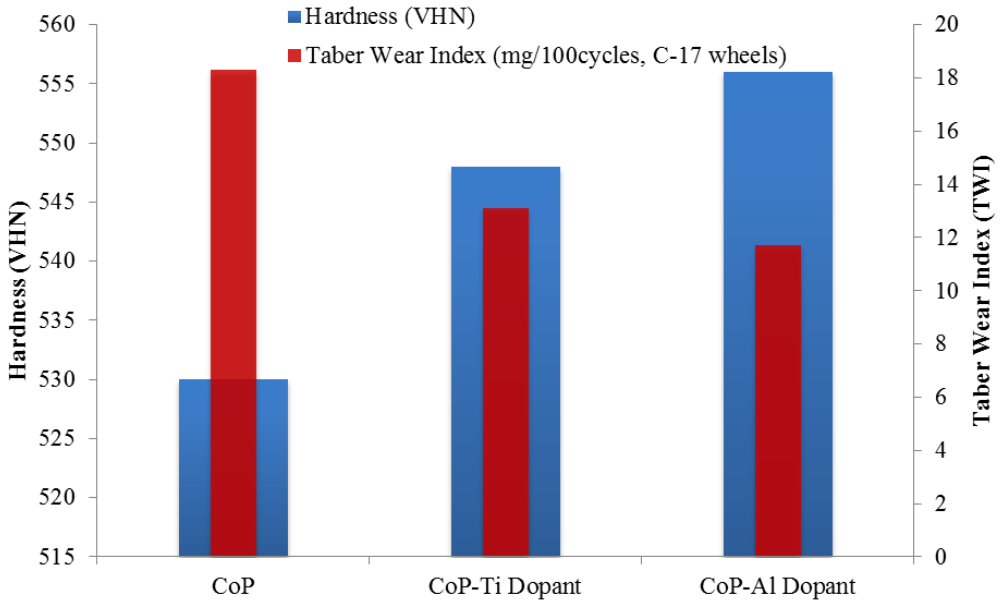

Figure 30 Hardness and Taber wear of CoP-Alumina and CoP-Ti Dopant system

As seen in Figure 30, an improvement in hardness and Taber wear is noted with the addition of dopants. Following this success, both Ti-dopant and Al-dopant were chosen for scale-up in Task 4.

Cirrus also developed a replenishment schedule for the two systems where:

- 50mL/L of Titania dopant solution added in the beaker before the first plating, replenishment of 6% of the original amount over an hour by dopants additions every 10 minutes.
- 2.5mL/L of Alumina dopant solution added in the beaker before the first plating, replenishment of 6% of the original amount over an hour by dopants additions every 10 minutes.

Cirrus Materials visited Integran at the beginning of Task 4 to facilitate technology transfer and scale-up of the two CoP-dopant systems. Further details regarding the technology transfer and scale-up at Integran are included in Task 4-3.

4.3 TASK 3 Development of specialized repair methods via brush plating

The optimized nCoP process from Task 1 and 2 was used to develop specialized repair methods through the use of brush/selective plating methods. Standard brush plating equipment was acquired and a preliminary brush plating setup was established at Integran. A detailed DOE was performed to study process variables including: flow rate of electrolyte, particulate loading, and electrical parameters.

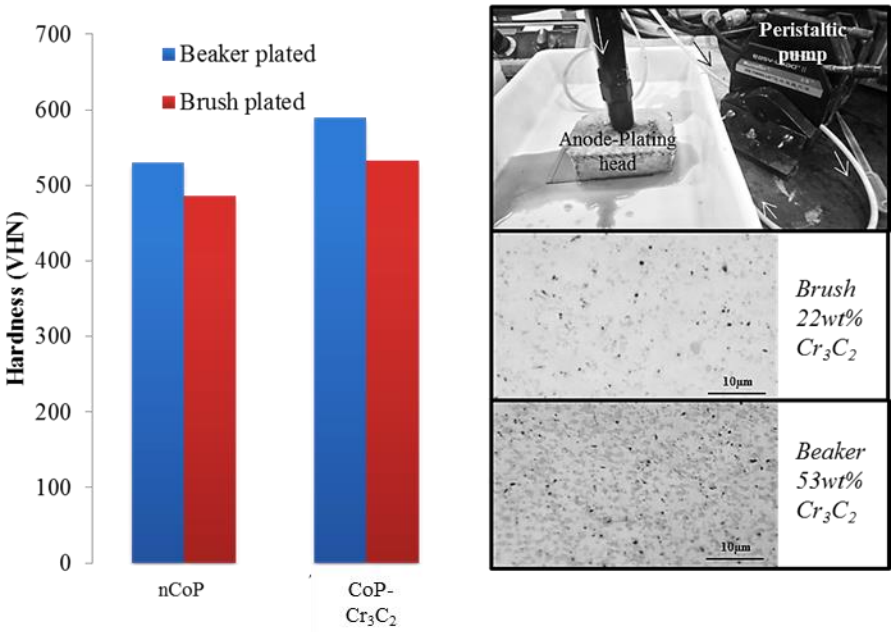

Figure 31 The brush plating setup (TR) and cross-sectional micrographs (BR) comparing brush plated and beaker plated deposit achieved with the same plating chemistry.

Figure 31 shows the difference in hardness between brush plated and beaker plated coatings as well as the brush plating setup and cross-sectional micrographs comparing brush plated and beaker plated deposit achieved with the same plating chemistry. Initial results demonstrate the ability to brush plate nCoP as well as nCoP-particle system. However, there is a discrepancy in hardness noted between the beaker and brush plated deposits. This may be due to a decrease in flow in the brush plated set-up; which may have resulted in reduced co-deposition of P in the deposit. However, as low flow is believed to be the root cause of this discrepancy, it may be addressed via a similar methodology as was addressed in the previous tasks. Furthermore, the use of 2nd phase particle systems was challenging because with solution flow the particles were trapped within the absorbent material (TuffWrap®) used to shield/line the anode/plating head, functioning almost as a particle filter, rendering the process messy and inefficient in co-depositing particles as seen in figure above. A quick solution was implemented to compensate for the insufficient co-deposition of particles by increasing particle loading in the plating solution. Table 9 compares properties of conventional plating (tank plating) and brush plating. Note the particle loading concentration required to achieve brush plating properties equivalent to ones achieved via tank plating.

Table 9 Conventional tank plating vs. Brush plating CoP and CoP-particle systems

	Particle loading in solution		Vol% Range (particles in the deposit)*		Phosphorus content (wt%)		Hardness (VHN)		Taber Wear (mg/1000cycles, CS-17 wheels)	
Set-up → **System ↓**	Tank Plating	Brush plating	Tank Plating	Brush plating	Tank Plating	Brush plating	Tank Plating	Brush plating	Tank Plating	Brush plating
CoP	-	-	-	-	1.1	0.7	528	513	18.3	18.9
CoP-SiC-Diamond	2x	4x	17 – 24	12 – 29	0.9	0.6	606	597	3.8	4.2
CoP-SiC-Cr_3C_2	2x	5x	46 - 57	31 - 53	0.9	0.5	605	582	4.1	5.7

* ImageJ was used to determine particle volume fraction. Numbers are based on SiC and Cr_3C_2 particles, diamond particles could not be seen via optical microscopy or SEM.

As seen in Table 9, despite the use of high particle loading volumes, the brush plating system produced deposits with lower particle content and lower phosphorus content. The higher particle loading also made solution handling very difficult, and in general the process was not deemed to be very user friendly. An alternative selective plating method was investigated using a technology/method that Integran recently developed for a project involving the repair of damaged steel piping in the Nuclear power stations. The technology involves an Encased Contact Free (ECF) Plating Apparatus whereby a localized plating head attaches to the surface to be repaired in which plating solution flows in and out. The plating head provides a spill free plating apparatus which is fabricated via 3D printing and can be customized to any surface. The plating head only coats the area to which it is attached and ideal for localized repair (see Figure 32) without the mess of brush plating. The apparatus uses a non-consumable anode and therefore re-optimization of nCoP chemistry was required.

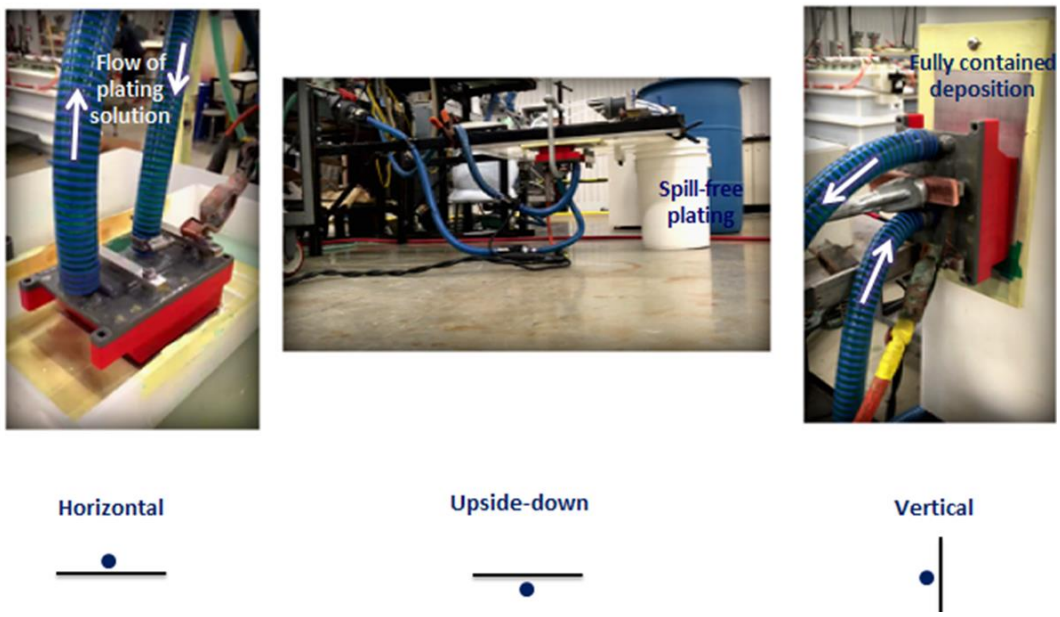

Figure 32 Encased Contact Free (ECF) Plating Apparatus

The effect of flow and pH on the deposit quality was studied. It was found that lower flow gave higher phosphorus content variability, therefore higher hardness variability, as compared to higher flow. However, very high flow resulted in very low Phosphorus deposition and non-uniform appearance. A mid-flow level was selected to balance Phos content in the deposit and to achieve good appearance.

Solution pH was found to influence both appearance and plating efficiency. High pH produced uneven deposits in both appearance and phosphorus content, where the variability was found to be amplified with flow conditions and direction. To address this, the pH was lowered which resulted in a more uniform deposit however this lowered the plating efficiency even further.

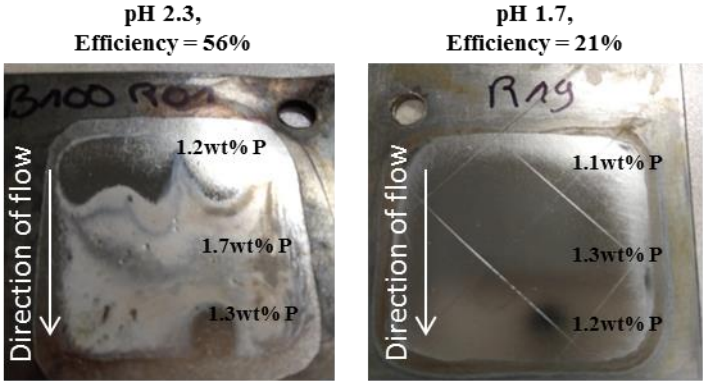

Figure 33 Effect of pH and flow on plating

Table 10 Deposit property comparison between Tank plated and ECF plated nCoP deposits

Property → / Chemistry → / System ↓	Phosphorus Content in the Deposit (wt% P)		Hardness (VHN)		Taber Wear (mg/1000cycles, CS-17 wheels)	
	Tank	ECF	Tank	ECF	Tank	ECF
CoP	1.0±0.13	1.3±0.09	528±18	617±13	18.32±0.55	17.02±0.26
CoP-Diamond	0.9±0.10	1.4±0.14	542±16	623±8	4.68±1.19	4.16±0.61
CoP-Alumina Dopant*	1.0±0.15	1.2±0.07	556±14	613±17	12.78±1.24	11.41±0.93

* The Al concentration in the CoP-alumina dopant deposit is not reported as SEM/EDS detected between 0.1 – 0.3 wt% Al in the deposits, which is within instrument error.

Phosphorus content was higher in deposits made via ECF plating as compared to tank plating. The Al concentration in the CoP-alumina dopant deposit is not reported as SEM/EDS detected between 0.1 – 0.3 wt% Al in the deposits, which is within instrument error. This has an effect on the hardness and Taber wear seen in Table 10. X-ray diffraction patterns of the two chemistries show that they are both nanocrystalline in nature but with different textures.

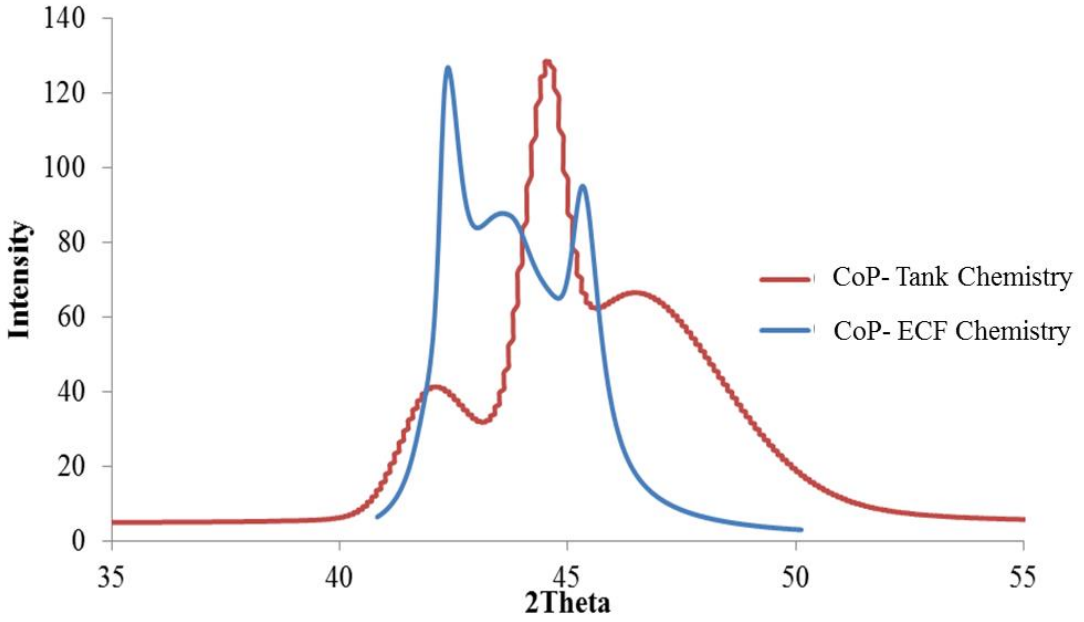

Figure 34 XRD patterns of baseline CoP from a Tank-based bath and the ECF apparatus

4.4 TASK 4 Final Process Stand-up

In this task the successful chemistries down-selected in the previous tasks were scaled-up to a 60L tank set-up. Chemistries that were scaled up included:

- Baseline CoP: used to plate at standard and alternative conditions
- CoP-Particle System: (CoP-Diamond and CoP-SiC-Diamond)
- CoP-Cirrus Dopant Systems: CoP- Titania and CoP-Alumina

4.4.1 Baseline CoP

The newly optimized CoP chemistry, which can operate under standard and alternative conditions was already validated in Task 1 and was therefore was able to be scaled-up without any further optimization.

4.4.2 CoP - Particle Systems

As previous results demonstrated that flow influences co-deposition of particles and phosphorus (and thus the mechanical properties), a short DOE was carried out to investigate the effect of particle loading on co-deposition and deposit properties on a tank scale (60L), due to the expected difference in flow between the beaker and tank set-up. The use of Nanovate B19 in this scale-up effort was avoided as it had resulted in decreased ductility.

4.4.2.1 CoP-Diamond

The first second-phase particle chemistry to be scaled up was the CoP-diamond chemistry.

Table 11 Effect of diamond loading concentration on hardness and Taber wear

Diamond concentration	Taber Wear (mg/1000 cycles, CS-17 wheels)	Hardness (VHN)
0.05x	8.5	526
0.1x	6.2	541
0.15x	4.7	568
0.25x	4.6	552
0.5x	4.3	576

As seen in the table, a small addition of diamond resulted in Taber wear ~ 4.7mg/100 cycles, as compared to beaker scale where only hybrid (multiple) particle system with B19 resulted in a similar Taber wear value of 4.12mg/1000 cycles with 1x diamond. As increases in diamond concentration did not result in significant improvement, the amount of diamond selected for testing in Task 5 was based on what provided the best performance at the lowest concentration. The addition of B19 was avoided as the dispersion of diamond in solution appeared to be adequate and to avoid the risk of decreased ductility, as previously it was noted that B19 made deposits more brittle.

4.4.2.2 CoP-SiC-Diamond

Following the findings from the diamond optimization trials, a similar approach of scaling the SiC

content and studying the influence on Hardness and Taber wear was studied. Unfortunately, there was little to no effect on the Taber wear with SiC addition, even with subsequent diamond addition. It is possible the solution was "saturated" with SiC which hindered co-deposition of Diamond particles and therefore the Diamond did not have as significant of an impact (Table 12). A similar effect was noted by a study investigating SiC and CNT. [11]

Table 12 Effect of SiC, diamond loading concentration on hardness and Taber wear

SiC concentration (g/L)	Taber Wear (mg/1000 cycles, CS-17 wheels)	Hardness (VHN)
0.2x	11.4	540
0.4x	12.6	524
0.8x	13.7	484
1x	13	545
1.5x	13.6	536
2x	11	535
2x SiC + 0.05x Diamond	12.4	496
2x SiC + 0.1x Diamond	13.1	484
2x SiC+ 0.25 Diamond	13.2	525

To test this "saturation" theory, beaker trials were carried out where the SiC concentration was kept low at 0.2x SiC.

Table 13 Effect of SiC diamond loading concentration on hardness and Taber wear – beaker study

SiC concentration (g/L)	Taber Wear (mg/1000 cycles, CS-17 wheels)	Hardness (VHN)
0.25x	13.4	541
0.2x SiC+ 0.1xDiamond	11	532
2x SiC + 0.1x Diamond	14.1	546

Once again, no significant influence was noted. Further investigations with the SiC and SiC-diamond system were therefore discontinued.

4.4.3 CoP- Cirrus Dopant Systems: Titania and Alumina Dopants

Cirrus Materials visited Integran to facilitate the technology transfer of their Cirrus Dopant™ technology. Fresh Titania and Alumina dopants were synthesized at Integran to be used for the

first set of plating trials to test reproducibility of the dopant technology.

Initial beaker trials with Cirrus-dopants in the nCoP solution at Integran produced deposits with lower hardness and higher Taber wear than the samples that were previously prepared at Cirrus. It was postulated that this could be due to insufficient replenishments – either dopant or phosphorous as both would be consumed quickly on a beaker scale when plating 4" x 4" Taber wear panels in 2L beakers.

Table 14 Cirrus Dopant properties

	Chemistry	Hardness (VHN)	Taber Wear Index (mg/1000cycles, C-17 wheels)
Titania Dopant	Cirrus sample sent April 2018 (beaker scale)	573	13.8
	Tech transfer May 2018 (beaker scale)	511	17.9
Alumina Dopant	Cirrus sample sent April 2018 (beaker scale)	566	11.3
	Tech transfer May 2018 (beaker scale)	523	14.1

A thick CoP-Alumina dopant deposit was produced with only Al-dopant replenishments. The cross-sectional hardness was studied as a function of thickness to check if hardness changes (i.e. Phosphorous is possibly is being "consumed" as function of plating time in the bath.)

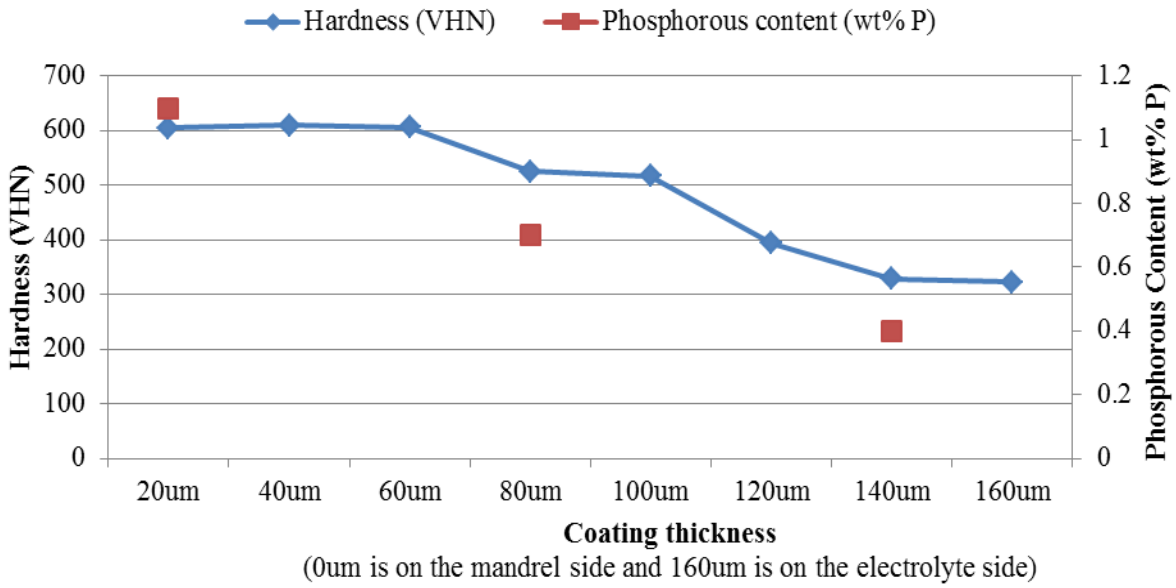

Figure 35 Hardness and P content as a function of thickness

As seen in Figure 36, hardness and P content decrease as plating time increases, therefore a P replenishment schedule needed to be developed. After a few iterations a replenishment schedule on a 30min interval for was determined for Nanovate™ A59 (Phosphorous containing additive) to maintain P content. The requirement for the Phosphorus replenishment may suggest that there is

an intrinsic incompatibility with the Cirrus Dopant and the nCoP process, as the replenishment amount for A59 represents a significant amount.

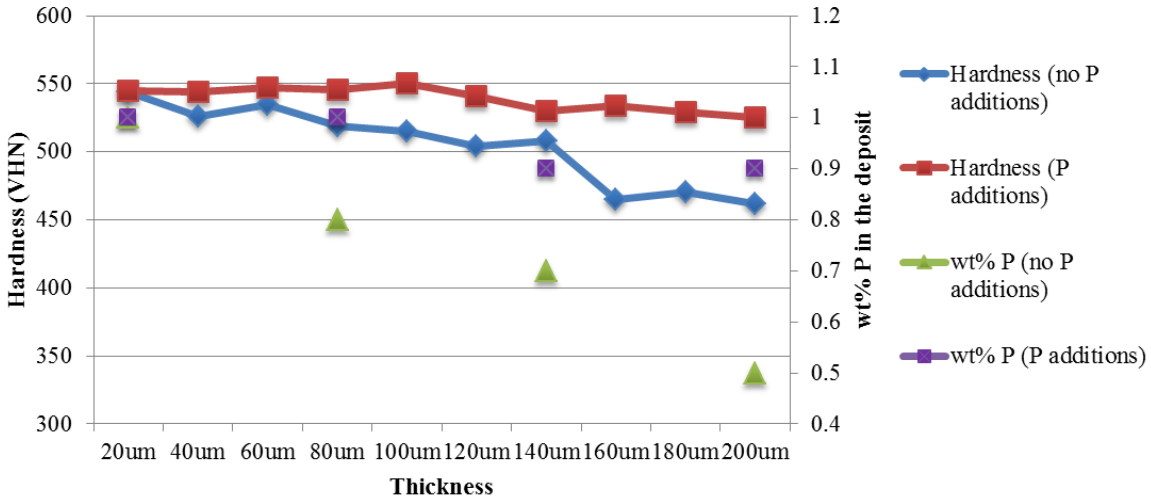

Figure 36 Hardness and P content as a function of thickness with and without P replenishments

The chemistry was then scaled-up to a 40L tank. Table below compares the beaker scale trials and the first set of tank trials. As it can be noted the tank trials produced results closer to results obtained from the samples sent by Cirrus for evaluation at the conclusion of Task 2B.

Table 15 Properties of CoP- Cirrus dopant deposits

	Chemistry	Hardness (VHN)	TWI (mg/1000cycles, C-17 wheels)
Titania Dopant	Cirrus sample sent April 2018 (beaker scale)	573	13.8
	Tech transfer May 2018 (beaker scale)	511	17.9
	Scale-up Trials 1 - 3 (tank scale)	548	13.1
Alumina Dopant	Cirrus sample sent April 2018 (beaker scale)	566	11.3
	Tech transfer May 2018 (beaker scale)	523	14.1
	Scale-up Trial 1 - 3 (tank scale)	556	11.7

4.4.4 Process Stability and Reliability

In order to ensure that all the samples produced throughout the sample production timeline for Task 5 were or high quality, AS9100 standard quality and maintenance protocol was followed:

1. Bath analysis: ICP and colorimeter for Co^{2+} and P content prior to each run
2. Regular pH monitoring. A special probe suitable for particle baths was acquired to maintain
3. Particle and dopant baths only: The tank had no filtration unit, to avoid losing dopant material and changing the bath chemistry over time.
4. Monitoring runs used to assess process stability, where every 5^{th} run was checked for hardness and composition to ensure deposit quality is not changing with bath Ah.

5. Followed replenishment schedule developed by Cirrus and Integran discussed earlier in Tasks 4.

4.5 TASK 5 Coating characterization, testing and evaluation

The core coating tests that were performed as part of Task 5 to demonstrate and validate the coating as a suitable alternative to Nickel and Chrome coatings included: deposit characterization, Hardness, Ductility, wear, corrosion performance and hydrogen embrittlement. Evaluation was carried out on the three systems successfully scaled up in Task 4:

1) Baseline CoP (developed and optimized in Tasks 1 and 4)
2) CoP-diamond (developed in Task 2A, optimized in Task 4)
3) CoP-alumina dopant (developed in Task 2B, optimized in Task 4)

4.5.1 Deposit characterization

All deposits were shiny, dense and uniform in appearance. Phosphorus content was 1.03±0.15 wt%P in all samples. X-Ray diffraction (XRD) patterns for the three systems are comparable, showing a nanocrystalline microstructure with a hexagonal close-packed crystal structure. Line broadening measurements on the XRD pattern indicate a grain size of <20nm was achieved. Minor variances in texture and broadening were observed, possible due to incorporation of particles.

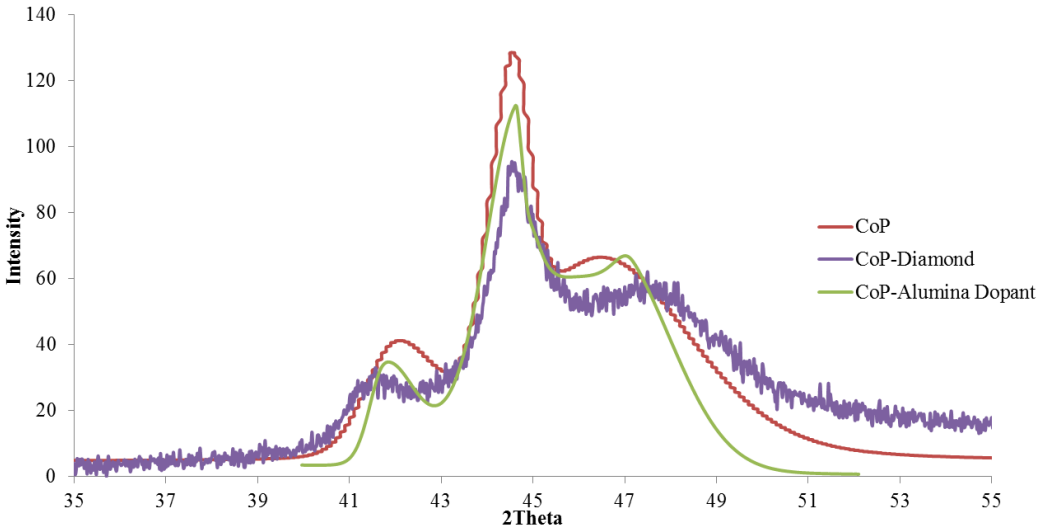

Figure 37 XRD pattern of down-selected CoP, CoP-diamond and CoP-alumina dopant

4.5.2 Hardness, Ductility and Wear testing:

The testing performed in this Task was performed as per ASTM standard procures listed in Section IV - Technical Approach (Table 9). The testing included: microhardness (as deposited and post heat treatment at 200°C), bend-ductility, sliding wear, coefficient of friction and Taber wear and were assessed on the following CoP systems:

1) Baseline CoP (plated under standard conditions 85°C)
2) CoP (plated under alternative conditions 70°C)
3) CoP-diamond
4) CoP-alumina dopant

Values reported are the average measurements performed on three samples. The samples were taken to fully represent the production timeline in case maintenance protocol highlighted in Task 4 was not sufficient to maintain constant plating conditions. For example a total of 11 CoP-diamond samples were produced and for Taber wear tests, samples number 2, 6, 11 were used.

Result trends obtained in Task 5 were similar to those obtained at a beaker scale (Table 16). A significant improvement in Taber wear is noted in the CoP-diamond system as compared to standard CoP. Particle addition did however lead to a slight decrease in %elongation and small increase in sliding wear rate.

Table 16 Mechanical properties of CoP, CoP (alternative conditions), CoP-diamond and CoP-Alumina dopant

PROPERTY	Test Method	Nanostructured CoP R3010 (Standard conditions, 85°C)	Nanostructured CoP R3010 (Alternative conditions – 70°C)	Nanostructured CoP-Diamond	Nanostructured CoP-Alumina Dopant
Hardness	**Vickers Microhardness**	532±13VHN	563±8VHN	569±7VHN	556±16VHN
		671±8VHN (post-HT)	696±12VHN (post-HT)	685±15VHN (post-HT)	663±23VHN (post-HT)
Ductility	**Bend Test**	5.29%	4.67%	3.12%	5.03%
Wear Volume Loss	**Pin-on-disc (against Al_2O_3 pin)**	6.76 x 10^{-6} mm^3/Nm	5.13 x 10^{-6} mm^3/Nm	7.05 x 10^{-6} mm^3/Nm	6.28 x 10^{-6} mm^3/Nm
Coefficient of Friction	**Pin-on-disc (against Al_2O_3 pin)**	0.40	0.52	0.66	0.50
Taber Wear	**CS-17 abrasive wheel**	18.32±0.16 mg/1000cycles	17.67±0.08 mg/1000cycles	4.88±0.29 mg/1000cycles	12.01±0.15 mg/1000cycles

4.5.3 Corrosion testing:

4.5.3.1 Salt Spray (ASTM B117)

Mild steel panels coated with the four CoP systems successfully scaled up in Task 4:

1) Baseline CoP (plated under standard conditions 85°C)
2) CoP (plated under alternative conditions – 70°C)
3) CoP-diamond (developed in Task 2A)
4) CoP-alumina dopant (developed in Task 2B)

Corrosion resistance of two coating thicknesses per CoP coating system/type was evaluated: 50µm and 100 µm. The motivation behind this was to see if there is a minimum coating thickness requirement to pass 1000hours of salt spray with pitting and formation of red rust.

All four coating systems passed 1000hour mark with no signs of red rust and pitting, however, all coatings did tarnish. (Figure 38) Also see complementary studies section for development of structural and tarnish resistant coating.

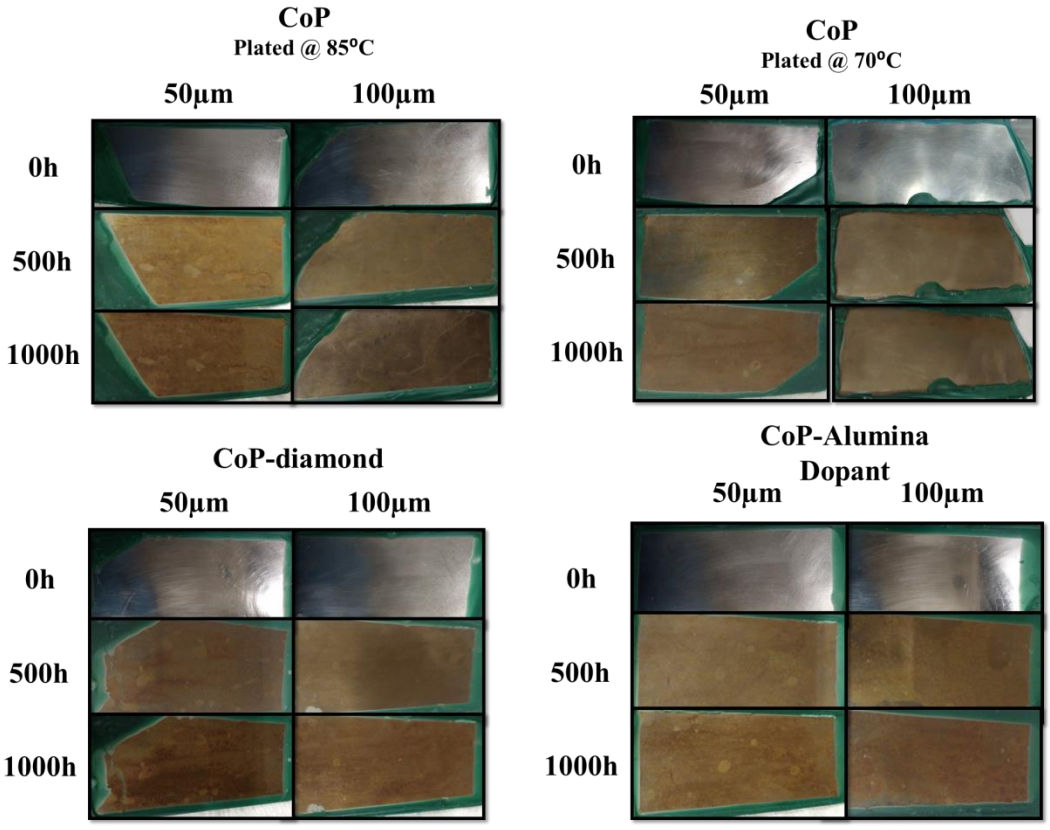

Figure 38 Progression of CoP coating systems with salt spray exposure

4.5.3.2 Linear Polarization Resistance, Galvanic compatibility

Corrdesa carried out LPR and galvanic compatibility testing. The scope of work comprised the following:

1. Linear Polarization Resistance (LPR) test- to determine recommended phosphorus content for optimum corrosion resistance and impact of dopant
2. Polarization data acquisition- according to NAVAIR protocol for galvanic corrosion simulation with Corrosion Djinn™
3. Galvanic coupling measurements- to quantify galvanic compatibility with relevant materials
4. Galvanic corrosion risk analyses with Djinn™- to compare Integran Co-P material performance with typical aerospace materials (Al 7075 and 4140 Steel).

Corrosion measurements were performed on the following CoP systems:

1) Baseline CoP (plated under standard conditions 85°C)
2) CoP (plated under alternative conditions 70°C)
3) CoP-diamond
4) CoP-alumina dopant

Based on long term and short term LPR measurements three coatings (nCoP, nCoP-diamond and nCoP-Alumina Dopant) were found to be best performing compared to the other 4 coatings. Figure 39 below shows the evolution after 24hr and 168hr exposure of the LPR and corrosion current for all the 7 coatings under study. They all lie in a similar range with the exception of nCoP (high Phos ~ 2 -2.5wt% Phos) which showed a higher potential. These findings indicated that coatings with the lowest corrosion rates were nCoP-diamond, nCoP-silicon carbide. This is followed by nCoP- low Phos, nCoP -Med Phos and nCoP- High Phos. The materials with the highest corrosion currents (rates) are the nCoP-Ti Dopant and nCoP-Al Dopant. Potentiodynamic polarization measurements were performed (Table 17) and the nCoP-diamond also showed lowest corrosion rate followed by nCoP baseline and the nCoP-alumina dopant. Overall, no significant effect of particle incorporation is seen on the corrosion rate but a detrimental effect of increasing phosphorus content on corrosion rate was observed.

Table 17 Corrosion current and estimated corrosion rate based on the Tafel extrapolation method

	Icorr (μA/cm^2)	**Corrosion Rate (mil/yr)**
nCoP-X	0.8	0.348
nCoP-SX	0.9	0.3915
nCoP-TD	1.5	0.6525
nCoP-AD	1.5	0.6525
nCoP	0.9	0.3915
nCo2P	1.3	0.5655
nCo4P	2	0.87

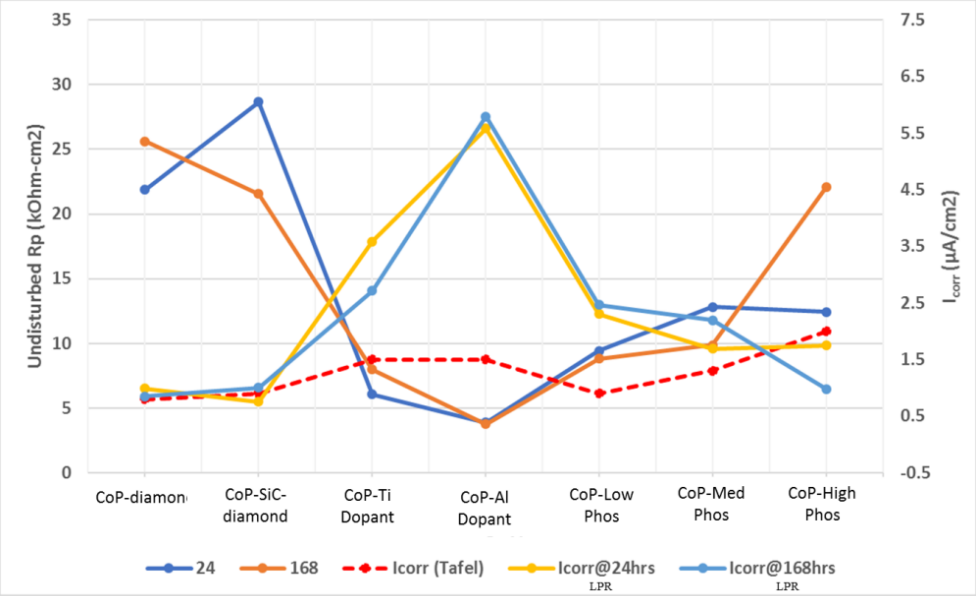

Figure 39 Polarization resistance and Icorr of the different CoP systems after 24h and 168h of exposure

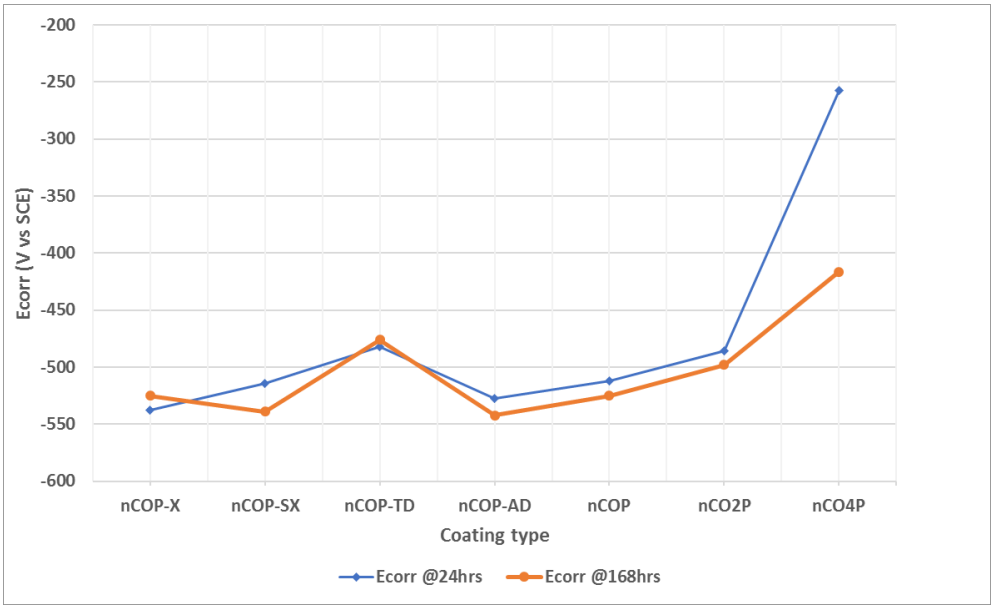

Figure 40 Corrosion potential after 24h and 168h of exposure

Long term galvanic measurements showed nCoP, nCoP-diamond and nCoP-Al Dopant resulted in similar galvanic currents (same order of magnitude) when coupled against 4130 HSS and Al 7075-T6. The coatings were all behaving cathodically when coupled against the Al 7075-T6 and 4130. The sharp dips in the current density were possibly due to replenishments made to the test cell with de-ionized water to compensate evaporated electrolyte. NOTE: all galvanic measurements were not conducted at the same time which explains the difference in electrolyte refilling events.

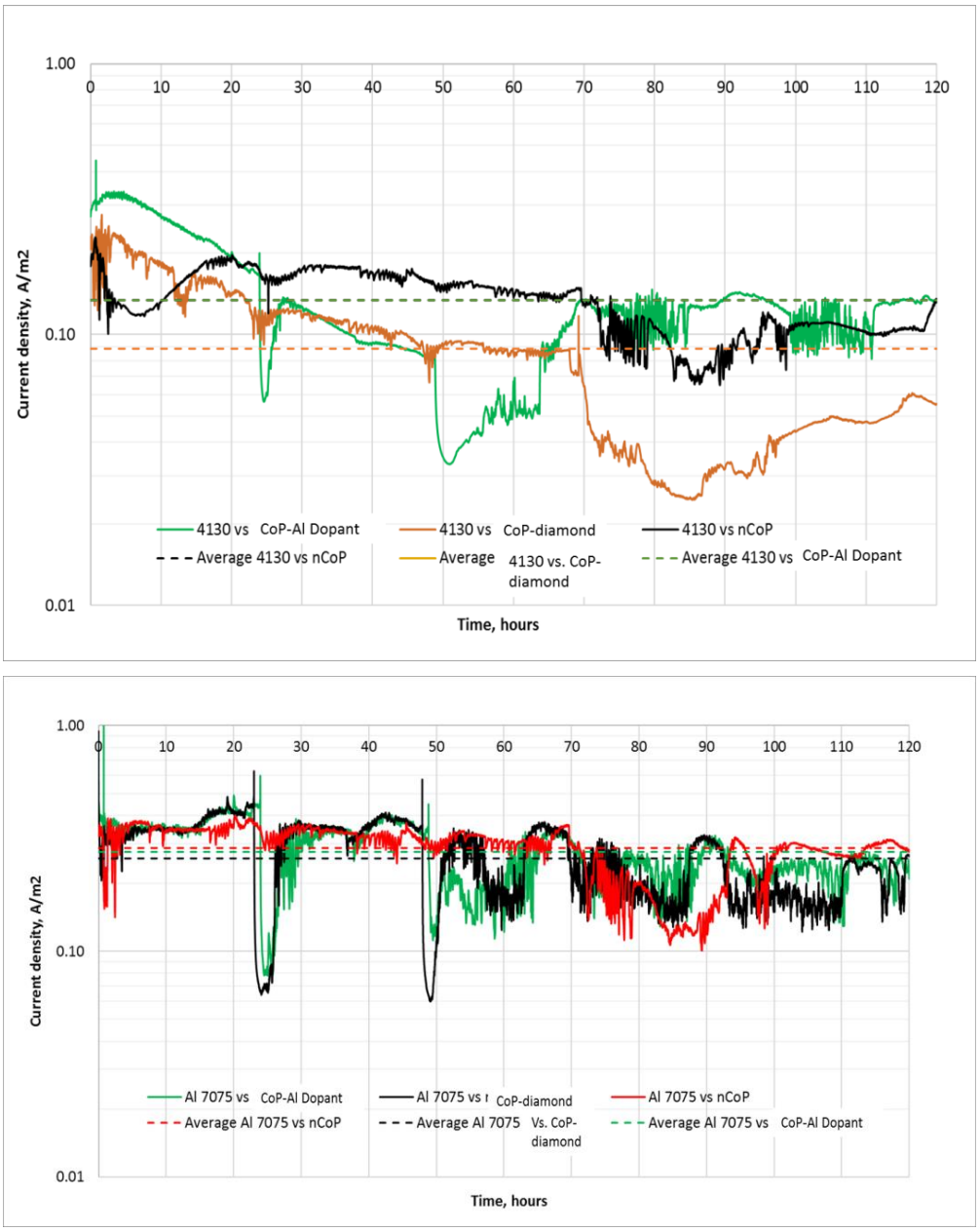

Figure 41 Galvanic coupling potential for 4130 and 7075 vs. nCoP, nCoP-diamond and nCoP-Alumina Dopant vs. time

For the full set of methods, results and corrosion data please see Appendix F for the full corrosion test report provided by Corrdesa.

4.5.4 **Hydrogen embrittlement testing: sustained load testing on notched bars**

Hydrogen embrittlement testing was carried out on the following coating systems, post-bake:

1) Baseline CoP
2) CoP (plated under alternative conditions)
3) CoP-diamond
4) CoP-alumina dopant

All coating systems passed post-HE relief bake at 375°F (+25/-0) for 24hrs, initiated within 4 hrs of plating. Please see Appendix E for all the results.

Table 18 Property Comparison Chart – Comparing CoP systems with Electroplated Ni and EHC

PROPERTY	Test Method	Electroplated Ni	Hard Chrome	Nanostructured CoP R3010	Nanostructured CoP R3010 (Task 1)	Nanostructured CoP-Diamond	Nanostructured CoP-Cirrus Dopant
Appearance	**Microscopy**	Pit/Pore/Crack Free	Micro-cracked	Pit/Pore/Crack Free	Pit/Pore/Crack Free	Pit/Pore/Crack Free	Pit/Pore/Crack Free
Microstructure	**TEM/XRD**	Microcrystalline	-	Nanocrystalline (grain size 5-15nm)	Nanocrystalline (grain size 5-15nm)	Nanocrystalline (grain size 5-15nm	Nanocrystalline (grain size 5-15nm
Hardness	**Vickers Microhardness**	100-150 VHN	Min. 600 VHN	532±13VHN	563±8VHN	569±7VHN	556±16VHN
		-	-	671±8VHN (post-HT)	696±12VHN (post-HT)	685±15VHN (post-HT)	663±23VHN (post-HT)
Ductility	**Bend Test**	10%	<1%	5.29%	4.67%	3.12%	5.03%
Wear Volume Loss	**Pin-on-disc (against Al_2O_3 pin)**	N/A	9 - 11 x 10^{-6} mm^3/Nm	6.76 x 10^{-6} mm^3/Nm	5.13 x 10^{-6} mm^3/Nm	7.05 x 10^{-6} mm^3/Nm	6.28 x 10^{-6} mm^3/Nm
Coefficient of Friction	**Pin-on-disc (against Al_2O_3 pin)**	N/A	0.7	0.40	0.52	0.66	0.50
Taber Wear	**CS-17 abrasive wheel**	42 mg/1000cycles	3-4 mg/1000cycles	18.32±0.16 mg/1000cycles	17.67±0.08 mg/1000cycles	4.88±0.29 mg/1000cycles	12.01±0.15 mg/1000cycles
Corrosion Resistance	**Salt Spray**	Protection Rating 8 (1000 h salt spray)	Protection Rating 2 (1000 h salt spray)	Protection Rating 8 (1000 h salt spray)	1000 h salt spray	1000 h salt spray	1000 h salt spray
Hydrogen Embrittlement	**Mechanical Hydrogen Embrittlement**	Pass with bake	Pass with bake	Pass with bake	Pass with bake	Pass with bake	Pass with bake

4.6 Complimentary Studies

1. Computational Dynamics

The nCoP, nCoP-diamond and nCoP-alumina dopant plating solutions were characterized to acquire the cathodic polarization curves and solutions efficiencies. This data was used as boundary conditions for conducting plating simulation using an arbitrary Hull Cell geometry with the multi-physics software Siemens Simcenter Star CCM+ and found that the plating efficiency of CoP is >90%, whereas CoP-diamond and CoP-Alumina dopant >80%. Please see Appendix F for the full report from Corrdesa.

2. Cirrus Dopant

Post scale-up, Cirrus materials investigated smaller particle size Zr-dopant system. Preliminary testing showed that the CoP-Zr system displayed a low coefficient of friction. Building on that Cirrus investigated dual dopant systems which displayed good microhardness (~ 600 VHN). A dual system (Zr-dopant and Al-dopant) sample displayed very high microhardness ranging from 600VHN to 3700 VHN. This result remains unexplained and further research is needed to provide a method to significantly improve dopant uptake in the substrate and coating hardness. Cirrus shipped two Taber wear panels to Integran to perform wear testing, one sample with the best zirconia dopant and the other with the dual dopant system. Preliminary evaluation indicated minor improvement in hardness and Taber wear, where the Zr-dopant had a taber wear of 11.43mg/1000 cycles and surface hardness of 579VHN. The dual dopant had a taber wear of 10.87mg/1000cycles and surface hardness of 584VHN. Please see appendix G for a full report produced by Cirrus Material Science on this development effort.

3. Structural-Tarnish Resistant Coating

In collaborative effort with VaporTech, Integran investigated a novel PVD topcoat to provide additional tarnish resistance and surface hardness to the nCoP coating. Four different thin-film PVD topcoats applied onto nCoP samples were investigated, including Chrome, CrN, Cr2N and ZrOC. The samples were tested for microhardness, corrosion and Taber wear performance. The top coats applied were less than 2um in thickness with an estimate hardness of greater than 1800 VHN. Only one top coat (ZrOC) was found to provide good tarnish resistance, with excellent Taber wear performance of 3.7mg/100cycles (CS-17 wheels) and >1000h of protection in Salt Spray with no evident sign of tarnishing. Surface hardness of this hybrid coating was found to be 817±13VHN.

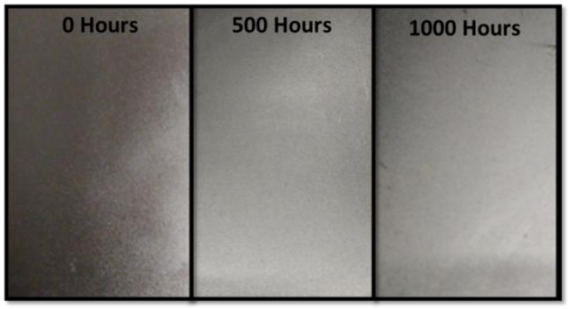

Figure 42 B117 results of the tarnish resistant hybrid coating

5. SUMMARY / CONCLUSIONS

The overall project objectives were successfully accomplished in this project. The main accomplishments in the project include:

- *nCoP Process Optimization* – Integran successfully optimized the nCoP deposition process such that nanostructured CoP coatings could be produced using DC-rectifiers at lower bath operating temperatures (as low as 70°C). Demonstration and validation testing confirmed that properties (hardness, wear, hydrogen embrittlement) were comparable to the standard nCoP coating previously demonstrated in WP-0411. The base nCoP coating (without particulate) meets and exceeds all of the electrolytic Ni properties and could likely be used as an alternative.

- *Nanometal Matrix Composite Development* – nCoP-composite coatings were successfully developed based on two different fabrication methods: i) co-deposition of second phase particulate (from particle suspension baths) showed significant improvement in abrasive wear performance over the baseline nCoP coating, achieving Taber wear as low as ~ 4mg/1000cycles for the nCoP-Diamond system (down from 18mg/1000cycles), and ii) development of nCoP-composite coatings based on the Cirrus Materials Science dopant technology in which co-deposited nanoparticles are formed in-situ achieved a Taber wear as low as ~ 11mg/1000cycles. Ductility testing performed on nCoP-composite samples fabricated from both methods showed that reasonable ductility was retained with the inclusion of the particles.
    - Out of all of the nCoP-composite coatings evaluated, only the nCoP-Diamond system had a Taber wear resistance similar to EHC.
    - The Cirrus Dopant Technology showed some improvement in Taber wear resistance, but did not meet that of the EHC. The nCoP process stability was also effected with the use of the Cirrus Dopants with significant phosphorous additive additions required to maintain phosphorus levels in the deposit

- *Substrate Compatibility for Repair Applications* – The nCoP process was successfully demonstrated to be suitable for repair of steel and aluminum substrates; providing good galvanic corrosion compatibility and excellent adhesion. The high hardness and excellent wear resistance of the nCoP coating was found to provide significantly enhanced surface durability to both steel and aluminum substrates. The excellent structural properties of the nanometal coating was also found to significantly enhance mechanical properties of aluminum substrates with a relatively thin layer of nanometal coating. Three-point bend tests performed on aluminum substrates coated with 100µm thick nCoP coatings showed a two-fold increase in flexural strength.

- *Demonstration of Novel Localized Repair Method for Thick Repairs* – A novel localized repair method was demonstrated on a modified nCoP-composite plating chemistry. Integran's Encased Contact Free (ECF) plating setup involves a fully contained plating head that can be attached to surfaces requiring repair. Plating solution is then pumped through the plating head resulting localized plating without the mess typically associated

with brush plating. Testing performed in the project demonstrated that the method was compatible with the nCoP-Composite coatings developed in the project.

Table 19 presents the benefits and drawbacks of each system that was successfully scaled-up.

Table 19 Benefits and Drawbacks of nCoP Composite Systems

System	Benefits	Drawbacks
All CoP systems	1. Can now be DC plated at a lower temperature → good for decreasing cost of implementation and ease of use. 2. Faster deposition rate and better efficiency than EHC - 125µm/hour vs. 15µm/hour. 3. Better sliding wear, ductility and corrosion performance than EHC. 4. Better Taber wear, sliding wear and hardness than Electrolytic Nickel 5. Electroplating data available enabling use of computational design and modelling of CoP electrochemical deposition processes	1. Hardness of as-deposited material is not as high as EHC.
CoP-Diamond	1. Taber wear resistance is similar to EHC 2. Low levels of added particulate do not significantly decrease ductility 3. Process is stable and repeatable	1. Fatigue data not available 2. Maintaining particle is suspension adds some complexity to the process
CoP-Alumina Dopant	1. Liquid additive i.e. easy to handle.	1. Taber wear resistance and hardness are not as high as EHC 2. Additions of Dopant need to be added continually during the process 3. Dopant additions have a negative effect on phosphorous levels in the bath, requiring significant additions of phosphorous to maintain deposit content

6. IMPLICATIONS FOR FUTURE RESEARCH AND BENEFITS

6.1 Overall Benefits

EHC Replacement
All CoP-based configurations (CoP, CoP-Diamond, CoP-Silicon Carbide, and CoP-Alumina Dopant) are fully dense, with great corrosion performance, good hydrogen embrittlement resistance and better sliding wear performance and ductility than EHC. This makes CoP a suitable candidate for applications requiring good sliding wear properties such as hydraulics.

For applications that require superior Taber wear resistance, CoP-Diamond system is a suitable replacement for EHC as it can be deposited at 125µm/hour vs EHC 15µm/hour. The fast deposition rate is also an asset for quicker repairs.

Nickel Replacement
All down-selected systems: CoP, CoP-Diamond, CoP-Silicon Carbide, and CoP-Alumina Dopant display better taber wear and hardness properties than Electroplated Ni. For full property comparison please see Table 18.

6.2 Future Work and Research

Fatigue
The original CoP (R3010) displays better fatigue properties than EHC, both in rotating beam fatigue and axial fatigue testing. However, the fatigue properties of the new CoP-Composite systems were not evaluated in this project but is required.

As most of the properties of the CoP matrix developed in task 1 are similar to the properties of the original CoP, it is anticipated that the fatigue performance will also be similar. The particle containing systems displayed good wear performance, corrosion resistance and still possessed reasonable ductility, however the fatigue performance has not been assessed. Fatigue testing should be carried out to determine the effect particles in the deposit has on the fatigue performance.

ECF Apparatus
Following the successful completion of this project, a few aspects present an interesting investigation opportunity to satisfy current environmental challenges being explored by the DoD, specifically the development and optimization of the ECF Plating apparatus for selective repair, application and stripping of coating would be interesting to pursue further.

As previously mentioned, the ECF was originally developed by Integran for repair application in the nuclear industry where it is critical for the repair process to be isolated from the environment. An opportunity lies in further investigating and developing the design and repair process associated around the ECF apparatus as application of ECF plating apparatus isolates the process from the environment but also the workers. This implies that application of ECF could result in improved coating lifecycle weapon system compliance to applicable environmental (40 CFR, Parts I and VII) and worker Occupational Health and Safety (29 CFR, Chapter XVII) regulations when

compared with current and legacy systems.

- Scalability: ECF apparatus can be molded to suit the substrate being repaired. Need to study the effect of depending on geometry and complexity of the substrate, optimize and understand the effect of flow conditions and other operating parameters.
- The chemistry used with the ECF system was a simple chemistry. Composite/layered coatings can easily be formed by switching the plating solution reservoir chemistry or by manipulating the incoming solution channels. However, further research is required to improve efficiency.

7. REFERENCES

[1] J. R. López, G. Stremsdoerfer, G. Trejo, R. Ortega, J. J. Pérez, Y. Meas, *Int. J. Electrochem. Sci.*, 7 (2012) 12244 - 12253

[2] T. Takenaka, T. Ono, Y. Narazaki, Y. Naka, M. Kawakami, Electrochimica Acta, 53(1) (2007): 117-121, https://doi.org/10.1016/j.electacta.2007.03.027

[3] G. Lin, W. Yang, Y. Wan, P. Tang, B. Wei, S. Zhang, *Journal of Rare Earths*, 27(2009) 259-263, https://doi.org/10.1016/S1002-0721(08)60231-8 .

[4] W. Chen, W. Gao, *Electrochimica Acta*, 55 (2010), 6865-6871

[5] S. Ghaziof, W. Gao, *Applied Surface Science*, 311 (2014), 635-642

[6] S. Ghaziof, W. Gao, *Journal of Alloys and Compounds*, 622 (2015), 918-924

[7] H. Gül, F. Kılıç, M. Uysal, S. Aslan, A. Alp, H. Akbulut. *Applied Surface Science 25*8, no. 10 (2012): 4260-4267.

[8] F. Kilic, H. Gul, S. Aslan, A. Alp, H. Akbulut. *Colloids and Surfaces a-Physicochemical and Engineering Aspects* 419, (2013): 53-60.

[9] J. W. Martin, Precipitation Hardening: Second Edition (1998), http://www.sciencedirect.com/science/book/9780750638852

[10] J. F. Archard, *Journal of Applied Physics*, 24 (1953) 981.

[11] M. Mosallanejad, A. Shafyei and S. Akhavan, "Simultaneous co-deposition of SiC and CNT into the Ni coating", *Canadian Metallurgical Quarterly*, vol. 55, no. 2, pp. 147-155, 2016.

8. APPENDICES

6.3 Appendix A – Comparison of nCoP and EHC processes and properties

Table A-1 nCoP and EHC process comparison

	nCoP	EHC
Deposition Method	Electrodeposition	Electrodeposition
Applicable Geometries	LOS and NLOS	LOS and NLOS
Efficiency	85-95%	15-35%
Deposition Rate	0.002”-0.008” per hour	0.0005”-0.001” per hour
Emission Analysis	Below OSHA limits	Cr^{+6}

Table A-2 nCoP and EHC properties comparison

	Test Method	Applicable Standard	nCoP	EHC
Appearance	Microscopy	-	Pit/Pore/Crack Free	Micro-cracked
Microstructure	TEM/XRD	-	Nanocrystalline (grain size 5-15nm)	-
Hardness	Vickers Microhardness	ASTM B578	530 – 600 VHN 600 – 750 VHN (heat treated)	Min. 600 VHN -
Ductility	Bend Test	ASTM B489	2-7%	<1%
Wear Volume Loss	Pin-on-disc (against Al_2O_3 pin)	ASTM G99	$6 – 7 \times 10^{-6}$ mm^3/Nm	$9 – 11 \times 10^{-6}$ mm^3/Nm
Coefficient of Friction	Pin-on-disc (against Al_2O_3 pin)	ASTM G99	0.4 - 0.5	0.7
Pin Wear	Pin-on-disc (against Al_2O_3 pin)	ASTM G99	Mild	Severe
Corrosion Resistance	Salt Spray	ASTM B117	Protection Rating 8 (1000 h salt spray)	Protection Rating 2 (1000 h salt spray)
Hydrogen Embrittlement	Mechanical Hydrogen Embrittlement	ASTM F519	Pass with bake	Pass with bake
Fatigue	Rotating Beam Fatigue	ISO 1143	Credit vs. EHC, Similar to vs. bare	Significant debit
	Axial Fatigue	ASTM E466	Credit vs. EHC and bare	Significant debit

6.4 Appendix B – Cirrus Year 1 report

Please see attached report.

SERDP WP2609

Summary Research Report – September 2017

1. Introduction

As the first year of programme WP2609 has completed, this document details the research outcomes, including the September most recent research results. It should be noted that the project started approximately 1 month later than expected, however the Year One objectives have been substantially achieved in the shorter timeframe. Section 2 of the document describes the programme research goals for the first year. Section 3 discusses experimental procedures. Section 4 discusses the bath stand-up results and issues. Section 5 presents the dopant selection process and provides a summary of dopant performance results. Section 6 presents and discusses coating hardness results. Section 7 presents and discusses coating wear resistance results. Section 8 discusses bath stability and maintenance issues. Section 9 presents the measurement on the Taber panels provided for Integran's testing. Section 10 summarises overall work to date and suggests future research directions

2. WP2609 Goals

In Year One, the project utilised Integran's existing nCoP bath chemistry and applied plating procedures, operating at laboratory scale. The primary objectives were:

a) *nCoP process stand-up at Cirrus*: logistics and plating line setup within the Cirrus Materials laboratory based at Rigg Electroplating Ltd in Auckland NZ, using Integran down-selected metal matrix from WP26-09 Task 1.

b) *Evaluate Dopant Compatibility with nCoP Chemistry:* analyze the formulation of the candidate nCoP bath for compatibility with the existing dopant chemistries and existing dopants. Based on preliminary analysis, select one of the existing dopants chemistries for a first level of evaluation. The evaluation is to be conducted at laboratory beaker scale to assess the selected dopant chemistry for stability and longevity when combined with the target bath. Work is to commence with $\leq$200 ml of the bath, with the objective of understanding the maximum quantity of the selected dopant that may be added to the nCoP chemistry while maintaining sufficiently small particle size in the electrolyte. Where required the selected dopant may be subject to minor modification to improve its stability in the target nCoP bath. A further test is to be performed to ensure that the dopant remains stable in the bath over an extended period. This test is to be performed by storing a bath doped at half the determined maximum level at room temperature and re-examining it for particles and precipitate at a regular interval.

c) *Determine Preferred Doping Levels*: The selected dopant for the initial task (b) is to be subjected to several plating tests to determine a preferred doping level with the dopant. Prior experience indicates that a doping level of between 0.5% by volume and 2% by volume works with many plating baths. While a wide range of doping levels may produce improved

coating performance there is typically a narrow range where the performance is optimized. During these experiments, small test baths are to be used and plating performed on mild steel (3 x 2 cm2) samples for simplicity. In each test, a new bath is to be used and a reference sample plated without dopant to evaluate the improvement. Samples are to be prepared on mild steel samples that have been appropriately pre-treated, and then plated using the optimum parameters for the bath (determined from the supplier TDS) to create coatings of approximately 10 - 20µM in thickness. Each sample is to be subject to hardness testing (which is a useful initial discriminant for coating improvement). Samples are also to be subject to surface and cross section analysis to ensure that the coatings are compact and without visible cracks and pores. From these results, one or two doping levels are to be selected for further analysis. The ideal outcome from this step is a range of doping levels at which the mechanical improvements are equivalent. The high end of this range is likely to be the preferred doping level and the low end of the range used to define the dopant exhaustion level for a bath.

d) *Confirm Coating Performance:* a second level of analysis is to be performed by coating selected target substrate samples with the optimum levels of dopant in baths of up to 6L capacity. This work is to begin with DC plating, and graduate to the target pulse plating waveforms. A new bath is to be used for coating each sample set, however depending on the sample size and batch capacity multiple samples may be plated at one time. These samples are to be coated to a target thickness agreed with Integran for their further evaluation. The test protocol for these samples, to be agreed with Integran, for tests initially performed at UoA facilities.

e) *Determine Bath Management Parameters*: provided Integran testing of samples confirms the initial results, further analysis of the coating process will be performed by Cirrus (NB: this task is still to be completed).

Once again, despite the late start of on the programme these objectives have been substantially achieved, it should be noted that, given the very low pH of the Integran nCoP bath, additional dopant optimisation for low pH nCoP may be worth consideration in Year Two. This is further discussed in section 6 below.

In Year Two, Cirrus programme goals are to support the adaptation of the doped nCoP process to brush plating.

3. Experimental Procedures

A variety of configurations and experimental procedures were used during the project. This section of the document outlines the essential elements of these procedures.

3.1. Substrates and Power

Three substrates were used in the project. These were:

Substrate	Size (mm)	Area (cm^2)	Pre-treatment Regime
Galvanised mild steel	20 x 30 x 1	13	1
Q Panel 4130 steel **Cut to 33 x 25.4 size also**	101.6 x 25.4 x 1.016	54.19	2

Taber TA	101.6 x 101.6 x 0.81	103.22 (ss) 239.37 (ds)	2

Figure 1: Substrates Used

The nCoP bath uses high current densities to achieve a nanostructured CoP coating. The TDS calls for a current density of 135 mA/cm^2, although both 165 mA/cm^2 and 80 mA/cm^2 were used at certain times. Given the substrates sizes above, high current power supplies were required. The initial DC plated samples (13 cm^2) required a maximum current of between 1A and 2A, well within the scope of laboratory power supplies, however the later samples required currents between 7A DC and 64A PP. For this reason, Cirrus acquired a high capacity Dynatronix pulse plating supply.

3.2. Pre-treatment

Two pre-treatment regimes were used for the samples, labelled 1 and 2 in Figure 1 above. The difference between these two pre-treatments was the acid pickling step, which was required to remove the zinc coating. The following is the procedure used.

- Acid pickling in 10% H_2SO_4 for 2 min at room temperature to remove Zn coating
- Rinse with tap followed by DI water
- Alkaline de-ruster (ADR) at room temp
    - 2 min cathodic at 10 mA/cm^2
    - 1 min anodic at 10 mA/cm^2
- Rinse with tap and DI water
- Immerse in '345' solution
    - 1 min cathodic at 10 mA/cm^2 cathodic
- Rinse with tap and DI water
- Immediately place in plating solution

The ADR used was a commercial solution METEX DYNAMO which is a chelated descaler that is mixed with sodium cyanide.

'345' solution is an acidic descaler supplied by PPS Industries.

3.3. Anodes

Cobalt anodes were used for all plating. For the early work solid cobalt sheet was selected, however all later plating was performed using bagged titanium mesh anode baskets with cobalt metal rounds. The Taber panels, being large could only be plated on one side with the available anode material.

3.4. Bath configurations

Three bath configurations were used for the project, which were:

- 250 mL beaker on hotplate with magnetic stirring
- 1.8 litre plastic container in insulated stainless-steel water bath. Heating was provided by two laboratory hot plates. Magnetic stirring of the bath was provided by one of the two hot plates
- 6 litre plastic container in the same water bath from above.

Due to the high temperature of the nCoP process, care was required to cover the plating containers and water baths to maintain reliable temperature control. In the larger baths, both the temperature of the water bath and the plating solution were controlled.

3.5. Measurement Equipment and Process

The morphology of coatings and the phosphorous and dopant coatings were measured by scanning electron microscope (SEM) with an energy dispersion spectroscopy (EDS) attachment. The phase structure and crystallite size of the coatings were determined by using X-ray diffraction (XRD). The hardness of coatings was measured by using microhardness tester (Struers DuraScan) with a Vickers diamond indenter. The applied load was 100 gf with a holding time of 10 s. At least 5 measurements under the same conditions were conducted, and the average value was calculated as the microhardness (HV). The wear property of the coatings was conducted by using a NANOVEA tribometer where the alumina ball of 6 mm in diameter acted as friction counterpart. The test was conducted with a load of 7 N and sliding speed of 100 rpm at room temperature with a relative humidity of ~50%. The concentration of P and Co in the bath solution was tested by using Inductively Coupled Plasma Mass Spectrometry (ICP-MS, Agilent 7700).

4. nCoP Process Stand-up Outcomes

Cirrus had several issues with successfully replicating the exact coating performance and composition results outlined in the Integran documentation. These were attributed to:

- The small scale of the initial plating works was not able to replicate plating performance in the larger tank.
- XRF set-up differences creating problems in comparing analysis results.
- Rapid dissolution of cobalt anodes resulting in unstable cobalt levels in the plating bath

Despite these factors, Cirrus and Integran agreed that the results obtained were sufficiently like lab scale plating results at Integran to provide a baseline for the program to continue. This section of the document presents the baseline coating performance to which the doped coatings were compared.

4.1. Coating Composition

A key aspect of the nCoP coating is it's nanostructure, XRD is often used to evaluate the crystalline structure of a coating with the crystal size determined by measuring the peak broadening from the spectra. Figure 2 shows the process reference spectra provided by Integran.

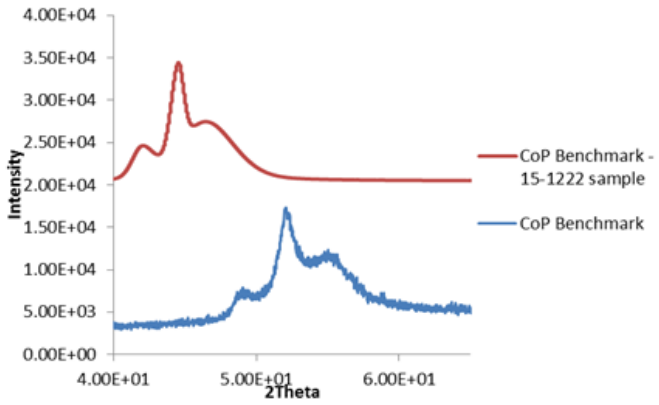

Figure 2: Integran XRD for nCoP

Unfortunately, the XRD measured by Cirrus had the form but not the substance of the Integran result. Ultimately, the results were determined to be sufficiently similar in curve shape to ascertain that a nanostructured coating was being produced at Cirrus.

Figure 3: Cirrus nCoP XRD Spectra

4.2. Coating Hardness

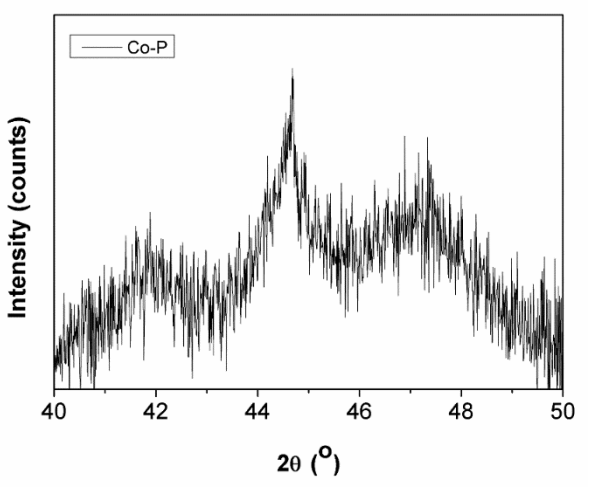

The coating hardness results initially varied widely, this was assumed to be due to the variation of phosphorous of the coatings. Figure 4 shows the early results evaluating the nCoP coating hardness on the cross section, here multiple thin layers were plated using various current densities. This process has worked in the past to rapidly identify a parameter range of interest. The intent was to find an optimum current density for evaluation of the dopant performance. The hardness achieved in all cases was less that the desired hardness for nCoP.

Current Density	**Knoop, $HK_{0.1}$**	
115 mA/cm^2	445.3 ± 25.45	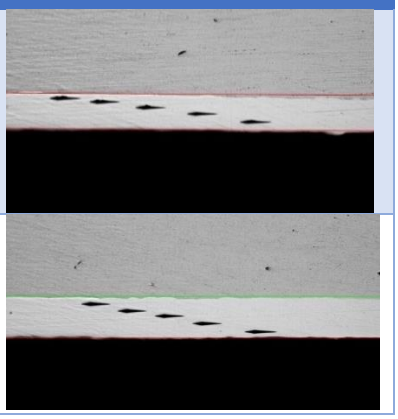
125 mA/cm^2	475.2 ± 16.41	
135 mA/cm^2	461.5 ± 18.56	
145 mA/cm^2	444.0 ± 7.48	
155 mA/cm^2	376.0 ± 35.42	
165 mA/cm^2	502.0 ± 7.00	
175 mA/cm^2	496.3 ± 9.29	
185 mA/cm^2	492.7 ± 6.03	
195 mA/cm^2	494.7 ± 10.69	
205 mA/cm^2	438.3 ± 18.72	

Figure 4: nCoP Initial Hardness Results

Based on these results it was decided to concentrate on plating at the standard current density 135 mA/cm^2 but also perform some work at the lower current density of 80 mA/cm^2. Furthermore, it was decided to always plate more than 50 microns and work with Vickers surface hardness. Figure 5 shows the best hardness obtained for the nCoP coating working on small scale. While the 80 mA/cm^2 with additional A59 additive achieved the best hardness; 135 mA/cm2 was selected as the reference hardness for dopant evaluation (530 $HV_{0.1}$). The measurement of phosphorous content using cross section SEM/EDS provided results were too varied to be used as an effective evaluation criterion.

Sample	**80 mA/cm^2**		**135 mA/cm^2**	
	Hardness	P %	Hardness	P %
Co-P	523.8±11.95	1.0	**531.0**±8.34	0.6
Co-P+4mL/L A59	571.8±13.07	0.9	-	-

Figure 5: Revised nCoP Hardness

4.3. Wear Resistance

The measurement of wear resistance using a Nanovea sliding tribometer proved to be somewhat problematic due to difficulty in measuring wear track width given the nodular surface structure, however the results for 7N load and 135 mA/cm^2, from Figure 6, was selected as a reference value for comparison with doped coatings. 248 µm was used as the reference wear resistance for the nCoP coating.

Coating	135 mA/cm^2 Wear track width µm		165 mA/cm^2 Wear track width µm	
	4N	7N	4N	7N
Co-P	~248	~318	~233	~295

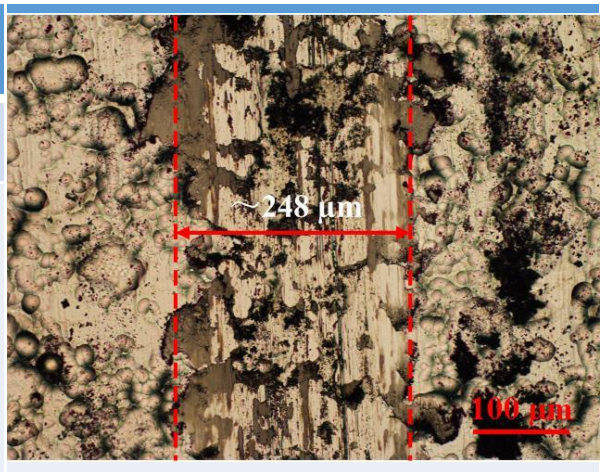

Figure 6: Wear Resistance of nCoP

4.4. Plating Bath Analysis

To understand the ionic concentration of the elements of the plating bath for dopant analysis a new bath and a bath that had been used to plate a set of evaluation samples was analysed using ICP. The results are shown in Figure 7, below.

Sample	Phosphorous	Cobalt
Old	12.69 g/L	73.77 g/L
New	12.12 g/L	69.43 g/L

Figure 7: ICP Analysis of Plating Solution

As may be seen the concentration of cobalt grows significantly during plating. This is assumed to be due to excessive anode dissolution because of the extremely acidic bath. The effect was exacerbated by the small bath volume compared to the anode area. This analysis lead to a change of process where that anodes were removed from the bath immediately after plating to minimise the change on cobalt concentration. Integran indicated that the cobalt and phosphorous concentrations were in the allowable range for the bath.

5. Dopant Selection

At the start of this programme, Cirrus selected three generic dopants: two organic dopants which develop nanoparticles of Titania and Zirconia respectively, and one aqueous dopant which develops Alumina nanoparticles. During the programme the formulation of the aqueous dopant was adapted for improved compatibility with the nCoP bath. This section describes the results of using the various dopants in the nCoP bath. In performing this work, coating hardness was used as a primary discriminant, thus the results here reflect this result. Later sections provide more detail on coating performance.

Initially, the bath compatibility of the dopants was tested by introducing a quantity of each dopant into a small quantity fresh nCoP bath. It was discovered that the aqueous dopant completely dissolved and remained in solution for extended periods. We have samples of bath over 6 months

old where there is no observable precipitate. The two organic dopants dissolved after stirring for a few minutes and remained in solution for experimental periods; however, both organic dopants precipitated if the solution was left for a week. In both cases, the precipitate could be re-dissolved with agitation. These aged, re-dissolved plating solutions still produce acceptable coatings.

5.1. Hardness of Standard Dopants

Initial evaluation of the selected dopants was performed using multi-layer plating. For each layer, the level of dopant was increased and approximately 8 microns of coating performed. Cirrus has found in the past that this approach allows the required dopant level to be rapidly assessed. In each case the plating current was 135 mA/cm^2, the solution temperature was 85℃, and magnetic stirring at 200 rpm was used. Figure 8 shows the results of the preliminary dopant concentration analysis. While the titania dopant required a slightly higher concentration of achieve peak hardness, 10 mL/L was chosen as the standard concentration used for the analysis.

Dopant Level	Knoop Hardness, $HK_{0.1}$		
	Al	Ti	Zr
2.5 mL/L	550.5 ± 17.68	549.0 ± 15.56	532.3 ± 27.10
5.0 mL/L	552.0	569.0 ± 4.24	549.3 ± 17.10
10.0 mL/L	560.5 ± 12.02	**573.5 ± 2.12**	**563.7 ± 23.46**
12.5 mL/L	**568.0 ± 14.14**	564.5 ± 2.12	547.7 ± 29.50
15.0 mL/L	559.0 ± 5.66	544.0 ± 15.56	541.0 ± 20.66
20.0 mL/L	542.0 ± 5.66	517.5 ± 28.99	519.0 ± 13.11
30.0 mL/L	448.5 ± 31.82	402.0 ± 137.18	427.7 ± 14.36

Figure 8: Dopant Evaluation Hardness Results

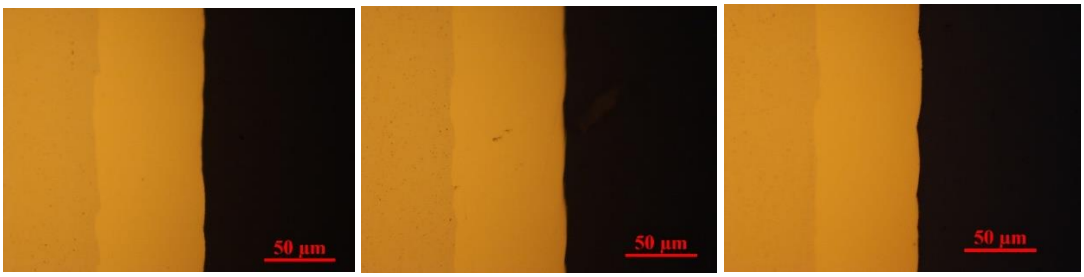

Figure 9: Seven Layer Doped nCoP Cross Sections (Al_2O_3, TiO_2, ZrO_2)

5.2. Dopant Development

During the research, a concern developed that the nitric acid component of the alumina dopant may be affecting the results. Cirrus evaluated other known approaches to creating the aqueous alumina dopant. Several formulations were tried including those peptised with hydrochloric, maleic, citric, lactic acids, etc. Of these hydrochloric appeared to show the most promising results. Figure 10 shows the results.

Coating	Hardness, $HV_{0.1}$
Co-P	531.0±8.34
Co-P+10 mL/L Al (HNO_3)	537.8±16.66
Co-P+10 mL/L Al (HCl)	551.4±9.21

Figure 10: Acid Comparison with Alumina Dopant

In all experiments, a reference nCoP samples was also produced. The table shows the reference together with the alumina dopant with the two acids. It should be

noted that the hardness results in Figure 10 are Vickers whereas the hardness results Figure 8 are Knoop the results for the original alumina dopant are substantially identical. Consequently, it was decided to use the hydrochloric acid for further work.

5.3. Coating Analysis of Gradient Doped Samples

One of the early concerns was whether the dopant was affecting the phosphorous content of the coatings. Thus, an LA-ICP/MS analysis of the gradient doped samples was performed.

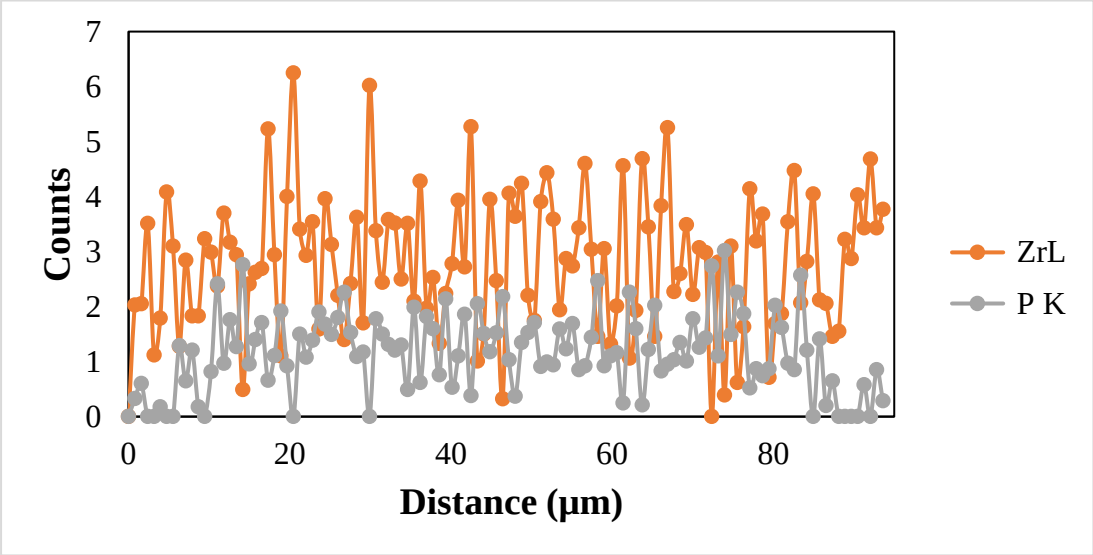

Figure 11: ICP Results for Gradient Zr Doped nCoP

Figure 11 the left side of the image represents the low (2.5 mL/L) Zr level while the right is the high level (30 mL/L). The Zr counts are high through the sample and the P counts low. Zr and P interference in the MS analysis may be the cause; however, the results show that the phosphorous levels remain high. In an analogous manner, the alumina doped sample was analysed, Figure 12 shows the results.

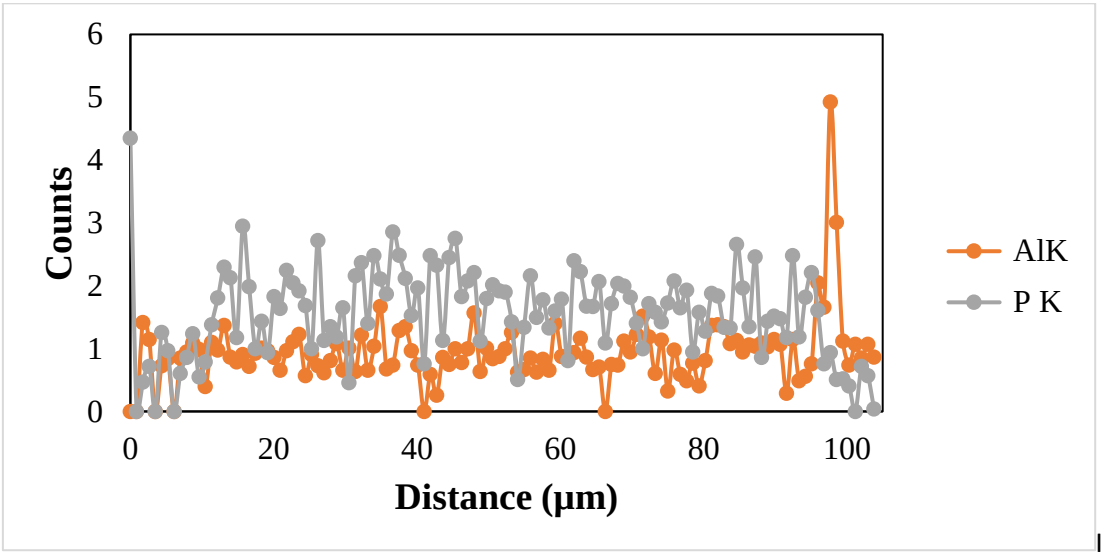

In

Figure 12: ICP Results for Gradient Al Doped nCoP

As may be seen the P counts remain high while the detected Al is low until the very high concentration. As with the previous result the dopant varies from 2.5 mL/L at the left to 30 mL/L at the right.

6. Doped nCoP Coatings Characterisation

Based on the preliminary dopant analysis, Cirrus decided to further investigate both the Zirconia and Alumina generating dopants. The stability of the Titania generating dopant was insufficient to continue the analysis, however it should be noted that the Titania generating dopant produced the hardest coatings. It is possible that formulation of an aqueous Titania generating dopant would produce better results, and this work is ongoing at Cirrus separate from the performance of this project. The majority of the results for Alumina generating dopant presented here were created using the dopant formulated with hydrochloric acid; results from the nitric acid based dopant are flagged.

Cirrus determined that the addition of 10 mL/L of dopant to the nCoP baths results in a hardness improvement between 5% and 8%, this concentration was selected as the doping level based on the initial evaluation of the available dopants.

6.1. Surface Morphology of Coated Surfaces

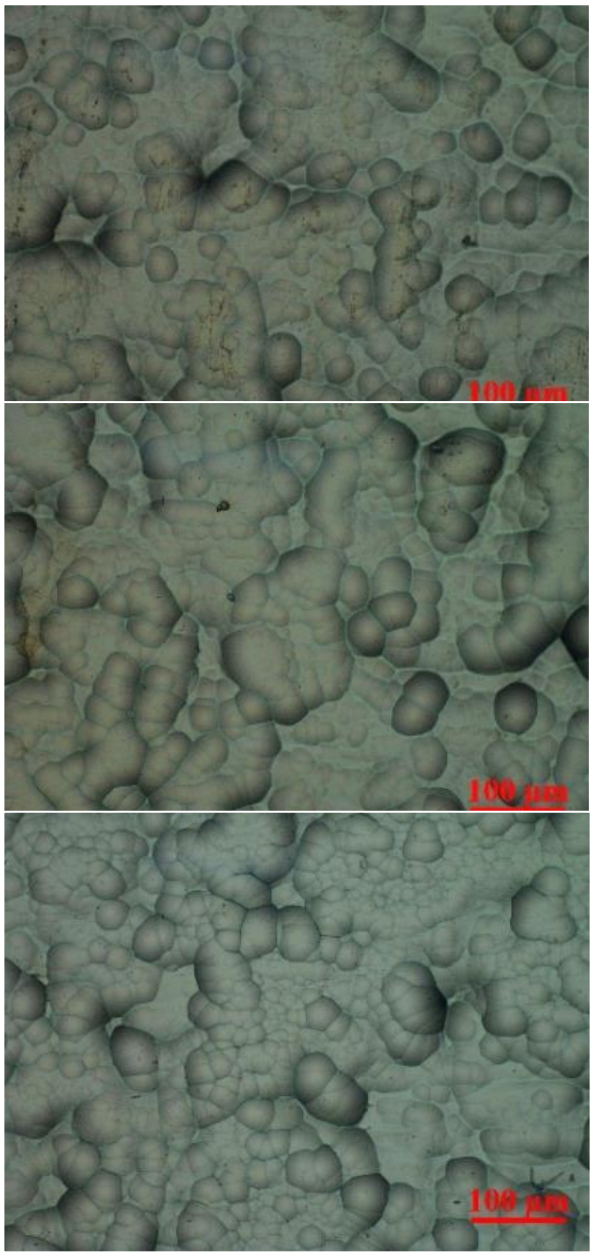

Figure 13: Optical 200 x Top: nCoP, Centre: nCoP + Zr, Bottom: nCoP + Al

A meaningful change in surface morphology often results from the addition of a dopant to a coating bath. This effect is frequently due to changing the grain size and the generation of more compact coating. In the case of the Integran nCoP bath such a change was not observed, probably due to a minimal grain size change. Here we present the both optical and SEM imagery for the doped and original coatings.

As may be observed, in Figure 13, the surface morphology of each of the coating shows a nodular structure typical of nCoP. While the surface of the coating plated from a bath with the organic Zirconia generating dopant is almost identical to that of the nCoP reference coating, the coating with the Alumina dopant shows a larger number of smaller nodules However, SEM imagery is required to further understand the coating morphology.

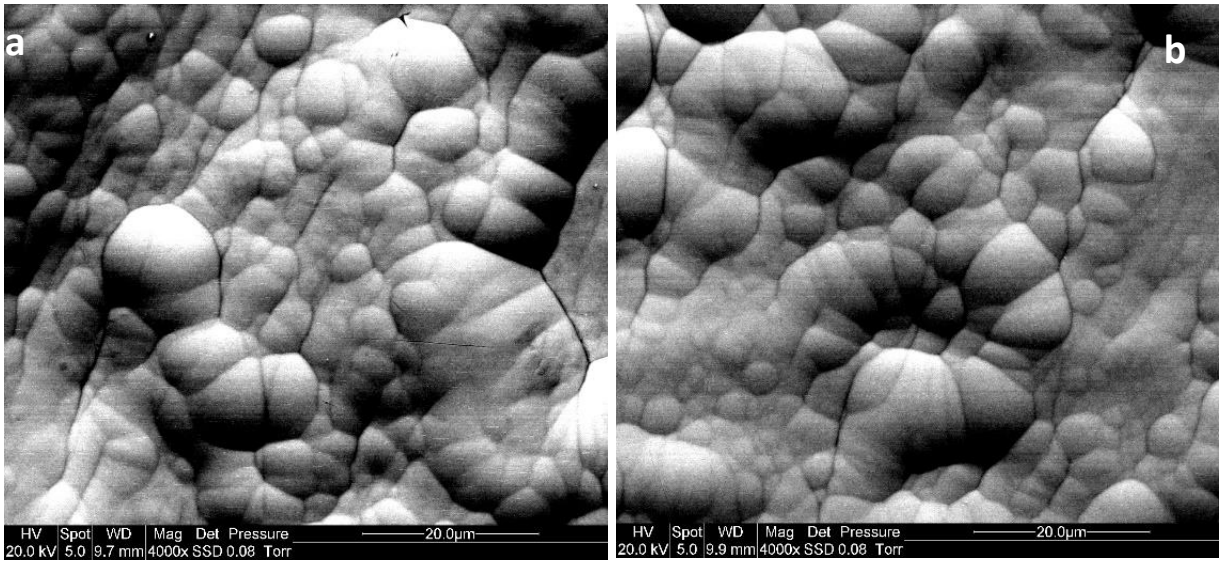

Figure 14: SEM of a) nCoP, b) nCoP + Zr, c) nCoP + Al

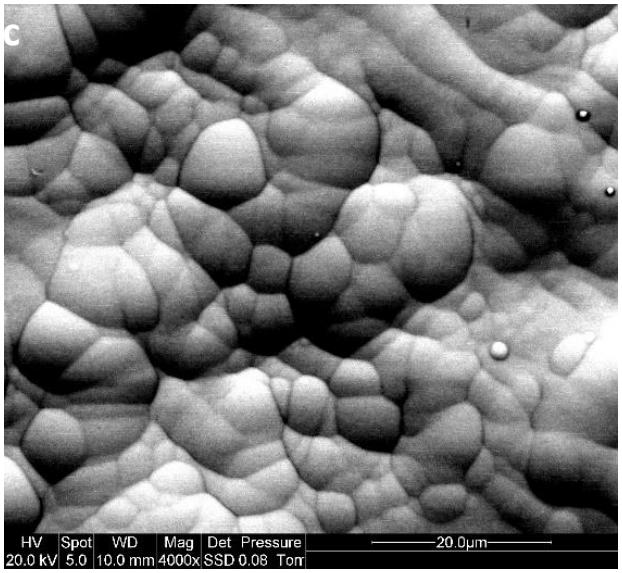

As may be observed in Figure 14 there are very minor differences between the surface morphology of the doped nCoP and nCoP coatings. Once again, there may be a slightly more nodular structure in the coating with the alumina generating dopant. This image is of the coating with the nitric acid based dopant.

The magnification of these images is insufficient to show the nCoP grain structure, which has an expected grain size of 20nm. Given this nanostructure, the presence of the dopant generated 40nm alumina particles are unlikely to significantly impact the grain size., That said, the dopant may provide additional nucleation sites for the grains and could affect the structure in this manner.

Figure 15: Dog-bone cross section a) nCoP + Al, b) nCoP

6.2. Thickness Distribution of Coated Surfaces

The early evaluation samples showed significant variation in hardness and wear resistance. After discussion with Integran, it was decided that the plating thickness should be increased to 100 microns per sample plated. Evaluation of samples with thicker plated coatings showed a significant dog-bone shape of the coating

thickness distribution. Figure 15 depicts several cross-section views of both a nCoP coating and a nCoP coating with alumina generating dopant. Both substrates were plated at 135 mA/cm2 with an expected coating thickness of 125 microns. While the dog-bone cross section may have been due to the small substrate size (20 x 30 mm) with the edges being a sizable percentage of the area there is also a left right variation in the coating thickness. This may have been due to the magnetic agitation. Figure 16 shows the estimated thickness of the coating by coating weight against the measured coating thickness at the centre for a series of samples plated in June and July 2017. The estimated thickness closely correlates with the expected thickness given the current and plating time. The plating thickness was estimated using the area of sample of 17.93 cm^2 plus the area of the wire used to hang the sample, of about as 3.6 cm^2.

Sample	Coating	Measurement			Estimated	Measured	
		Before Cleaning	After Plating	Plating Weight	Thickness (µm)	Left (µm)	Right (µm)
28/6-S1	nCo-P	7.7138	10.1121	2.3983	~125		
28/6-S2	nCo-P	7.8150	10.2284	2.4143	~125	73	102
28/6-S3	nCo-P	7.8415	10.2654	2.4239	~126		
28/6-S4	nCo-P	8.0554	10.4941	2.4387	~127		
29/6-S1	nCo-P+10mL/L Zr	7.7961	10.2100	2.4139	~125		
29/6-S2	nCo-P+10mL/L Zr	7.8029	10.2226	2.4197	~126		
29/6-S3	nCo-P+10mL/L Zr	7.7538	10.1773	2.4235	~126	112	80
29/6-S4	nCo-P+10mL/L Zr	7.8934	10.3241	2.4307	~126		
3/7-S1	nCo-P+10mL/L Al (HCl)	7.9404	10.3541	2.4137	~125		
3/7-S2	nCo-P+10mL/L Al (HCl)	7.9103	10.3278	2.4175	~126		
3/7-S3	nCo-P+10mL/L Al (HCl)	7.9432	10.3743	2.4311	~126	71	104
3/7-S4	nCo-P+10mL/L Al (HCl)	8.0021	10.4248	2.4227	~126		

Figure 16: Measured and Estimated Thickness

6.3. Surface Hardness of Coated Surfaces

As noted previously doped nCoP achieves a 5% - 8% improvement in hardness over standard nCoP. Coating hardness improvements produced by incorporation of nanoparticles in the coating are created by a combination of Hall-Petch strengthening due to grain refinement and precipitation hardening due to dispersed ceramic particles in the matrix. It is believed that due to the nanostructure of nCoP coating the Hall Petch mechanism will have minor impact; however, precipitation hardening is still possible with the ceramic phase impeding dislocation movement and increasing hardness. The impact may be limited by the relatively large particle size produced by aqueous dopants. Figure 17 shows the measured hardness results over several samples. The improvement is relative to the reference hardness of 531 $HV_{0.1}$ for nCoP of developed during the process stand-up. In all instances, the measured hardness is an average of five readings and is presented together with the standard deviation in the readings.

Sample Ref	Coating	Hardness $HV_{0.1}$	Improvement
29/6_S2	nCoP+10mL/L Zr	570.8± 8.73	7.5%
5/5_S5	nCoP+10mL/L Zr	566.6±8.76	6.8%
3/7_S3	nCoP+10mL/L Al	577.6± 6.19	8.67%
8/5_S4	nCoP+10mL/L Al	551.4±9.21	3.8%
8/5_S2	nCoP+10 mL/L Ti	551.0±17.76	3.8%

Figure 17: Hardness Results

As these results show, there is a considerably variation in the measured hardness values with samples produced later having higher hardness results, these samples were plated with thicker coatings.

6.4. Coating Composition

Several coated samples were evaluated for elemental composition, both XRF and SEM/EDS were used for this analysis. The XRF results showed significant variation while SEM/EDS was reasonable consistent. Figure 18, suggests that the dopant suppressed the phosphorous uptake in the coating, thus there may be two hardness effects of the dopant, one being an increase due to the presence of hard particles and one being a reduction due to lower coating phosphorous content. Note that 28/6_S2 exhibited higher hardness that previous nCoP coatings produced with an average hardness of 546.2± 8.64 $HV_{0.1}$, this may be due to a higher than normal phosphorous content.

Sample	Coating	Co	P	Zr	Al	Ti
		Wt%				
13/1_S4	nCoP+10mL/L Zr	98.81	0.96	0.23	-	-
13/1_S4	nCoP+10mL/L Ti	98.93	1.05	-	-	0.03
12/1_S8	nCoP+10mL/L Al	98.59	1.09	-	0.31	-
29/6_S3	nCoP+10mL/L Zr		1.03	0.16		
3/7_S3	nCoP+10mL/L Al		1.04	-	0.1	-
28/6_S2	nCoP		1.1			

Figure 18: Elemental Analysis of Coatings

6.5. Wear Resistance

Unlike with hardness where the improvement created by the dopants was slight, more significant improvements in wear resistance were observed. The data presented here is a combination of several wear resistance measurements. In all cases these results presented are for a 7-newton load at 100 rpm and 10 minutes of wear, with the "Wear" column in Figure 19 showing the average width of the generated wear track in microns. As with the hardness measurements, the improvement percentage shown below is relative to the nCoP measurement during process stand-up at Cirrus.

Sample Ref	Coating	Wear (µm)	Improvement
8/5_S2	nCoP+10mL/L Ti	270	15.1%
8/5_S3	nCoP+10mL/L Al	287	9.7%
5/5_S5	nCoP+10mL/L Zr	273	14.1%
3/7_S3	nCoP+10mL/L Al	280	11.9%
29/6_S3	nCoP+10 mL/L Zr	281	11.6%
8/3_S4	nCoP+10 mL/L Zr	277	12.8%
8/3_S6	nCoP+10mL/L Al (HNO_3)	261	17.9%

Figure 19: Coating Wear Resistance

Given the relatively low measured improvement in coating hardness, the mechanism to improve wear resistance requires explanation. This could be due to the quantity of hard particles in the coating. In prior dopant work with sub 12nm particles, Cirrus seldom directly measured secondary particle presence in the coating using XRF or SEM/EDS. In general, either TEM or LA/ICP-MS are required to estimate secondary particle concentration in doped coatings. That said, with the nCoP coating detectable quantities of particles have been observable by XRF and SEM/EDS. This is likely due the nano-structured coating offering more grain boundary sites where particles may be adsorbed, increasing particle uptake.

A further complication in this work was the difficulty of directly measuring the width of wear tracks due to the coating surface morphology. Figure 20 shows two wear track images for nCoP coatings with alumina generating dopants which illustrate the measurement problem

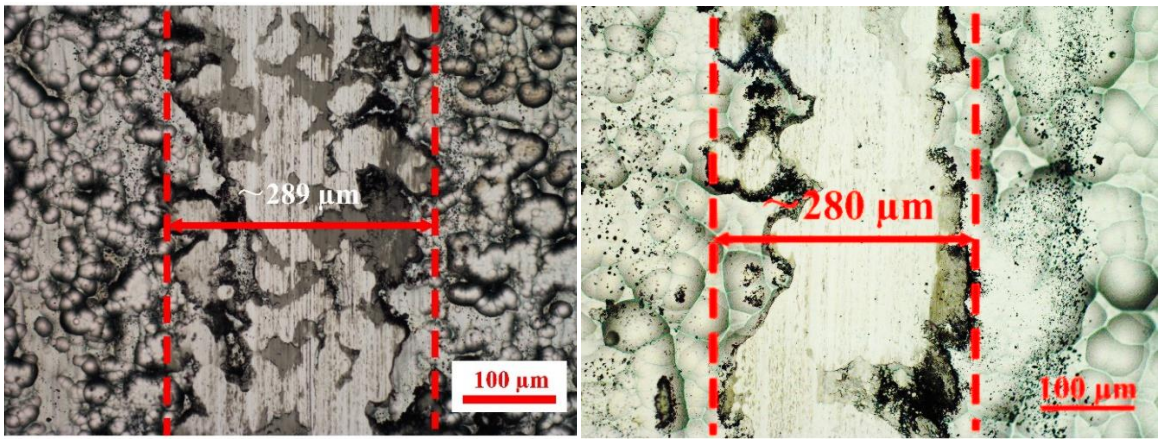

Figure 20: Two nCoP + Al Wear Tracks

7. Bath Stability and Reuse.

During all coating evaluation activities, Cirrus retained each used bath with each dopant for later evaluation. While these baths had varying levels of dopant added, it was estimated that the total dopant per bath would be sufficiently close to 10 mL/L to allow effective reuse of the bath. In our reuse study, we used both the bath "as saved" as well as a formulation adjusted to increase the dopant to 20 mL/L. The purpose of the increased dopant level was to see if this effected the wear resistance. This section of the report discusses the results obtained in the reuse and stability study. For each bath, several samples were plated to an expected coating thickness of 125 microns.

7.1. Coating Structure

SEM studies were performed of the surface of the coating made with the used baths. Figure 21 shows three views of the surface of the coating produced with the used nCoP bath doped containing Zirconia producing dopant. The surface morphology is very different from that observed with a fresh bath (Figure 14), there are significantly greater microstructure on the surface. The used bath with zirconia dopant contained a discernible precipitant, this was reintegrated by vigorous agitation, however larger particles are likely to remain. These larger particles possibly created the changed surface morphology.

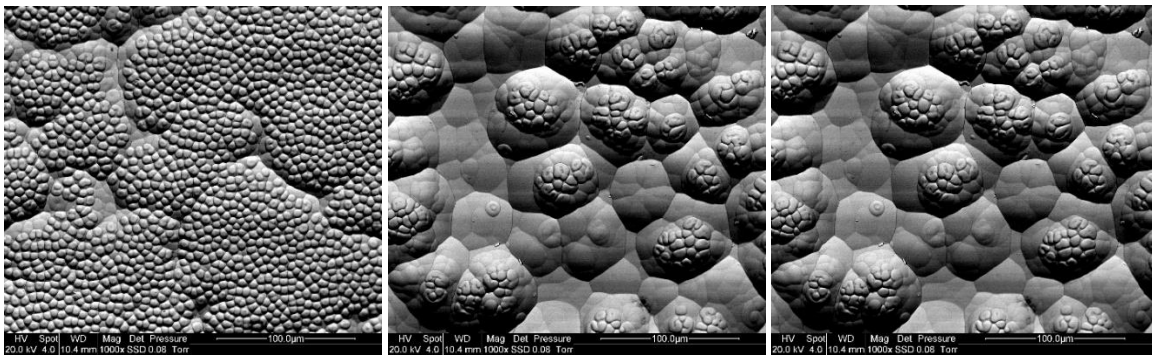

Figure 21: Three views of nCoP + 20 mL/L Zr from a used bath

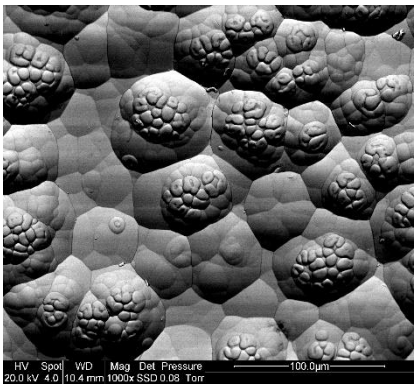

By comparison the used bath with the alumina dopant exhibited a morphology that was little changed from that observed with a fresh bath. Figure 22 shows a single view of this coating which is substantially the same as that produced from a fresh bath (Figure 14). The nodules exhibit a slightly more developed substructure but this may be due to the increased dopant content.

Figure 22: nCoP with 20 mL/L A from used bath

The SEM/EDS results measured from these SEM images are informative, here we observed similar levels of dopant in both the used bath and new bath. The detected Al is 0.25% by weight while the detected Zr is 0.19% by weight. The aluminium was higher than previous measurements (Figure 18) while the Zirconium is lower. It's worth noting that this may reflect the ability of the instrument to accurately measure the elements.

7.2. Hardness and Wear Resistance

From our prior analysis, we would have expected the hardness of these more highly doped baths to be lower than those with optimum dopant and this was the case; however, the wear resistance shows interesting results.

Samples	Hardness ($HV_{0.1}$)	Wear (µm) (as plated)	Wear (µm) (polished)
Co-P+20mL/L Zr	491.8±19.23	251	269
Co-P+20 mL/L Al	556.2±3.35	299	310

Figure 23: Used Bath Performance

While the coating with the zirconia generating dopant exhibited substantially poorer hardness that the equivalent fresh bath (~568 HV), the wear resistance was improved (~274 µm). These samples were tested as plated and lightly polished to remove some of the more significant surface features. The polished wear for the for the zirconia doped sample was substantially the same as the coating from a fresh bath.

The coating with the alumina generating dopant produced a hardness that is little different from the 10 mL/L doped fresh bath (577 HV) but the wear performance was substantially worse, although difficulties with measuring the wear track width may have impacted this result.

While initial results are consistent with gradual secondary particle depletion profiles Cirrus and measured in other works, more analysis is required to understand bath remediation and performance over time for the nCoP bath. This may be due to the nanostructure of the coating and/or the low pH and operating parameters of the bath.

8. Pulse Plated Sample Characterisation

In early August 2017, Cirrus received and commissioned a Dynatronix pule power supply. This allowed us to investigate the difference between DC plating and pulse plating on the mechanical properties of doped nCoP coating. This section of the report presents the results. It should be noted that the research on pulse plating was accomplished with used plating bath as the supply of fresh plating bath was substantially depleted, consequently the results achieved may be considered sub-

optimum. Here we are especially concerned with the depletion of the phosphorous in the bath. Some ICP analysis results are provided in section 8.3.

8.1. Bath Configuration

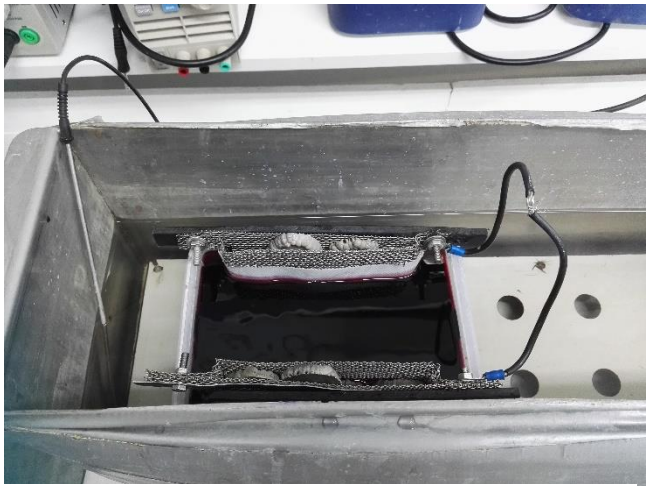

Figure 25: 1.8 Litre Bath Configuration

The availability of the larger power supply supported plating samples of a larger size. This necessitated upscaling our plating bath. We worked Limitations on available anode cobalt material and the larger sample size required that we create two separate baths; one for plating Q-panel substrates and one for Taber panel substrates. These baths were 1.8L and 6L capacity respectively. Maintaining 85℃ bath temperatures in the larger capacity baths necessitated an insulated water bath. The scale up equipment (depicting the 1.8L Q-Panel plating apparatus) is shown in Figure 25.

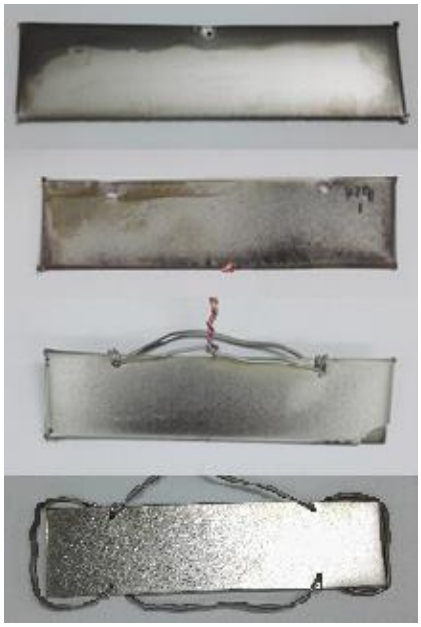

Figure 24: Q Panel Samples

Initially there was some problems plating sampled in the larger scale baths, the images in Figure 24 show various samples. From the top, the samples plated using a single contact point exhibited extreme burning on the upper edge. Transitioning to dual contact points showed improved results, however as bath had been used for many trials depleted organic elements resulted in poor overall plating. In the third image, we changed the anode basket arrangement to provide better anode current distribution and used a heavier gauge wire for connecting the substrate. The plating was very thick and non-adherent on the edges, the lower right corner shows where the plating was peeled off. The final sample shows a sample generated with a four-point connection scheme with a burn wire. This shows a bright surface with a few dull spots where the burn wire is too close to the surface. A jig with providing four titanium contact points and a stainless-steel burn wire was used for all analysis samples. A burn wire was used for some Taber samples (below)

8.2. Surface Morphology

The transition from DC plating to pulse plating resulted in significant changes in surface morphology for samples without dopant but less significant changed for doped samples. However, it appeared that pulse plated samples with dopant exhibited a more compact smoother structure.

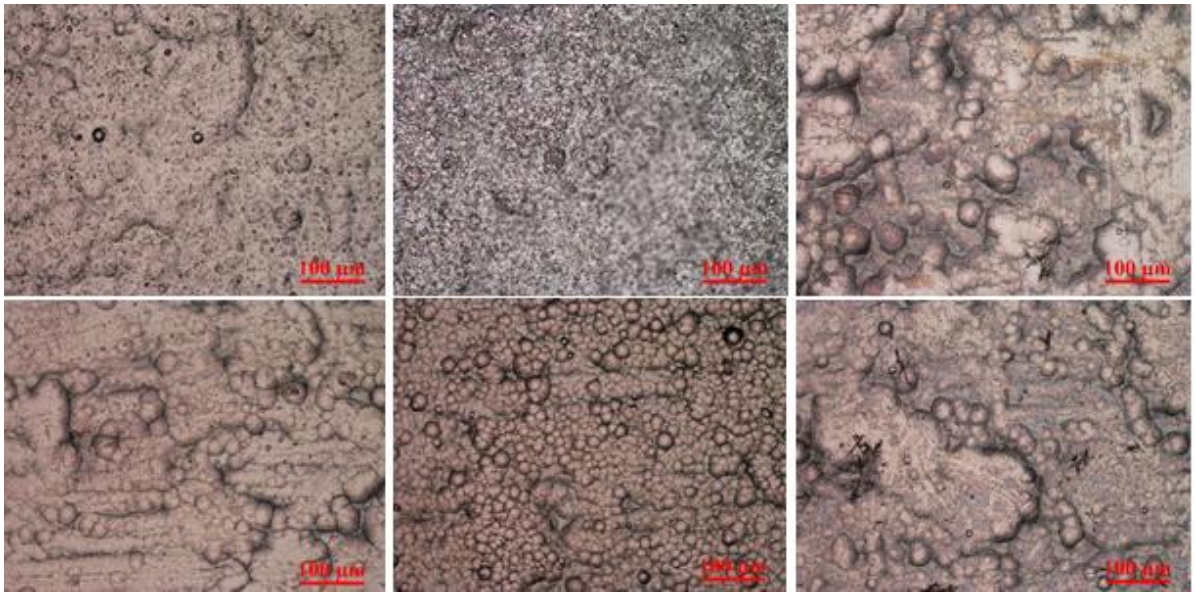

Figure 26: Surface Morphologies 200X, top DC, bottom PC. (left to right nCoP, Al doped, Zr doped)

8.3. Hardness

The hardness of the samples varied significantly from our prior results, note that these results were obtained with used bath and thus could be expected to have high Co concentration relative to the P concentration. Figure 27 summarises the measured hardness values.

Sample	DC Plating	Pulse Plating
nCoP	524.0±20.04	553.4±20.89
nCoP + 10 mL/L Zr dopant	549.2±14.08	562.6±11.87
nCoP + 10 mL/L Al dopant (HCl)	542.0±3.00	592.4±24.30

Figure 27: Pulse Plating Hardness

Clearly these results show interesting trends compared to the DC results. Cirrus have observed that in general pulse plating results in an increased uptake of particles in the coating when compared to DC plating. This is possible du to two effects, replaced of dopant particles near the cathode during the 'OFF' period and disruption of the double layer allowing increased particle uptake.

The plating performed was suboptimum and no exploration of pulse parameters was performed. We used the Integran standard pulse configuration. However, the measured hardness for the Al dopant is significantly improved over the DC case.

8.4. Wear Resistance

As with hardness we observed improvements in wear resistance in pulse plated sampled. In addition, a possible change in wear mechanism for Zr doped samples was suggested by the CoF measurements

Sample	DC Plating	Pulse Plating
nCoP	323	290
nCoP + 10 mL/L Zr dopant	263	238
nCoP + 10 mL/L Al dopant (HCl)	268	244

Figure 28: Pulse Plating Wear Track Widths

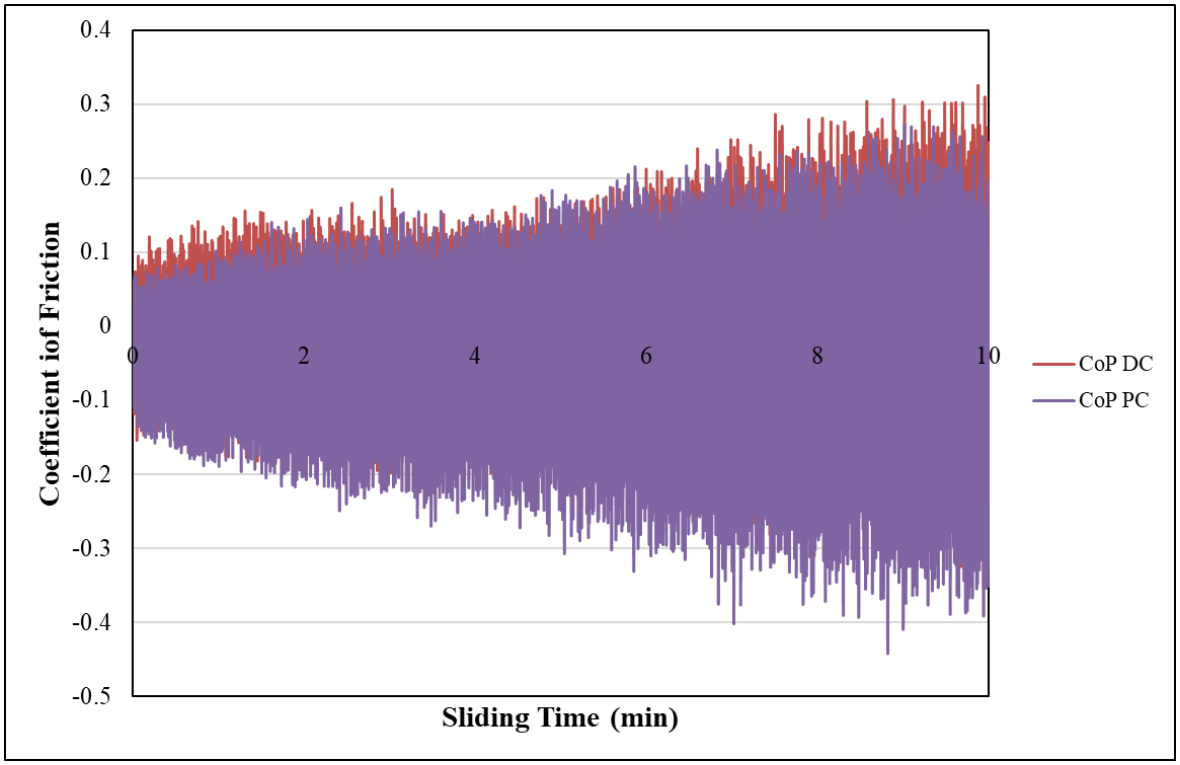

Figure 29: CoP CoF

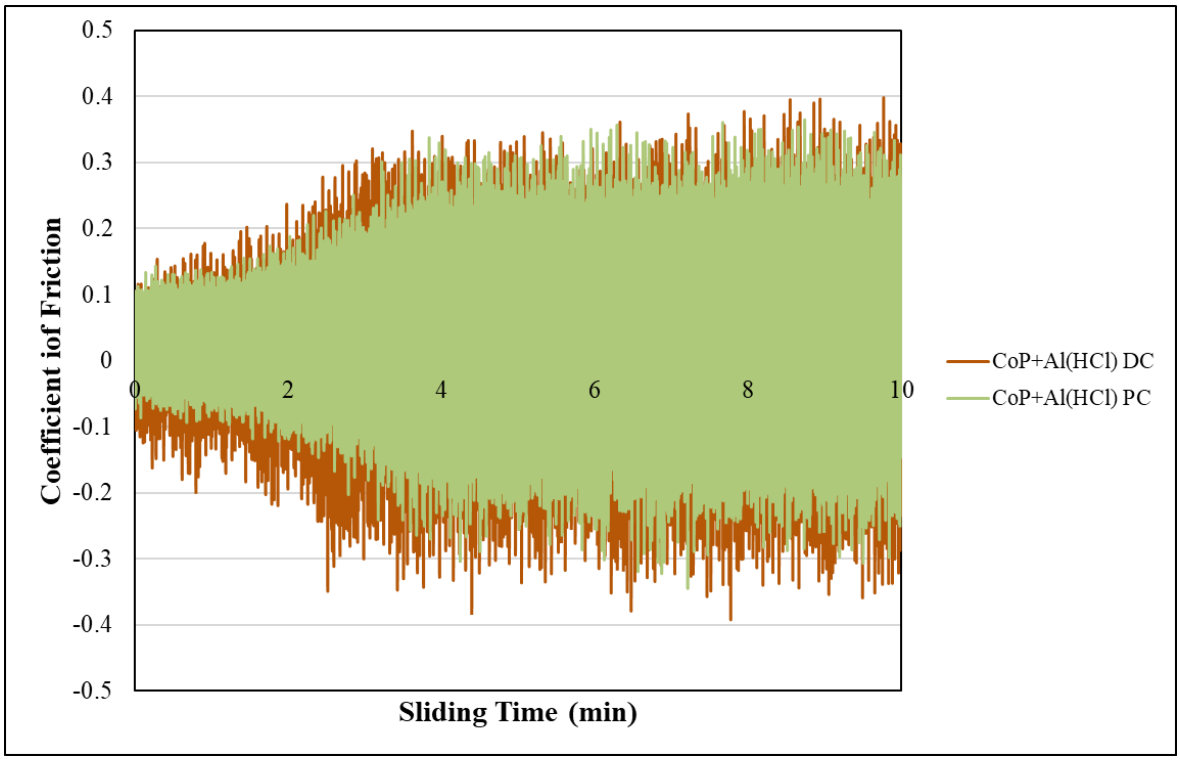

Figure 30: CoP with Al Dopant CoF

Figure 29 and Figure 30 depict the friction curves for the base nCoP coating and the Al doped nCoP coating. The nCoP shows a slow increase in friction as the surface wears while the Al shows a rapid increase in friction. This probably indicates that the Al doped coating suffers ablative

wear initially and then has improved abrasive wear characteristics (as illustrated by the lower wear trach width.

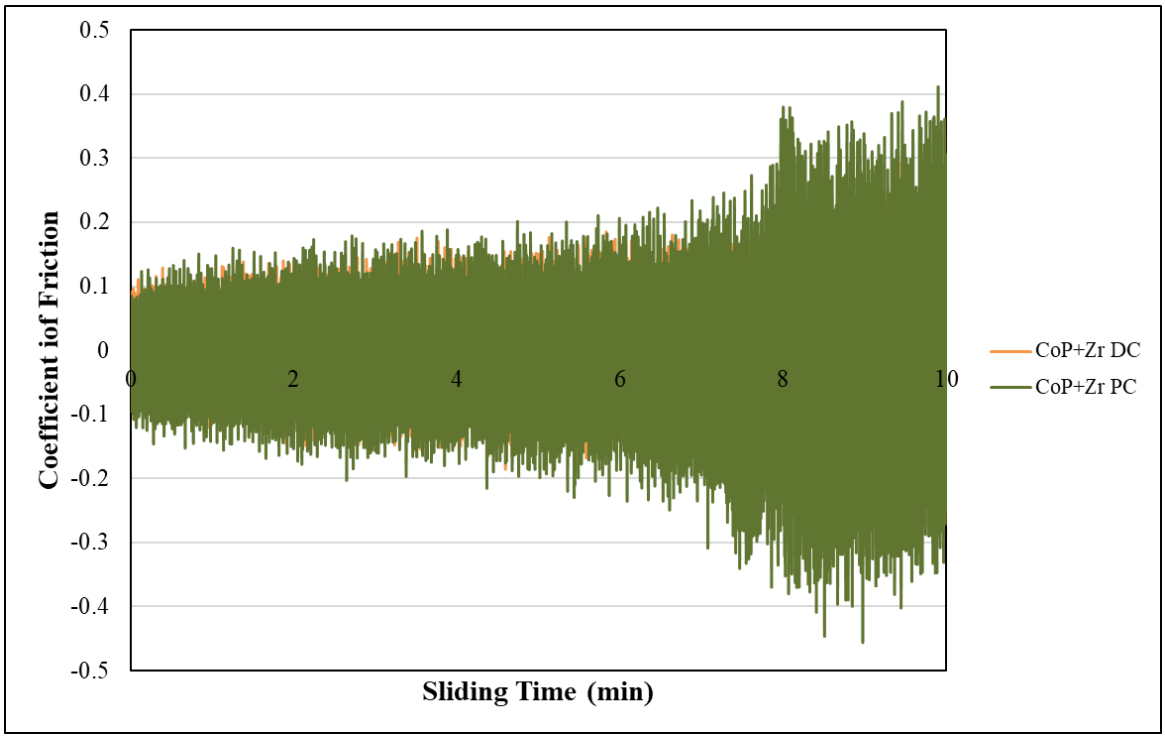

Figure 31: nCoP with Zr CoF

Figure 31 shows the zirconia doped coating which exhibits a completely different wear characteristic from with the plain nCoP or alumina doped nCoP. Clearly here the hard coating had very low abrasive wear initially – after some time either the harder surface layer or the alumina wear ball is changing the nature of the wear.

8.5. ICP Results

To understand whether our work with used solutions would produce valid results we conducted ICP analyses of the various used solutions. Figure 32 shows the results of this analysis

Sample Description	Raw Data				Normalised			
	Co	P	Al	Zr	Co	P	Al	Zr
	g/l	g/l	g/l	g/l	g/l	g/l	g/l	g/l
Used ~10mL/L Al	68.750	13.010	0.016	-	68.750	13.010	0.016	-
Used 20mL/L Al top-up	66.788	12.395	0.027	-	68.750	12.759	0.027	-
Used post plating 1	69.691	12.930	0.027	-	68.750	12.755	0.027	-
Used post plating 2	75.110	14.187	0.036	-	68.750	12.986	0.033	-
Al dopant	-	-	1.222	-				
Used ~13.3 mL/L Zr	72.840	13.154	-	0.110	72.840	13.154	-	0.110
Used 20 mL/L Zr top-up	75.113	13.440	-	0.105	72.840	13.034	-	0.102
Used post plating	78.949	14.177	-	0.153	72.840	13.080	-	0.141
Used filtered	75.694	13.092	-	0.000	72.840	12.599	-	0.000
Used solution nCoP	74.810	13.838	-	-				

Figure 32: ICP Analysis

To perform ICP analysis it was necessary to dilute the samples 1000 times, this created significant measurement errors preventing easy comparison of different samples, consequently Cirrus normalised the results using the cobalt measurement for the original sued solution. While we expect the amount cobalt to grow slightly as plating occurs due to excessive dissolution of the anodes we believe this to be the best way to compare samples. Highlighted figures show where the results obviously have some other introduced error.

The results show that the phosphorous content of the bath is not significantly influenced by plating and this we can expect changed in phosphorous in the coatings to be because of the introduction of dopant. This may be due to the dopant complexing with the cobalt ions and increasing the reduction of cobalt at the surface relative to phosphorous.

As expect the volumes of dopant in the coated surface is very small and we see little reduction of the concentration of dopant due to plating.

The filtered solution with zirconium dopant shows no remaining zirconium indicating significant agglomeration.

The measured dopant metal concentrations are in the bath are line with the metal concentrations on to dopant itself.

9. Taber Samples

Cirrus have prepared several Taber wear panels for further evaluation by Integran. These samples were created in the 6-litre bath configuration and plated on one side. We performed hardness testing on one side of these samples to validate their performance prior to shipping. These samples were made using a burn wire to encourage uniform deposition.

Cirrus measured hardness on the edge of these samples as 540 $HV_{0.1}$ for DC plating and 567 $HV_{0.1}$, for pulse plating, while these are slightly lower than typically measured they are in the ball park. Several factors may have affected these measurements, the plating at the edges, where the measurements were taken, may be affected by the burn wire. The plating thickness may be slightly lower (due to the area of the burn wire). We do however expect to get indicative results from the samples.

10. Conclusions and Further Work.

The programme to date has generated results that indicate that a liquid dopant can improve the mechanical properties of nCoP deposited under typical conditions. The improvement in hardness is between 5% and 8% while the improvement in wear resistance is between 8 and 16%. Improvements observed with pulse plating are higher than this.

The organic dopants produce the better improvements in mechanical properties, however the current formulations are not stable in the low pH of the nCoP. The Titania generating dopants agglomerate and precipitate after a few hours while the zirconia generating dopants precipitate after a few days. The aqueous alumina dopant produces moderate hardness and wear resistance improvements; however, it shows consistent stability in the nCoP bath. The reason for this difference may be the size of particles created by the dopant with Alumina typically creating particles of approximately 40-nm, while organic dopants create particles below 12-nm. Cirrus expect that the smaller particles more easily integrate with the nCoP grain structure and thus result in improved coating properties.

Cirrus have an ongoing project to develop new and improved dopants and expect that we can either create an aqueous dopant with a smaller particle size or an organic dopant that remains stable in both low and high pH baths. Cirrus expect that the outcomes of this project may be able to feed into the SERDP work in year two.

The use of pulse plating shows some interesting improvements on coating mechanical properties at higher dopant concentrations which requires further investigation. This should also form part of the year two SERDP work.

The work on during the second year of the project should focus on the areas outline above. Figure 33 shows a proposed workplan for this effort.

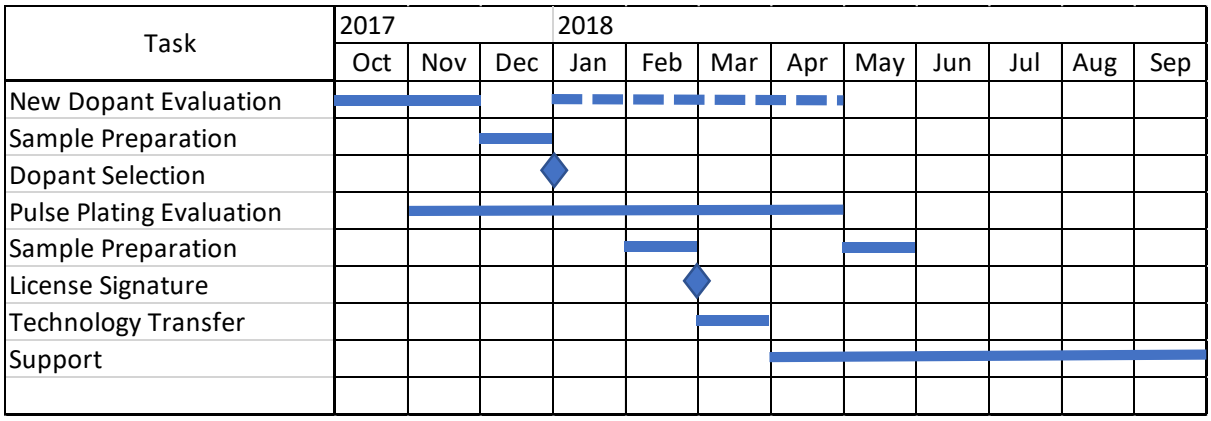

Figure 33: WP2609 Year 2 Work Proposal

6.5 Appendix C – Salt Spray Chamber at Integran (as per ASTM B117)

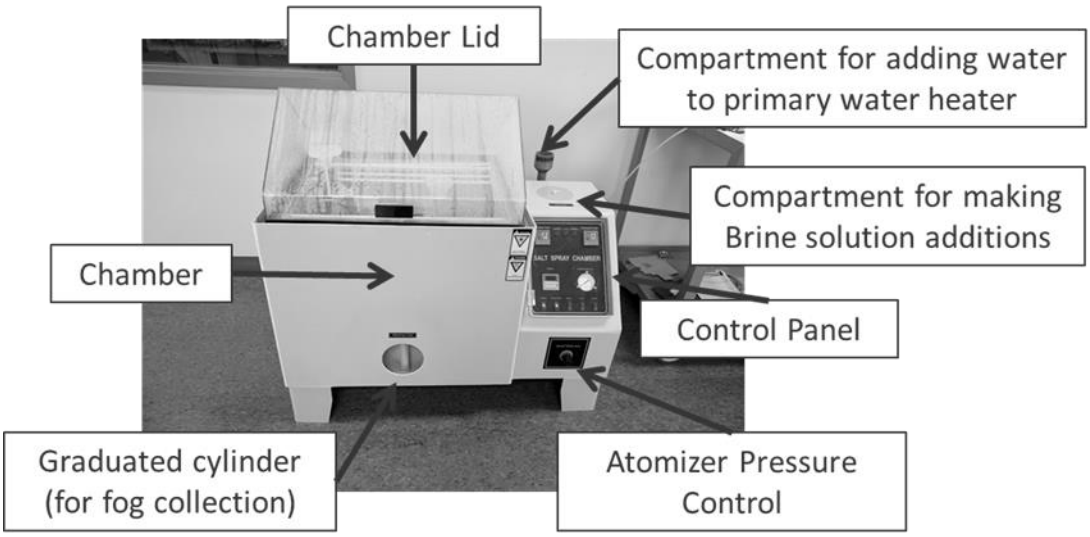

Figure C-1 Salt Spray Chamber

Operating conditions:

- Saline solution: 3.5% NaCl
- Chamber temperature: 35°C
- Record of pH of collected "fog" on regular basis
- Deposits monitored at the following intervals: 24h, 48h, 72h, 96h, 200h, 500h, 1000h.

6.6 Appendix D – Coefficient of friction (μ) and sliding wear rate (SWR) with particle addition

In general, the coefficient of friction and sliding wear rate tests both increase with particle additions. Data was obtained from Pin-on-disk tests, using an Al_2O_3 pin.

Table D-1 Effect of particle size on coefficient of friction and sliding wear rate

particle size (nm)	particle loading (g/L)	Average Coefficient of friction (μ)	SWR* (10E-6 mm^3/Nm) weight loss-basis
40	0	0.58	12.41
	0.2x	0.48	8.36
	0.4x	0.53	13.86
	0.8x	0.58	19.05
	1x	0.59	17.46
	1.5x	0.58	17.37
	2x	0.62	18.33
	4x	0.63	21.44
500	0	0.58	12.41
	0.2x	0.58	8.91
	0.4x	0.59	12.3
	0.8x	0.55	22.89
	1x	0.65	21.11
	1.5x	0.69	25.01
	2x	0.71	27.82
	4x	0.75	28.69
1000	0	0.58	12.41
	0.2x	0.65	6.54
	0.4x	0.67	14.22
	0.8x	0.67	25.17
	1x	0.69	23.82
	1.5x	0.74	33.01
	2x	0.78	27.45
	4x	0.71	26.33

As seen in the table higher particle loading and therefore co-deposition results in higher coefficient of friction and sliding wear rate (SWR). Note SWR was calculated on a mass-loss basis and not volume loss.

6.7 Appendix E – Hydrogen Embrittlement Results

Please see attached the test results for:

5) Baseline CoP
6) CoP (plated under alternative conditions – 70degC, 80mA/cm2 developed in Task 1)
7) CoP-diamond
8) CoP-alumina dopant

STANDARD CoP

ASSURED Testing Services

www.assuredtestingservices.com
388 Servidea Drive
Ridgway, PA 15853 USA
P: +1 814-773-3224
F: +1 814-773-3225

ISO 17025 | NADCAP Accredited
AAMA Component Testing
CAGE 5HSJ7

TEST REPORT -22190

CLIENT BILL TO

BILL TO: ONMISSISS--2267 OurSupplier ID
Integran Technologies, Inc.
6300 Northam Drive

Mississauga ON L4V1H7
CANADA Supplier Code
Ph: 416-675-6266

CLIENT SENT TO

SENT TO: ONMISSISS--2267 OurSupplier ID
Integran Technologies, Inc.
6300 Northam Drive

Mississauga ON L4V1H7
CANADA Supplier Code
Ph: 416-675-6266

Test Report#:22190 **Entry Date:** Monday, April 23, 2018

Contact: Ijya Srivastava/ Andy Robertson

PO#: CC using PO 6419 Q#101316INTG

Hydrogen Embrittlement Testing IAW ASTM F519.
Notched 1a.1 bars were loaded at 75% nominal notched fracture strength.
Notched Fracture Strength - 8778 pounds.

Part Test Information

PART NUMBER	LOT NUMBER	S#	SAMPLE DESCRIPTION

TEST SPECIFICATION NAME	TEST PROCEDURE NAME	HOURS	CYCLES

TEST RESULTS	INDATE	OUTDATE	TESTCNT	RETCNT	REQ	COMP	REQ	HOURS	COMP

Notched Bars

ASTM F519 — Hydrogen Embrittlement ASTM F519-17

	01-May-18	09-May-18	4	0	200	200		

Results: 4 of 4 PASS with no fracture.

Requirements: A plating/coating process shall be considered non-embrittling if none of the plated/coated specimens fracture within 200 hours after loading. If 1 of 4 samples fractures, samples are reloaded for remaining exposure, and then step loaded as per section 11.2.

Michele Singer

Revision# 1.12 Date 2/16/18

End Of Report

Michele Singer

Assistant Laboratory Manager

ASSURED Testing Services
www.assuredtestingservices.com
388 Servidea Drive
Ridgway, PA 15853 USA
P: +1 814-773-3224
F: +1 814-773-3225

ISO 17025 | NADCAP Accredited
AAMA Component Testing
CAGE 5HSJ7

BILL TO: ONMISSISS--2267
Integran Technologies, Inc.
6300 Northam Drive
Mississauga ON L4V1H7
CANADA
Ph: 416-675-6266

SENT TO: ONMISSISS--2267
Integran Technologies, Inc.
6300 Northam Drive
Mississauga ON L4V1H7
CANADA
Ph: 416-675-6266

Entry Date: Wednesday, August 22, 2018
Purchase Order#: CC using 6668 Q#101316INTG
Primary Contact: Ijya Srivastava/ Andy Robertson

TEST REPORT - 23103

SET 1: CoP (ALTERNATIVE CONDITIONS)
SET 2: CoP - DIAMOND
SET 3: CoP - ALUMINA DOPANT

Hydrogen Embrittlement Testing IAW ASTM F519.
Notched 1a.1 bars were loaded at 75% nominal notched fracture strength.
Notched Fracture Strength - 8622 pounds.

Part and Test Information

Test Result

Results: 4 of 4 PASS with no fracture.

Requirements: A plating/coating process shall be considered non-embrittling if none of the plated/coated specimens fracture within 200 hours after loading. If 1 of 4 samples fractures, samples are reloaded for remaining exposure, and then step loaded as per section 11.2.

Test Specification Name	ASTM F519-17a
Test Procedure Name	Hydrogen Embrittlement ASTM F519-17a
Part Number	Set 1
Lot Number	
Sample Description	Notched Bars
In Date	28-Aug-18
Out Date	05-Sep-18
Test Count	4
Return Count	4

Cycles		Hours	
Required		Required	200
Hours/Cycle		Completed	200
Completed			

Test Result

Results: 4 of 4 PASS with no fracture.

Requirements: A plating/coating process shall be considered non-embrittling if none of the plated/coated specimens fracture within 200 hours after loading. If 1 of 4 samples fractures, samples are reloaded for remaining exposure, and then step loaded as per section 11.2.

Test Specification Name	ASTM F519-17a
Test Procedure Name	Hydrogen Embrittlement ASTM F519-17a
Part Number	Set 2
Lot Number	
Sample Description	Notched Bars
In Date	28-Aug-18
Out Date	05-Sep-18
Test Count	4
Return Count	4

Cycles		Hours	
Required		Required	200
Hours/Cycle		Completed	200
Completed			

Printed 9/11/2018 3:48:50 PM

TEST REPORT - 23103

Assured Testing Services

BILL TO:	ONMISSISS--2267 Integran Technologies, Inc.	SENT TO	ONMISSISS--2267 Integran Technologies, Inc.

Test Result

Results: 4 of 4 PASS with no fracture.

Requirements: A plating/coating process shall be considered non-embrittling if none of the plated/coated specimens fracture within 200 hours after loading. If 1 of 4 samples fractures, samples are reloaded for remaining exposure, and then step loaded as per section 11.2.

Test Specification Name	ASTM F519-17a
Test Procedure Name	Hydrogen Embrittlement ASTM F519-17a
Part Number	Set 3
Lot Number	
Sample Description	Notched Bars
In Date	28-Aug-18
Out Date	05-Sep-18
Test Count	4
Return Count	4

Cycles		Hours	
Required		Required	200
Hours/Cycle		Completed	200
Completed			

Michele Singer

Assistant Laboratory Manager

Michele Singer

Revision# 1.13 Date 7/26/18

End Of Report

6.8 Appendix F – Corrdesa Final Report

Please see attached the report from Corrdesa highlighting results from:

1) LPR tests
2) Galvanic Compatibility tests
3) Plating simulations

List and details of coating codes used by Corrdesa:

	Corrdesa Coating Designation	Coating Description	Chemistry
1	nCoP	Standard CoP, Low P (0.8 – 1.3wt% P)	Baseline
2	nCo2P	Standard CoP, med P (1.4 – 1.9wt% P)	
3	nCo4P	Standard CoP, high P (2.0 – 2.5wt% P)	
4	nCoP-X	CoP-diamond	Integran Particle
5	nCoP-SX	CoP-Silicon carbide-diamond	
6	nCoP-TD	CoP-titania dopant	Cirrus Dopant
7	nCoP-AD	CoP- alumina dopant	

ADVANCED NANOCRYSTALLINE COBALT ALLOYS AND COMPOSITES AS ALTERNATIVES FOR CHROMIUM AND NICKEL PLATING IN REPAIR OPERATIONS

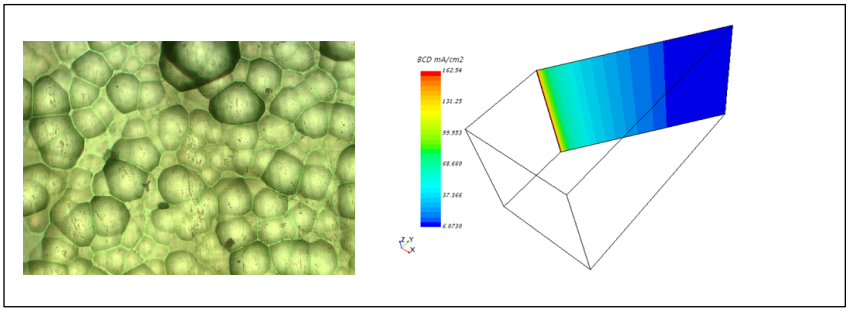

Doc type: Report

Contract Number: SERDP WPSON 16-04

Report #: R17-011-01

Authors: Siva Palani, Alan Rose
Date: Nov 30, 2018
Corrdesa Report #: R17-011-01

RECORD OF CHANGES

Version	Date	Changes
Original	11/30/2018	Original

1. Contents

List of Figures

LIST OF TABLES

1. Introduction

This aim of the project reported here was to investigate and analyze the corrosion performance of Integran developed novel nanocrystalline cobalt-phosphorus embedded with second-phase hard particles. This also included composite coatings with dopants from Cirrus technology. The work consisted of making electrochemical measurements using various techniques to quantify the corrosion behavior of coatings provided by Integran to study the impact of various Phosphorous content and dopant from a corrosion standpoint. Furthermore, we utilized computational fluid dynamics, electroplating and galvanic corrosion design software in order to predict deposition rates and aid in material selection.

The Scope of Work therefore comprised the following:

1. **Linear Polarization Resistance (LPR) test-** to determine recommended phosphorus content for optimum corrosion resistance and impact of dopant
2. **Polarization data acquisition**- according to NAVAIR protocol for galvanic corrosion simulation with Corrosion Djinn™
3. **Galvanic coupling measurements-** to quantify galvanic compatibility with relevant materials
4. **Galvanic corrosion risk analyses with Djinn™-** to compare Integran Co-P material performance with typical aerospace materials
5. **Characterization of Integran's Co-P plating solutions**- to enable future electroplating simulations to aid in process scale-up and plant design

2. Experimental

2.1. Approach

Linear Polarization Resistance (LPR) measurement method was used as a screening method (Task 1) in order to initially rank 7 different types of coatings in terms of corrosion current and consequently the corrosion rate:

	Coating Designation	Chemistry
1	nCoP	Baseline
2	nCo2P	
3	nCo4P	
4	nCoP-X	Integran Particle
5	nCoP-SX	
6	nCoP-TD	Cirrus Dopant
7	nCoP-AD	

Table 1: List of coatings investigated during initial screening study

And finally, the rest of the tasks were performed on 3 down-selected coatings from the LPR measurements.

2.2. Data Acquisition

All the electrochemical corrosion measurements i.e. LPR, Potentiodynamic polarization curve and galvanic measurements were conducted in 3.5 wt.% NaCl with near neutral pH (buffered) under bulk and naturally-aerated electrolyte conditions. They were measured with a 3-electrode setup using the Princeton Applied Research (PAR) and also Corrdesa designed electrochemical flat cell with working electrode area of 1cm^2 (Figure 1). In order to minimize crevice, a Teflon gasket and masking paint is used for the PAR and Corrdesa cell respectively. The measurement details are as below:

1) Equipment and Ancillary
   - Equipment: Gamry Reference 600/ Ivium nStat Potentiostat
   - Reference: Saturated Calomel Electrode
   - Counter: Platinum Mesh/ Graphite Rod

2) Potentiodynamic Polarization Curve Measurement Procedure:

- Scan Rate: 0.1 mV/sec
- All anodic and cathodic scans begin at the OCP (Open circuit potential) after 1-hour pre-exposure in the electrolyte
- OCP and applied potentials referenced vs. Saturated Calomel Electrode (SCE)
- Potential Scan Range: -1800 mV to up to 0 mV vs. SCE
- 3.5% NaCl solution in deionized water at stagnant condition under room temperature (25±3°C). Solution is refreshed for every scan.

- Electrochemical cell is placed in a Faraday cage
- All specimens are cleaned ultrasonically in acetone for 10 min followed by ethanol/IPA for 10 min, and air-dried at room temperature

3) Linear Polarization Resistance Measurement Procedure:

- Equipment: Gamry Reference 600/ Ivium nStat Potentiostat
- Scan Rate: 0.1 mV/sec
- All scans begin from more cathodic to anodic potentials versus OCP
- OCP and applied potentials referenced vs. Saturated Calomel Electrode (SCE)
- Potential Scan Range: -15 mV to +15 mV vs. OCP
- 3.5% NaCl solution in deionized water at stagnant condition under room temperature (25±3°C).
- Electrochemical cell is placed in a Faraday cage.
- All specimens are cleaned ultrasonically in acetone for 10 min followed by ethanol/IPA for 10 min, and air-dried at room temperature.

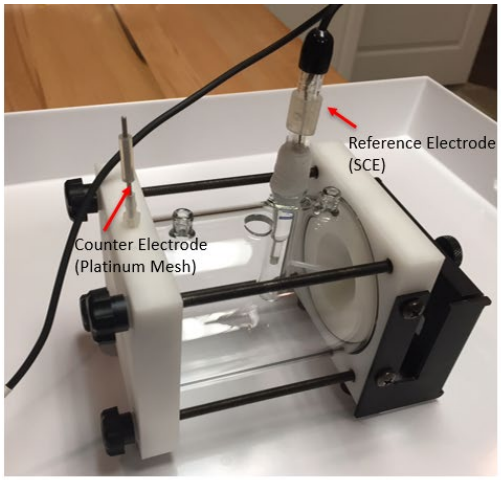

PAR flat cell

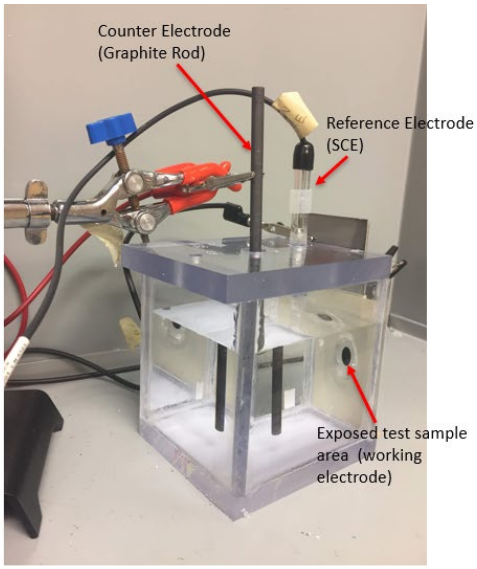

Corrdesa flat cell

Figure 1: Electrochemical cells used for electrochemical measurements.

3. Results

3.1. Linear Polarization Resistance (LPR) measurements

The LPR technique, also referred to as "linear polarization", is an experimental electrochemical technique that estimates the small signal changes in electric current when potential is perturbed by Ecorr±15 mV (G102, 1994). The slope of the resulting curve over this range is the polarization resistance. In this work, LPR measurements for the duration up to 8 days (192 hours) were conducted on all the coatings listed in Table 1. All measurements were at least repeated twice.

a)

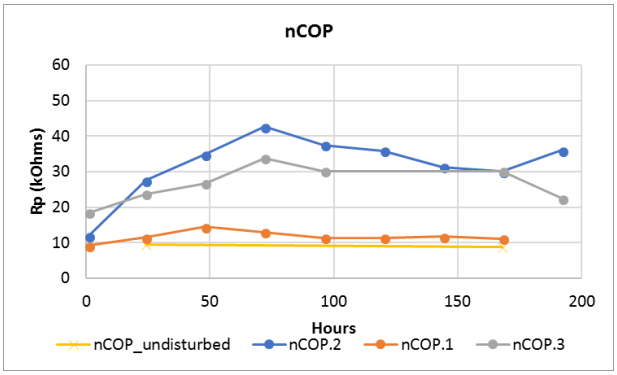

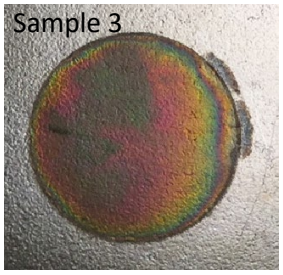

b)

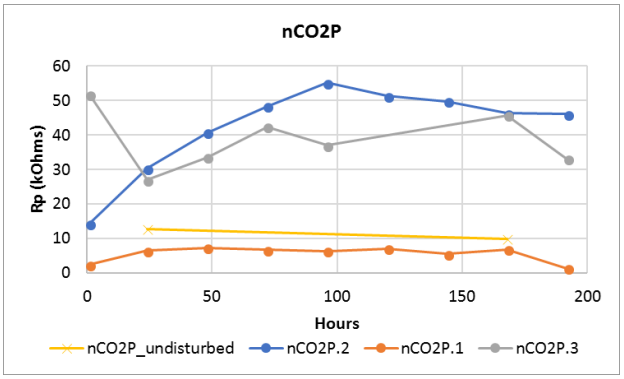

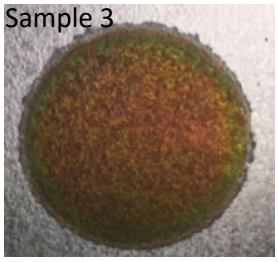

c)

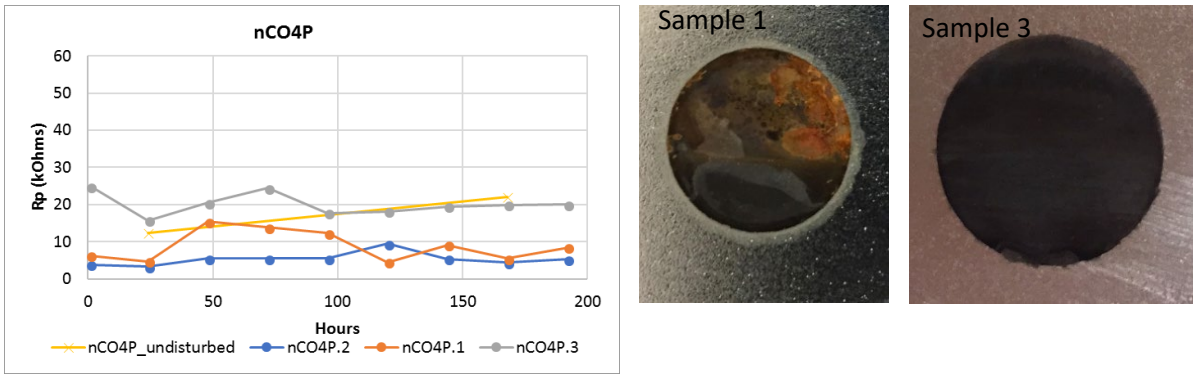

Figure 2: Long term LPR measurements on a) nCoP (Low Phos) b) nCo2P (Medium Phos) and c) nCo4P (High Phos) coatings

The undisturbed measurements in the graphs denote on these samples the LPR measurements which were executed at the 24 hours mark and at168 hours without intermediate measurements.

a)

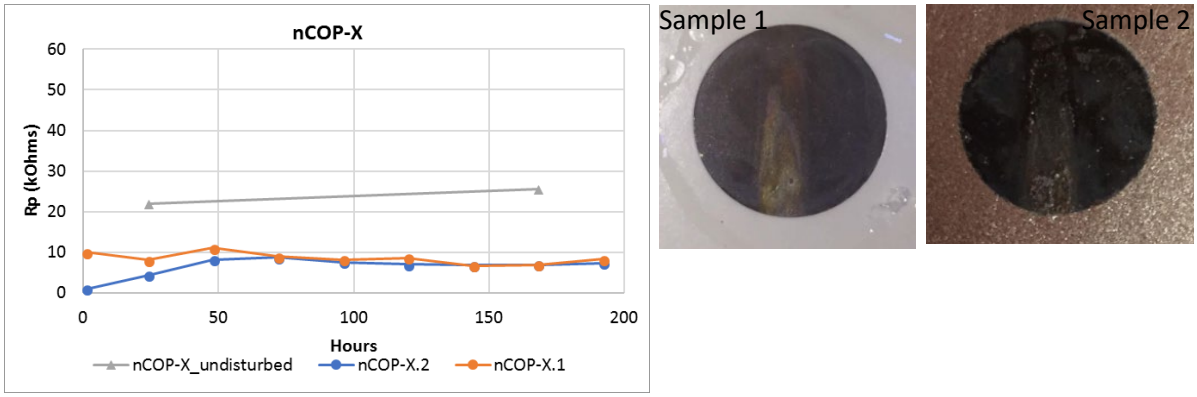

b)

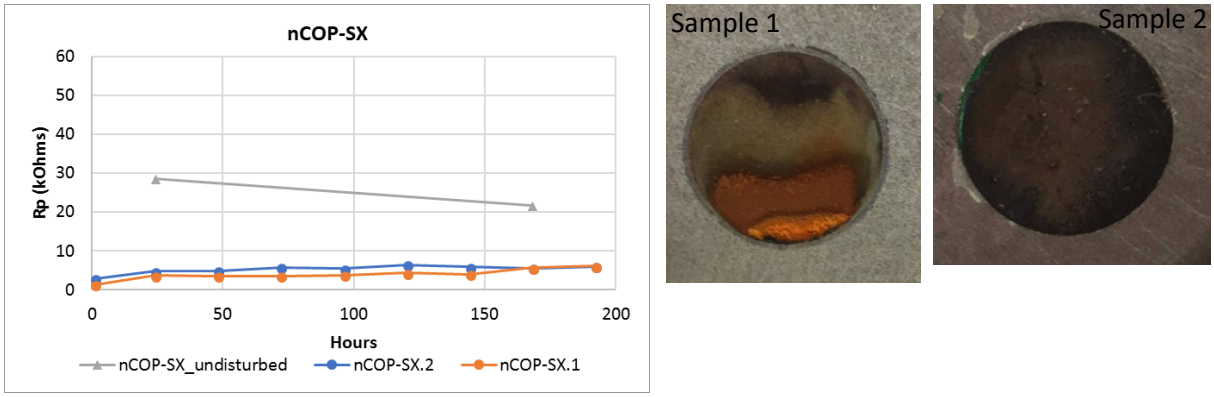

Figure 3: Long term LPR measurements on a) nCoP-X b) nCoP-SX coatings with Integran particles

a)

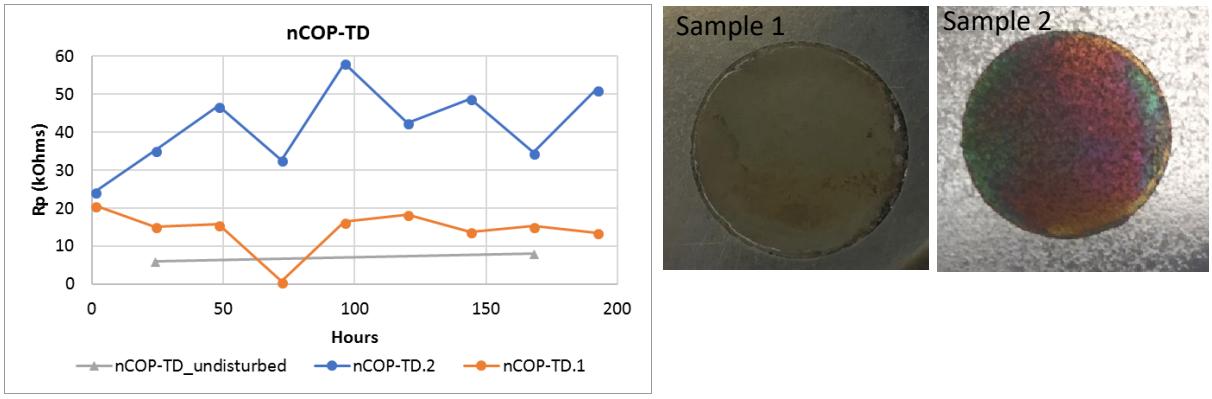

b)

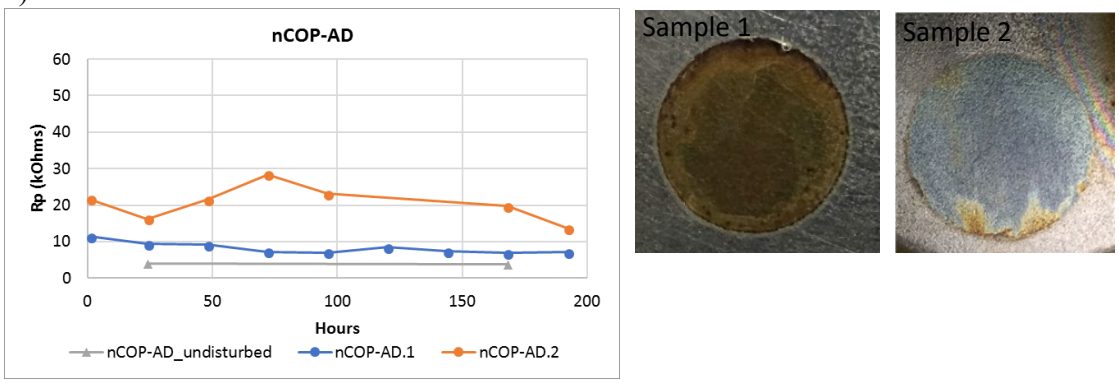

Figure 4: Long term LPR measurements on a) nCoP-X b) nCoP-SX coatings with Cirrus particles

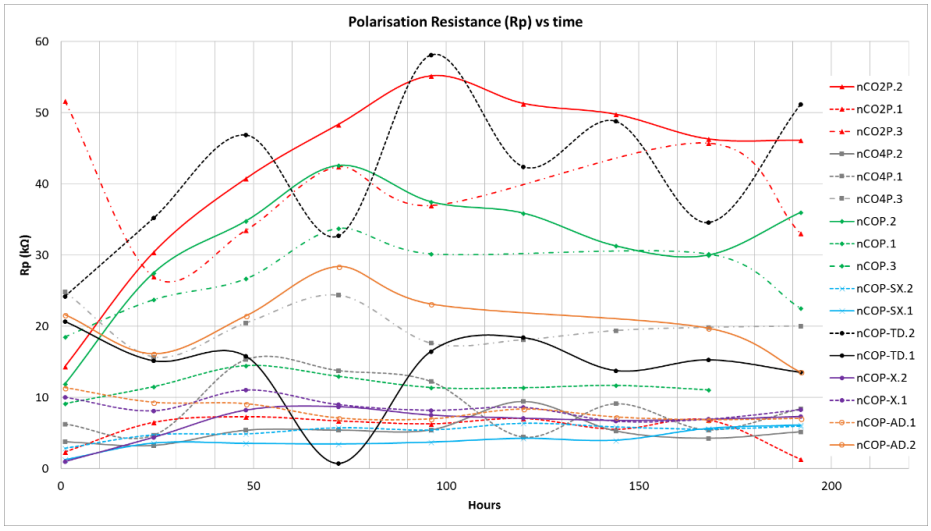

Figure 5: Summary of LPR evolution versus time for all the investigated coatings and repeats.

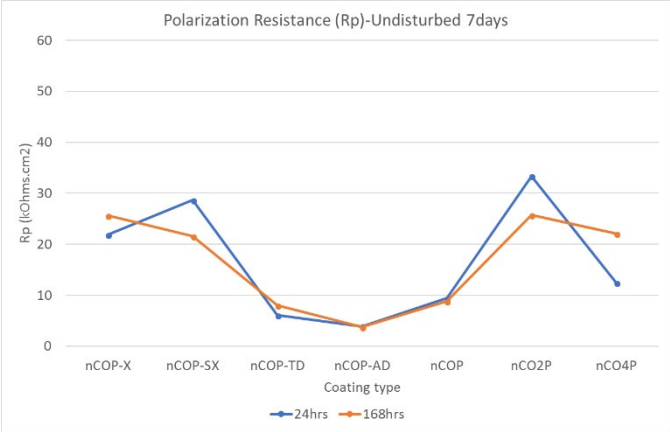

Figure 6: Undisturbed LPR comparison between 24 hours and at 168 hours for all the investigated coatings.

For the estimation of corrosion rate, in addition to LPR we also used the Tafel extrapolation method since the polarization behavior of the coatings were rather linear in the Tafel region. Therefore, polarization curves for all the 7 coatings were measured. Each cathodic and anodic branches of the curves were measured on separate specimens to ensure we capture the true polarization behavior. Then, the estimation of Icorr was done using Gamry's Echem Analyst software's E Log vs I Fit which performs a linear least square fit of Log(i) versus potential in the selected region. The slope of the line is the Beta coefficient for the half reaction in which you are interested. The current at which the fitted line goes through Ecorr is Icorr (Figure 7).

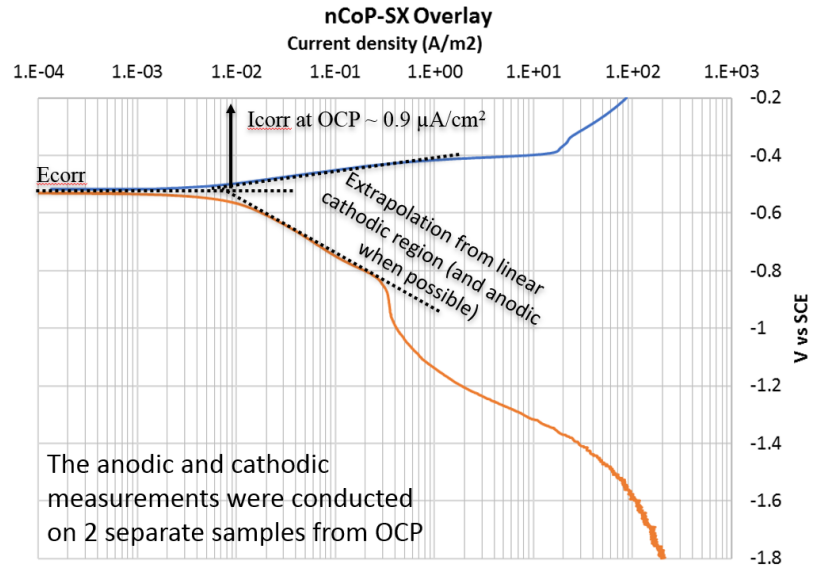

Figure 7: Tafel extrapolation for Icorr and Ecorr estimation

Figure 8 to Figure 10 shows the polarization curves measured on all 7 coatings in accordance to the polarization measurement protocol generated with NAVAIR after 1-hour exposure under OCP condition.

a)

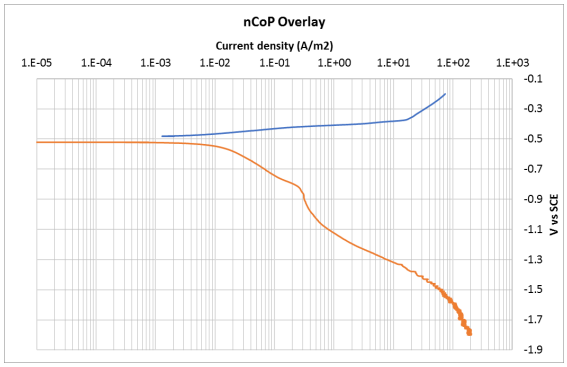

b)

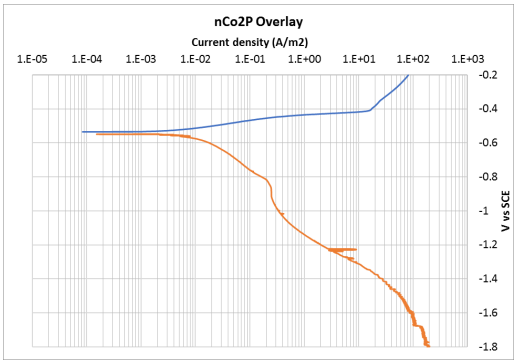

c)

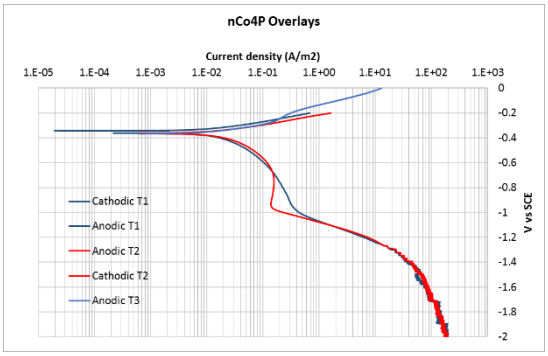

Figure 8: Polarization curves of a) nCoP (Low Phos) b) nCo2P (Medium Phos) and c) nCo4P (High Phos) coatings

a)

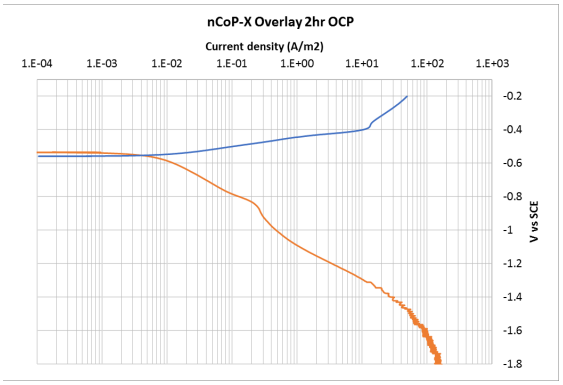

b)

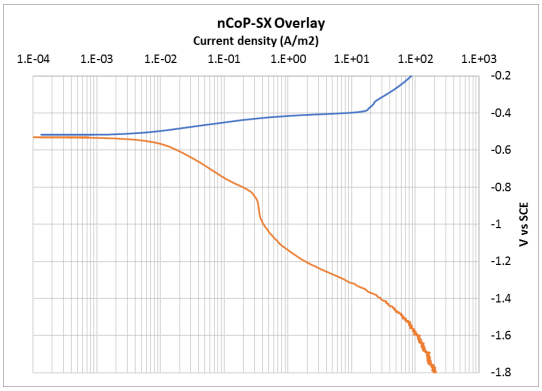

Figure 9: Polarization curves of a) nCoP-X b) nCoP-SX coatings with Cirrus particles

a) b)

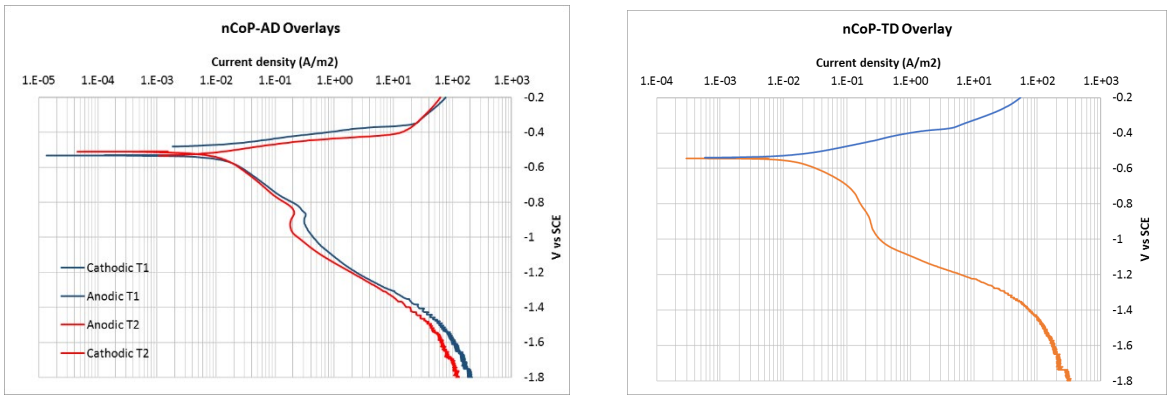

Figure 10: Polarization curves of a) nCoP-AD b) nCoP-TD coatings with Integran particles

	Estimation	
	Icorr ($\mu A/cm^2$)	**Corrosion Rate (mil/yr)**
nCoP-X	0.8	0.348
nCoP-SX	0.9	0.3915
nCoP-TD	1.5	0.6525
nCoP-AD	1.5	0.6525
nCoP	0.9	0.3915
nCo2P	1.3	0.5655
nCo4P	2	0.87

Table 2: Corrosion current and rate estimation based on the Tafel extrapolation method

Table 2 shows the estimated corrosion current and the resulting corrosion rate estimation based on the Tafel extrapolation method as shown in Figure 7. The nCoP baseline with low Phosphorus and with Integran particles resulted in a lower corrosion rate. Figure 11 depicts the measured LPR values at 24 hours and at 168 hours and the resulting, estimated corrosion currents based on both Tafel extrapolation and LPR method. The plots titled "24" and "168" are referring to the left axis "Undisturbed Rp", while the plots titled "Icorr (Tafel)", "Icorr@24hrs" and "Icorr@168hrs" are referring to the right axis. Tafel slope of 0.1 and 0.2 V/decade was used anodic and cathodic respectively for calculating the Icorr coming from the LPR measurements. This value was decided to be a good estimate also after cross checking using the Electrochemical Frequency Modulation technique which measures the actual Tafel slopes. The Icorr (Tafel) was measured from polarization curve after 1-hour OCP exposure. Using LPR method with a-priori knowledge of βa and βc, can be used to indirectly compute Icorr. The polarization resistance can be expressed as:

$$R_p = \frac{1}{2.303 I_{corr}} \left(\frac{\beta_a \beta_c}{\beta_a + \beta_c}\right) \quad \text{Eq.1}$$

This expression can be re-written for Icorr to arrive at the Stern-Geary equation

$$I_{corr} = \frac{\beta}{R_p} \quad \text{Eq.2}$$

where β = 2.303 [βaβc / (βa + βc)] is a constant of proportionality.

The discrepancy between the corrosion currents (i_corr) measured by Tafel data in the polarization curves vs. LPR for the "nCoP-AD" and "nCoP-TD" materials could be caused due to samples from different batches (different coating composition) were used.

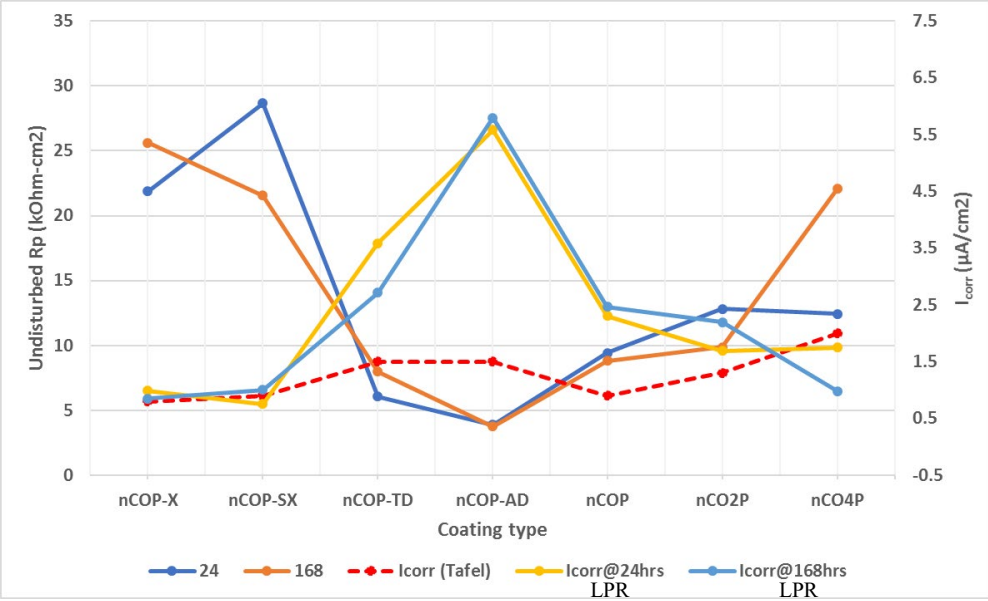

Figure 11: Summary of polarization resistance and the estimated corrosion currents versus time

Figure 12 shows the corrosion potential evolution for all the 7 coatings under study. They all lie in the range -550 to 475 mV vs SCE except for nCo4P which showed much higher potential, possibly due to higher Phosphorous content. Its Ecorr value also drifted close to -250 mV during the period of 7 days. These findings indicate that coatings with the lowest corrosion currents (rates) would be nCoP-X, nCoP-SX. This is followed by nCoP, nCo2P and nCo4P. The materials with the highest corrosion currents (rates) are the nCoP-TD and nCoP-AD.

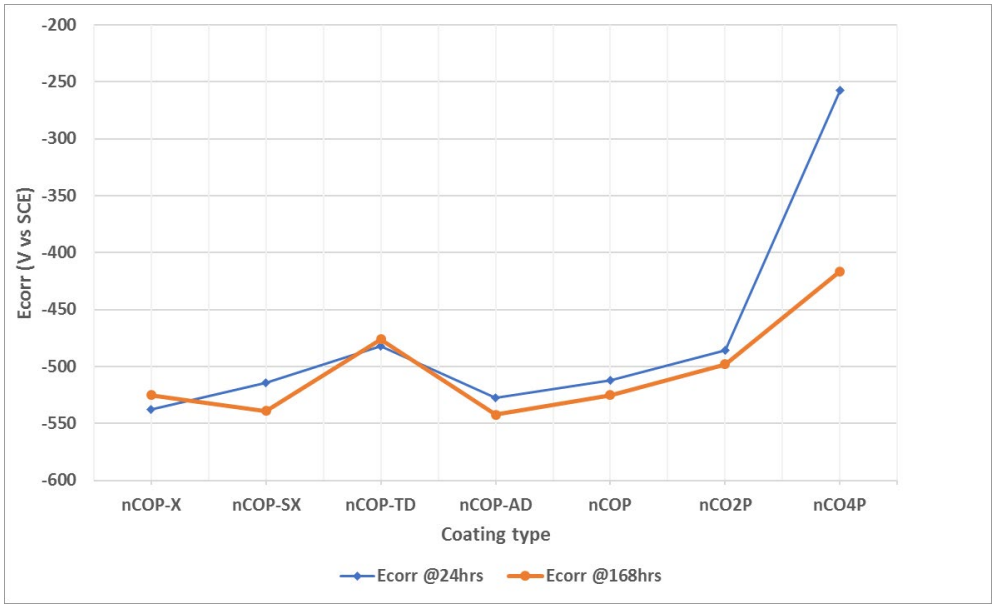

Figure 12: Corrosion potential after 24 hours and 168 hours

3.2. Polarization Behavior measurement for Corrosion Djinn™ analysis

Eventually nCoP, nCoP-X and nCoP-AD coatings were found to be promising and consequently selected, moving forward to the rest of the planned tasks. So, potentiodynamic polarization curves in accordance to NAVAIR measurement protocols were measured on the 3 coatings for the full range of potentials. A total of 3 polarization curves were measured for each coating. These curves are as shown in Figure 13. These curves were then post processed and uploaded into Corrosion Djinn software tool for executing galvanic corrosion risk assessments with aerospace relevant materials.

a)

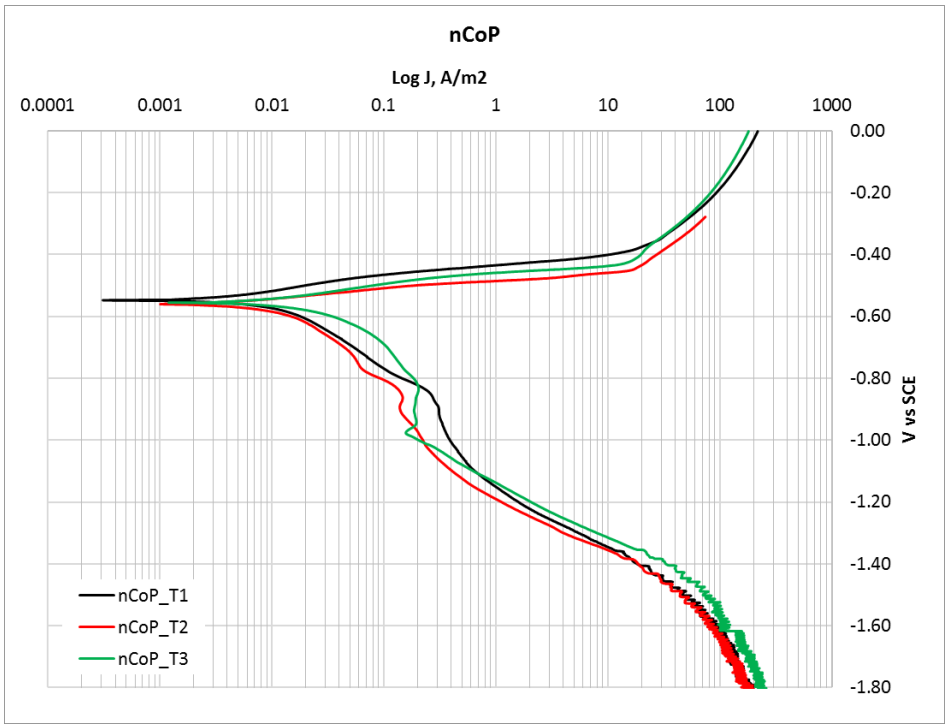
nCoP
Log J, A/m2
0.0001
0.001
0.01
0.1
1
10
100
1000
0.00
-0.20
-0.40
-0.60
-0.80
-1.00
-1.20
-1.40
-1.60
-1.80
V vs SCE
nCoP_T1
nCoP_T2
nCoP_T3

b)

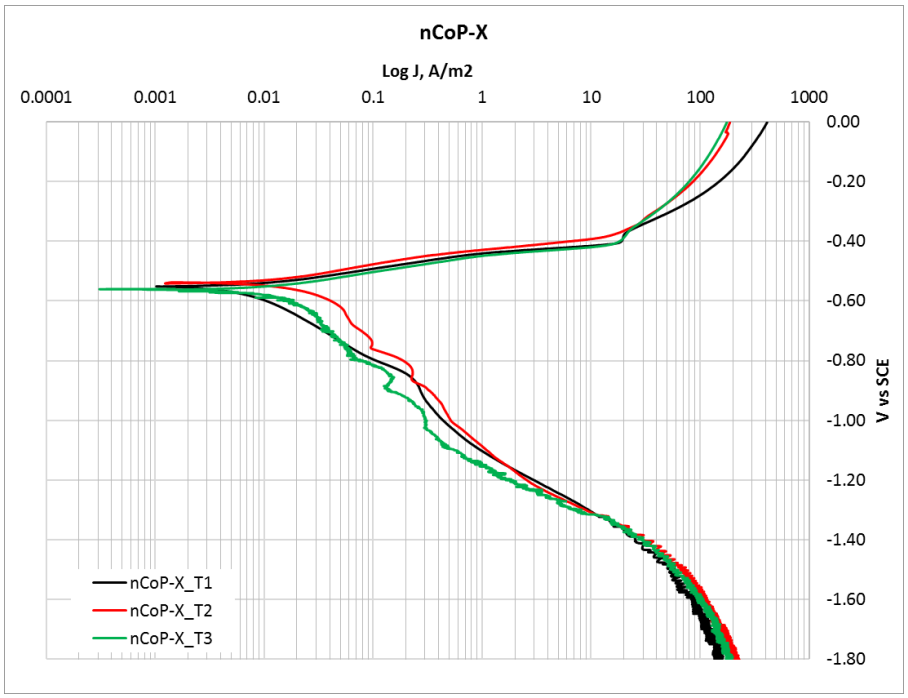
nCoP-X
Log J, A/m2
0.0001
0.001
0.01
0.1
1
10
100
1000
0.00
-0.20
-0.40
-0.60
-0.80
-1.00
-1.20
-1.40
-1.60
-1.80
V vs SCE
nCoP-X_T1
nCoP-X_T2
nCoP-X_T3

c)

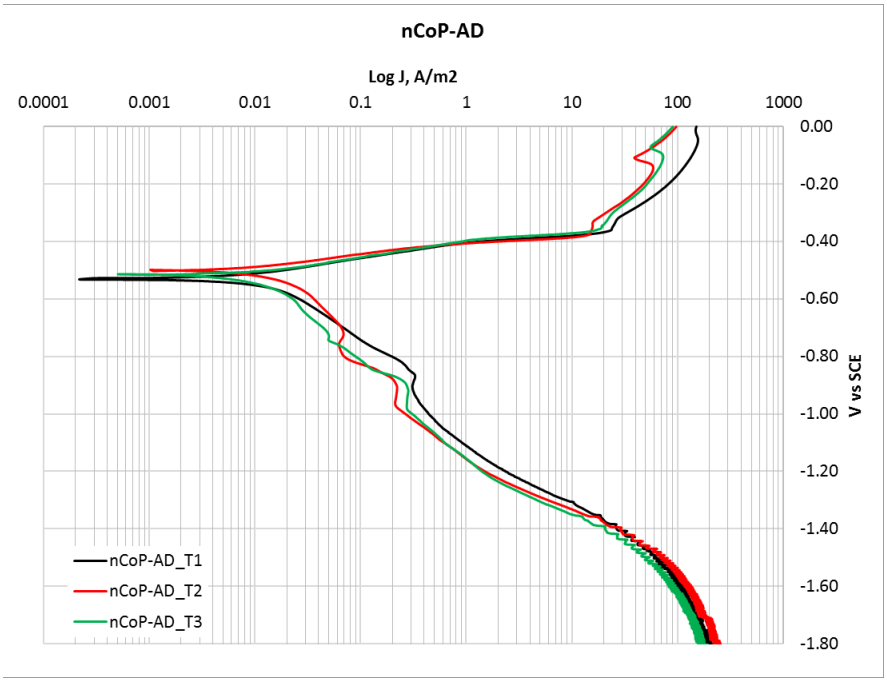

d)

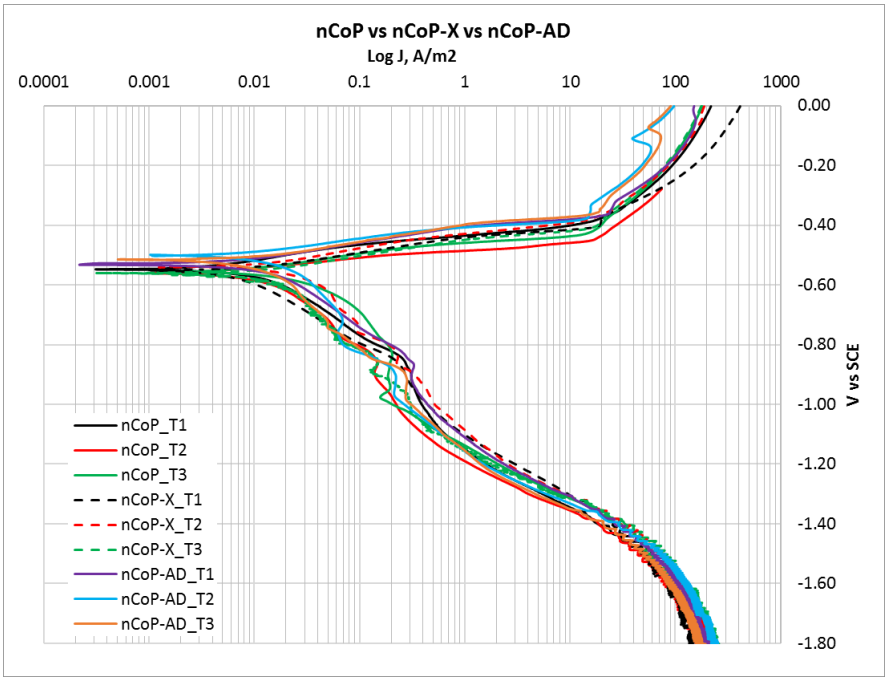

Figure 13: Complete polarization curves of a) nCoP b) nCoP-X c) nCoP-AD and d) overlay of all three coatings

All 3 coatings have very similar and reproducible anodic behavior in comparison to the cathodic behavior where there was larger spread in the oxygen reduction reaction regime. The nCoP-AD showed the most noble OCP followed by nCoP-X and nCoP Baseline. From corrosion standpoint, it is found that the nCoP-X is the best followed by nCoP baseline and the nCoP-AD. This is based on the LPR and polarization measurements conducted.

3.3. Galvanic corrosion risk analysis with Corrosion Djinn™ analysis

In support of these tasks Corrdesa provided Integran with limited access to the Corrosion Djinn software tool so that they could carry out their own analyses with any aerospace relevant material of interest. The Djinn database already contains many materials and coatings typically used in air and land vehicles. So, the addition of nCoP coatings data to the database enables us to compare with other aerospace materials from the perspective of galvanic risk.

Corrosion Djinn enables materials engineers and designers to assess dissimilar materials for galvanic incompatibility according to MIL-STD-889. The Djinn database already contains many modern materials and coatings typically used in air and land vehicles. By adding the polarization curves of the nCoP, nCoP-X and nCoP-AD, we are now able to perform galvanic corrosion risk analyses in conjunction with other aerospace materials. All 3 measured polarization curves for each coating were uploaded into Djinn. Please refer to Appendix 1 for sample report on analyses done with Al 6061-T6, 4130 high strength steel and 15-5 Stainless steel materials. Al 6061-T6 and 4130 are both more anodic (sacrificial) when compared to all the nCoP coatings whereas the 15-5 was more cathodic (noble). However, the analysis also showed that despite 4130 being anodic versus the coatings its self-corrosion rate was higher than the galvanic corrosion rate when coupled to these 3 coatings. In contrast, the Al 6061-T6 which was also anodic versus the coatings showed much lower self-corrosion rate. This means in the case of 4130, although the coating is more cathodic the galvanic effect is lower when compared to its own corrosion rate.

3.4. Galvanic coupling measurement

The purpose of this task is to quantify the galvanic effect or interaction when these coatings are contacted with typical aerospace materials such as Al 7075-T6 or 4130 high strength steel. Therefore, zero resistance ammetry (ZRA) galvanic coupling measurements between these 3 coatings with Al 7075-T6 and 4130 were conducted over the course of 5 days. The resulting galvanic current and mixed potential were recorded every 2 seconds. The surface area of both the anode and cathode were kept constant at $1cm^2$ during all the galvanic measurements in order to simulate 1:1 cathode to anode ratio. The electrolyte was in stagnant condition without stirring in order correlate with all the polarization measurements and also not to artificially accelerate the galvanic corrosion considering it is a long-term measurement. In general, both Al 7075-T6 and 4130 were behaving anodic in all cases when galvanically coupled to the coatings. In other words, all the coatings acted more noble causing Al 7075 and 4130 to corrode preferentially.

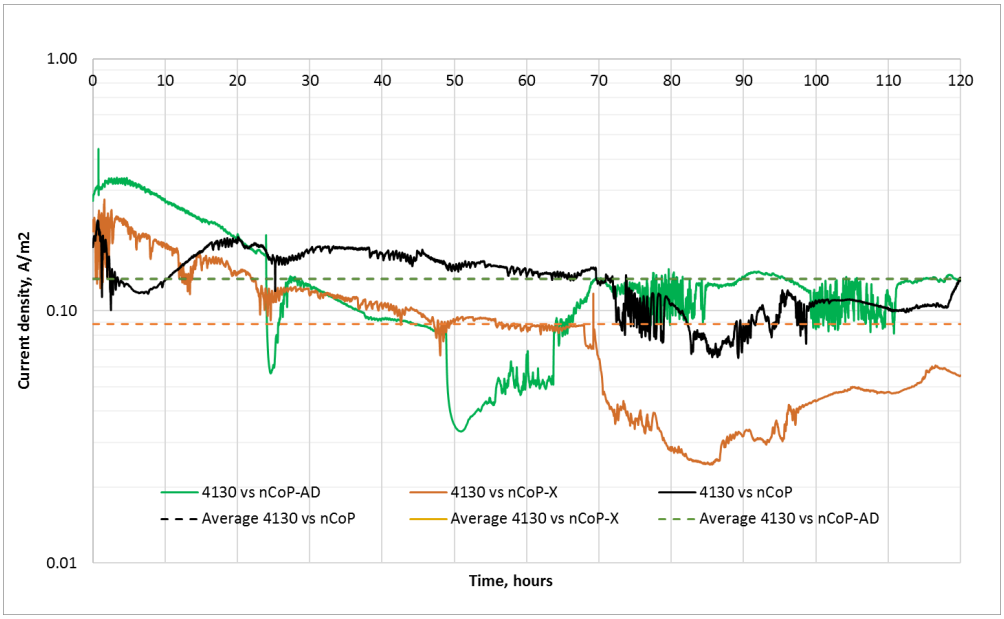

Figure 14: Galvanic current density for 4130 vs. nCoP, nCoP-X and nCoP-AD vs. time

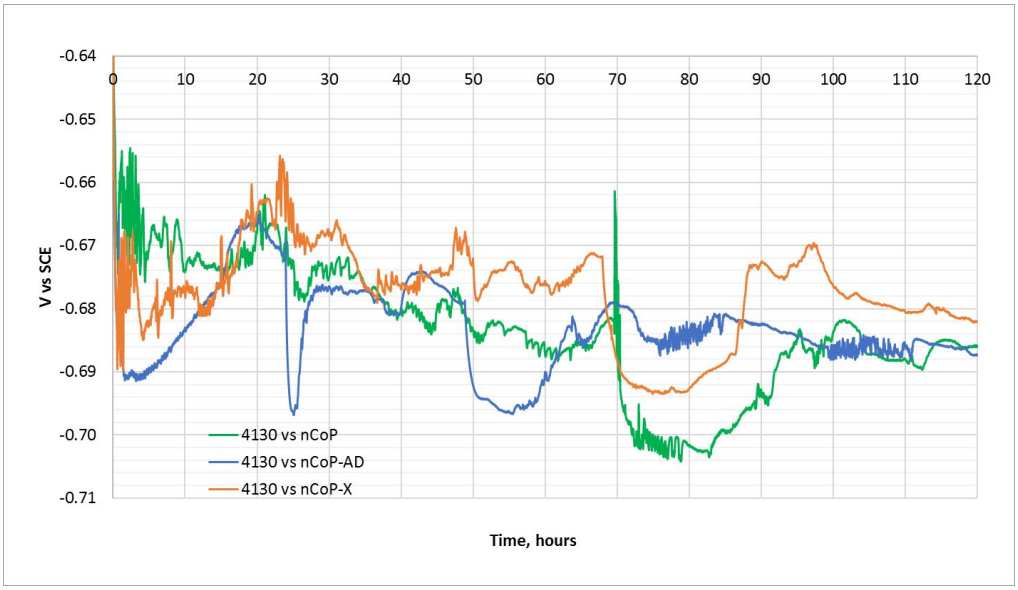

Figure 15:Galvanic coupling potential for 4130 vs. nCoP, nCoP-X and nCoP-AD vs. time

Figure 14 shows individual galvanic current measurements for the 3 coatings when coupled against bare 4130 high strength steel for 5 days. The dotted straight lines denote the 5 days average of galvanic current density values. Figure 15 shows the corresponding galvanic potentials measured simultaneously during the galvanic current measurements. It should be noted that the drastic dip in current density values e.g. at around 50 hrs. and at around 70 hrs. for nCoP-AD and nCoP-X respectively were caused while refilling the cell with de-ionized water to compensate evaporated electrolyte. Please note that all these galvanic measurements were not conducted at the same time which explains the difference in electrolyte refilling events.

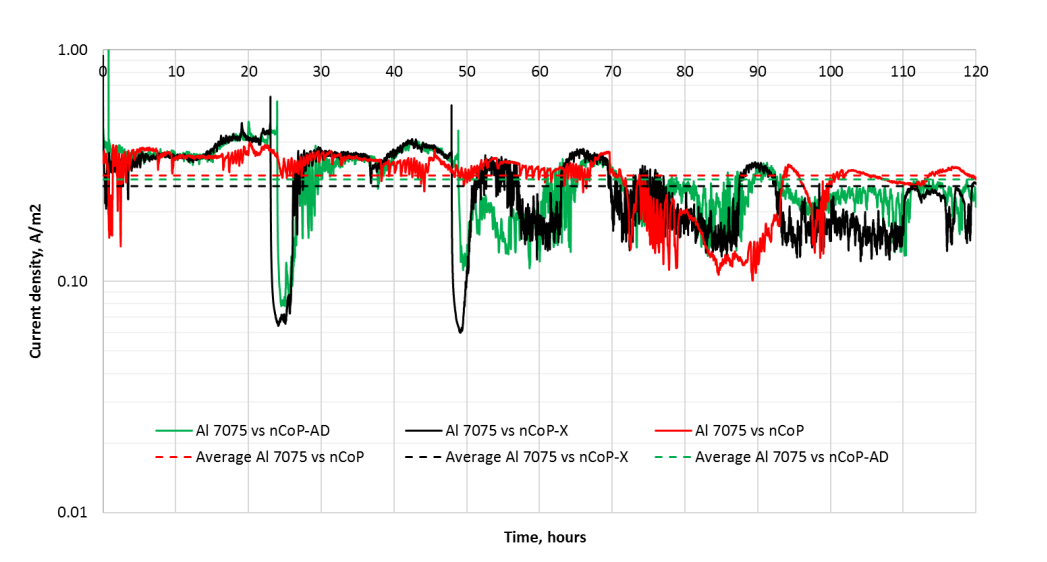

Figure 16: Galvanic current density for Al 7075-T6 vs. nCoP, nCoP-X and nCoP-AD vs. time

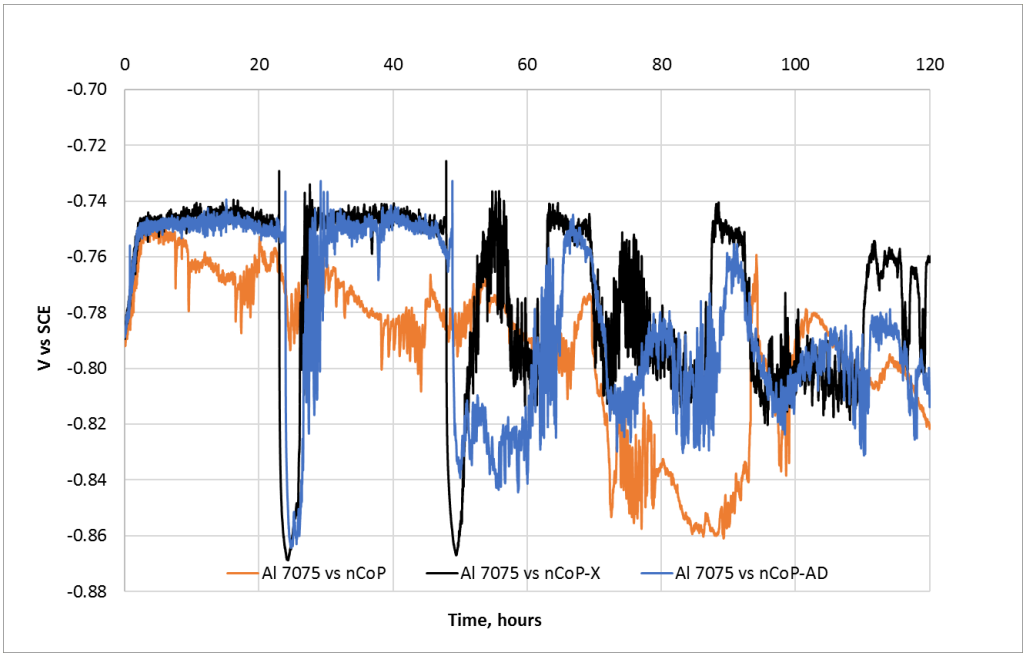

Figure 17: Galvanic coupling potential for Al 7075-T6 vs. nCoP, nCoP-X and nCoP-AD vs. time

Figure 16 shows individual galvanic current measurements for the 3 coatings when coupled against bare Al 7075-T6 for 5 days. Again, the drastic dip in current density values e.g. at around 23 hrs. and at around 48 hrs. for nCoP-AD and nCoP-X were caused while electrolyte replenishment in the cell due to evaporation. Figure 17 shows the corresponding galvanic potentials measured simultaneously during the galvanic current measurements.

3.5. Plating electrolyte characterization

Three electrolytes were received from Integran, namely, nCoP-Baseline, nCoP-X and nCoP-AD. The polarization measurements were executed using a rotating disc electrode (RDE) at 400rpm connected to Gamry Reference 600 potentiostat/galvanostat, at 78°C-82°C, representative of a relatively well mixed tank flow. The electrode setup used is shown in Figure 18.

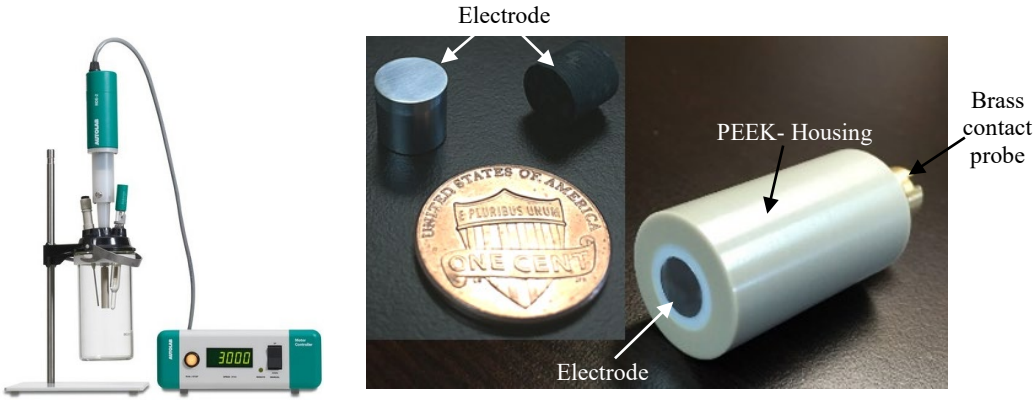

Figure 18: RDE setup and electrode system

3.5.1. Cathodic polarization and efficiency

For each experiment, the RDE was equipped with a stainless steel 316 (SS 316) electrode. All the measurements were conducted using galvanostatic method i.e. constant current mode. The cathodic polarization and the resulting plating efficiency result for (NANOVATE S3010™) nCoP-Baseline, nCoP-X and nCoP-AD electrolytes are shown in Figure 19 through Figure 21, as well as being tabulated in Table 4. In general, the currents were held under galvanostatic conditions for at least 15 minutes for the highest current density i.e. -2000 A/m^2 region and gradually increased to about 1 hour at the lowest current density region i.e. -100 A/m^2 as the plating process becomes less efficient.

a)

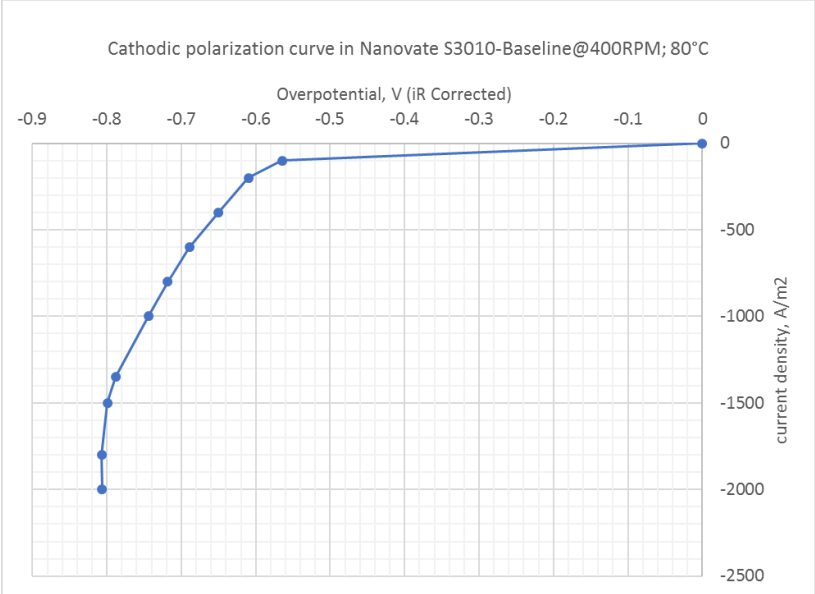

b)

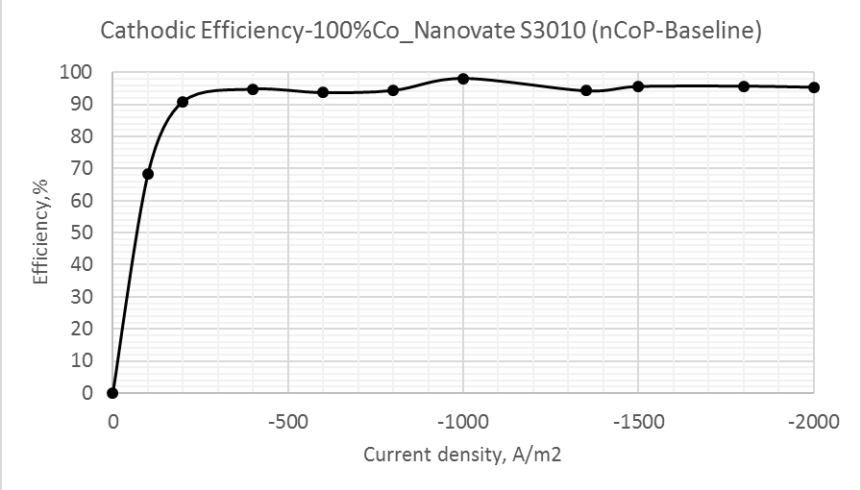

Figure 19: a) Cathodic polarization measurements of fresh Nanovate S3010-nCoP b) *Plating efficiency of the fresh* Nanovate S3010-nCoP

a)

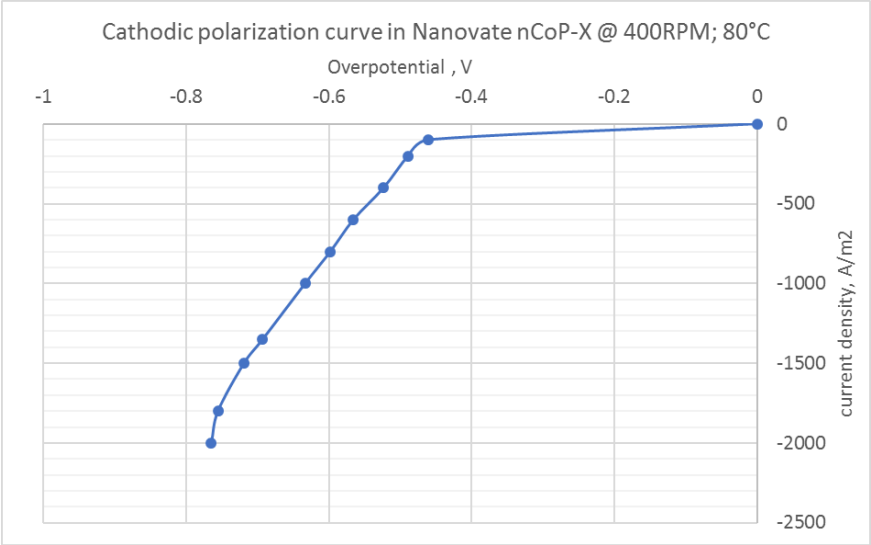

b)

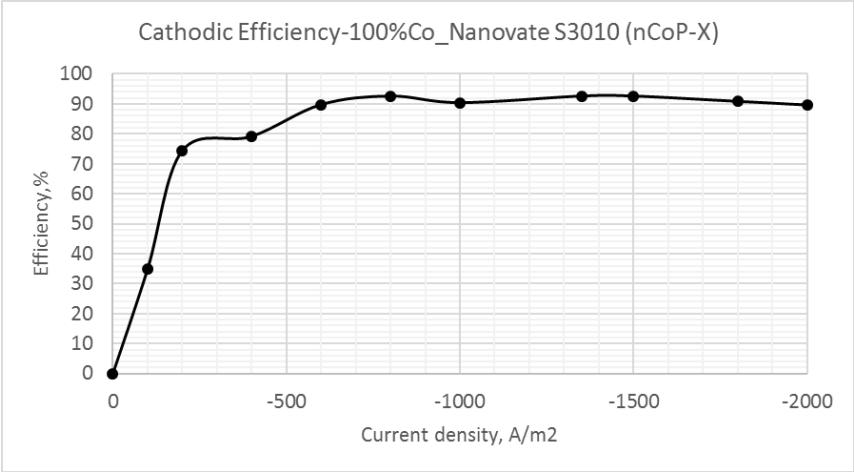

Figure 20: a) Cathodic polarization measurements of fresh Nanovate S3010-nCoP-X b) Plating efficiency of the fresh *Nanovate S3010-nCoP-X*

a)

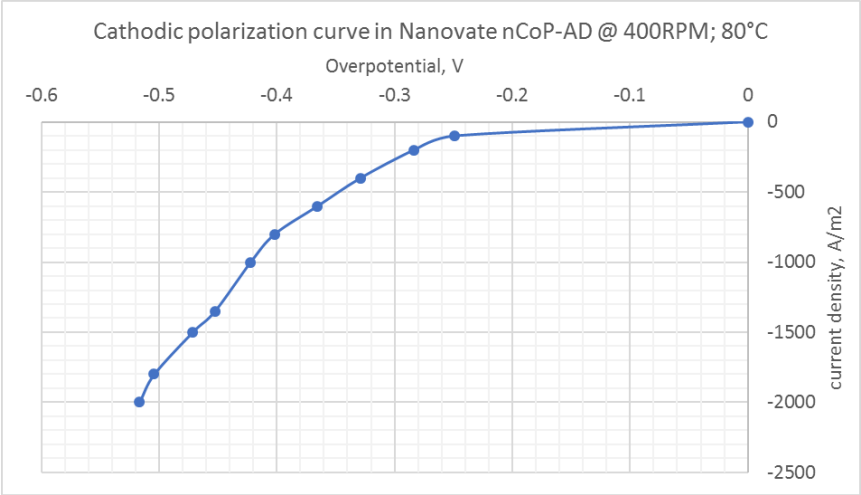

b)

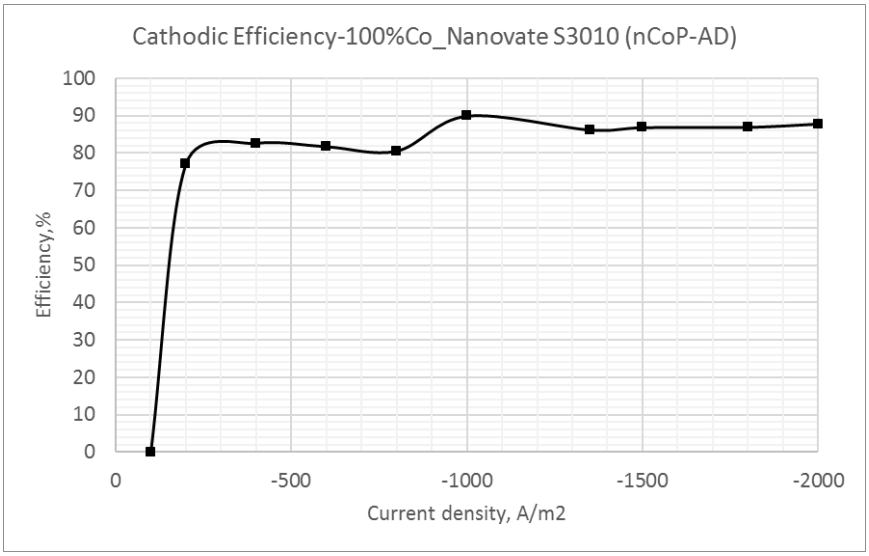

Figure 21: a) Cathodic polarization measurements of fresh Nanovate S3010-nCoP-AD b) Plating efficiency of the fresh *Nanovate S3010-nCoP-AD*

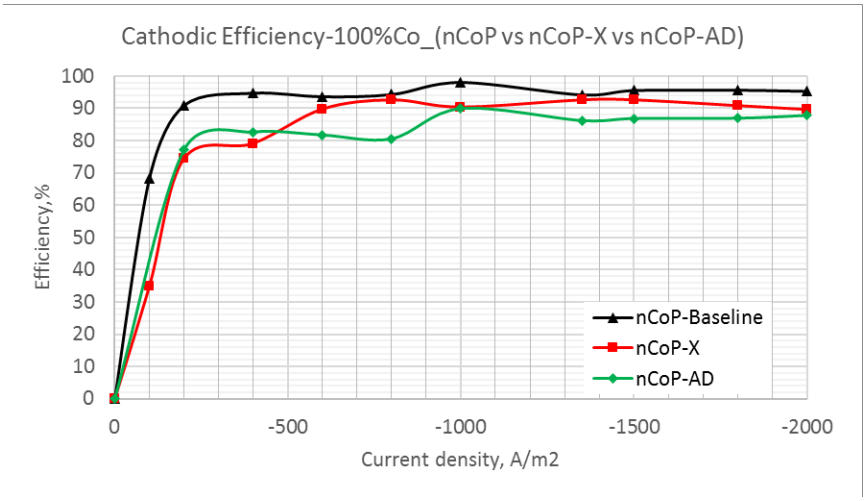

Figure 22: Summary of plating efficiencies for all 3 solutions

The plating efficiency shows how effectively the imposed current is used for plating process for reduction of Cobalt (II) to solid Cobalt according to reaction below:

$$Co^{2+} + 2e^{-} \rightarrow Co \qquad \text{Eq. 3}$$

The plating process efficiency can be expressed according to Faraday's law:

$$\Delta m = -\frac{M\Delta t\theta j}{zF} \qquad \text{Eq. 4}$$

where:

θ : efficiency of plating

z : valence for Cobalt (2)

M : atomic weight of Cobalt (58.9332 g/mol)

j : local cathodic current (mA)

Δm : weight gain (g)

Δt : plating duration (s)

F : Faraday's constant (96485)

For each efficiency calculation, the RDE electrode weight is measured before and after the experiment using an analytical balance with 0.0001g precision. The measured weight gain is compared with the theoretical weight gain to capture cathodic efficiency of the 3 plating solutions. Since the Phosphorous content in these 3 solutions were expected to be about 1%, all the plating efficiencies were calculated based on 100 % contribution from Cobalt.

Nanovate S3010	nCoP-Baseline	nCoP-X	nCoP-AD
Conductivity (S/m) @ 80°C	11.2	9.9	13.8
Current density (A/m^2)	**Efficiency (%)**		
-2000	95.4	89.6	87.8
-1800	95.7	90.8	86.9
-1500	95.6	92.6	86.8
-1350	94.3	92.6	86.2
-1000	98.1	90.4	89.9
-800	94.4	92.6	80.6
-600	93.7	89.7	81.7
-400	94.8	79.1	82.7
-200	90.9	74.4	77.1
-100	68.3	34.9	-
0	0.0	0.0	0.0

Table 3: Tabulated summary of cathodic plating efficiency and conductivity

3.5.2. **Anodic polarization**

Anodic polarization curves of the Cobalt anode supplied by Integran was measured in all 3 nCoP electrolytes. The curves were measured potentiodynamically at a scan rate of 0.5 mV/s. The electrolyte conditions were similar to plating conditions: well agitated; 78-82 °C.

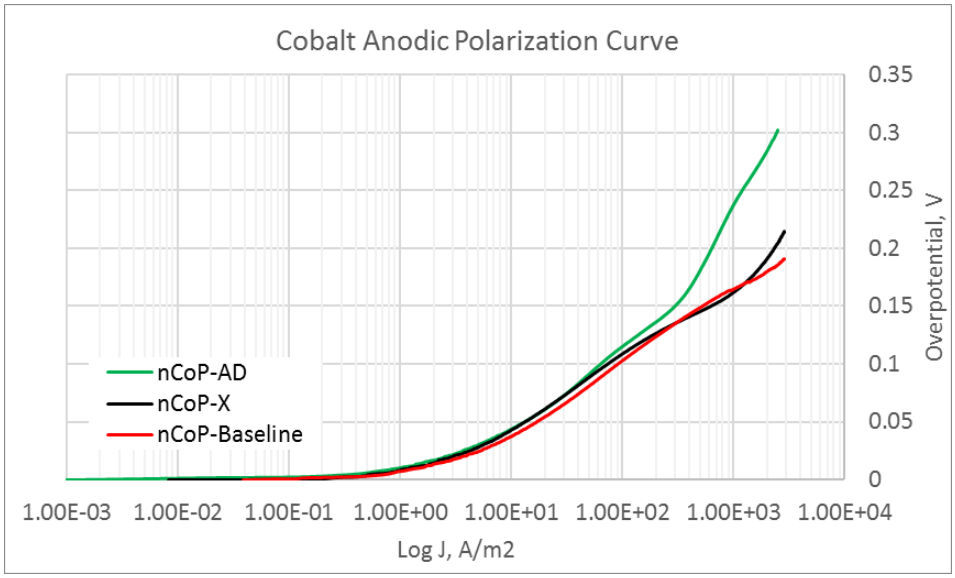

Figure 23: Anodic polarization curves of Cobalt in nCoP, nCoP-X and nCoP-AD electrolytes

3.5.3. **Plating simulations**

The objective of gathering the polarization data is so that in the future, we will have the necessary information available to execute plating simulations. This can bring substantial benefit, with the use of the multi-physics software Siemens Simcenter Star CCM+, as it will be possible to construct a simulation model of an arbitrary plating tank and insert the CAD information of articles to be plated, such as landing gear for example. Clearly this capability will be useful when there is a need to scale-up the process and design plating plant. For now, however, we will demonstrate the use of the plating polarization data and the CCM+ modeling on a simpler but informative geometry.

The properties of the surface coating obtained by electrolytic deposition depend on many factors, one of the most important factors affecting the quality of the deposit is the current density during the deposition. To study this affect and to determine optimal plating conditions in practice, many electroplaters use a Hull cell, a trapezoidal structure composed of two nonparallel electrodes and two insulating walls. Since the cathode is tilted with respect to the anode, a wide variation in current densities along the cathode surface can be obtained in a single experiment, thereby permitting the observation of the quality of deposits produce over a wide range of plating conditions.

3.5.3.1. Theoretical Model

In the absence of concentration gradients, the current density (i) locally at any point in the cell can be determined from the gradient of the local potential (φ) by Ohm's law as follows;

$$\nabla^2 = 0 \qquad \text{in the electrolyte}$$

$$\frac{\partial \phi}{\partial \xi} = 0 \qquad \text{along the insulating walls}$$

$$\phi = V_A \qquad \text{along the anode}$$

along the cathode

$$-\kappa\frac{\partial\phi}{\partial\xi} = i(\phi, V_C)$$

where ξ is a surface normal. The local current density at the cathode surface depends on the local potential in the electrolyte and the potential of the electrode. For electrodeposition of a single species, the surface kinetics may be represented by the Butler Vollmer equation

$$i = i_o\left\{e^{\left(\frac{\eta}{\beta_a}\right)} - e^{\left(\frac{\eta}{\beta_c}\right)}\right\}$$

$$\eta = V_c - \phi$$

whether potentials are measured with respect to a reference electrode of the same kind as a working electrode, i_o is the exchange-current density and β_a and β_c are the anodic and cathodic Tafel slopes. Alternatively, the relationship on the cathode boundary can be represented by the polarization curve for the cathode material.

In practice, it is common to distinguish between the primary current distribution, which results uniquely from resistance effects (ohmic drop) and the secondary current distribution, where the shape of the distribution is influenced by both the electrolyte resistance **and** the electrode kinetic resistance, which are provided, directly by the measured polarization curves already reported in the previous sections. The primary current distribution is, in fact, simply the secondary current distribution in the limited very rapid kinetics.

3.5.3.2. Using Star CCM+ for modeling the electroplating in a Hull cell

The aim of this section is to introduce some elements of using CCM+ for simulating electroplating in the Hull cell geometry.

In CCM+ the dimensions of the Hull cell were parameterized, Figure: 24, so for example, the short side of 48mm was entered as the parameter $ShortSide. This will enable a quick rebuild of a Hull cell geometry (and remesh) by simply changing the parameters.

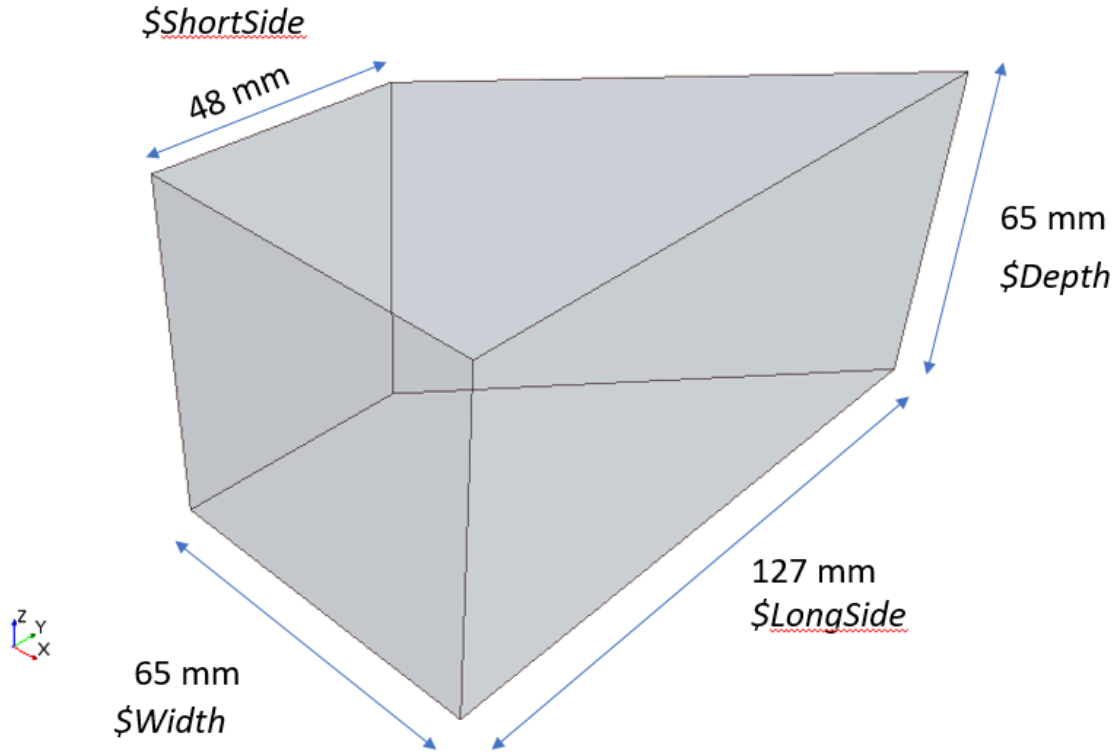

Figure: 24 Hull cell

CCM+ allows you to import CAD from a number of packages, it also comes with its own native CAD capability, called CAD-Modeler. Since the Hull cell geometry is quite simple, we used CAD-Modeler, to create a 2D sketch which was then extruded.

A 'part' was then created from this geometry and the surfaces were labeled according to Figure: 25, to enable setting of boundary conditions. The remaining faces were labeled as 'Sides'.

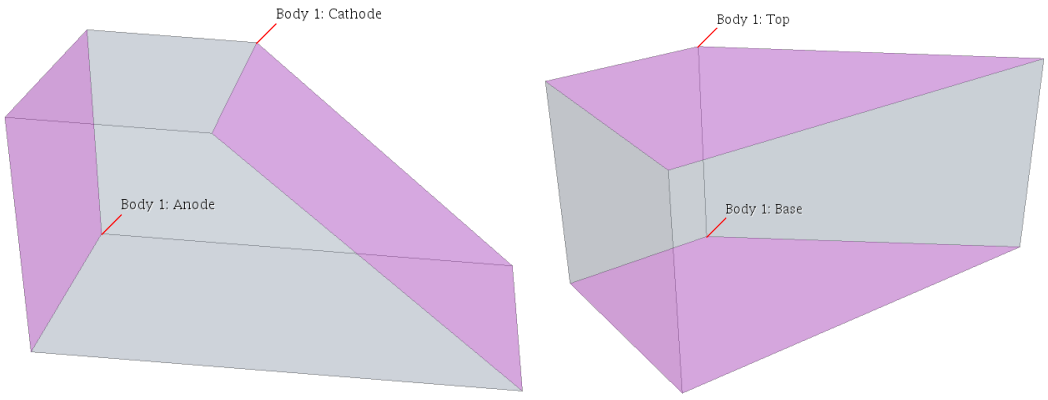

Figure: 25 Boundary surface names for Hull Cell

In the Tools menu, Universal parameters were defined;

- BaseSize
- AnodePotential
- CathodePotential

These were used in the mesh and setting of boundary conditions. The mesh was created using a 'Directed Mesh Operation'.

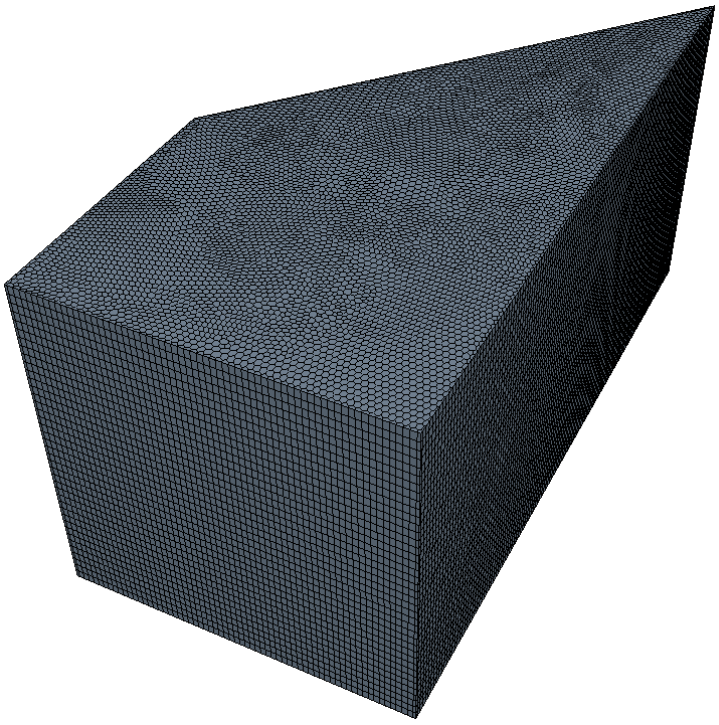

Figure: 26 Computational mesh for Hull cell

In the Tools/Parameters menu we defined parameters that can be later referenced in boundary conditions, Table 4.

Table 4 Tools/parameters

BaseSize	1 mm (+ mesh refinement check with 0.25mm)
AnodePotential	3.3 V
CathodePotential	0 V
Electrical conductivity of the CoP solution (for baseline solution)	11.2 S/m

The aim of this modeling task is to gather necessary plating data for future simulation should Integran need to design scaled-up plating processes. The reason for choosing the Hull cell was to conveniently

illustrate the impact of a changing geometry and plating efficiency. Whether we use constant voltage or current does not matter with this objective in mind. This software was used in double precision mode. For future work, the mesh for example could be refined very easily as this was introduced as an easily changed parameter. The result of a finer mesh, for this Hull cell configuration is to only impact the *peakiness* of the current density magnitude towards the end of the cathode as will be shown later.

3.5.3.3. Simulation results

The current density distribution on the cathode for the baseline solution is shown Figure 27.

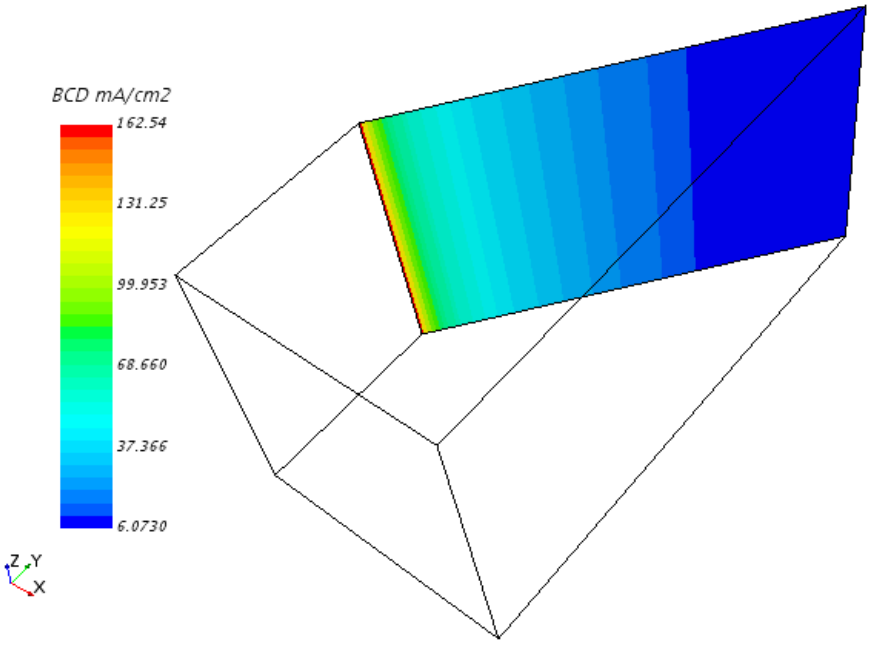

Figure 27 Secondary current density distribution on cathode – for Baseline CoP solution

2D XY plots of current density on cathode are quite informative. This can be done by non-dimensionalizing the distance along the cathode from vertex-5 to vertex-6 shown in Figure 28. The *plating thickness rate* can be calculated by applying Faraday's law.

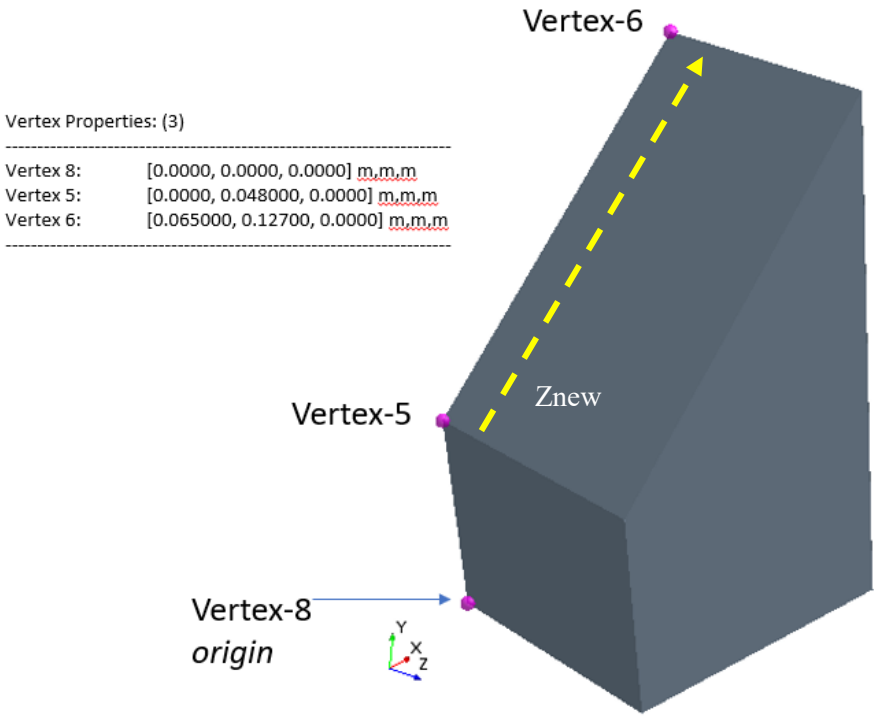

Figure 28: Hull cell geometry and definition of plot line along cathode

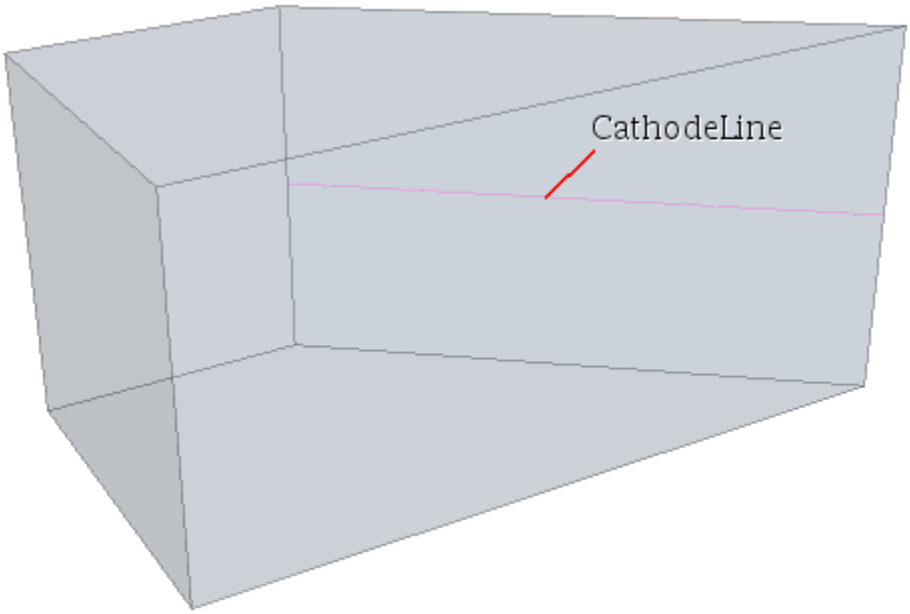

Figure 29: Line on which to plot current density or plating thickness rate as a function of evolved distance along cathode

The current density plots and the plating thickness rate along the cathode are shown in Figure 30 and Figure 31 respectively. The impact of the hydrogen evolution reaction is captured by the application of the plating efficiency factor.

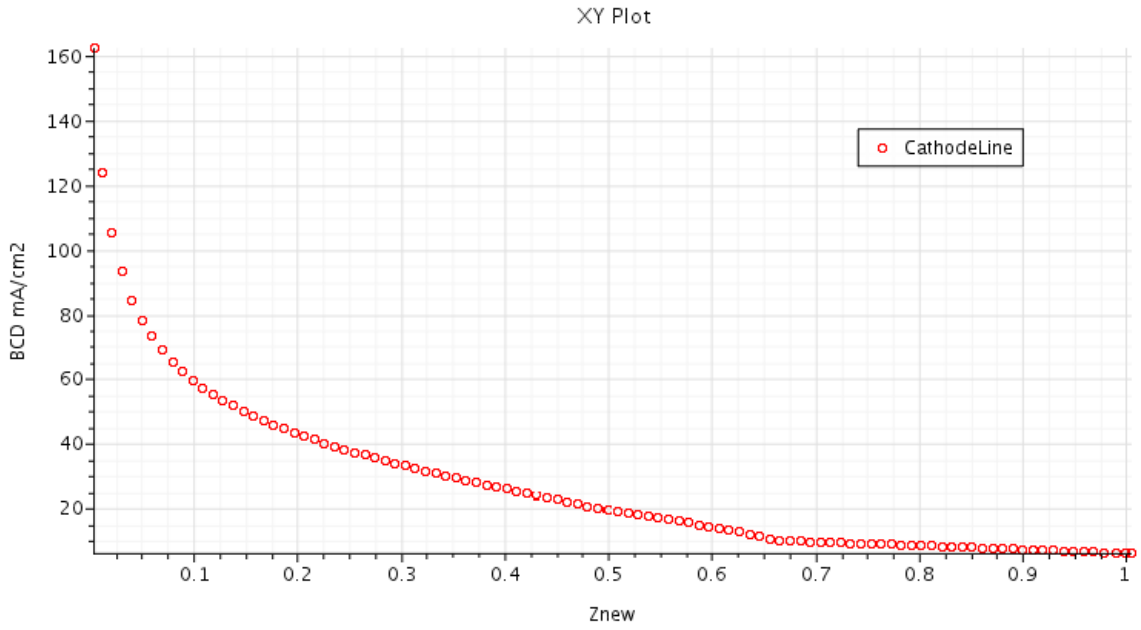

Figure 30: Boundary current density on cathode – for Baseline CoP solution

We can also see how the plating thickness rate varies with the boundary current density on the cathode for each of the three solutions, see Figure 31. A target current density range of 80-150 mA/cm^2 has been proposed by Integran and observing Figure 32, it would seem, from the higher gradient, that the Baseline solution would perform slightly less consistently than the others, that is, the plating thickness rate varies more readily over the current density range.

As stated earlier in Table 4 a minimum mesh size of 1 mm was used. Figure 33 and Table 5 show very similar results for a finer mesh base size of 0.25mm except for the very end of the cathode, where essentially, we have a big jump from a region of maximum current density to zero current density on the adjacent insulating surfaces. Of course, in reality, in production, one would avoid such geometries/issues, by the use of robbers or custom, auxiliary anodes etc.

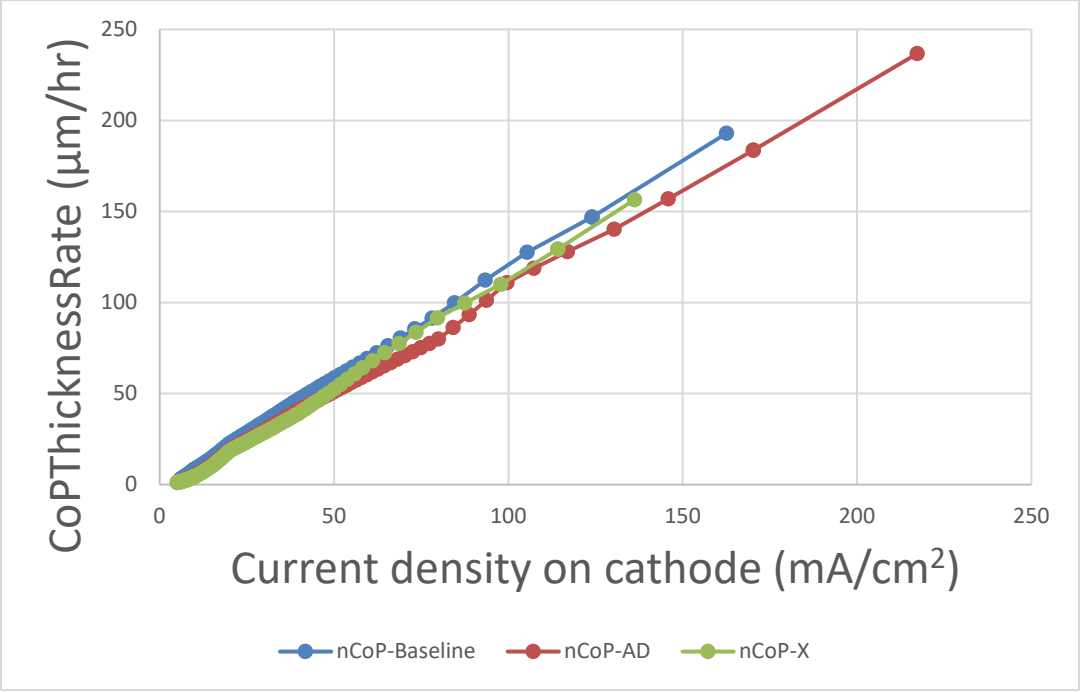

Figure 31: CoP plating thickness rate as function of cathode current density for each of the solutions

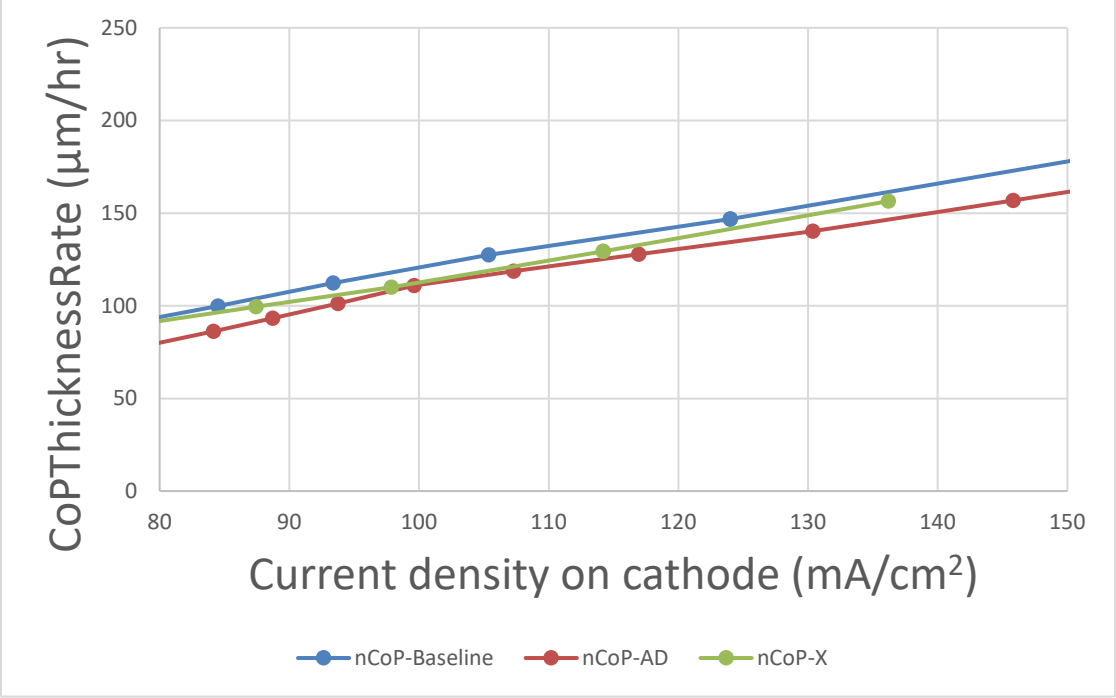

Figure 32: CoP plating thickness rate within the target range of current density for each of the solutions

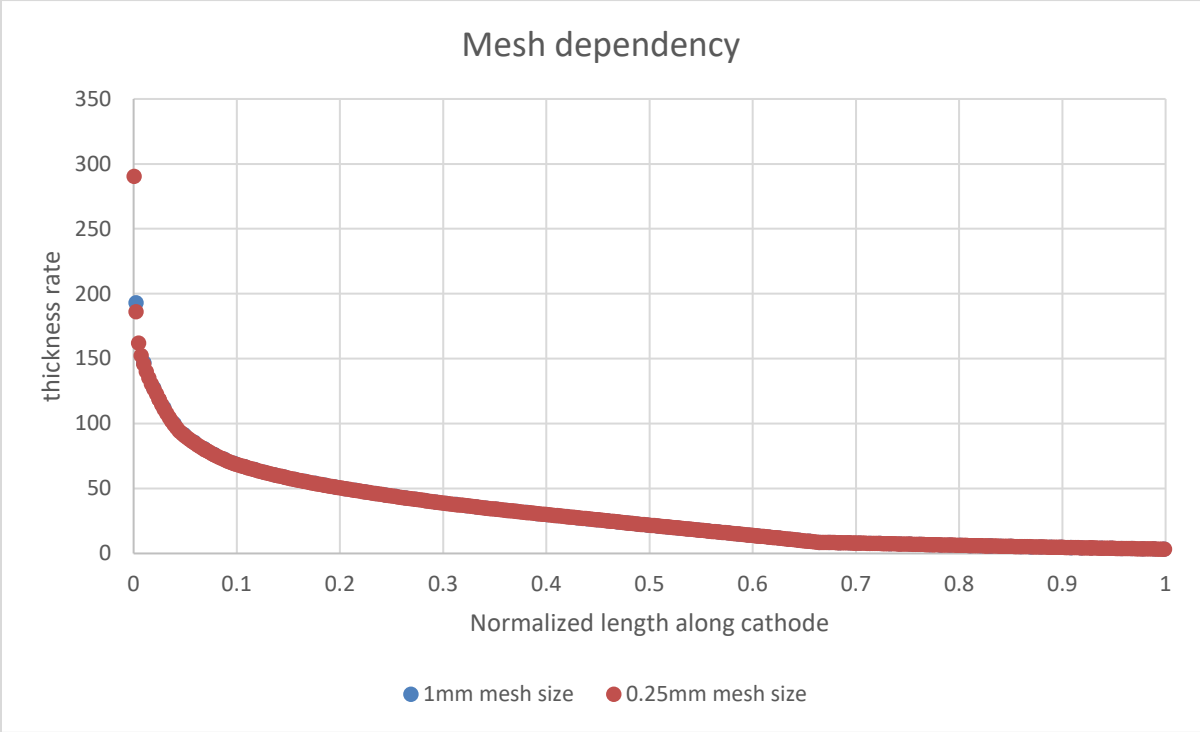

Figure 33 Mesh dependency of computational solution

Table 5 Mesh dependency impact

Mesh size =>	**1 mm**	**0.25 mm**
Minimum	3.1	3.1
Average	31.9	31.0
Maximum	192.9	290.2

4. Summary

In this work we have analyzed the corrosion performance of the Integran developed novel nanocrystalline cobalt-phosphorus embedded with second-phase hard particles. This also included composite coatings with dopants from Cirrus technology. The corrosion performance of these coatings was analyzed using electrochemical techniques i.e. short term and long-term Linear Polarization Resistance (LPR) measurements, Potentiodynamic Polarization and galvanic measurements and Corrosion Djinn analyses. Following are the summary of findings:

- Based on long term and short term LPR measurements finally three coatings (nCoP, nCoP-X and nCoP-AD) were found to be best performing compared to the other 4 coatings (nCo2P, nCo4P, nCo-SX and nCoP-TD).
- Consequently, based on potentiodynamic polarization measurements the nCoP-X showed lowest corrosion rate followed by nCoP baseline and the nCoP-AD. This is based on the LPR and polarization measurements conducted.
- Long term galvanic measurements showed nCoP, nCoP-X and nCoP-AD resulted in similar galvanic currents (same order of magnitude) when coupled against 4130 HSS and Al 7075-T6. The coatings were all behaving cathodically when coupled against the Al 7075-T6 and 4130.
- Similarly, example Corrosion Djinn Analyses also showed that the nCoP, nCoP-X and nCoP-AD coatings were cathodic when compared against 4130, Al 6061-T6 but anodic when compared against 15-5 Stainless. However, the analysis also showed that 4130 has higher self-corrosion rate when compared to the corrosion rate due to galvanic interaction with the coatings.
- Additionally, the nCoP, nCoP-X and nCoP-AD plating solutions were characterized in order acquire the cathodic polarization curves and solutions efficiencies. These data were than used as boundary conditions for conducting an example plating simulation using an arbitrary Hull Cell geometry with the multi-physics software Siemens Simcenter Star CCM+.

Corrosion Djinn - nCoP vs Al 6061-T6

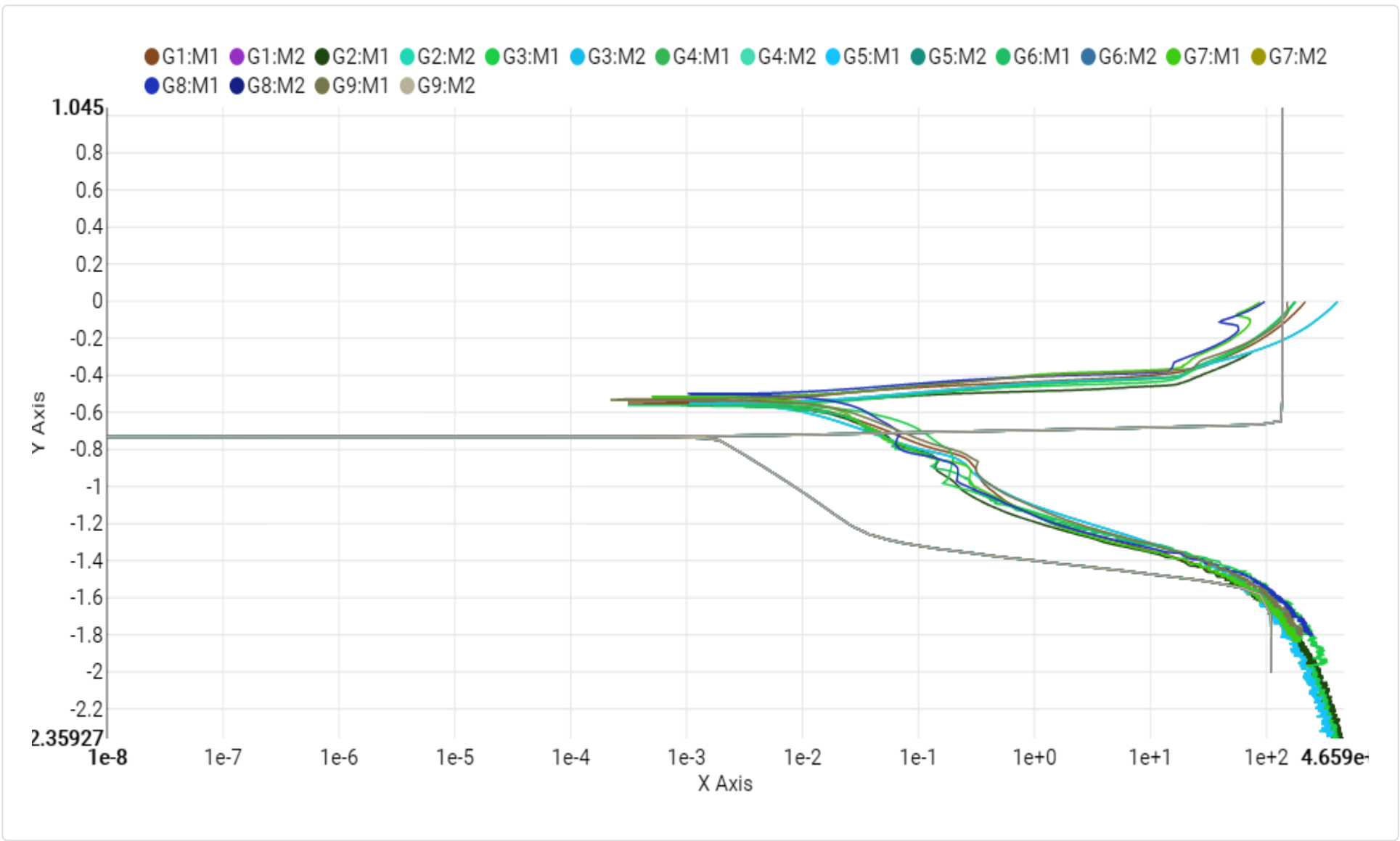

Group 1

Environment 3.5% NaCl

Material 1 (Cathode)

Substrate

Any - COATING ONLY

Designation

None

Coating

nCo-P C1+A3

Treatment

None

OCP	-5.47e-1 V_{SCE}
Self Corrosion Rate	1.09e+1 microns/year
	4.35e-1 mils/year
Galvanic Acceleration Factor	

Material 2 (Anode)

Substrate

Aluminum

Designation

6061-T6

Coating

None

Treatment

None

OCP	-7.31e-1 V_{SCE}
Self Corrosion Rate	2.08e+0 microns/year
	8.33e-2 mils/year
Galvanic Acceleration Factor	2.97e+1

Potential Difference	1.84e-1 V
Mixed Potential	-7.11e-1 V_{SCE}
Galvanic Corrosion Current Density	5.94e-2 Am^{-2}
Galvanic Corrosion Rate	6.19e+1 microns/year
	2.47e+0 mils/year

Group 2

Environment 3.5% NaCl

Material 1 (Cathode)

Substrate

Any - COATING ONLY

Designation

None

Coating

nCo-P A1+C3

Treatment

None

OCP	-5.60e-1 V_{SCE}
Self Corrosion Rate	1.09e+1 microns/year
	4.35e-1 mils/year
Galvanic Acceleration Factor	

Material 2 (Anode)

Substrate

Aluminum

Designation

6061-T6

Coating

None

Treatment

None

OCP	-7.31e-1 V_{SCE}
Self Corrosion Rate	2.08e+0 microns/year
	8.33e-2 mils/year
Galvanic Acceleration Factor	2.43e+1

Potential Difference	1.71e-1 V
Mixed Potential	-7.12e-1 V_{SCE}
Galvanic Corrosion Current Density	4.86e-2 Am^{-2}
Galvanic Corrosion Rate	5.05e+1 microns/year
	2.02e+0 mils/year

Group 3

Environment 3.5% NaCl

Material 1 (Cathode)

Substrate

Any - COATING ONLY

Designation

None

Coating

nCo-P A2+C2

Treatment

None

OCP	-5.55e-1 V_{SCE}
Self Corrosion Rate	1.09e+1 microns/year
	4.35e-1 mils/year
Galvanic Acceleration Factor	

Material 2 (Anode)

Substrate

Aluminum

Designation

6061-T6

Coating

None

Treatment

None

OCP	-7.31e-1 V_{SCE}
Self Corrosion Rate	2.08e+0 microns/year
	8.33e-2 mils/year
Galvanic Acceleration Factor	5.55e+1

Potential Difference	1.76e-1 V
Mixed Potential	-7.07e-1 V_{SCE}
Galvanic Corrosion Current Density	1.11e-1 Am^{-2}
Galvanic Corrosion Rate	1.15e+2 microns/year
	4.62e+0 mils/year

Group 4

Environment 3.5% NaCl

Material 1 (Cathode)

Substrate

Any - COATING ONLY

Designation

None

Coating

nCo-P X A2+C1

Treatment

None

OCP	-5.52e-1 V_{SCE}
Self Corrosion Rate	1.09e+1 microns/year
	4.35e-1 mils/year
Galvanic Acceleration Factor	

Material 2 (Anode)

Substrate

Aluminum

Designation

6061-T6

Coating

None

Treatment

None

OCP	-7.31e-1 V_{SCE}
Self Corrosion Rate	2.08e+0 microns/year
	8.33e-2 mils/year
Galvanic Acceleration Factor	2.02e+1

Potential Difference	1.79e-1 V
Mixed Potential	-7.13e-1 V_{SCE}
Galvanic Corrosion Current Density	4.05e-2 Am^{-2}
Galvanic Corrosion Rate	4.21e+1 microns/year
	1.68e+0 mils/year

Group 5

Environment 3.5% NaCl

Material 1 (Cathode)

Substrate

Any - COATING ONLY

Designation

None

Coating

nCo-P-X A3+C2

Treatment

None

OCP	-5.52e-1 V_{SCE}
Self Corrosion Rate	1.09e+1 microns/year
	4.35e-1 mils/year
Galvanic Acceleration Factor	

Material 2 (Anode)

Substrate

Aluminum

Designation

6061-T6

Coating

None

Treatment

None

OCP	-7.31e-1 V_{SCE}
Self Corrosion Rate	2.08e+0 microns/year
	8.33e-2 mils/year
Galvanic Acceleration Factor	2.02e+1

Potential Difference	1.79e-1 V
Mixed Potential	-7.13e-1 V_{SCE}
Galvanic Corrosion Current Density	4.05e-2 Am^{-2}
Galvanic Corrosion Rate	4.21e+1 microns/year
	1.68e+0 mils/year

Group 6

Environment 3.5% NaCl

Material 1 (Cathode)

Substrate

Any - COATING ONLY

Designation

None

Coating

nCo-P X A4+C3

Treatment

None

OCP	-5.61e-1 V_{SCE}
Self Corrosion Rate	1.09e+1 microns/year
	4.35e-1 mils/year
Galvanic Acceleration Factor	

Material 2 (Anode)

Substrate

Aluminum

Designation

6061-T6

Coating

None

Treatment

None

OCP	-7.31e-1 V_{SCE}
Self Corrosion Rate	2.08e+0 microns/year
	8.33e-2 mils/year
Galvanic Acceleration Factor	2.18e+1

Potential Difference	1.70e-1 V
Mixed Potential	-7.13e-1 V_{SCE}
Galvanic Corrosion Current Density	4.36e-2 Am^{-2}
Galvanic Corrosion Rate	4.54e+1 microns/year
	1.82e+0 mils/year

Group 7

Environment 3.5% NaCl

Material 1 (Cathode)

Substrate

Any - COATING ONLY

Designation

None

Coating

nCo-P AD A5+C4

Treatment

None

OCP	-5.15e-1 V_{SCE}
Self Corrosion Rate	1.09e+1 microns/year
	4.35e-1 mils/year
Galvanic Acceleration Factor	

Material 2 (Anode)

Substrate

Aluminum

Designation

6061-T6

Coating

None

Treatment

None

OCP	-7.31e-1 V_{SCE}
Self Corrosion Rate	2.08e+0 microns/year
	8.33e-2 mils/year
Galvanic Acceleration Factor	2.38e+1

Potential Difference	2.16e-1 V
Mixed Potential	-7.12e-1 V_{SCE}
Galvanic Corrosion Current Density	4.75e-2 Am^{-2}
Galvanic Corrosion Rate	4.95e+1 microns/year
	1.98e+0 mils/year

Group 8

Environment 3.5% NaCl

Material 1 (Cathode)

Substrate

Any - COATING ONLY

Designation

None

Coating

nCo-P AD A3+C3

Treatment

None

OCP	-5.01e-1 V_{SCE}
Self Corrosion Rate	1.09e+1 microns/year
	4.35e-1 mils/year
Galvanic Acceleration Factor	

Material 2 (Anode)

Substrate

Aluminum

Designation

6061-T6

Coating

None

Treatment

None

OCP	-7.31e-1 V_{SCE}
Self Corrosion Rate	2.08e+0 microns/year
	8.33e-2 mils/year
Galvanic Acceleration Factor	3.36e+1

Potential Difference	2.30e-1 V
Mixed Potential	-7.10e-1 V_{SCE}
Galvanic Corrosion Current Density	6.73e-2 Am^{-2}
Galvanic Corrosion Rate	7.00e+1 microns/year
	2.80e+0 mils/year

Group 9

Environment 3.5% NaCl

Material 1 (Cathode)

Substrate

Any - COATING ONLY

Designation

None

Coating

nCo-P AD A4+C1

Treatment

None

OCP	-5.31e-1 V_{SCE}
Self Corrosion Rate	0.00e+0 microns/year
	0.00e+0 mils/year
Galvanic Acceleration Factor	

Material 2 (Anode)

Substrate

Aluminum

Designation

6061-T6

Coating

None

Treatment

None

OCP	-7.31e-1 V_{SCE}
Self Corrosion Rate	2.08e+0 microns/year
	8.33e-2 mils/year
Galvanic Acceleration Factor	3.74e+1

Potential Difference	2.00e-1 V
Mixed Potential	-7.10e-1 V_{SCE}
Galvanic Corrosion Current Density	7.48e-2 Am^{-2}
Galvanic Corrosion Rate	7.78e+1 microns/year
	3.11e+0 mils/year

Corrosion Djinn - nCoP vs 4130

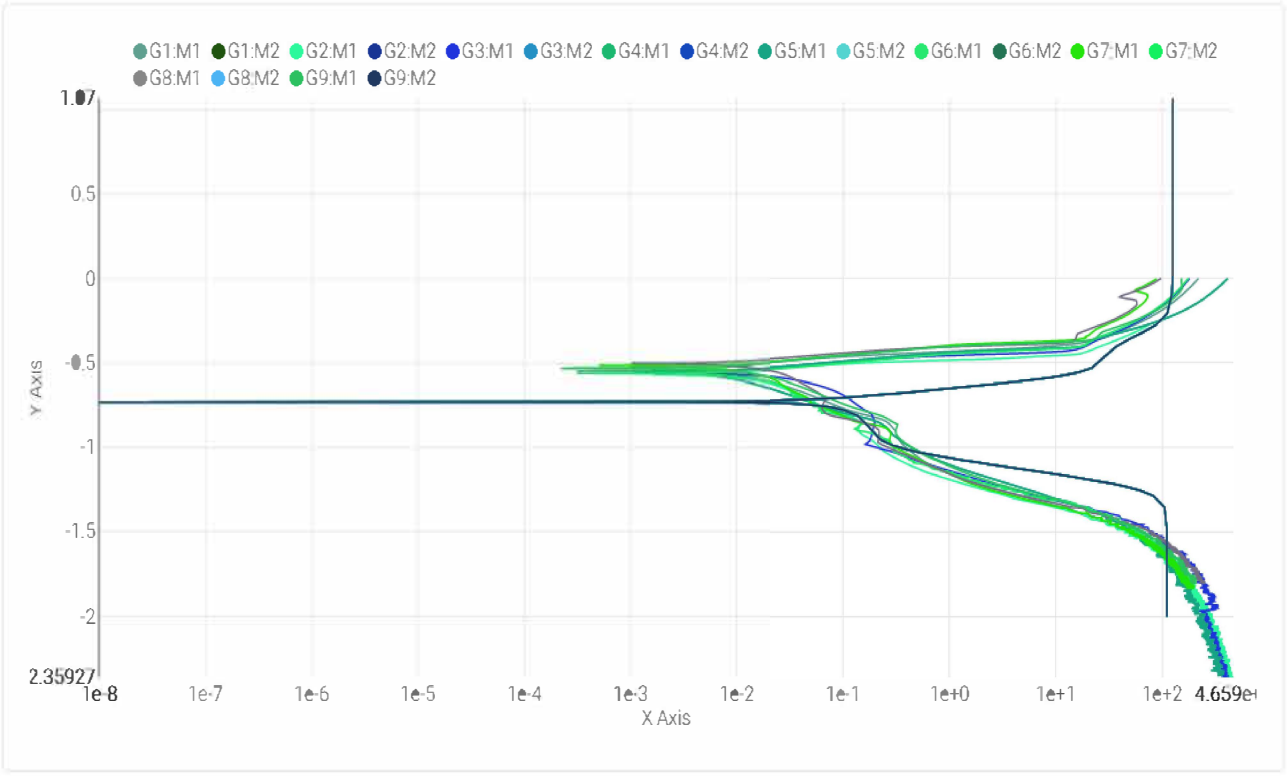

Group 1

Environment 3.5% NaCl

Material 1 (Cathode)

Substrate

Any - COATING ONLY

Designation

None

Coating

nCo-P C1+A3

Treatment

None

OCP	-5.47e-1 V_{SCE}
Self Corrosion Rate	1.09e+1 microns/year
	4.35e-1 mils/year
Galvanic Acceleration Factor	

Material 2 (Anode)

Substrate

Steel, high strength

Designation

4130

Coating

None

Treatment

None

OCP	-7.29e-1 V_{SCE}
Self Corrosion Rate	7.47e+1 microns/year
	2.99e+0 mils/year
Galvanic Acceleration Factor	9.30e-1

Potential Difference	1.82e-1 V
Mixed Potential	-7.13e-1 V_{SCE}
Galvanic Corrosion Current Density	6.06e-2 Am^{-2}
Galvanic Corrosion Rate	6.94e+1 microns/year
	2.78e+0 mils/year

Group 2

Environment 3.5% NaCl

Material 1 (Cathode)

Substrate

Any - COATING ONLY

Designation

None

Coating

nCo-P A1+C3

Treatment

None

OCP	-5.60e-1 V_{SCE}
Self Corrosion Rate	1.09e+1 microns/year
	4.35e-1 mils/year
Galvanic Acceleration Factor	

Material 2 (Anode)

Substrate

Steel, high strength

Designation

4130

Coating

None

Treatment

None

OCP	-7.29e-1 V_{SCE}
Self Corrosion Rate	7.47e+1 microns/year
	2.99e+0 mils/year
Galvanic Acceleration Factor	7.64e-1

Potential Difference	1.69e-1 V
Mixed Potential	-7.16e-1 V_{SCE}
Galvanic Corrosion Current Density	4.98e-2 Am^{-2}
Galvanic Corrosion Rate	5.70e+1 microns/year
	2.28e+0 mils/year

Group 3

Environment 3.5% NaCl

Material 1 (Cathode)

Substrate

Any - COATING ONLY

Designation

None

Coating

nCo-P A2+C2

Treatment

None

OCP	-5.55e-1 V_{SCE}
Self Corrosion Rate	1.09e+1 microns/year
	4.35e-1 mils/year
Galvanic Acceleration Factor	

Material 2 (Anode)

Substrate

Steel, high strength

Designation

4130

Coating

None

Treatment

None

OCP	-7.29e-1 V_{SCE}
Self Corrosion Rate	7.47e+1 microns/year
	2.99e+0 mils/year
Galvanic Acceleration Factor	1.67e+0

Potential Difference	1.74e-1 V
Mixed Potential	-7.04e-1 V_{SCE}
Galvanic Corrosion Current Density	1.09e-1 Am^{-2}
Galvanic Corrosion Rate	1.25e+2 microns/year
	4.99e+0 mils/year

Group 4

Environment 3.5% NaCl

Material 1 (Cathode)

Substrate

Any - COATING ONLY

Designation

None

Coating

nCo-P X A2+C1

Treatment

None

OCP	-5.52e-1 V_{SCE}
Self Corrosion Rate	1.09e+1 microns/year
	4.35e-1 mils/year
Galvanic Acceleration Factor	

Material 2 (Anode)

Substrate

Steel, high strength

Designation

4130

Coating

None

Treatment

None

OCP	-7.29e-1 V_{SCE}
Self Corrosion Rate	7.47e+1 microns/year
	2.99e+0 mils/year
Galvanic Acceleration Factor	6.49e-1

Potential Difference	1.77e-1 V
Mixed Potential	-7.17e-1 V_{SCE}
Galvanic Corrosion Current Density	4.23e-2 Am^{-2}
Galvanic Corrosion Rate	4.84e+1 microns/year
	1.94e+0 mils/year

Group 5

Environment 3.5% NaCl

Material 1 (Cathode)

Substrate

Any - COATING ONLY

Designation

None

Coating

nCo-P-X A3+C2

Treatment

None

OCP	-5.52e-1 V_{SCE}
Self Corrosion Rate	1.09e+1 microns/year
	4.35e-1 mils/year
Galvanic Acceleration Factor	

Material 2 (Anode)

Substrate

Steel, high strength

Designation

4130

Coating

None

Treatment

None

OCP	-7.29e-1 V_{SCE}
Self Corrosion Rate	7.47e+1 microns/year
	2.99e+0 mils/year
Galvanic Acceleration Factor	6.49e-1

Potential Difference	1.77e-1 V
Mixed Potential	-7.17e-1 V_{SCE}
Galvanic Corrosion Current Density	4.23e-2 Am^{-2}
Galvanic Corrosion Rate	4.84e+1 microns/year
	1.94e+0 mils/year

Group 6

Environment 3.5% NaCl

Material 1 (Cathode)

Substrate

Any - COATING ONLY

Designation

None

Coating

nCo-P X A4+C3

Treatment

None

OCP	-5.61e-1 V_{SCE}
Self Corrosion Rate	1.09e+1 microns/year
	4.35e-1 mils/year
Galvanic Acceleration Factor	

Material 2 (Anode)

Substrate

Steel, high strength

Designation

4130

Coating

None

Treatment

None

OCP	-7.29e-1 V_{SCE}
Self Corrosion Rate	7.47e+1 microns/year
	2.99e+0 mils/year
Galvanic Acceleration Factor	6.67e-1

Potential Difference	1.68e-1 V
Mixed Potential	-7.17e-1 V_{SCE}
Galvanic Corrosion Current Density	4.35e-2 Am^{-2}
Galvanic Corrosion Rate	4.98e+1 microns/year
	1.99e+0 mils/year

Group 7

Environment 3.5% NaCl

Material 1 (Cathode)

Substrate

Any - COATING ONLY

Designation

None

Coating

nCo-P AD A5+C4

Treatment

None

OCP	-5.15e-1 V_{SCE}
Self Corrosion Rate	1.09e+1 microns/year
	4.35e-1 mils/year
Galvanic Acceleration Factor	

Material 2 (Anode)

Substrate

Steel, high strength

Designation

4130

Coating

None

Treatment

None

OCP	-7.29e-1 V_{SCE}
Self Corrosion Rate	7.47e+1 microns/year
	2.99e+0 mils/year
Galvanic Acceleration Factor	7.42e-1

Potential Difference	2.14e-1 V
Mixed Potential	-7.16e-1 V_{SCE}
Galvanic Corrosion Current Density	4.84e-2 Am^{-2}
Galvanic Corrosion Rate	5.54e+1 microns/year
	2.22e+0 mils/year

Group 8

Environment 3.5% NaCl

Material 1 (Cathode)

Substrate

Any - COATING ONLY

Designation

None

Coating

nCo-P AD A3+C3

Treatment

None

OCP	-5.01e-1 V_{SCE}
Self Corrosion Rate	1.09e+1 microns/year
	4.35e-1 mils/year
Galvanic Acceleration Factor	

Material 2 (Anode)

Substrate

Steel, high strength

Designation

4130

Coating

None

Treatment

None

OCP	-7.29e-1 V_{SCE}
Self Corrosion Rate	7.47e+1 microns/year
	2.99e+0 mils/year
Galvanic Acceleration Factor	1.04e+0

Potential Difference	2.28e-1 V
Mixed Potential	-7.12e-1 V_{SCE}
Galvanic Corrosion Current Density	6.76e-2 Am^{-2}
Galvanic Corrosion Rate	7.74e+1 microns/year
	3.10e+0 mils/year

Group 9

Environment 3.5% NaCl

Material 1 (Cathode)

Substrate

Any - COATING ONLY

Designation

None

Coating

nCo-P AD A4+C1

Treatment

None

OCP	-5.31e-1 V_{SCE}
Self Corrosion Rate	0.00e+0 microns/year
	0.00e+0 mils/year
Galvanic Acceleration Factor	

Material 2 (Anode)

Substrate

Steel, high strength

Designation

4130

Coating

None

Treatment

None

OCP	-7.29e-1 V_{SCE}
Self Corrosion Rate	7.47e+1 microns/year
	2.99e+0 mils/year
Galvanic Acceleration Factor	1.15e+0

Potential Difference	1.98e-1 V
Mixed Potential	-7.10e-1 V_{SCE}
Galvanic Corrosion Current Density	7.52e-2 Am^{-2}
Galvanic Corrosion Rate	8.61e+1 microns/year
	3.44e+0 mils/year

Corrosion Djinn - nCoP vs 15-5 PH

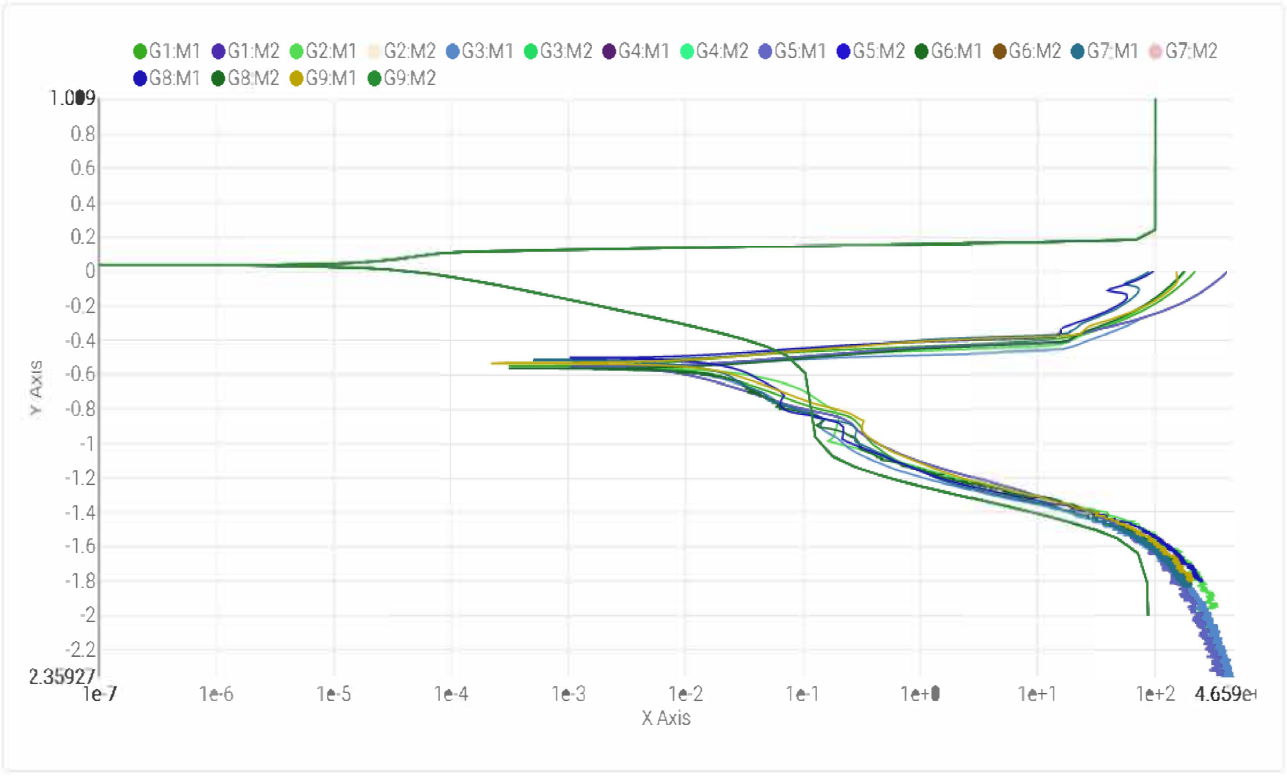

Group 1

Environment 3.5% NaCl

Material 1 (Anode)

Substrate

Any - COATING ONLY

Designation

None

Coating

nCo-P C1+A3

Treatment

None

OCP	-5.47e-1 V_{SCE}
Self Corrosion Rate	1.09e+1 microns/year
	4.35e-1 mils/year
Galvanic Acceleration Factor	6.61e+0

Material 2 (Cathode)

Substrate

Stainless steel

Designation

15-5 PH

Coating

None

Treatment

None

OCP	3.79e-2 V_{SCE}
Self Corrosion Rate	3.57e-2 microns/year
	1.43e-3 mils/year
Galvanic Acceleration Factor	

Potential Difference	5.85e-1 V
Mixed Potential	-4.73e-1 V_{SCE}
Galvanic Corrosion Current Density	6.61e-2 Am^{-2}
Galvanic Corrosion Rate	7.18e+1 microns/year
	2.87e+0 mils/year

Group 2

Environment 3.5% NaCl

Material 1 (Anode)

Substrate

Any - COATING ONLY

Designation

None

Coating

nCo-P A2+C2

Treatment

None

OCP	-5.55e-1 V_{SCE}
Self Corrosion Rate	1.09e+1 microns/year
	4.35e-1 mils/year
Galvanic Acceleration Factor	7.67e+0

Material 2 (Cathode)

Substrate

Stainless steel

Designation

15-5 PH

Coating

None

Treatment

None

OCP	3.79e-2 V_{SCE}
Self Corrosion Rate	3.57e-2 microns/year
	1.43e-3 mils/year
Galvanic Acceleration Factor	

Potential Difference	5.93e-1 V
Mixed Potential	-5.01e-1 V_{SCE}
Galvanic Corrosion Current Density	7.67e-2 Am^{-2}
Galvanic Corrosion Rate	8.34e+1 microns/year
	3.34e+0 mils/year

Group 3

Environment 3.5% NaCl

Material 1 (Anode)

Substrate

Any - COATING ONLY

Designation

None

Coating

nCo-P A1+C3

Treatment

None

OCP	-5.60e-1 V_{SCE}
Self Corrosion Rate	1.09e+1 microns/year
	4.35e-1 mils/year
Galvanic Acceleration Factor	8.01e+0

Material 2 (Cathode)

Substrate

Stainless steel

Designation

15-5 PH

Coating

None

Treatment

None

OCP	3.79e-2 V_{SCE}
Self Corrosion Rate	3.57e-2 microns/year
	1.43e-3 mils/year
Galvanic Acceleration Factor	

Potential Difference	5.98e-1 V
Mixed Potential	-5.12e-1 V_{SCE}
Galvanic Corrosion Current Density	8.01e-2 Am^{-2}
Galvanic Corrosion Rate	8.71e+1 microns/year
	3.48e+0 mils/year

Group 4

Environment 3.5% NaCl

Material 1 (Anode)

Substrate

Any - COATING ONLY

Designation

None

Coating

nCo-P X A2+C1

Treatment

None

OCP	-5.52e-1 V_{SCE}
Self Corrosion Rate	1.09e+1 microns/year
	4.35e-1 mils/year
Galvanic Acceleration Factor	7.60e+0

Material 2 (Cathode)

Substrate

Stainless steel

Designation

15-5 PH

Coating

None

Treatment

None

OCP	3.79e-2 V_{SCE}
Self Corrosion Rate	3.57e-2 microns/year
	1.43e-3 mils/year
Galvanic Acceleration Factor	

Potential Difference	5.90e-1 V
Mixed Potential	-4.99e-1 V_{SCE}
Galvanic Corrosion Current Density	7.60e-2 Am^{-2}
Galvanic Corrosion Rate	8.27e+1 microns/year
	3.31e+0 mils/year

Group 5

Environment 3.5% NaCl

Material 1 (Anode)

Substrate

Any - COATING ONLY

Designation

None

Coating

nCo-P-X A3+C2

Treatment

None

OCP	-5.52e-1 V_{SCE}
Self Corrosion Rate	1.09e+1 microns/year
	4.35e-1 mils/year
Galvanic Acceleration Factor	7.60e+0

Material 2 (Cathode)

Substrate

Stainless steel

Designation

15-5 PH

Coating

None

Treatment

None

OCP	3.79e-2 V_{SCE}
Self Corrosion Rate	3.57e-2 microns/year
	1.43e-3 mils/year
Galvanic Acceleration Factor	

Potential Difference	5.90e-1 V
Mixed Potential	-4.99e-1 V_{SCE}
Galvanic Corrosion Current Density	7.60e-2 Am^{-2}
Galvanic Corrosion Rate	8.27e+1 microns/year
	3.31e+0 mils/year

Group 6

Environment 3.5% NaCl

Material 1 (Anode)

Substrate

Any - COATING ONLY

Designation

None

Coating

nCo-P X A4+C3

Treatment

None

OCP	-5.61e-1 V_{SCE}
Self Corrosion Rate	1.09e+1 microns/year
	4.35e-1 mils/year
Galvanic Acceleration Factor	7.91e+0

Material 2 (Cathode)

Substrate

Stainless steel

Designation

15-5 PH

Coating

None

Treatment

None

OCP	3.79e-2 V_{SCE}
Self Corrosion Rate	3.57e-2 microns/year
	1.43e-3 mils/year
Galvanic Acceleration Factor	

Potential Difference	5.99e-1 V
Mixed Potential	-5.09e-1 V_{SCE}
Galvanic Corrosion Current Density	7.91e-2 Am^{-2}
Galvanic Corrosion Rate	8.60e+1 microns/year
	3.44e+0 mils/year

Group 7

Environment 3.5% NaCl

Material 1 (Anode)

Substrate

Any - COATING ONLY

Designation

None

Coating

nCo-P AD A5+C4

Treatment

None

OCP	-5.15e-1 V_{SCE}
Self Corrosion Rate	1.09e+1 microns/year
	4.35e-1 mils/year
Galvanic Acceleration Factor	6.35e+0

Material 2 (Cathode)

Substrate

Stainless steel

Designation

15-5 PH

Coating

None

Treatment

None

OCP	3.79e-2 V_{SCE}
Self Corrosion Rate	3.57e-2 microns/year
	1.43e-3 mils/year
Galvanic Acceleration Factor	

Potential Difference	5.53e-1 V
Mixed Potential	-4.67e-1 V_{SCE}
Galvanic Corrosion Current Density	6.35e-2 Am^{-2}
Galvanic Corrosion Rate	6.91e+1 microns/year
	2.76e+0 mils/year

Group 8

Environment 3.5% NaCl

Material 1 (Anode)

Substrate

Any - COATING ONLY

Designation

None

Coating

nCo-P AD A3+C3

Treatment

None

OCP	-5.01e-1 V_{SCE}
Self Corrosion Rate	1.09e+1 microns/year
	4.35e-1 mils/year
Galvanic Acceleration Factor	5.85e+0

Material 2 (Cathode)

Substrate

Stainless steel

Designation

15-5 PH

Coating

None

Treatment

None

OCP	3.79e-2 V_{SCE}
Self Corrosion Rate	3.57e-2 microns/year
	1.43e-3 mils/year
Galvanic Acceleration Factor	

Potential Difference	5.39e-1 V
Mixed Potential	-4.56e-1 V_{SCE}
Galvanic Corrosion Current Density	5.85e-2 Am^{-2}
Galvanic Corrosion Rate	6.36e+1 microns/year
	2.54e+0 mils/year

Group 9

Environment 3.5% NaCl

Material 1 (Anode)

Substrate

Any - COATING ONLY

Designation

None

Coating

nCo-P AD A4+C1

Treatment

None

OCP	-5.31e-1 V_{SCE}
Self Corrosion Rate	0.00e+0 microns/year
	0.00e+0 mils/year
Galvanic Acceleration Factor	Infinity

Material 2 (Cathode)

Substrate

Stainless steel

Designation

15-5 PH

Coating

None

Treatment

None

OCP	3.79e-2 V_{SCE}
Self Corrosion Rate	3.57e-2 microns/year
	1.43e-3 mils/year
Galvanic Acceleration Factor	

Potential Difference	5.69e-1 V
Mixed Potential	-4.69e-1 V_{SCE}
Galvanic Corrosion Current Density	6.46e-2 Am^{-2}
Galvanic Corrosion Rate	7.02e+1 microns/year
	2.81e+0 mils/year

6.9 Appendix G – Cirrus Final Report

Please see attached the final report from Cirrus Materials.

[i] SFMRB Metal Finishing Industry Market Survey 2000-2001, Report No. 6, Surface Finishing Industry Council, American Electroplaters and Surface Finishers Society, the Metal Finishing Suppliers Association, and the National Association of Metal Finishers.

SERDP WP2609

Summary Research Report – October 2018

1. Introduction

The timeframe for WP2609 programme is two years. This document details only the year 2 research summaries and final conclusions. Information concerning the year 1 research results can be found in last year's report.

Over all the programme showed that the adoption of Cirrus Dopant™ with Integran's nCoP process can produce good improvements in both hardness and wear resistance. Aqueous dopants evaluated in the second year of the programme showed enhanced results against those evaluated in the first year. Under optimum conditions the hardness of the coating can be improved by about 10-12% using the new alumina dopants. Wear performance using pin on disk wear testing can improve outcomes by 10-18%. Work has been performed to understand the required dopant replenishment regimes, however further work is required to ensure that these regimes operate at beyond laboratory scale.

The technology has been successfully transferred to Integran, however further work is required for them to achieve results comparable to those obtained by Cirrus.

Dual dopants show very interesting results which have yet to be fully validated but suggest in certain circumstances a hardness improvement of 80-90% may be possible.

This document is intended to be read together with the year 1 report (included as Annex A) Section 2 reiterates the overall programme research goals. Section 3, which covers experimental procedures, is left blank and reference can be made to last year's report for details. Section 4 discusses new dopants developments, including novel and potentially important work on dual dopant applications. Section 5 discusses the requirements of dopant replenishment and presents experimental results. Section 6 presents conclusions both for year 2 and for the overall programme.

2. WP2609 Goals

In Year One, the project utilised Integran's existing nCoP bath chemistry and applied plating procedures, operating at laboratory scale. The primary objectives were:

a) *nCoP process stand-up at Cirrus*: logistics and plating line were established within the Cirrus Materials laboratory based at Rigg Electroplating Ltd in Auckland NZ, using Integran down-selected metal matrix from WP26-09 Task 1.

b) *Evaluate Dopant Compatibility with nCoP Chemistry:* the formulation of the candidate nCoP bath was analysed for compatibility with the existing dopant chemistries and existing dopants. Based on preliminary analysis, one of the existing dopants chemistries was selected for a first level of evaluation. The evaluation was conducted at laboratory beaker scale to assess the selected dopant chemistry for stability and longevity when combined with the target bath.

Work commenced with ≤200mL of the bath, with the objective of understanding the maximum quantity of the selected dopant that may be added to the nCoP chemistry while maintaining sufficiently small particle size in the electrolyte. Where required the selected dopant was subjected to minor modification to improve its stability in the target nCoP bath. A further test was performed to ensure that the dopant remains stable in the bath over an extended period. This test was performed by storing a bath doped at half the determined maximum level at room temperature and re-examining it for particles and precipitate at a regular interval.

c) *Determine Preferred Doping Levels*: The selected dopant for the initial task (b) was subjected to several plating tests to determine a preferred doping level with the dopant. Prior experience indicated that a doping level of between 0.5% by volume and 2% by volume works with many plating baths. While a wide range of doping levels may produce improved coating performance there is typically a narrow range where the performance is optimized. During these experiments, small test baths were used, and plating performed on mild steel (3 x 2 cm2) samples for simplicity. In each test, a new bath was used, and a reference sample plated without dopant to evaluate the improvement. Samples were prepared on mild steel substrates that had been appropriately pre-treated, and then plated using the optimum parameters for the bath (determined from the supplier TDS) to create coatings of approximately 10 - 20μm in thickness. Each sample was subjected to hardness testing (which is a useful initial discriminant for coating improvement). Samples were also subjected to surface and cross section analysis to ensure that the coatings were compact and without visible cracks and pores. From these results, one or two doping levels were selected for further analysis. The ideal outcome from this step was a range of doping levels at which the mechanical improvements are equivalent. The high end of this range was likely to be the preferred doping level and the low end of the range used to define the dopant exhaustion level for a bath.

d) *Confirm Coating Performance:* a second level of analysis was performed by coating selected target substrate samples with the optimum levels of dopant in baths of up to 6L capacity. This work begun with DC plating and graduated to the target pulse plating waveforms. A new bath was used for coating each sample set, however depending on the sample size and batch capacity multiple samples may have been plated at one time. These samples were coated to a target thickness agreed with Integran for their further evaluation. The test protocol for these samples was agreed with Integran and performed at UoA facilities.

e) *Determine Bath Management Parameters*: provided Integran testing of samples confirmed the initial results, further analysis of the coating process was performed by Cirrus (NB: this task ongoing).

In Year Two, the project utilised Integran's existing nCoP bath chemistry and plating procedures, operating at laboratory scale. The primary objectives were:

f) *nCoP process stand-up at Cirrus*: logistics and plating line re-established within the Cirrus Lab, initially based at Rigg Electroplating Ltd in Auckland, NZ, and later at Cirrus Materials Science Ltd, using Integran down-selected metal matrix from WP26-09 Task 1.

g) *New Dopant Evaluation:* the formulation of the candidate nCoP bath was analysed for compatibility with the existing dopant chemistries and existing dopants. Preliminary analysis suggested the organic dopant (titania or zirconia dopant) caused precipitation in the bath, while alumina aqueous dopant remain stable in the bath and did not precipitate. A high concentration Al dopant was developed to reduce the volume of dopant to be added in the bath. Ultimately, new titania and zirconia aqueous dopants were developed to replace the organic dopants for this application.

h) *Development sub-license, technology transfer & support*: Documentation on the preparation, doping, handling, and of replenishing dopant for nCoP baths was provided to Integran. Technical support was provided initially on-site in Toronto, and then remotely from New Zealand.

i) *Confirm Coating Performance:* Several coated Taber wear panels were provided to Integran to evaluate the wear performance for different dopants with nCoP. A variety of smaller size samples was also provided for Cordessa, LLC for evaluate the corrosion performance.

3. Experimental Procedures

As reported in the on the completion Year 1 research report at Annex A.

4. Dopant Selection

During the first year of this programme, Cirrus selected three generic dopants for evaluation, these were: two organic dopants which develop nanoparticles of titania and zirconia respectively, and one aqueous dopant which develops alumina nanoparticles. During the programme the formulation of the aqueous dopant was adapted for improved compatibility with the nCoP bath.

In year 2, Cirrus evaluated three additional dopants, being: high concentration alumina dopant, together with aqueous titania and zirconia dopant formulations. (NB: these dopants were developed independently of the programme under a New Zealand Government research grant).

4.1 Alumina Aqueous

In the year 1 programme, we discovered that 10 mL/L Al dopant is optimum providing better microhardness and wear resistance in the nCoP coatings. However, 10 mL/L represents a bath dilution of 1% by volume. By increasing the particle concentration in the dopant, we aim achieve similar results with lower volume of dopant, reducing the impact on the underlying bath chemistry. Importantly, this improvement limits the dilution of the plating bath and reduces the introduction of non-functional additives. The development is critical when dopant replenishment is considered as such non-functional additives may accumulate in the bath.

Figure 1 shows both the microhardness and wear track widths for nCoP doped with two high concentration alumina dopants. Here 0.025 and 0.075 represents 2.5 and 7.5 times the standard dopant particle concentration.

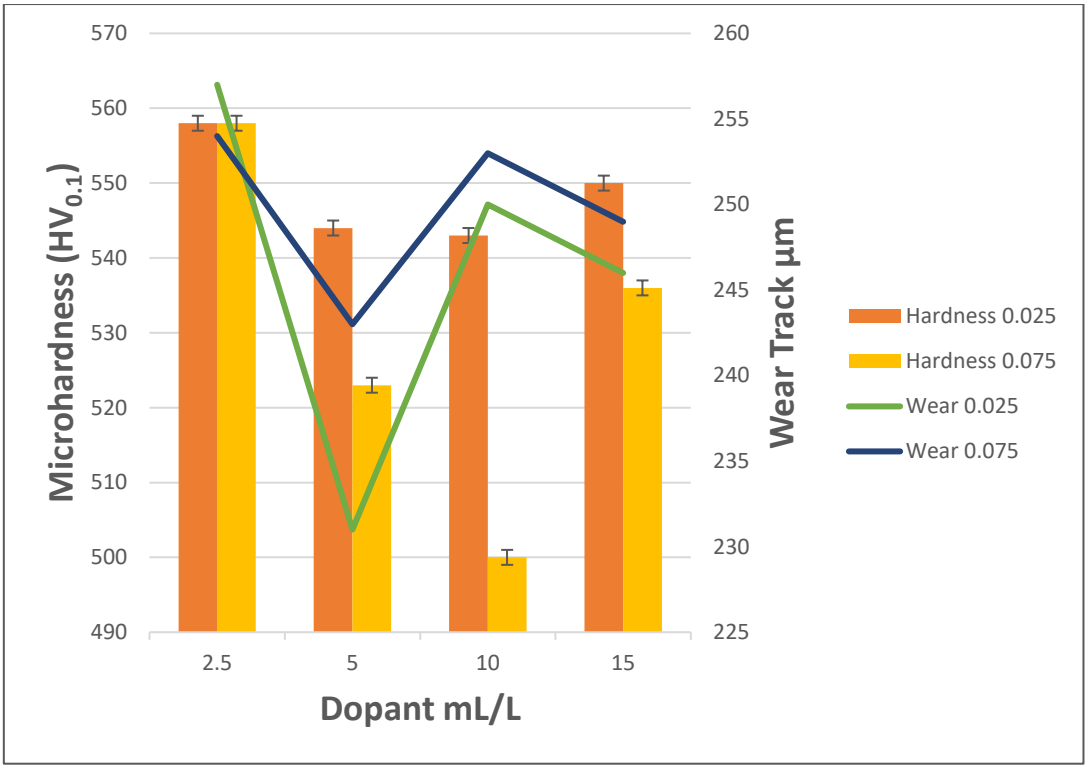

Figure 1: Microhardness and wear tracks of CoP doped with different concentration of alumina.

The results indicate that both dopants exhibited the highest microhardness at the dopant level at 2.5 mL/L, which is 25% of the dopant level reported in year 1. It is interesting to note that the best wear and best hardness required different dopant concentrations. Further work is required to understand the underlying mechanisms.

Figure 2Figure 2 depicts the distribution of the particle size against the intensity for concentration alumina dopants with different particle concentrations. The concentrations of 2.5x and 7.5x were selected from an analysis of particle zeta potential. Cirrus' research indicates that if the zeta potential of a dopant is greater and -25mV the dopant is likely to be stable and the particles will be incorporated into a coating. The average particle sizes are summarized in Table 1; however, these measurements are for the dopant alone. Due to the opacity of the nCoP bath it was not possible to check the particle size in the bath, which is assumed to be smaller than in dopant, as no precipitation was observed. As expected, the results show that increasing the concentration of alumina particles by 2.5 times standard increases the particle size by up to 4 times, however the growth in particle size stabilises with the further increase in alumina particles to 7.5 times standard.

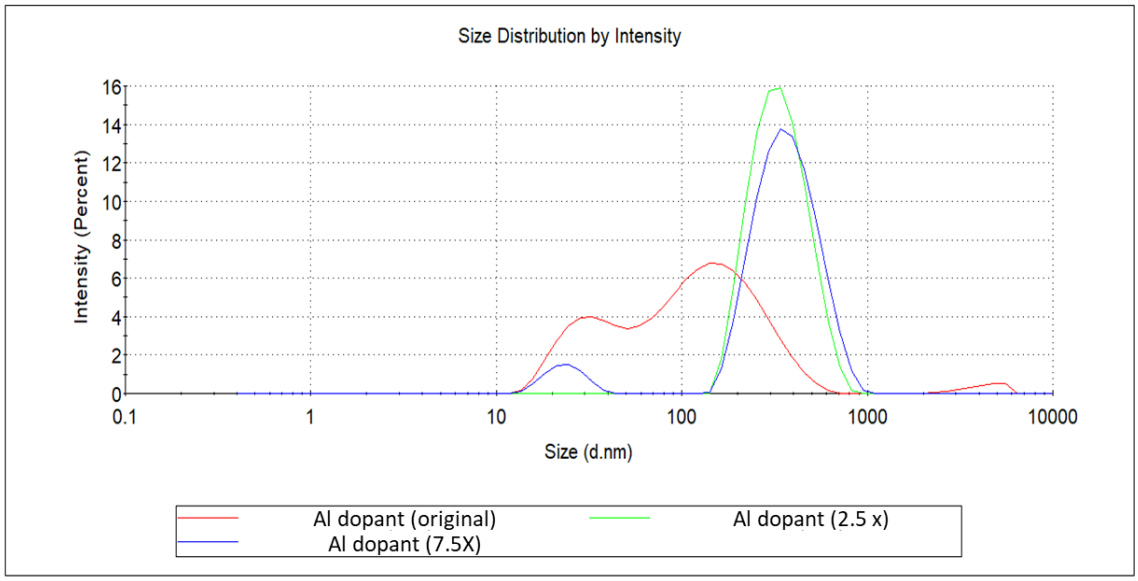

Figure 2: Distribution of particles size determined by zetasizer.

Table 1: Average of distribution of particles size.

Sample	Test (Z-Ave)			Average (d. nm)	STDEV
	1	2	3		
Al Dopant (original)	73.9	73.65	74.45	74.00	0.41
Al Dopant (2.5X)	311.3	310.7	310.7	310.90	0.35
Al Dopant (7.5X)	261.2	262.2	247.5	256.97	8.21

4.2 Titania Aqueous Dopant

Development of a substantially aqueous titania dopant was quite difficult and conducted under an NZ Government research grant to ensure dedicated resources could be deployed for this research. The results of this separate project are reported elsewhere, unfortunately it was not possible to develop a stable dopant with a high concentration of titania particles. Once considered stable, the new aqueous titania dopants were added to the WP2609 project for testing with nCoP.

Initial evaluation of the selected dopants was performed using samples plated at 135 mA/cm^2 for 20 min on a commercially sourced Q-panel substrate. Table 2 shows the initial microhardness for the newly developed titania aqueous dopant, with very little improvement observed. However, the increase at 15 mL/L suggested evaluation should be conducted at higher dopant levels.

Table 2: Microhardness of new developed titania aqueous dopant

Sample Descriptions	Microhardness ($HV_{0.1}$)
nCoP (reference)	512±9
nCoP+5mL/L Ti	510±2

nCoP+10mL/L Ti	497±5
nCoP+15mL/L Ti	533±2

Figure 3 shows results for hardness and wear obtained with an aqueous titania dopant and high doping levels. As may be observed, a doping level of 50mL/L exhibited both a high wear resistance and hardness. This suggests that titania can be a useful dopant for nCoP but a formulation with a higher particle concentration is required to be practical. Cirrus has not begun developing such a formulation yet.

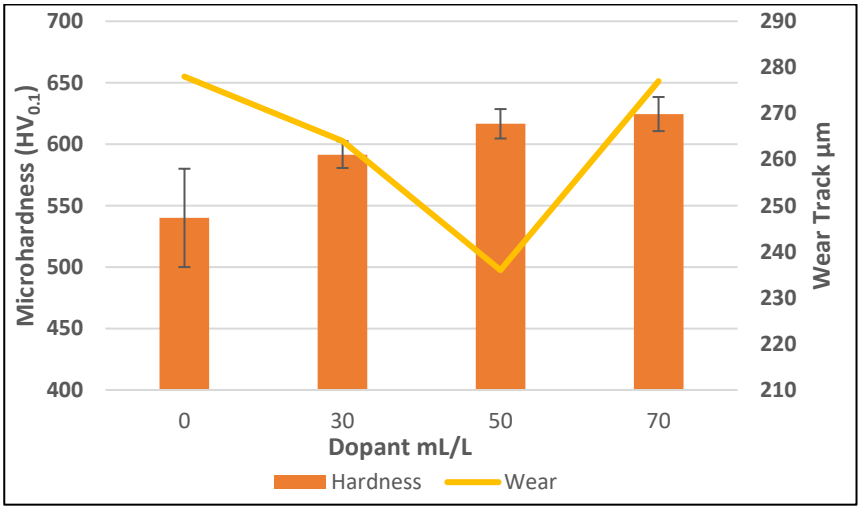

Figure 3: Microhardness and wear tracks of CoP doped with different level of titania dopant.

4.3 Zirconia Aqueous Dopant

Under the auspices of an NZ Government research grant, Cirrus researched multiple approaches to creating an aqueous zirconia dopant, initially for use in electroless plating. The most successful approach yielded several candidate aqueous zirconia dopants. Once introduced to WP2906, the best of these only produced a 5% hardness improvement when incorporated into the nCoP bath, and many resulted in over-doping, where the zeta-potential of particles in the bath is over-come and particle agglomeration occurs during the deposition process.

Figure 4 shows the surface morphology of the samples when over-doped (at 25mL/L), here we were looking for a harness improvement; however, despite the porosity introduced by over-doping, the surface morphology appears refined. The porous structure of the deposit, caused by over-doping, might explain the low hardness improvement.

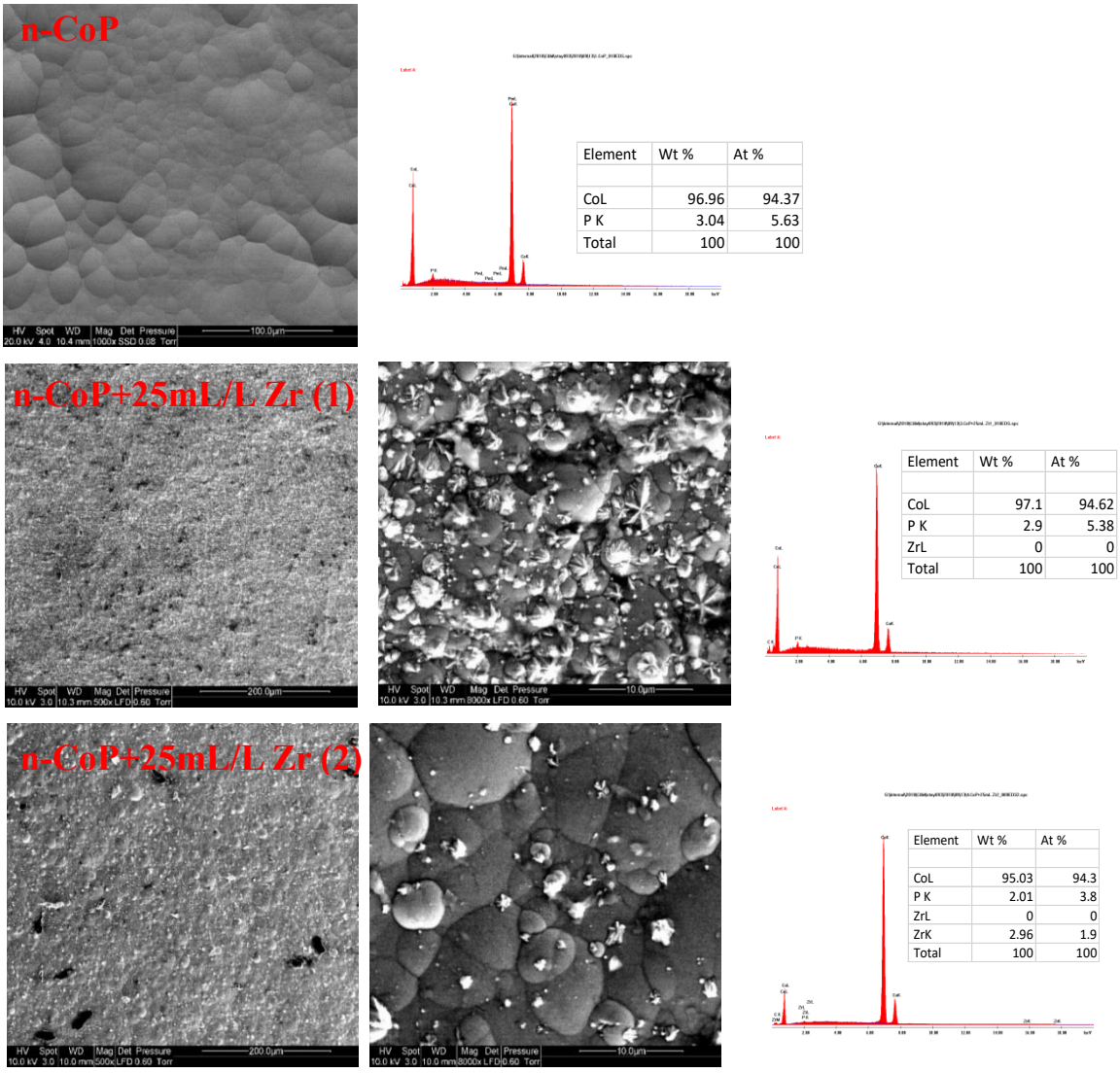

Figure 4: SEM morphology and EDS of undoped n-CoP coating and using different formulation of Zr dopant.

Despite the minimal hardness improvement, the change surface morphology for the two formulations (Zr (1) and Zr (2)) had a significant effect on the co-efficient of friction, as shown in Figure 5. Here 10mL/L of dopant was incorporated into nCoP bath. The wear testing was performed on a Nanovea Tribometer operating in linear mode at 100 rpm with a 7N load.

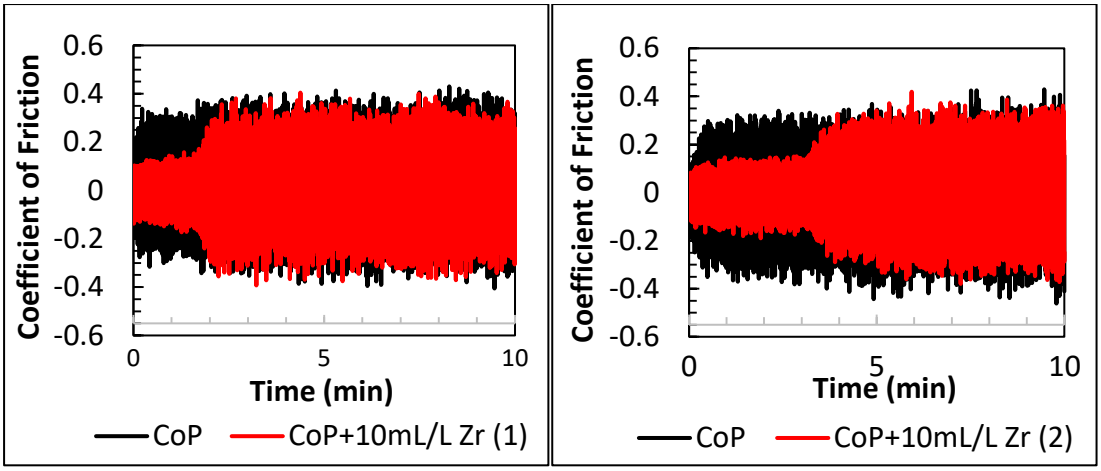

Figure 5: Coefficient of Friction for CoP+10mL/L zirconia aqueous dopant.

The finer surface morphology appears to improve the co-efficient of friction with the two dopant formulations producing different results.

As can be observed, the aqueous zirconia dopant lowered the co-efficient of friction but did not improve the microhardness of the coating. Following this, the dopant formulation was further modified (Zr 3) to eliminate the porous microstructure. Figure 6 shows the optical microscopy images for the three variants of zirconia dopant using 25 mL/L in each case to exacerbate the over-doping effect. As may be observed, Zr-3 dopant formulation eliminated the porous microstructure; however, the hardness improved remained steady at 5-7%.

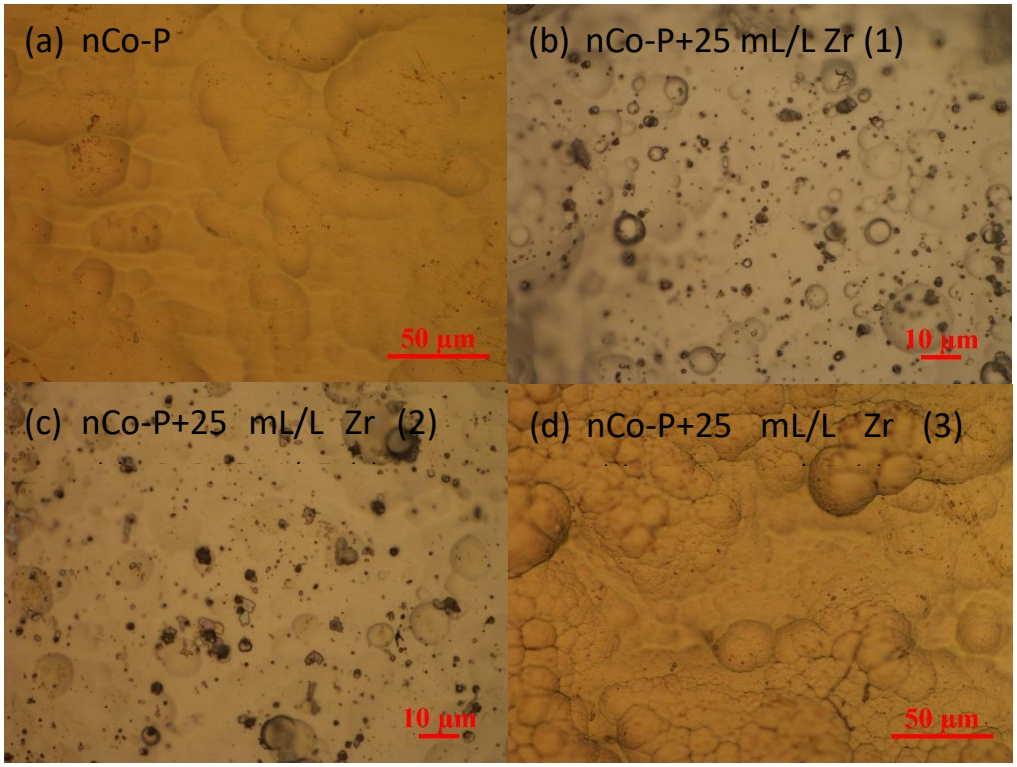

Figure 6: Optical microscopy images of coating with different recipe of Zr aqueous dopant.

4.4 Dual Dopant Analysis

Given the improved hardness results achieved with the improved alumina dopant, and the lower co-efficient of friction achieved with the zirconia dopant, Cirrus pivoted the research work to apply dual dopants. Dual dopant work with nCoP must be considered preliminary, as the remaining time on the programme was insufficient to conduct a full evaluation with this electrolyte.

Firstly, two Taber panels were produced for Integran to perform wear testing (one with the best zirconia dopant and the other with the dual dopants) and the results of this testing will be reported separately by Integran. While preparing dual dopant samples we plated two minor analysis samples both before and after plating the Taber panel. During all plating dopant replenishment was performed (see Section 5). The results of testing on these "analysis samples" is reported here.

The arrangement of the samples in the plating bath is shown in Figure 7, in the following analysis the samples are referred to as:

- Time: before or after – depending on whether the samples were plated first or last.
- Position: left or right – depending on their position in the bath; and
- Connection: direct or indirect – depending on the connection to the plating supply.

As may be seen in the results in Table 3, when working with dual dopants in a nCoP electrolyte depositing with DC power, these distinctions are important.

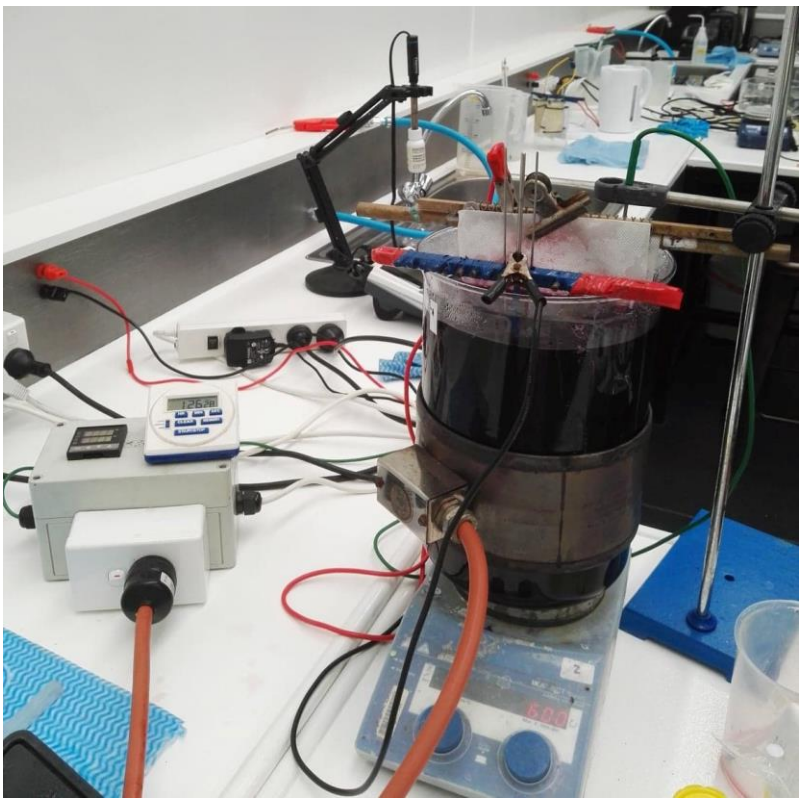

Figure 7: Sample Plating Arrangement

The results suggest the connection has a direct and currently unexplained effect on the plating rate for the sample. The coating weight for the directly connected samples are in all cases about half that of those connected via the cathode bar, however the total deposited nCoP in both cases is about the same. Secondly the samples plated after the Taber panels are harder than those

plated before. Finally, and most obviously sample three showed a very large and unexplained increase in hardness.

Table 3: Dual Dopant Results with 2.5mL/L Al and 10mL/L Zr dopants

Sample	Time	Position	Connection	Hardness $HV_{0.1}$	Weight grams	Wear Track µm
1	Before	Left	Direct	599.29±10.74	0.249	255
2	Before	Right	Indirect	581.14±14.65	0.736	255
3	After	Right	Direct	928.54±308.90	0.332	245
4	After	Left	Indirect	607.43±27.26	0.623	227

The differing plated thickness, as measured by the weight, is probably a result of the connection between the substrate and the cathode supply using a crocodile clip, however this does not explain why the sample directly connected to the supply was the lightest. The differences in hardness before and after preparation of the Taber sample could be explained by the dopant replenishment regime. However, sample 3 remains unexplained and further research may provide a method to significantly improve dopant uptake in the substrate and coating hardness.

Table 4 shows the 14 measurements taken on the surface of sample 3. As may be seen the hardness varies widely between typical values around 600 and an extreme value of 3700. These changes are associated with the coating morphology as seen below.

Table 4: Sample 3 Hardness Analysis

Test Point	*Hardness $HV_{0.1}$*	*Diagonal*	*Diagonal 1*	*Diagonal 2*
1	666	16.688	15.844	17.532
2	603	17.532	17.403	17.662
3	1373	11.623	11.429	11.818
4	1328	11.818	13.247	10.39
5	776	15.455	15.844	15.065
6	1487	11.169	11.039	11.299
7	790	15.325	15.455	15.195
8	661	16.753	17.013	16.494
9	687	16.429	16.104	16.753
10	824	15	15.974	14.026
11	1206	12.403	12.857	11.948
12	943	14.026	14.026	14.026
13	727	15.974	15.974	15.974
14	3702	7.078	7.273	6.883
Average	**928.54**			
STDEV	**308.90**			

Figure 8 shows the surface morphology observed through optical microscopy during hardness testing for the four samples, as may be seen the surface morphology of samples 2 and 4 is very

similar while 1 and 3 is also similar. Sample 1 & 3, with inclusions, are typically harder than the samples without and the area where the hardness is taken shows a finer structure, especially sample 3, the image for which is associated with measurement 11 above. Sample 3 also shows many more inclusions with perhaps a finer structure. Cirrus believes these to be agglomerated particles, however SEM analysis is required to confirm this understanding. The presence of the large particles

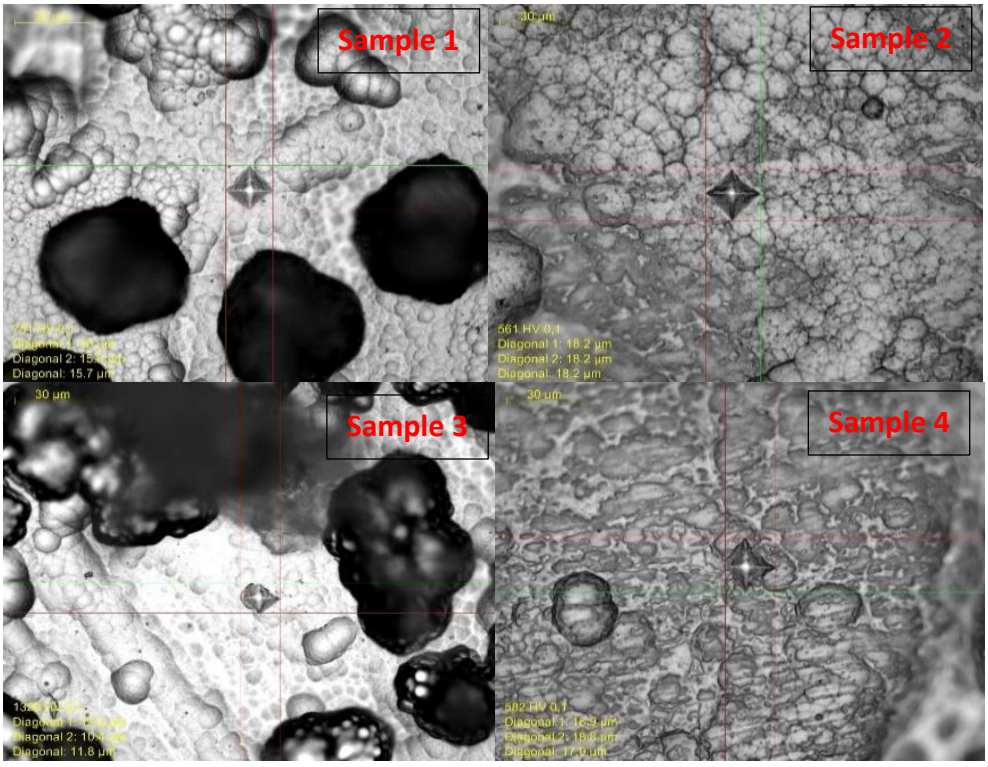

Figure 8: Surface Morphology Dual Dopant - Samples 1-4

Wear testing was performed on all samples using the same equipment and parameters as for the prior dopant work, however the results are only reported for two representative samples.

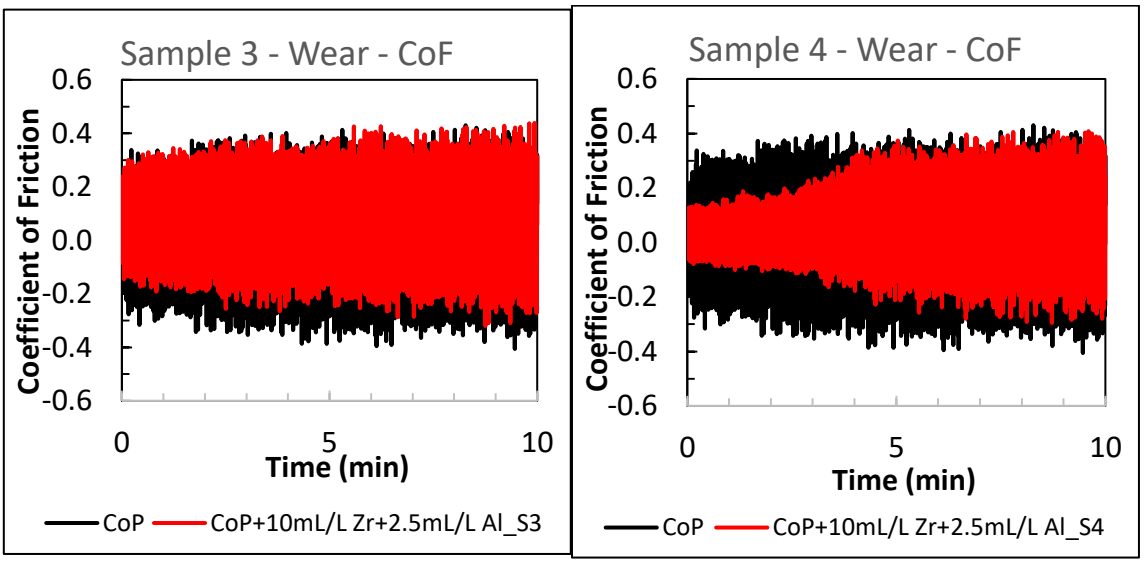

Figure 9: Dual Doped Sample CoF

As may be observed in Figure 9 the samples with the inclusions have higher CoF while being harder. Ideally, the harder structure would be maintained with smaller inclusions.

5. Dopant Replenishment

During the research, dopant depletion during deposition of a thick coating was allowed for. Dopant depletion calculations were performed based on the particle density in a coating derived from SEM/EDS analysis; unfortunately, this analysis is not deemed to be highly accurate due to the low levels of particles and the measurement error in EDS. That said, the calculation confirmed that dopant depletion would occur, and early validation with simple nickel coatings confirmed the importance of replenishment. Table 5 shows the microhardness of nickel with and without alumina dopant replenishment, indicating that both the hardness and measurement consistency improved when dopant is replenished during the plating process. Designing replenishment levels require an understanding of both particle concentration and size in the coating and the bath.

Table 5: Microhardness of Ni coating with and without alumina replenishment.

Sample	**Hardness ($HV_{0.1}$)**	
Test Point	**Ni+10 mL/L Al**	**Ni+10 mL/L Al+0.1mL/L / min**
1	476	495
2	467	495
3	464	495
4	464	489
5	467	499
AVERAGE	**467.6**	**494.6**
STDEV	4.93	3.58

An indicative nCoP dopant replenishment regime was developed from the nickel bath work and validated with dopant consumption experiments in nCoP. Samples were plated in a nCoP bath initially doped with 10 mL/L of alumina dopant, and then with successively lower controlled dopant levels, withdrawing some of the plated sample every minute while simultaneously adjusting the plating current. The result was a surface which should have continuously reducing dopant levels that was tested by nano-scratch as a measure of surface hardness. Figure 10 shows the scratch test results, which clearly show significant dopant depletion after six minutes of plating, while results are not entirely consistent the upward trend is obvious

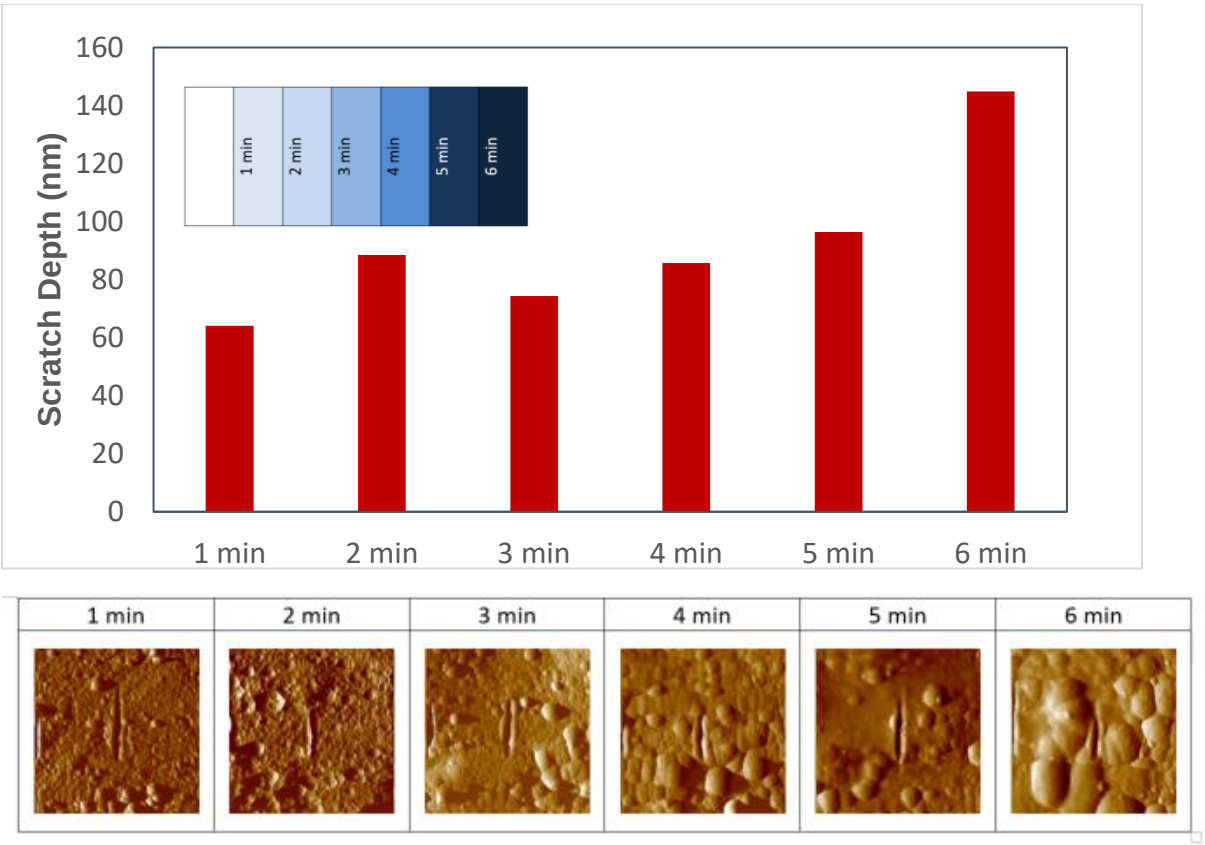

Figure 10: Scratch test for CoP+10mL Al dopant deposit at different time.

Next, we examined the influence of alumina dopant replenishment regimes on the micro-hardness of a plated sample. Each sample was DC plated for an hour at 135 mA/cm^2. Based on prior analysis, we calculated the 6% dopant depletion per hour at this plating current for nCoP. Two replenishment regimes were selected one where replenishment occurred every 5 min and the other every 10 min. In each case a 'second sample' was sample plated after replenishment was completed.

Figure 11 shows the results of this work; based on the micro-hardness, a 5 min replenishment regime appears to exceed the optimum dopant level and the micro-hardness drops slightly, while a 10-minute replenishment regime maintains a level of hardness consistent with the previous results. While a replenishment regime of 6% per hour with dopant additions every 10 minutes appears appropriate (at laboratory scale) to maintain the optimum level of dopant inside the bath, a repeat sample did not completely validate this method.

Additional work should evaluate the actual dopant concentration in both the bath and coating, typically via ICP-MS analysis, though with the small volumes involved, ICP analysis is prone to dilution and measurement errors. Developing a better bath analysis approach will advance both the understanding of dopant replenishment and incorporation.

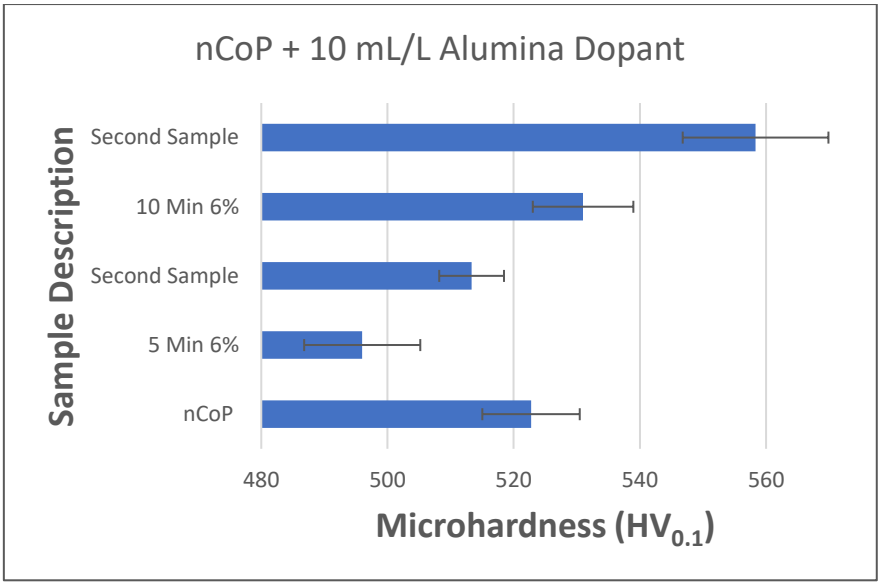

Figure 11: Effect of replenishment rate for Al dopant on microhardness properties.

6. Conclusions

Over all the programme showed that the adoption of Cirrus Dopant™ with Integran's nCoP process can produce good improvements in both hardness and wear resistance. Aqueous dopants evaluated in the second year of the programme showed enhanced results against those evaluated in the first year. Under optimum conditions the hardness of the coating can be improved by about 10-12% using the new alumina dopants. Wear performance using pin on disk wear testing can improve outcomes by 10-18%. Work has been performed to understand the required dopant replenishment regimes, however further work is required to ensure that these regimes operate at beyond laboratory scale.

The technology has been successfully transferred to Integran, however further work is required for them to achieve results comparable to those obtained by Cirrus. Cirrus have completed some preliminary industrialisation with and understanding of the required dopant replenishment regime of 6% per hour when plated at standard conditions. Furthermore, the newly developed high concentration dopants require minimum bath dilution and introduce minimal unwanted products.

Dual dopants show very interesting results which have yet to be fully validated but suggest in certain circumstances a hardness improvement of 80-90% may be possible. However, significant work still remains to understand the mechanisms involved and produce repeatable results.

Annex A – Year 1 Report